LIPOIC ACID PROTEIN LIGASES IN *Plasmodium* SPP.

by

DIPL. BIOL.
SVENJA GÜNTHER

THESIS SUBMITTED FOR THE DEGREE OF
DOCTOR OF PHILOSOPHY

NOVEMBER 2007

DIVISION OF INFECTION AND IMMUNITY
INSTITUTE OF BIOMEDICAL AND LIFE SCIENCES
UNIVERSITY OF GLASGOW

Abstract

Protozoan parasites of the genus *Plasmodium* are the causative agent of malaria. The four human pathogenic species infect more than 500 million people each year, causing the death of at least 1 million people. The most severe form of human malaria is caused by *P. falciparum*, which is responsible for 90% of the malaria deaths. A major problem in the treatment of this disease is resistance of the parasites against most of the existing chemotherapies. Therefore, there is an urgent need to identify, validate and assess potential new drug targets. The prerequisite of a potential drug target is that it should not be of significance for the human host or it should be sufficiently different from the human counterpart, so that parasite-specific inhibition is feasible. Lipoic acid metabolism in *Plasmodium* differs from that of mammals in some ways and therefore it might be a promising target for the development of new antimalarials. This study investigated the importance of lipoic acid ligation in *P. falciparum* using reverse genetic approaches, to assess whether this pathway has potential for drug design. In addition, a spectrophotometric assay system was developed that allowed the biochemical characterisation of lipoic acid ligases and can be adapted to high-throughput screening approaches of inhibitors for these enzymes.

Lipoic acid, also known as 6,8-thioctic acid, is an essential cofactor of α-keto acid dehydrogenase complexes (KADH) and the glycine cleavage system (GCV). The KADH include the pyruvate dehydrogenase (PDH), branched chain α-keto acid dehydrogenase (BCDH) and α-ketoglutarate dehydrogenase (KGDH), which are an integral part for any cell's metabolism. In *Plasmodium* spp. the lipoic acid dependent enzyme complexes are found in the apicoplast, a plastid related organelle, and in the mitochondrion and thus two organelle specific lipoylation pathways are present in these parasites. Biosynthesis of the cofactor occurs in the apicoplast. Octanoyl-[acyl carrier protein]: protein N-octanoyltransferase (LipB) catalyses the attachment of octanoyl-acyl carrier protein (octanoyl-ACP) to the PDH and lipoic acid synthase (LipA) then catalyses the insertion of two sulfurs into the octanoyl-chain to form lipoamide. In the mitochondrion, scavenged lipoic acid is ligated to the enzyme complexes by the action of lipoic acid protein ligase A (LplA1), in an ATP-dependent reaction. However, a second lipoate protein ligase A (LplA2) was identified in the genome of *P. falciparum*, but its subcellular localisation could not be predicted using the available prediction programs. To further analyse its localisation, parasites were generated expressing full length LplA2 in frame with green

fluorescent protein (GFP). In addition, immunofluorescence analyses on wild-type parasites using LplA2 specific antibodies were performed. These studies showed that LplA2 is dually targeted to the apicoplast as well as to the mitochondrion, raising the question about potential redundancy between the ligases present in the parasites. To further analyse this possibility, knock-out studies of *lplA1* and *lplA2* were performed in the human and rodent malaria parasites *P. falciparum* and *P. berghei*, respectively. Knock-out studies showed that LplA1 and LplA2 are non-redundant and strongly suggested that LplA1 is crucial for intraerythrocytic development, whereas LplA2 is essential for sexual development in the mosquito. According to these results it appears that (1) a key regulator of lipoic acid metabolism in *Plasmodium* spp. is stage specific expression of the relevant proteins and (2) both ligases are potential drug targets as knock-out of *lplA1* appeared impossible in the blood stages and knock-out of *lplA2* resulted in the interruption of parasite sexual development in the mosquito, and thus transmission of the parasites would be blocked if LplA2 was inhibited.

To further analyse the biochemical properties of *P. falciparum* LplA1 and LplA2, a spectrophotometric assay system was developed, which is also suitable for the development of a high-throughput assay system. The spectrophotometric assay monitors the first part of the LplA reaction - the activation of lipoic acid by ATP. The released pyrophosphate is converted to phosphate which is detected by acidic ammonium molybdate. Using the *Escherichia coli* LplA protein as a positive control, kinetic parameters for the bacterial protein were determined that are in reasonable agreement with the published data. The results validate the assay and suggest that it might be suitable for inhibitor screening in the future.

Author's declaration

I hereby declare that I am the sole author of this thesis and performed all of the work presented, with the following exceptions:

Chapter 3

• Parasite lines expressing various KADH-GFP fusion proteins were generated and analysed by Dr Paul McMillan and Prof Sylke Müller.

• The construct LplA1-KO-pHH1 was generated and transfected by Dr Carsten Wrenger.

• GC-MS analyses were performed by Dr Terry K. Smith, University of Dundee.

• Thin smears of *P. falciparum* taken every eight hours to analyse the progression through the intraerythrocytic developmental cycle were made by Prof Sylke Müller, Eva Patzewitz, Dr Janet Storm and myself. Images were taken by Prof Sylke Müller.

Chapter 4

• Some of the fluorescence images were taken by Prof Sylke Müller.

Chapter 5

• The construct LplA1-pASK-IBA3 was generated by Dr Carsten Wrenger.

• LC-tandem mass spectrometry analyses were performed by Dr Richard Burchmore of the Sir Henry Wellcome Functional Genomics Facility, University of Glasgow.

• MALDI-TOF mass spectrometry analyses were performed by the Fingerprints proteomics facility, University of Dundee.

• CD spectrum analyses were performed by Dr Sharon Kelly of the protein characterisation facility, University of Glasgow.

Svenja Günther

Publications

Günther S., Wallace L., Patzewitz E.M., McMillan P.J., Storm J., Wrenger C., Bissett R., Smith T.K. and Müller S. (2007)
Apicoplast lipoic acid protein ligase B is not essential for *Plasmodium falciparum*.
PLoS Pathog 3(12): e189. doi:10.1371/journal.ppat.0030189

Günther S., McMillan P.J., Wallace L.J. and Müller S. (2005)
Plasmodium falciparum possesses organelle-specific alpha-keto acid dehydrogenase complexes and lipoylation pathways.
Biochemical Society Transactions 33: 977-980

Acknowledgement

Here is the space to thank everyone who has somehow contributed to this work in the last years. Might it have been intellectually, financially, by keeping me focused or by keeping me sane...

First and foremost I would like to thank my supervisor Prof Sylke Müller for her invaluable assistance, support and guidance throughout the last four years. I am grateful that she gave me the opportunity to work on this exciting project in the first place, and for being such an excellent mentor. Her expertise, enthusiasm and her suggestions as well as her encouragements and persistence helped me at all times, especially during the difficult ones. Thanks for always pushing me a wee bit further.

The "Müller lab" was a brilliant place to work. I want to thank all the lab members, past and present, for there support, help, encouragement and (most important) for the fun time! In particular I want to thank Anne, Eva, Janet, Lynsey, Paul and Susan A. for their help with the culture whenever it was needed. I also want to thank Lesley for reading my thesis, giving advice and putting the commas at the right spot.

Thanks to everyone on level 5 and 6.

I wish to thank Prof Kai Matuschewski for giving me the opportunity to work in his lab on *Plasmodium berghei*. He and everyone in his lab helped and taught me how to do it, and I am deeply grateful for that. I had a fantastic three months in Heidelberg!

I am grateful to my assessor Prof Graham H. Coombs for his sound advice. His suggestions helped to stay focused on the most important things.

Everyone of the Boehringer Ingelheim Fonds deserves a big thank you! Not only because of the sincere friendship to my bank account, but moreover for the personal support. In particular, I would like to thank Monika Beutelspacher, Claudia Walther and Hermann Fröhlich for the fantastic Hirschegg and Blaubeuren meetings, for giving me the opportunity to go to conferences and workshops all over the world and for staying in contact and further supporting me in my career as a scientist.

I wish to thank the Gornik's Go, Günter, Fiona and Daniel who accepted me as a family member and who gave me shelter and food during my time in Heidelberg. Thanks for making it feel like home.

A big, big thank you goes to my family. To my brother Marcus, who introduced me to LaTeX and to whom I am deeply grateful for his help, advice and tremendous efforts to make this thesis look the way it does. To my parents Marlis and Rainer, I owe special gratitude. Without their support and understanding it would have been impossible to get this far.

Last, but certainly not least, I want to thank Sebastian. With his encouragement and understanding, his incredible amount of patience and his love he supported me all the way through and enabled me to finish this work.

für meine eltern

Contents

List of Figures

List of Tables

Abbrevations

μg	microgram
μl	microliter
μM	micromolar
3' UTR	Three prime untranslated region
5' UTR	Five prime untranslated region
[Fe-S]	Iron-sulphur cluster
A	Adenine
aa	Amino acid
ACP	Acyl carrier protein
AdoMet	S-Adenosyl-methionine
ADP	Adenosine diphosphate
AHT	Anhydrotetracycline
AMP	Adenosine monophosphate
AmpR	Ampicillin resistance cassette
ATP	Adenosine triphosphate
BCDH	Branched chain α-keto acid dehydrogenase complex
bp	base pairs
BPL	Biotin protein ligase
BSA	Bovine serum albumin
BSD	Blasticidin-S-deaminase
C	Cytosine
C-terminal	Carboxy terminal
CD	Circular dichroism
cDNA	Complementary DNA
CmR	Chloramphenicol resistance cassette
CO_2	Carbon dioxide
CoA	Coenzyme A
Da	Daltons
DABCO	1,4-Diazabicyclo[2.2.2]octane
DAPI	4',6-Diamidino-2-phenylindole dihydrochloride
DHFR/TS	Dihydrofolate reductase/thymilidate synthase
DHPS	Dihydropteroate synthase

DIC	Differential interference contrast
DMSO	Dimethyl sulphoxide
DNA	Deoxyribonucleic acid
dNTP	Deoxynucleotide triphosphate
DT	Dihydrofolate reductase/thymilidate synthase
DTT	Dithiothreitol
E1	Dehydrogenase protein of KADH
E2	Acyltransferase protein of KADH
E3	Dihydrolipoamide dehydrogenase (LipDH) protein of KADH
Ec	*Escherichia coli*
ECL	Enhanced chemiluminescence
EDTA	Ethylenediamine tetraacetic acid
EGTA	Ethylene glycol tetraacetic acid
ER	Endoplasmatic reticulum
FAD	Flavin adenine dinucleotide
G	Guanine
g	gram
GCV	Glycine cleavage system
gDNA	Genomic DNA
GFP	Green fluorescent protein
GMP	Guanosine monophosphate
GTP	Guanosine triphosphate
h	Hour(s)
hDHFR	Human dihydrofolate reductase
HEPES	4-(2-hydroxyethyl)-1-piperazineethanesulfonic acid
IFA	Immunofluorescence analysis
IgG	Immunoglobulin G
IPTG	Isopropyl-β-D-thiogalactopyranoside
K_m	Michaelis constant
KADH	α-Keto acid dehydrogenase complex
KAHRP	Knob-associated histidine rich protein
KanR	Kanamycin resistance cassette
kb	kilobases
kDa	kilo daltons
KGDH	α-Ketoglutarate dehydrogenase complex
kpsi	Kilo pound-force per square inch

L	liter
LA	Lipoic acid
LB	Luria Bertani
LipA	Lipoic acid synthase
LipB	Octanoyl-[acyl carrier protein]:protein N-octanoyltransferase
LipDH	Dihydrolipoamide dehydrogenase (E3) protein of KADH
LplA	Lipoic acid protein ligase A
M	molar
MCS	Multiple cloning site
MDa	mega dalton
mg	milligram
min	Minute(s)
ml	milliliter
mM	millimolar
MOPS	3-(N-morpholino)propanesulfonic acid
N-terminal	Amino terminal
NAD^+	Nicotinamide adenine dinucleotide, oxidised form
NADH	Nicotinamide adenine dinucleotide, reduced form
$NADP^+$	Nicotinamide adenine dinucleotide phosphate, oxidised form
NADPH	Nicotinamide adenine dinucleotide phosphate, reduced form
Ni-NTA	Nickel-nitrilotriacetic acid
nm	Nanometers
OD	Optical density
ORF	Open reading frame
PAGE	Polyacrylamide gel electrophoresis
Pb	*Plasmodium berghei*
PBS	Phosphate buffered saline
PCR	Polymerase chain reaction
PDH	Pyruvate dehydrogenase complex
Pf	*Plasmodium falciparum*
PfCAM	*Plasmodium falciparum* calmodulin
PfCRT	*Plasmodium falciparum* chloroquine resistance transporter
PfEMP-1	*Plasmodium falciparum* erythrocyte membrane protein-1
PFGE	Pulse field gel electrophoresis
PfHRPII	*Plasmodium falciparum* histidine rich protein 2
PfHRPIII	*Plasmodium falciparum* histidine rich protein 3

PfHsp86	*Plasmodium falciparum* heat shock protein 86
Pi^{2-}	Inorganic phosphate
PMSF	Phenylmethyl sulphonyl fluoride
PPi	Pyrophosphate
PVM	Parasitophorous vacuole
ROS	Reactive oxygen species
rpm	Revolutions per minute
SD	Standard deviation
SDS	Sodium dodecyl sulphate
sec	Secund(s)
SRP	Signal recognition particle
T	Thymine
Ta	*Thermoplasma acidophilum*
TAE	Tris-Acetate containing EDTA
TBE	Tris-Borate containing EDTA
TCA	Tricarboxylic acid
TCEP	Tris(2-carboxyethyl)phosphine
Tet	Tetracycline
Tg	*Toxoplasma gondii*
THF	Tetrahydrofolate
TPP	Thiamine pyrophosphate
Tris	Tris [hydroxymethyl] aminomethane
TrxPx1	2-Cys peroxiredoxin
U	Unit
UV	Ultraviolet
V	Volt
V_{max}	Maximum velocity
v/v	Volume per volume
w/v	Weight per volume
WHO	World health organisation
WT	Wild-type
ZeoR	Zeocin resistance cassette
°C	Degree Celsius

1. Introduction

1.1. Malaria

Malaria is one of the most important infectious diseases in the world. About 40% of the world's population lives in malaria endemic areas and is therefore at risk of the disease (Greenwood and Mutabingwa, 2002). Each year, more than 500 million people become infected, resulting in the death of more than 1 million people. Many of them are young children and pregnant woman. Most of the malaria cases occur in tropical Africa, but Asia and South America are also affected (Figure 1.1) (WHO, 2007).

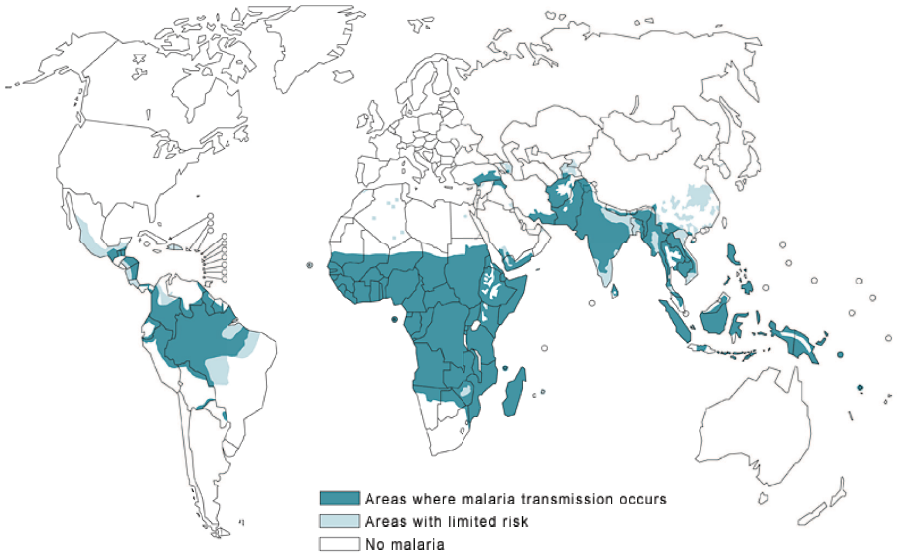

Figure 1.1.: Distribution of malaria in 2005
This figure displays the regions were malaria transmission occurred in 2005. White are the regions without malaria, pale blue are regions with limited risk and dark blue are the areas where malaria transmission occurs. This image was taken from the World Health Organisation (WHO) (http://www.who.int/en/).

Malaria is caused by protozoan parasites of the genus *Plasmodium*. These parasites belong to the phylum of *Apicomplexa* that are defined by the presence of apical organelles required for invasion of their host cell. Many different *Plasmodium* species are known which can infect different vertebrate hosts including primates, rodents, birds and reptiles. The four following species *P. falciparum*, *P. vivax*, *P. ovale* and *P. malariae* can cause the disease in humans. Each of these four species is responsible for unique malaria outcomes.

P. malariae, for example, undergoes a three day intraerythrocytic development cycle resulting in recurring fever attacks every 72 hours, whereas the other three species undergo a two day intraerythrocytic development cycle (Cook, 1996). *P. vivax* and *P. ovale* are able to form dormant stages in the hepatocytes. These stages are known as hypnozoites and they can survive for up to 20 years (Cogswell, 1992). On the contrary, *P. falciparum* and *P. malariae* are not able to form dormant stages. *P. falciparum* infection results in the most severe clinical symptoms of malaria and causes 90% of the malaria deaths. The most widespread parasite is *P. vivax*, responsible for $\sim$80% of the worldwide malaria cases.
All *Plasmodium* parasites are transmitted by female mosquitoes of the genus *Anopheles*. Of the $\sim$380 *Anopheles* species only 60 can transmit malaria (Cook, 1996). The female mosquitoes themselves become infected during a blood-meal from an infected person and transmit the parasites to the next person with the next blood-meal. The parasite's life cycle including the host switch between human and mosquito is explained in more detail in the following section.

1.2. Life cycle of malaria parasites

Plasmodium parasites possess a complex life cycle, which switches between sexual and asexual development (Figure 1.2). The sexual development (gamogony) as well as sporogony takes place in the *Anopheles* mosquito whereas the parasites proceed through asexual development (schizogony) in the human host. The asexual development in the parasite's life cycle begins with the injection of infective sporozoites into the human by a female *Anopheles* mosquito during a blood meal. The sporozoites migrate via the blood and lymph systems to the liver where they invade hepatocytes. Here, the first asexual reproduction (exoerythocytic schizogony) takes place. The sporozoites differentiate to schizonts, which can produce up to 30,000 merozoites (Prudêncio et al., 2006). Upon rupture of the hepatocyte, the merozoites are released into the blood stream where they immediately invade erythrocytes, in which the second asexual reproduction (intraerythrocytic schizogony) occurs. Invasion is coordinated by the apical organelles of the merozoite and results in the invagination of the erythrocyte plasma membrane to form the parasitophorous vacuole, which surrounds the parasite and separates it from the erythrocyte cytosol (Gaur et al., 2004, Cowman and Crabb, 2006). Within the parasitophorous vacuole, the parasite matures through the three different developmental stages. During early intraerythrocytic development (1-18 hours after invasion) the parasites are in the ring stage. In this stage the parasites show only low metabolic activity, although the parasite begins to modify its host cell and it starts to endocytose and digest the host cell

cytoplasm. The parasite matures into the trophozoite stage (18-28 hours after invasion), in which the host cell cytoplasm is ingested to obtain nutrients from the host cell. Particulary important is the haemoglobin, which is used as an amino acid source by the parasite (Banerjee et al., 2002). Degradation of haemoglobin takes place in the parasite's food vacuole and the remaining haem is converted into haemozoin, also known as malaria pigment (Egan et al., 2002). Additionally, during the trophozoite stage RNA and protein synthesis occurs at a high level and DNA synthesis is initiated (Arnot and Gull, 1998). During the schizont stage (28-48 hours after invasion) *Plasmodium* parasites go through multiple rounds of DNA replication and nuclear divisions to form a syncytial cell with 8-32 nuclei (Arnot and Gull, 1998). Finally, the schizont undergos cytokinesis and mononucleated merozoites are formed which are released upon rupture of the erythrocyte (Doerig et al., 2000). Back in the blood stream, the merozoites infect more erythrocytes in which they can continue the intraerythrocytic development cycle. This phase of the parasites development is responsible for the symptoms of malaria. Rupture of infected erythrocytes and the subsequent release of merozoites into the blood stream causes for example the symptomatic cycling of fever observed in malaria patients (Miller et al., 2002).

Some merozoites will not proceed through the intraerythrocytic development cycle, but will instead undergo gametocytogenesis during which they differentiate into either female macrogametocytes or male microgametocytes (Talman et al., 2004). These are taken up by a female *Anopheles* mosquito during a blood-meal and the sexual development within the mosquito starts. The macrogametocytes form spherical macrogametes and each microgametocyte divides into 4-8 exflagellated microgametes (Sinden et al., 1978). Fusion of macro- and microgametes in the mosquito's midgut leads to the formation of the diploid zygote which develops to the motile ookinete. The ookinete migrates through the midgut epithelium and matures at the basal lamina into the immobile oocyst (Matuschewski, 2006). The oocyst goes through several rounds of asexual replication to form sporozoites. These are released and travel to the salivary gland of the mosquito where they invade the gland cells (Matuschewski, 2006). With the next blood meal of the mosquito these highly infective sporozoites are injected into the human body, allowing the cycle of infection between the human and mosquito host to continue.

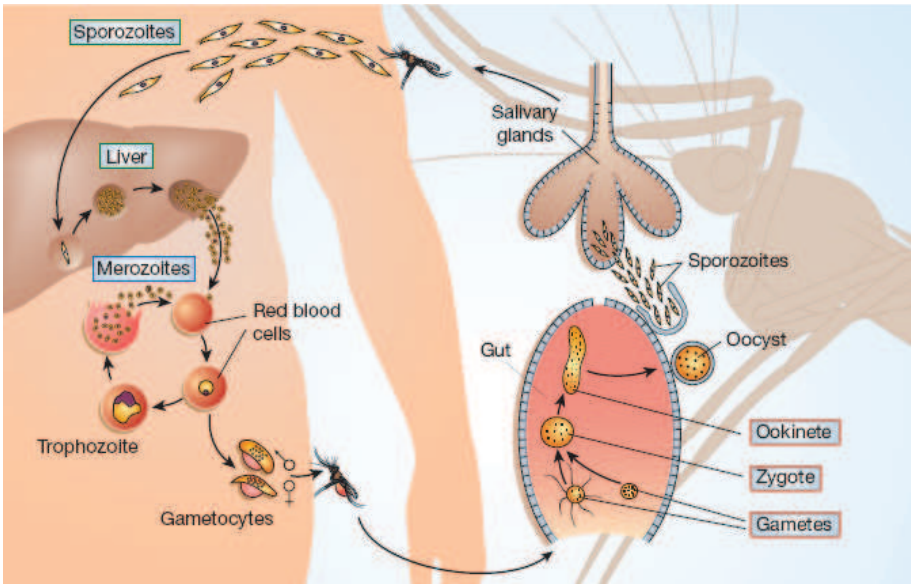

Figure 1.2.: Life cycle of malaria parasites
Plasmodium parasites possess a complex life cycle that switches between asexual development in the human host, and sexual development in the mosquito host. A female anopheline mosquito injects sporozoites into the blood stream of the human host during a blood meal. The sporozoites migrate to the liver and invade hepatocytes. They reproduce asexually until thousands of merozoites are formed and released through rupture of the hepatocyte. In the blood stream, the merozoites invade erythrocytes in which they undergo the intraerythrocytic development cycle, resulting in the release of merozoites. These invade more erythrocytes in which they either continue the intraerythrocytic development cycle or undergo gametocytogenesis, during which they form either female or male gametocytes. These are taken up by a mosquito during a blood meal and the sexual development in the mosquito's midgut starts. The female gametocytes develop into spherical macrogametes and the male gametocytes into 4-8 exflagellated microgametes. A macro- and a microgamete fuse to form the zygote, which develops into the motile ookinete. The ookinete traverses the midgut epithelium where it develops into an oocyst in which sporozoites are formed. These are released and enter the mosquito's salivary glands ready to infect the human host with the next blood meal of the mosquito. The image was taken from Ménard (2005) with permission from Nature Publishing Group.

1.3. *Plasmodium falciparum*

P. falciparum infections are responsible for the most severe form of malaria and can result in cerebral malaria or pregnancy-related malaria. These disease outcomes are specific to *P. falciparum* infections and are attributable to two phenomena of the infected erythrocytes called sequestration and rosetting (Miller et al., 2002). During the intraerythrocytic developmental cycle, *P. falciparum* remodels the erythrocyte surface in a way that allows the infected erythrocyte to adhere to the vascular endothelium (Kyes et al., 2001). Cy-

toadherence is mediated by the antigenically variant *P. falciparum* erythrocyte membrane protein 1 (PfEMP-1) on the surface of the infected erythrocytes (Kyes et al., 2001). It is probably anchored in the plasma membrane by a putative transmembrane domain and is associated on the cytoplasmic site with other parasite encoded proteins. These consist predominantly of the knob-associated histidine rich protein (KAHRP), and together they form protrusions on the erythrocyte surface known as "knobs" (Kilejian, 1979, Crabb et al., 1997). PfEMP-1 interacts with several molecules expressed by endothelial cells including CD36, intercellular adhesion molecule 1 (ICAM-1) and chondroitin sulfate A (CSA), to promote adhesion to these cells. Data suggest that PfEMP-1 mediated adhesion to ICAM-1 plays an important role in cerebral malaria (Turner et al., 1994) and that adhesion to CSA contributes to pregnancy-related malaria (Fried and Duffy, 1996). Sequestration to the endothelium also occurs in a number of other organs including the heart, liver and kidneys, resulting in the blockage of the microvascular blood flow in the affected organs (Miller et al., 2002). In addition, sequestration also prevents the infected erythrocytes being recognised and cleared by the spleen, and thus helps the parasite to evade the host immune system (Miller et al., 2002). Rosetting is the second phenomenon of *P. falciparum* infected erythrocytes and consists of the attachment of infected cells to uninfected erythrocytes. Again, this effect is mediated by the variant antigen family PfEMP-1, and it was suggested that complement receptor 1 (CR1) on the surface of uninfected erythrocytes plays a key role in the rosetting phenotype (Rowe et al., 1997).

P. falciparum is the most studied parasite of the human infective *Plasmodium* species, possibly because *P. falciparum* causes the most lethal form of malaria. Moreover, the ability to culture these parasites *in vitro* has contributed largely to the study of this parasite in more detail (Trager and Jensen, 1976). In 2002, the *P. falciparum* genome project was completed (Gardner et al., 2002) and it has been widely used as a valuable tool to further analyse these parasites. The completed genome is especially helpful in the quest for new antimalarial drug targets and potential vaccine candidates. The nuclear genome of *P. falciparum* is 22.9 megabase (Mb) in size comprising 14 chromosomes varying in size between 0.643 and 3.29 Mb. With 80.6% of the genome consisting of (A+T), it is the genome containing the highest (A+T) levels sequenced to date. In introns and intergenic regions it even reaches (A+T) levels up to 90%. About 5300 protein encoding genes were predicted, of which only 40% displayed sufficient similarities with genes in other organisms to predict their potential protein function (Gardner et al., 2002).

1.4. Chemotherapies

Currently, the main way to combat malaria is by chemotherapy using different antimalarial drugs. However, widespread resistance against many of these drugs is a serious problem, and therefore the identification of potential new antimalarial drug targets and the development of new drugs is urgently required (Hyde, 2007). Vector control and insecticide-treated mosquito nets are other possibilities to prevent infection with *Plasmodium* parasites and "control" the disease, however, this is difficult to implement and maintain in countries which are affected (Greenwood et al., 2005, Hill et al., 2006). Additionally, great efforts are being taken to find and develop a vaccine against *Plasmodium* parasites and although some progress has been made, this is still elusive (Targett, 2005, Matuschewski and Mueller, 2007).

1.4.1. Quinoline antimalarials

Quinoline-based antimalarial drugs have been widely used in the treatment of malaria, but resistance against these compounds is a major problem. Chloroquine, a 4-aminoquinoline, was the antimalarial drug of choice for several decades due to it being highly effective and cheap to produce (Cook, 1996). However, resistance has spread leaving only a few areas in the world where malaria treatment with chloroquine is still successful (Winstanley and Ward, 2006). Chloroquine is believed to target the polymerisation of toxic haem. It enters the food vacuole and binds to haem, thus preventing its polymerisation to haemozoin (Egan et al., 1997, Leed et al., 2002). As a result, the concentration of toxic haem increases causing enhanced oxidative stress, membrane damage and eventually parasite death (Loria et al., 1999). Chloroquine resistant parasites accumulate less chloroquine in their food vacuole, which is associated with mutations in the multidrug resistance transporter and chloroquine resistance transporter (Mu et al., 2003). Another phenomenon observed in resistant parasites is that they contain higher levels of glutathione. It is thought that glutathione detoxifies free haem and therefore protects the parasites from the increased haem levels (Ginsburg and Golenser, 2003).
Primaquine, a 8-aminoquinoline, is used in combination therapy with other antimalarials (mainly with chloroquine) in the treatment of *P. vivax* and *P. ovale* malaria (Galappaththy et al., 2007). Primaquine is active against the dormant stages of these parasites and thus is used to kill hypnozoites in the liver to prevent relapse of the disease (Winstanley and Ward, 2006). The precise mode of action of primaquine is not known, but it is believed to act on the mitochondria of the parasites (Foley and Tilley, 1998, Schlitzer, 2007).

Other compounds used for malaria treatment are the methanolquinolines mefloquine (known as Lariam®) and quinine, and halofantrine, a phenanthrene methanol (Bray et al., 2005, Hyde, 2007). Quinine is a naturally occurring compound, which is extracted from chinona bark. It is used as a prophylactic and in combination with antimalarial antibiotics for the treatment of malaria. Mefloquine, quinine and halofantrine also enter the parasite's food vacuole but their exact mode of action is not known, although it is believed to be different from chloroquine's mode of action (Foley and Tilley, 1998, Schlitzer, 2007).

1.4.2. Artemisinin

Artemisinin is another naturally occurring compound found in the shrub *Artemesia annua*. It has been used in China in the treatment of different diseases including malaria for centuries. Its precise mode of action is not known. Several ways how artemisinin affect parasites have been suggested. One possible mode of action is the inhibition of the production of haemozoin by alkylation of haem (Meshnick, 1998). It has also been shown that artemisinin and its derivates are redox active, producing reactive oxygen species and thus increase oxidative stress for the parasites (Dong and Vennerstrom, 2003). In addition, artemisinin was also shown to inhibit the serco/endoplasmatic reticulum Ca^{2+} ATPase (Eckstein-Ludwig et al., 2003). Artemisinin based combination therapies (ACT) are now recommended by the WHO for treatment of malaria due to widespread resistance against other antimalarials such as chloroquine or antifolates.

1.4.3. Antifolates

Antifolates have been successfully used as antimalarials, but resistance against these compounds has widely spread. Antifolates used in malaria therapy affect *de novo* folate biosynthesis by inhibiting either the dihydrofolate reductase-thymilidate synthase (DHFR-TS) or the hydroxymethylpterin pyrophosphokinase-dihydropteroate synthase (HPPK-DHPS) (Hyde, 2007). Drugs like pyrimethamine or proguanil (which is metabolised to the active form cycloguanil) inhibit DHFR activity whereas sulfonamides and sulfone act on DHPS activity (Hyde, 2007). These compounds were initially used in monotherapy, but resistant parasites developed quickly (Gregson and Plowe, 2005). Combination of DHFR inhibitors with DHPS inhibitors showed synergistic effects in the treatment of malaria and thus a combination of pyrimethamine and sulfadoxine (known as Fansidar®) is used for the treatment of *falciparum* malaria (Gregson and Plowe, 2005, Hyde, 2007). However, resistance against these compounds has widely spread, which are caused by several point mutations in the respective genes resulting in different grades of

resistance against these compounds. It was shown that pyrimethamine resistance is caused by four point mutations within the DHFR gene (Wu et al., 1996), and resistance against sulfadoxine is due to point mutations within the DHPS gene (Triglia et al., 1998). A combination of these mutations in parasite populations is responsible for the pyrimethamine-sulfadoxine treatment failure. Since 2003 a combination of chlorproguanil and dapsone (known as LapDap®) has been used as an antimalarial, but some resistance against this drug has already been reported and thus it is currently tested in combination with artemisinins (Schlitzer, 2007).

1.4.4. Atovaquone

Atovaquone is another compound used in chemotherapy of malaria. It is a structural analog of ubiquinone and thus targets and inhibits cytochrome bc_1 in the mitochondrial inner membrane, resulting in the collapse of the membrane potential (Sherman, 2005). In monotherapy, parasites with point mutations in the cytochrome b gene emerged quickly conferring resistance against atovaquone (Kessl et al., 2005). In combination with proguanil (known as Malarone®), it is more effective against parasites and also induces less resistance (Hyde, 2007). The precise synergistic mechanism of atovaquone and proguanil is not yet fully understood, but it appears that it is not associated with proguanil's function as an antifolate precursor; rather, it appears to sensitise the mitochondrion for atovaquone action (Sherman, 2005). However, the production of this drug is problematic, as it is very expensive, and therefore not available for people living in malaria endemic areas.

1.4.5. Antibiotics

Several antibiotics exhibit antimalarial activities and doxycycline, tetracycline and clindamycine are currently used in combination therapies (CDC, 2007). Generally it is believed that antibiotics affect pathways present in the apicoplast, the plastid-related organelle, and/or in the mitochondrion due to their bacterial origin (Goodman et al., 2007). It was suggested that clindamycine inhibits protein translation in the apicoplast, as it does in the related parasite *Toxoplasma gondii* (Camps et al., 2002). Doxycycline and tetracycline also inhibit protein translation and it is believed that they affect the mitochondrion (Prapunwattana et al., 1988). Recent data, however, also suggest an effect on the apicoplast (Dahl et al., 2006, Goodman et al., 2007). Other antibiotics affect parasite viability *in vitro* and *in vivo* and they will be discussed in more detail below.

1.5. Structure of *Plasmodium falciparum*

The asexual stages of *P. falciparum* mature in a 48 hour development cycle within an erythrocyte. They contain a number of distinct organelles which play crucial roles during their life cycle (Sherman, 2005). Figure 1.3 displays a 3D reconstruction image of a merozoite, the invasive form of the parasite, taken from Bannister et al. (2000).

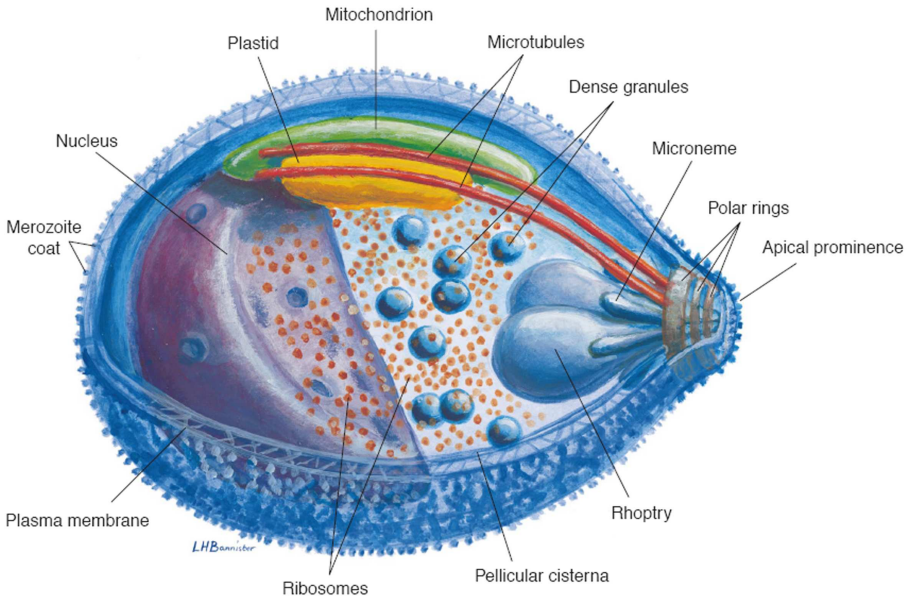

Figure 1.3.: Organisation of a *P. falciparum* merozoite
This image displays a reconstituted 3D image of a *P. falciparum* merozoite based on serial electron microscope slides. The image is taken from Bannister et al. (2000) with permission from Elsevier.

The rhoptries, micronemes, dense granules and polar rings at the apical end are also known as the apical organelles. They are formed during schizogony and are the key players in invasion of the host cell. Other unique *Plasmodium* compartments include the parasitophorous vacuole, which is generated during the invasion process and surrounds the parasites in the erythrocyte cytoplasm. Also unique for *Plasmodium* parasites are the cytostome and the food vacuole which are involved in endocytosis of host cell cytoplasm and hemoglobin digestion. Membranous structures called Maurer's clefts are generated within the infected erythrocyte which are believed to play a role in protein trafficking to the erythrocyte membrane. It is suggested that the Maurer's clefts are generated by vesicles that bud from the parasitophorous vacuole membrane (Spycher et al., 2006). Another organelle unique to most apicomplexan parasites is the apicoplast, a plastid-related organelle. It is closely associated with the mitochondrion throughout the intraerythrocytic

development cycle of the parasites. Because the apicoplast and the mitochondrion have been thoroughly investigated in this thesis, both organelles are described in more detail below.

1.5.1. The apicoplast

The apicoplast is a plastid-related organelle present in almost all apicomplexan parasites. *Apicomplexa* like *Cryptosporidium* once possessed a plastid but lost it over time (Huang et al., 2004). The apicoplast was acquired by secondary endosymbiosis of an already plastid-bearing organism. Therefore, this organelle is surrounded by four membranes (McFadden and Roos, 1999). The precise origin of the apicoplast is still controversial, but it probably is derived from a red algae rather than a green algae (Sherman, 2005). During the intraerythrocytic developmental stages, the apicoplast is closely associated with the mitochondrion and, like this organelle, it elongates and branches out during schizogony. Late in schizogony, the branched apicoplast divides so that each newly formed merozoite contains a new apicoplast (van Dooren et al., 2005).

The apicoplast has retained its own 35 kb circular genome, and most of the 30 proteins encoded by it play a role in their own synthesis (Wilson et al., 1991). This suggests that after the endosymbiosis event the majority of the genes encoded in the genome of the engulfed algae were transferred into the parasite nucleus. Genome analysis of *P. falciparum* revealed that $\sim$10% of the nucleus encoded proteins are likely to be targeted to the apicoplast (Gardner et al., 2002), and the mechanisms governing protein targeting to the apicoplast will be explained in Chapter 1.6.4.

Inhibition of apicoplast DNA replication, transcription and translation by various antibiotics leads to death of the parasites, suggesting a crucial role of this organelle for parasite viability (Waters and Janse, 2004, Goodman et al., 2007). Indeed, some antibiotics are currently used in combination therapies for the treatment of malaria (see 1.4.5). Interestingly, antibiotics can cause two distinct drug kinetic responses. Antibiotics like ciprofloxacin, rifampicin and thiostrepton cause an immediate effect whereas clindamycin and tetracycline result in the delayed death of the parasites (Goodman et al., 2007). The "delayed death phenotype" is also observed in *T. gondii*. He et al. (2001) engineered *T. gondii* mutants that are not able to segregate the apicoplast during endodygeny and thus they produced parasites, which lack the apicoplast. These apicoplast lacking parasites grew normally and were able to invade another host cell, however, then growth stopped

and the parasites died (He et al., 2001). These experiments suggest that the "delayed death phenotype" relates to apicoplast function and in that respect it was proposed that the apicoplast might be essential for the establishment of the parasitophorous vacuole (He et al., 2001). The "delayed death phenotype" occurs in both apicomplexan parasites but interestingly, ciprofloxacin, an apicoplast replication inhibitor, causes immediate death in *P. falciparum* but delayed death in *T. gondii*, suggesting that the apicoplast pathways might fulfil different roles in *Plasmodium* and *Toxoplasma* parasites (Fichera et al., 1995, Goodman et al., 2007).

The apicoplast is a non-photosynthetic plastid which contains a number of different biochemical pathways. Fatty acid biosynthesis, for instance, occurs in the apicoplast. Like in bacteria and plants, fatty acids in *Plasmodium* parasites are synthesised via the type II pathway, which consists of single enzymes acting in concert to catalyse the condensation, dehydration and reduction reactions (Ralph et al., 2004, White et al., 2005). Acetyl-CoA is required in the first step of the pathway, and is provided by the pyruvate dehydrogenase complex (PDH), which is also present in the apicoplast (Foth et al., 2005, McMillan et al., 2005). Acetyl-CoA becomes carboxylated by acetyl-CoA carboxylase to form manoyl-CoA, which is the committing step in fatty acid biosynthesis. Not all apicomplexan parasites possess a type II fatty acid synthesis pathway. Parasites like *Cryptosporidium* synthesise fatty acids via the type I pathway in the cytosol, which is also present in mammals and yeast (Zhu et al., 2000). The type I pathway consists of one protein (fatty acid synthase), which contains all enzymatic reaction sites required for fatty acid synthesis (Smith et al., 2003). Interestingly, the apicomplexan parasites *T. gondii* and *Eimera tenella* seem to possess both fatty acid biosynthesis pathways, type II in the apicoplast and type I potentially in the mitochondrion (Zhu, 2004, Mazumdar et al., 2006), suggesting that differences exist in fatty acid metabolism between various *Apicomplexa*. Inhibition of *Plasmodium* fatty acid synthesis by thiolactomycin, an inhibitor of the condensing enzymes FabB (β-ketoacyl-ACP synthase I), FabF (β-ketoacyl-ACP synthase II) and FabH (β-ketoacyl-ACP synthase III) killed parasites *in vitro* (Waller et al., 1998). Triclosan also killed parasites *in vitro* and was even able to clear mice infected with the rodent malaria parasite *P. berghei* (Surolia and Surolia, 2001). It was shown that Triclosan inhibits FabI (enoyl-ACP reductase) activity (Surolia and Surolia, 2001), making fatty acid biosynthesis a potential antimalarial drug target.

Another important biosynthetic pathway present in the apicoplast is the non-mevalonate

dependent isoprenoid biosynthesis. Like in bacteria and plants, the pathway in *Plasmodium* parasites is 1-deoxy-D-xylulose-5-phosphate (DOXP) dependent. It was shown that the antibiotic fosmidomycin inhibits DOXP reductoisomerase (catalysing the second step in the pathway), killing *P. falciparum in vitro* and *in vivo* (Jomaa et al., 1999). Currently fosmidomycin is used in clinical trials and it shows particularly promising results in combination with clindamycin (Wiesner et al., 2002, Na-Bangchang et al., 2007).

Haem is an essential prosthetic group of, for example, cytochromes and is involved in oxygen- and electron-transport. Although *Plasmodium* parasites generate free haem through uptake and digestion of host cell haemoglobin, they rely on haem biosynthesis (Surolia and Padmanaban, 1992). The pathway is divided between different compartments including the apicoplast, mitochondrion and also possibly the cytosol (Ralph et al., 2004). The first step of the reaction, the synthesis of δ-aminolevulinate from glycine and succinyl-CoA, is catalysed by the δ-aminolevulinate synthase, which is located in the mitochondrion (Varadharajan et al., 2002, Sato et al., 2004). The enzymes catalysing the subsequent reactions in haem biosynthesis are present in the apicoplast (Sato et al., 2004, van Dooren et al., 2006). However, the localisation of the last three enzymes in the biosynthesis process, namely HemF (coproporphyrinogen oxidase), HemG (protoporphyrinogen oxidase) and HemH (ferrochelatase) is not clear, although HemH possibly contains a N-terminal mitochondrial targeting peptide suggesting mitochondrial localisation (Ralph et al., 2004). On the contrary, HemG does not possess an obvious N-terminal targeting peptide and thus could be a cytosolic protein. However, the mammalian HemG is targeted to the mitochondrion by unknown internal targeting signals, a mechanism that could also apply for the *Plasmodium* enzyme (Morgan et al., 2004, Dailey et al., 2005). Prediction of HemF localisation is difficult because it contains several introns at the N-terminus (Ralph et al., 2004). Further analyses are required to determine the exact localisation of the last enzymes of the haem biosynthesis pathway.

Plasmodium possess different pathways for iron-sulphur ([Fe-S]) cluster biosynthesis. The parasites are able to synthesise [Fe-S] cluster in the apicoplast as well as in the mitochondrion (Seeber, 2002). The pathway in the apicoplast is likely to be responsible for providing [Fe-S] cluster for enzymes like lipoic acid synthase (LipA), ferredoxin, tRNA methylthiotransferase or IspG and IspH, both of which are involved in isoprenoid biosynthesis.

1.5.2. The mitochondrion

The mitochondrion in *Plasmodium* parasites was derived through primary endosymbiosis of an α-proteobacterium resulting in an organelle surrounded by two membranes (van Dooren et al., 2006). The appearance of mitochondria in *Plasmodium* parasites varies between different species and life cycle stages. *P. falciparum* intraerythrocytic stages contain a single mitochondrion without cristae, whereas *P. falciparum* gametocytes contain multiple cristate mitochondria (Rudzinska, 1969, van Dooren et al., 2006). During the intraerythrocytic development, the mitochondrion changes its morphology along with the apicoplast. The mitochondrion elongates and branches during schizogony before it divides. Multiple organelles are formed, which are segregated to the single merozoites (van Dooren et al., 2005).

The mitochondrion in *Plasmodium* has retained a small 6 kb genome, which only encodes three proteins, the cytochrome b, cytochrome c oxidase I and cytochrome c oxidase III, in addition to 20 fragmented rRNAs (Sherman, 2005). Most of the genes of the mitochondrial genome were transferred to the parasites nuclear genome (Adams and Palmer, 2003). Consequently, mitochondrial proteins encoded in the nucleus have to be transported to the mitochondrion, and the precise mechanisms of mitochondrial protein targeting will be described in Chapter 1.6.5.

One of the most important functions of the mitochondrion in mammals is the generation of ATP by oxidative phosphorylation, the main energy source for the cell. Therefore, it was somewhat surprising when it was shown that the primary source of energy for *P. falciparum* intraerythrocytic stages is provided by glycolysis (Bryant et al., 1964). Most of the pyruvate generated during glycolysis is metabolised into lactate rather then into acetyl-CoA like in mammals (Sherman, 2005). In mammals, this step is catalysed by PDH, which links glycolysis with the TCA cycle. Because of these findings in *Plasmodium*, it was initially thought that the parasites do not possess a TCA cycle. However, the genome project revealed the presence of genes encoding all necessary proteins in the genome (Gardner et al., 2002). Further analyses on the protein level, however, revealed some differences to the mammalian counterpart, giving reason to speculate about the precise function of the *Plasmodium* TCA cycle. Citrate synthase, the first enzyme in the cycle, is present in *Plasmodium* blood stages and it was confirmed to localise to the mitochondrion (Tonkin et al., 2004). Aconitase, catalysing the second step, the isomerisation of citrate to isocitrate, is also present in the blood stages. It was shown that the enzyme

possesses aconitase activity *in vitro* and localises to multiple destinations including the mitochondrion, cytosol and food vacuole (Hodges et al., 2005). The third enzyme in the TCA cycle is the isocitrate dehydrogenase. A potential mitochondrial enzyme was identified in the *P. falciparum* genome, and biochemical analyses revealed that the reaction of the *P. falciparum* enzyme is $NADP^+$ dependent in contrast to the mammalian enzyme, which requires NAD^+ (Wrenger and Müller, 2003). Because NADPH is produced during the reaction, which can not be fed into the electron transport chain, it was suggested that the isocitrate dehydrogenase might be involved in mitochondrial redox control. The subsequent conversion of α-ketoglutarate to succinyl-CoA is catalysed by the multienzyme complex α-ketoglutarate dehydrogenase, which is present in the mitochondrion (Günther et al., 2005, McMillan et al., 2005). The generated succinyl-CoA is either used for haem biosynthesis or it is converted to succinate by the succinyl-CoA synthase. The protein consists of α and β subunits and homologues were identified in the *P. falciparum* genome (van Dooren et al., 2006). The next enzyme in the TCA cycle is the succinate dehydrogenase, which catalyses the conversion of succinate to fumarate. Additionally, succinate dehydrogenase is also involved in oxidative phosphorylation (complex II), and a functional homologue of the enzyme was identified in *P. falciparum* (Suraveratum et al., 2000, Takeo et al., 2000). Fumarate is then converted into malate by a fumarate hydratase. The homologue identified in *P. falciparum* showed, however, more similarity to the bacterial iron-sulphur cluster containing class I protein than to the class II protein found in yeast and mammals (Flint et al., 1992, Gardner et al., 2002). In the final step of the TCA cycle, malate is converted to oxaloacetate, catalysed by malate dehydrogenase. *P. falciparum* possess a homologue of this enzyme, however, it does not appear to localise to the mitochondrion (Lang-Unnasch, 1995). Instead, a malate-quinone oxidoreductase was identified with potential mitochondrial localisation. In *Helicobacter pylori*, this enzyme replaces malate dehydrogenase in the TCA cycle, which has also been suggested for *P. falciparum* (Kather et al., 2000, Gardner et al., 2002). Malate-quinone oxidoreductase is a membrane bound flavoprotein which uses ubiquinone as electron acceptor and thus provides electrons for the electron transport chain (Uyemura et al., 2004). Although potential homologues of all TCA cycle enzymes were identified, more studies are required to investigate their precise functions and confirm their predicted subcellular localisation. At the moment it can only be speculated whether the *Plasmodium* TCA cycle in the intraerythrocytic stages provides reducing equivalents for the electron transport chain located at the inner mitochondrial membrane. Since *Plasmodium* intraerythrocytic stages seem to rely on glycolysis as their main energy source, it could be that the TCA cycle fulfills a biosyn-

thetic role by providing molecules for other biochemical pathways such as succinyl-CoA for haem biosynthesis. Other life cycle stages, however, might rely on the TCA cycle as the prime energy source.

Plasmodium parasites maintain a membrane potential across their inner mitochondrial membrane (Srivastava et al., 1997). This is achieved by electron transport across the membrane into the intermembrane space, which is the basis of oxidative phosphorylation in mammals. The electrons, which are transported in *Plasmodium*, are provided by several dehydrogenases located in the inner membrane, which use ubiquinone as the electron acceptor. These dehydrogenases include a single-subunit NADH dehydrogenase, dihydroorotate dehydrogenase, glycerol-3-phosphate dehydrogenase and malate-quinone oxidoreductase (van Dooren et al., 2006). In mammals, electrons are provided by the TCA cycle and are transferred to the electron transport chain by complex I, a multi-subunit NADH dehydrogenase. This enzyme is absent in *Plasmodium* parasites (Gardner et al., 2002) but, as already mentioned above, the parasites possess several other dehydrogenases, which can provide electrons. *P. falciparum* also has homologues of complex II, complex III and complex IV, which are responsible for the re-oxidisation of ubiquinone and generation of the membrane potential by pumping protons into the intermembrane space. Generally, ATP synthesis is driven by this membrane potential and is catalysed by ATP synthase. However, homologous for only some ATP synthase subunits were identified in the *P. falciparum* genome (Gardner et al., 2002), suggesting that *Plasmodium* mitochondria are not able to synthesise ATP via this route.

If the electron transport chain does not result in the production of ATP what other function might it have? Painter and colleagues recently suggested, that the main function of the electron transport chain is to regenerate ubiquinone, and thus to provide oxidised ubiquinone for dihydroorotate dehydrogenase (Painter et al., 2007). Dihydroorotate dehydrogenase is part of the pyrimidine biosynthesis pathway, which is essential for parasite survival. *P. falciparum* are unable to scavenge pyrimidines and therefore rely on the *de novo* synthesis. Dihydroorotate dehydrogenase is therefore a potential antimalarial drug target, and by using high-throughput screening some potential *Plasmodium* specific inhibitors have already been identified (Baldwin et al., 2005).

Parts of the folate metabolism are also present in the mitochondrion, which is very important for parasite viability, as it is a target of several antimalarial drugs. Despite the

importance of this pathway, its precise function is not very well understood (Hyde, 2005). It is thought to be the main source of one-carbon (C1) units for other metabolic pathways, including pyrimidine biosynthesis, which is required for DNA synthesis, and methionine biosynthesis.

As mentioned above, [Fe-S] cluster biosynthesis occurs in the mitochondrion as well as in the apicoplast. Mitochondrial proteins which require [Fe-S] cluster include for example members of the electron transport chain, the aconitase and potentially the fumarate hydratase. [Fe-S] cluster dependent enzymes are also found in the cytosol, and it is debated whether the [Fe-S] cluster for these enzymes are provided by the mitochondrial pathway, as it is the case in other organisms, or whether the apicoplast [Fe-S] cluster biosynthesis pathway provides [Fe-S] cluster for the cytosolic proteins (van Dooren et al., 2006).

1.6. Protein targeting

Protein targeting in *Plasmodium* parasites is a very complex process, and multiple destinations to target proteins exist. The following sections describe briefly what is known so far about protein targeting to various destinations in *Plasmodium* parasites.

1.6.1. Protein targeting to the host cell

During the intraerythrocytic development cycle, the parasite remodels the erythrocyte, a process which requires protein trafficking. It was shown that proteins targeted to the host cell contain the *Plasmodium* export element/vacuolar targeting signal (PEXEL/VTS) for translocation across the parasitophorous vacuole membrane (Hiller et al., 2004, Marti et al., 2004). However, how the proteins get across this membrane is not known. Two routes for transport to the erythrocyte membrane have been described. Proteins targeted to the host cell like KAHRP or PfEMP-3 contain a typical signal peptide at their N-terminus that allows co-translational import into the secretory pathway (Wickham et al., 2001, Lopez-Estraño et al., 2003). The proteins are transported to the parasitophorous vacuole and the PEXEL/VTS signal allows transport across the parasitophorous vacuole membrane. In the erythrocyte cytosol, the proteins interact with the Maurer's clefts, but how they are transported to the cytoplasmatic side of the erythrocyte membrane is unclear. Transport of PfEMP-1 to the erythrocyte membrane requires a different mechanism, since PfEMP-1 does not contain a classical signal peptide and thus its entry into the secretory system is not clear. Data suggest that PfEMP-1 enters the ER via its putative transmem-

brane domain and is then transported to the parasitophorous vacuole membrane (Knuepfer et al., 2005). It has been suggested that PfEMP-1 is packaged into the Maurer's clefts while they are forming by budding off the parasitophorous vacuolar membrane (Spycher et al., 2006), and recently it was shown that *P. falciparum* skeleton binding protein 1 (PfSBP-1) is involved in this process (Maier et al., 2007). It seems that PfSBP-1 is also required for PfEMP-1 trafficking to the erythrocyte surface (Maier et al., 2007). Furthermore, exported proteins were identified without an obvious PEXEL/VTS motif (Blisnick et al., 2000, Spycher et al., 2003, Spielmann et al., 2006), suggesting yet another potential trafficking route for these proteins. Potentially, these proteins are also exported while the Maurer's cleft are formed, but further analyses are required to support this hypothesis.

1.6.2. Protein targeting to the food vacuole

Host cell haemoglobin is endocytosed by the cytostome and is subsequently transported to the food vacuole. Here, haemoglobin is digested by several proteases, which are targeted to the food vacuole via the secretory system, requiring ER and Golgi transport (Tonkin et al., 2006a). However, a food vacuole targeting peptide has not yet been described, although recently it was shown that the first 120 amino acids of the cysteine protease falcipain-2 are sufficient to target GFP to the food vacuole (Dasaradhi et al., 2007). These data suggest that trafficking to the food vacuole might be mediated by a potential N-terminal targeting peptide, but further analyses are required to support this finding. After entry into the secretory system, two pathways for trafficking to the food vacuole were described. The first was observed for the aspartic protease plasmepsin II, which is involved in the first steps of haemoglobin degradation (Klemba et al., 2004a). The protein contains a transmembrane domain and is transported through the ER as a membrane protein. It is trafficked to the cytostome and from there it is delivered to the food vacuole, possibly through vesicular transport. In the food vacuole, the transmembrane domain is cleaved releasing plasmepsin II into the food vacuole (Klemba et al., 2004a). A similar trafficking mechanism was proposed for falcipain-2, which also contains a transmembrane domain (Dasaradhi et al., 2007). Interestingly, no classical signal peptide is found at the N-terminus of this protein. But as already suggested for PfEMP-1 import into the secretory system, the hydrophobic transmembrane domain might facilitate the import into the ER. Another route of trafficking was described for dipeptide aminopeptidase I, which contains no transmembrane domain (Klemba et al., 2004b). It was shown that the protease enters the endomembrane system and targets to the food vacuole via the parasitophorous vacuole, where it is taken up again during endocytosis and transported to the food vacuole.

1.6.3. Protein targeting to the apical organelles

Protein trafficking to the apical organelles is not very well understood in *P. falciparum*. It is known that targeting to the rhoptries in *P. falciparum* and *T. gondii* is via the ER and Golgi (Howard and Schmidt, 1995), thus the proteins possess a classical N-terminal signal peptide. Within the secretory system a second targeting step is required and for *T. gondii* it has been shown that this is accomplished by either a tyrosin-based motif at the C-terminus of the proteins, or by the interaction with other proteins. Indeed, targeting of membrane proteins to the micronemes also requires a tyrosin-based and acidic amino acid-based motif in *T. gondii* (Cristina et al., 2000, Hoppe et al., 2000). These features are also found in some *Plasmodium* proteins, however, for the *P. falciparum* rhoptry-associated protein 1 (RAP-1) and for the micronemal erythrocyte binding antigen 175 (EBA-175), it was shown that the C-terminal tyrosin-based motifs are not required for correct targeting to the organelles (Baldi et al., 2000, Gilberger et al., 2003). It was suggested that the proteins potentially are transported in concert with other proteins, which escort them to the correct organelle. Recently, Treeck and colleagues demonstrated that a luminal cysteine rich region at the C-terminus of EBA-175 together with correct timing of expression is crucial for micronemal targeting of this protein (Treeck et al., 2006). Although this cysteine rich region is highly conserved in the EBL-superfamily, it is not found in other micronemal proteins like apical membrane antigen 1 (AMA-1) or subtilisin like protease (SUB2), suggesting that multiple mechanisms facilitate micronemal protein targeting (Treeck et al., 2006). Not very much is known about protein targeting to the dense granules. The only requirement shown so far for correct targeting in *P. falciparum* was correct timing of expression. A GFP fusion protein of the ring infected erythrocyte antigen (RESA) was only targeted to the dense granules when under control of its endogenous promoter (Rug et al., 2004).

1.6.4. Protein targeting to the apicoplast

Since most of the proteins originally encoded by the plastid genome were transferred into the nuclear genome, a machinery to import apicoplast proteins encoded by the nucleus had to be developed. In plants, which contain a primary plastid, proteins designated for the plastid contain a N-terminal transit peptide for translocation into the plastid (Vothknecht and Soll, 2000, Jackson-Constan and Keegstra, 2001). The transit peptide is rich in basic amino acids and thus contains a positive net-charge, and additionally contains a chaperone binding site. The transit peptide interacts with protein complexes within the plastid membranes, which facilitate the post-translational protein import. These protein complexes are

known as Toc and Tic (Translocon at the outer/inner membrane of chloroplasts) (Soll and Schleiff, 2004). During protein import, the transit peptide is cleaved once it has passed the inner membrane, catalysed by a stromal processing peptidase producing the mature protein (Richter and Lamppa, 1998). The situation in apicomplexan parasites is somewhat more complicated than in plants, because the apicoplast is a secondary plastid surrounded by four membranes rather than two. Thus, proteins targeted to the apicoplast possess, in addition to the transit peptide, a signal peptide that allows import into the secretory pathway (van Dooren et al., 2001). Nuclear encoded proteins that are directed to the apicoplast possess a bipartite leader sequence that firstly imports the protein co-translationally into the secretory system and secondly directs it to the apicoplast (Waller et al., 2000). It was also suggested that apicoplast targeting through the secretory pathway is Golgi independent and diverts straight from the ER to the apicoplast (DeRocher et al., 2005, Tonkin et al., 2006b). Toc and Tic homologues were identified in the *P. falciparum* genome, and it is speculated that they span the four apicoplast membranes to promote protein import into the apicoplast (Mullin et al., 2006).
The likelihood of an apicoplast localisation of a protein can be estimated on the basis of the bipartite leader sequence using several prediction programs including SignalP and the *Plasmodium* specific PATS (prediction of apicoplast targeted sequences) (Nielsen et al., 1997, Zuegge et al., 2001).

1.6.5. Protein targeting to the mitochondrion

Most of the mitochondrial proteins are encoded in the nucleus and thus need to be imported into the mitochondrion. Mitochondrial protein import occurs post-translationally, and targeting is facilitated via different pathways. The most widespread method for mitochondrial protein import is via a N-terminal transit peptide, but internal signals and transmembrane domains are also able to facilitate mitochondrial protein import (Pfanner and Geissler, 2001). Mitochondrial protein import in *P. falciparum* has so far been shown to be accomplished by N-terminal transit peptides, which if fused to green fluorescent protein (GFP) direct GFP into the mitochondrion (Sato et al., 2003). Import of the protein across the two mitochondrial membranes is achieved by the protein complexes Tom and Tim (Translocase of the outer/inner membrane) (Pfanner and Geissler, 2001). Homologues of the Tom and Tim complexes were identified in the *P. falciparum* genome, suggesting that mitochondrial protein import in *Plasmodium* is similar to mitochondrial protein import in other organisms (van Dooren et al., 2006).
As for apicoplast proteins, the potential mitochondrial localisation can be predicted by the

nature of the transit peptide using programs like MitoProt, Predotar or the *P. falciparum* specific PlasMit (Claros and Vincens, 1996, Bender et al., 2003, Small et al., 2004).

1.6.6. Dual protein targeting

In plants it has been shown that some proteins have multiple destinations and that these proteins are dually targeted to different organelles (Silva-Filho, 2003). Different mechanisms can be involved in the regulation of this process. Alternative splicing is one possibility or the duplication of the gene with the acquisition of different 5' ends can determine the location of the protein. Alternative translation initiation or translation initiation from non-AUG start codons are other ways of regulation. Post-translational modifications as well as ambiguous targeting sequences can also play important roles in determining the final localisation of a protein (Silva-Filho, 2003).
Multiple targeting has also been observed in *P. falciparum*. The zinc metalloprotease falcilysin was shown to be targeted to the food vacuole, to the apicoplast and also likely to the mitochondrion (Ponpuak et al., 2007). In the food vacuole, falcilysin participates in the degradation of haemoglobin, whereas in the apicoplast and mitochondrion it was suggested that it may be involved in transit peptide degradation. Different mechanisms that might be involved in the multiple targeting of falcilysin were discussed by Ralph (2007) and include potential post-translational modifications, alternative splicing and/or alternative translation initiation. Recently, dual targeting was also demonstrated in *T. gondii*. Pino and colleagues showed dual targeting of proteins to the apicoplast and mitochondrion (Pino et al., 2007). The functions of the dually targeted proteins in *T. gondii* are required by both organelles and the authors suggest that the main mechanism involved is bimodal targeting. Generally, with the bimodal mechanism, dual localisation of a protein is achieved by the different "organelle import machineries" recognising different parts of the protein. In apicomplexan parasites one crucial step for dual targeting to the apicoplast and the mitochondrion is the import into the secretory pathway. Bimodal targeting suggests that the signal peptide of these dual targeted proteins is weak and is not recognised by the signal recognition particle (SRP) at all times, resulting in some proteins trafficking to the apicoplast via the secretory system and some proteins being post-translationally imported into the mitochondrion. However, Pino and colleagues have also shown that different translation initiation and differential splicing can affect the protein localisation, and are likely to play a role in dual protein targeting (Pino et al., 2007).
Dual protein targeting in *Plasmodium* and *Toxoplasma* might allow the parasites to adapt quickly to changes in their environment, but the precise mechanisms controlling dual tar-

geting remain elusive and require further analyses.

1.7. Lipoic acid

Lipoic acid (6,8-thioctic acid or 1,2-dithiolane-3-pentanoic acid) and its reduced form, dihydrolipoic acid, are naturally occurring thiol compounds, which were first isolated 1951 by Reed and colleagues (Reed et al., 1951) (Figure 1.4). Most of the lipoic acid present in the cell is found in the protein-bound form, as it is an essential cofactor of the α-keto acid dehydrogenase complexes (KADH) and the glycine cleavage system (GCV). However, apart from being a cofactor of these enzyme complexes, lipoic acid and its reduced form are potent antioxidants with a low redox potential of -0.32 V (Jocelyn, 1967).

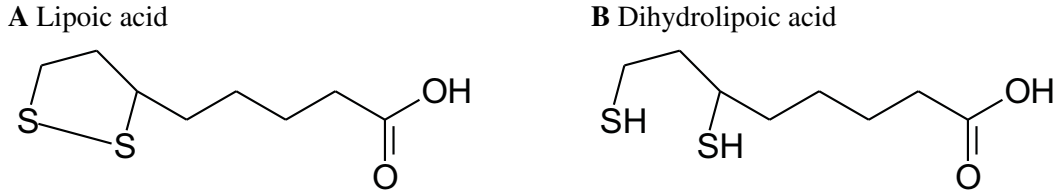

Figure 1.4.: Chemical structure of (A) lipoic acid and its reduced form (B) dihydrolipoic acid

1.7.1. Lipoic acid functions as an antioxidant

Due to the low redox potential, lipoic acid is not only able to scavenge reactive oxygen species (ROS), but also has the power to reduce other disulfides such as glutathione disulfide (GSSG) or vitamin C non enzymatically (Jones et al., 2002). In this respect, lipoic acid has been suggested as the "antioxidant of antioxidants" (Bilska and Wlodek, 2005). Lipoic acid and dihydrolipoic acid are also able to chelate redox active metal ions such as iron, thus preventing the production of highly reactive hydroxyl radicals through the Fenton reaction (Packer et al., 1995, Suh et al., 2004b). The antioxidant characteristics of lipoic acid could also play a role in *Plasmodium*, which is continuously exposed to oxidative stress produced by host immune response but also by its own metabolism, particulary during haemoglobin degradation (Müller, 2004). But not only free lipoic acid might act as an antioxidant. In *Mycobacterium tuberculosis* it has been shown that protein-bound lipoic acid reduces a thioredoxin-like protein and thus contributes to the pathogen's antioxidant defense (Bryk et al., 2002). *P. falciparum* and *T. gondii* thioredoxin can also be

reduced by free lipoic acid *in vitro*, suggesting a potential function of lipoic acid in the defense of oxidative stress in these parasites (Akerman and Müller, 2005). More research is required to elucidate the potential role of lipoic acid as an antioxidant in apicomplexan parasites.

Generally, the interest in lipoic acid has increased due to its antioxidant activities and its pharmacologic properties are extensively investigated. It was, for example, shown that lipoic acid has beneficial effects in the therapy of diabetes type 1 and type 2, which are both associated with increased oxidative stress (Packer et al., 2001). Type 1 diabetes is caused by autoimmune destruction of the insulin generating β-cells in the pancreas, whereas in type 2 diabetes insulin resistance is one of the major problems (Packer et al., 1995). The elevated glucose level in diabetes patients leads to an increase of ROS causing increased oxidative stress, which can be reduced by lipoic acid (Packer et al., 1995, 2001, Bilska and Wlodek, 2005). In type 2 diabetes, administration of lipoic acid additionally increased glucose uptake into the cells by activating the insulin signalling cascade (Packer et al., 2001, Konrad, 2005). Lipoic acid has also been shown to exhibit beneficial effects in the treatment of other diseases associated with oxidative stress, such as neurodegenerative diseases like Alzheimer's disease (Holmquist et al., 2007).

Additionally, lipoic acid can affect gene transcription regulation by influencing redox sensitive transcription factors present in the cytosol, by either promoting or inhibiting their translocation to the nucleus (Zhang and Frei, 2001, Suh et al., 2004a). One redox sensitive transcription factor is nuclear factor-κB (NF-κB), and its translocation to the nucleus is prevented by lipoic acid (Zhang and Frei, 2001, Bilska and Wlodek, 2005). This is particularly interesting in the treatment of diseases like cancer or acquired deficiency syndrome (AIDS), because active NF-κB plays an important role in the progress of these diseases (Patrick, 2000, Bilska and Wlodek, 2005). Another redox sensitive transcription factor influenced by lipoic acid is nuclear factor erythroid2-related factor 2 (Nrf2). In contrast to NF-κB, nuclear translocation of Nrf2 is increased and causes, for example, an increased production of γ-glutamylcysteine synthetase (GCS), which catalyses the first step in glutathione synthesis (Suh et al., 2004a). This suggests that lipoic acid is not only able to reduce GSSG in the cell, but also increases its production.

Due to the antioxidant properties of lipoic acid, the cosmetic industry has also shown extensive interest in lipoic acid, particularly because it was shown to reduce the signs of skin ageing (Beitner, 2003).

Lipoic acid research covers many different areas, since this compound seems to have a variety of different effects. Beside its antioxidant properties, it is an essential cofactor of several multienzyme complexes involved in energy and folate metabolism, and amino acid degradation. Its role as a cofactor is of particular interest in this thesis, and lipoic acid functions in these complexes and its production and attachment will be explained in the following sections.

1.7.2. Lipoic acid functions as a cofactor of multienzyme complexes

1.7.2.1. α-Keto acid dehydrogenase complexes

Lipoic acid is a covalently attached cofactor of KADHs and is essential for their catalytic activity. KADHs consist of multimers of three independent proteins, namely a substrate specific α-keto acid decarboxylase (E1), an acyltransferase (E2) and a dihydrolipoamide dehydrogenase (E3). These multienzyme complexes can be up to 10 MDa in size. In eukaryotes three KADHs are present, the pyruvate dehydrogenase (PDH), the branched chain α-keto acid dehydrogenase (BCDH) and the α-ketoglutarate dehydrogenase (KGDH) (Perham, 2000).

Generally, KADHs convert an α-keto acid, NAD^+ and coenzyme A (CoA) to CO_2, NADH and acyl-CoA and the reaction mechanism is shown in Figure 1.5. The substrate specific E1 subunit contains thiamine pyrophosphate (TPP) as a cofactor, and catalyses the decarboxylation of a α-keto acid, generating CO_2 and acyl-TPP bound to the protein. Subsequently, the acyl-group is transferred to the lipoamide-group of the E2 subunit, which is covalently attached to a specific lysine residue of the acyltransferase subunit. The lipoamide transfers the acyl-group from the E1 subunit to coenzyme A to form acyl-CoA. The last step in the reaction is the re-oxidation of dihydrolipoamide by the FAD containing E3 subunit producing NADH (Reed and Hackert, 1990, Perham, 2000).

The E2 subunits form homo-trimers, which assemble to either 24mers in a cubic organisation or 60mers in a pentagonal dodecahedron organisation (Reed and Hackert, 1990). This high molecular mass oligomer can be considered as the core of the multienzyme complexes, and E1 and E3 subunits bind to this core. The E2 protein consists of three distinct domains. The N-terminal part of the protein is the lipoyl-domain, which contains the signature lysine residue that is post-translationally modified by attachment of lipoic acid. This domain is followed by a subunit binding domain, which confers binding of the E1 and E3 subunits to the E2 core structure. Subsequent to this is a catalytic domain found

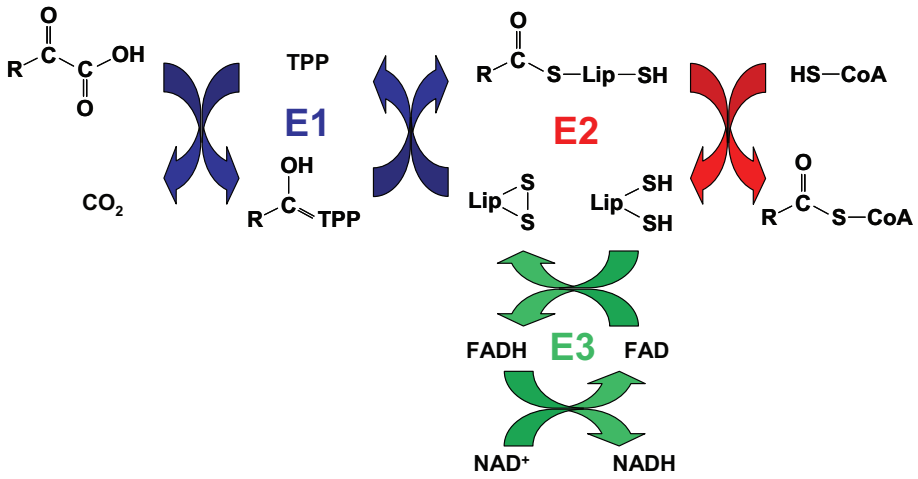

Figure 1.5.: General reaction mechanism of KADHs
The thiamine pyrophosphate dependent decarboxylase subunit (E1; blue) catalyses the decarboxylation of an α-keto acid and the subsequent reductive acylation of the lipoyl-group bound to the acyltransferase (E2; red). The E2 subunit catalyses the transfer of the acyl-group to CoA. The third subunit, the dihydrolipoamide dehydrogenase (E3; green), re-oxidises the reduced lipoyl-group of the E2-subunit with NAD^+ as the final electron acceptor.
Abbreviations: RCOCOOH, α-keto acid; TPP, thiamine pyrophosphate; RCOH-TPP, hydroxyacyl-thiamine pyrophosphate; RCO-S-LipSH, acyl-lipoamide; $LipS_2$, lipoamide; $Lip(SH)_2$, dihydrolipoamide; CoASH, Co-enzyme A; RCO-CoA, acyl-CoA

at the C-terminus, which catalyses the transfer of the acyl-rest to coenzyme A producing acyl-CoA and dihydrolipoamide. The domains are separated by flexible linker regions, which are ~20-30 amino acids long, and rich in the amino acids proline and alanine, giving them flexibility (Perham, 1991). Thus, these flexible linkers allow the lipoyl-domain to function as a "swinging-arm", transporting reaction intermediates from the E1 to the E2 and E3 subunits (Aevarsson et al., 1999, Mooney et al., 2002). E2 subunits possess one to three lipoyl-domains depending on the complex and organism they occur in. In *in vitro* assays it was shown that the lipoyl-domains alone can be expressed and are recognised by the lipoic acid attaching enzymes, and thus become post-translationally lipoylated (Ali and Guest, 1990, Dardel et al., 1990, Quinn et al., 1993). Figure 1.6 displays a schematic diagram of the *P. falciparum* KADH-E2 subunits and the H-protein, which is part of the glycine cleavage system described below.

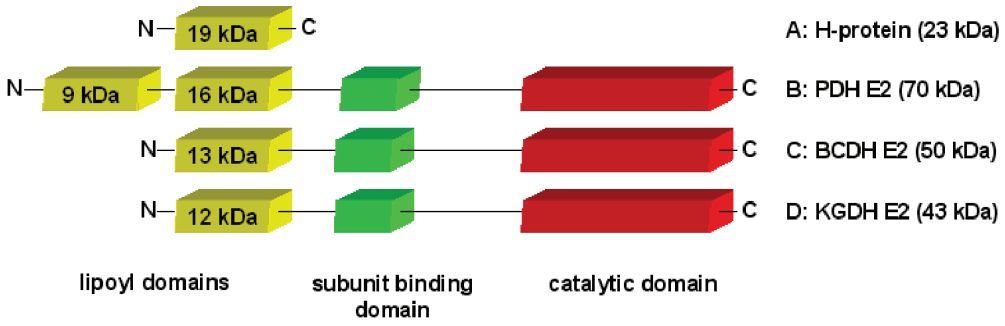

Figure 1.6.: Schematic diagram of *P. falciparum* H-protein and KADH-E2 subunits
This figure displays schematically the structure of *P. falciparum* H-protein (A), PDH-E2 (B), BCDH-E2 (C) and KGDH-E2 (D). The KADH-E2 subunits consist of three domains, the lipoyl domains at the N-terminus (yellow), a substrate binding domain (green) and the catalytic domain at the C-terminus (red). The PDH-E2 possesses two lipoyl domains (9 kDa and 16 kDa in size) whereas the BCDH-E2 and KGDH-E2 only possess one lipoyl domain each (13 kDa and 12 kDa). The H-protein only consists of lipoyl-domain.

The E1 proteins confer substrate specificity to the complexes and require TPP and Mg^{2+} as cofactors for their activity. The dihydrolipoamide dehydrogenase (E3) is a flavoprotein, which is responsible for the re-oxidation of dihydrolipoamide. In most organisms, the dihydrolipoamide dehydrogenase is shared between the different multienzyme complexes (Bourguignon et al., 1996). However, some organisms contain KADH specific E3 subunits (Lutziger and Oliver, 2000).

The PDH catalyses the oxidative decarboxylation of pyruvate to acetyl-CoA. The enzyme complex is generally found in the mitochondrion where it links glycolysis with the TCA cycle. Plants possess an additional PDH enzyme complex, which is present in the plastid, where it provides acetyl-CoA and NADH for fatty acid biosynthesis (Mooney et al., 2002). The situation in apicomplexan parasites is unique since these parasites possess only one PDH, which is present in the apicoplast (Foth et al., 2005). Accordingly, they possess two organelle specific E3 proteins (McMillan et al., 2005).

BCDH is located to the mitochondrion where it is involved in the degradation of the branched-chain amino acids valine, leucine and isoleucine. First, the branched-chain amino acid transaminase catalyses the production of the branched chain α-keto acids. Valine is converted into α-ketoisovaleric acid, leucine into α-ketoisocaproic acid and isoleucine into α-keto-β-methylvaleric acid. These α-keto acids are then oxidative decarboxylated by BCDH generating isobutyryl-CoA, isovaleryl-CoA and α-methylbutyryl-

CoA, respectively. Eventually, the acyl-CoA products can be converted to acetyl-CoA and/or succinyl-CoA for usage in the TCA cyle (Anderson et al., 1998). Homologues of BCDH-E1 and BCDH-E2 were identified in *P. falciparum*, and it has been shown that this enzyme complex is present in the mitochondrion (Günther et al., 2005, McMillan et al., 2005).

The KGDH is also found in the mitochondrion where it catalyses the oxidative decarboxylation of α-ketoglutarate to succinyl-CoA as an integral part of the TCA cycle. Succinyl-CoA is also used for the biosynthesis of haem, whereas NADH is fed into the respiratory chain via complex I (NADH dehydrogenase). *P. falciparum* also possesses a KGDH, which is located in the mitochondrion (Günther et al., 2005, McMillan et al., 2005).

1.7.2.2. Glycine cleavage system

The glycine cleavage system (GCV) represents another mitochondrial multienzyme complex, which is dependent on lipoic acid. It catalyses the oxidative decarboxylation and deamination of glycine, generating CO_2, NH_3, NADH and N^5,N^{10}-methylene tetrahydrofolate (CH_2-THF), and the reaction mechanism is shown in Figure 1.7. The GCV consists of multiple copies of four protein subunits, namely P-protein, H-protein, T-protein and L-protein. The P-protein is a pyridoxal phosphate dependent decarboxylase, which catalyses the decarboxylation of glycine and the reductive methylamination of the lipoamide, which is covalently attached to the H-protein. The T-protein requires THF for its activity, and catalyses the transfer of methylene to THF and the subsequent release of NH_3. The H-protein then reacts with the L-protein, the dihydrolipoamide dehydrogenase described above, to oxidise the dihydrolipoamide with NAD^+ as the final electron acceptor. The released CH_2-THF reacts with another glycine molecule, resulting in the formation of serine, a reaction that is catalysed by serine hydroxymethyltransferase (SHMT), which is closely associated with the GCV (Douce et al., 2001).

Overall, the reaction mechanism of the GCV is very similar to the one observed in KADHs, with lipoic acid function as a shuttle transporting reaction intermediates to the different active sites in the complex. As the lipoyl-moieties in the KADH-E2 subunits, lipoic acid is covalently attached via an amide linkage to the ε-amino group of a conserved lysine residue of the H-protein. Structurally, the H-protein is related to the lipoyl-domains of the KADH-E2 subunits and could be seen as the "lipoyl-domain" of the GCV (Figure 1.6).

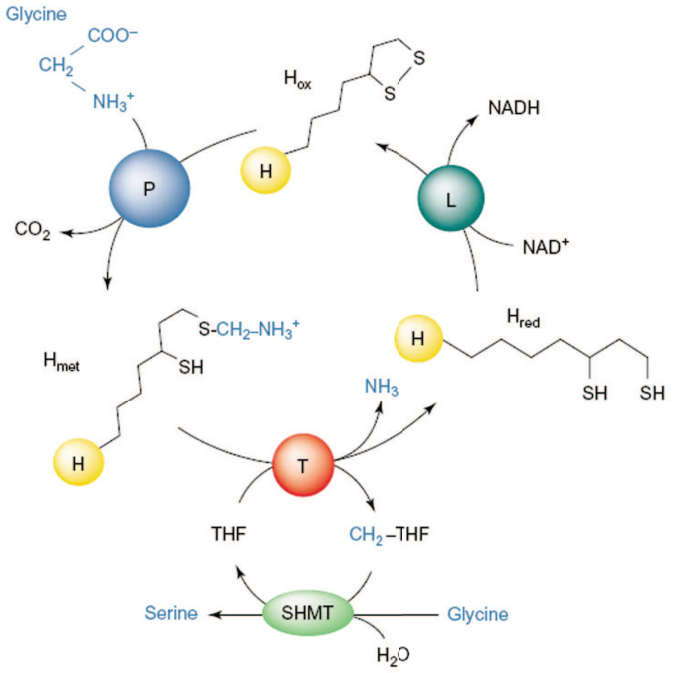

Figure 1.7.: Reaction mechanism of the glycine cleavage system
The P-protein, a pyridoxal phosphate dependent decarboxylase, catalyses the decarboxylation of glycine and the subsequent transfer of the methylamine-group to the lipoamide-group of the H-protein. The methylamine-group is passed on the T-protein, which catalyses its deamination. The L-protein is responsible for the re-oxidization of the dihydrolipoamide of the H-protein with NAD^+ as the final electron acceptor. A serine hydroxymethyltransferase associated with the glycine cleavage system catalyses the reaction of glycine with the methyl-group bound to tetrahydrofolate to form serine. The image is taken from Douce et al. (2001) with permission from Elsevier.
Abbreviations: P, P-protein; H, H-protein; T, T-protein; L, L-protein, SHMT, serine hydroxymethyltransferase; THF, tetrahydrofolate; H_{met}, methylaminated H-protein; H_{red}, reduced form of H-protein; H_{ox}, oxidized form of H-protein

A detailed structure of the GCV is not known, but the subunit stoichiometry of plant GCV was investigated and it was shown to contain four P-protein homo-dimers, 27 H-protein monomers, nine T-protein monomers and two L-protein homo-dimers, with the H-proteins forming the core of this complex (Oliver et al., 1990). Homologues of all subunits, except for the P-protein, have been identified in the *P. falciparum* genome. Further analyses suggest that the GCV is present in the mitochondrion, since all identified subunits possess potential mitochondrial transit peptides at their N-termini (Salcedo et al., 2005).

1.7.3. Lipoic acid metabolism

Lipoic acid is post-translationally attached to the KADH-E2 subunits and to the H-protein of the GCV. It is ligated to the ε-amino group of a conserved lysine residue of the KADH-E2 and the H-protein (Reche and Perham, 1999, Douce et al., 2001). This is achieved by either of the pathways displayed in Figure 1.8. Lipoic acid can be synthesised *de novo* and biosynthesis requires two enzymes. First, the octanoyl-ACP:protein N-octanoyl transferase (LipB) covalently attaches octanoyl-acyl carrier protein (ACP) to the enzyme complexes (Cronan et al., 2005, Zhao et al., 2005). The octanoyl-ACP used as a precursor for lipoic acid synthesis is provided by fatty acid biosynthesis (Gueguen et al., 2000, Miller et al., 2000). In a second step, two sulphurs are inserted into the C_8-chain of the octanoyl-moiety at positions six and eight, to form the lipoyl-arm. This reaction is catalysed by lipoic acid synthase (LipA), an S-adenosyl-methionine (AdoMet)-dependent, [Fe-S] cluster-containing enzyme, which shows a high degree of mechanistic similarity to biotin synthase (Miller et al., 2000, Zhao et al., 2003, Cicchillo et al., 2004a). Lipoic acid can also be salvaged from the environment, and scavenged lipoic acid is ligated directly to the enzyme complexes by either of the two known salvage pathways. The first involves one enzyme, a lipoic acid protein ligase A (LplA), which attaches scavenged lipoic acid in a single ATP-dependent reaction (Cronan et al., 2005). The second salvage pathway consists of two enzymes that catalyse the attachment of lipoic acid to the enzyme complexes. Lipoic acid is initially activated by the lipoate-activating enzyme using ATP or GTP, and is then ligated to the enzyme complexes by a lipoyltransferase (Fujiwara et al., 1999, 2001, 2007).

Almost all organisms are able to synthesise lipoic acid using the above described biosynthesis pathway, generally found in their mitochondrion. Plants possess two biosynthesis pathways, one being present in the mitochondrion and the other found in the plastid (Yasuno and Wada, 2002). Mammals possess the genes encoding for the proteins comprising the biosynthesis pathway, and lipoic acid synthase has been shown to be essential for embryogenic development (Yi and Maeda, 2005). However, later on, mammals seem to rely primarily on the uptake of lipoic acid through vitamin transporters (Prasad and Ganapathy, 2000). The scavenged lipoic acid is then ligated to the enzyme complexes by the salvage 2 pathway. In contrast, bacteria possess the salvage 1 pathway and scavenged lipoic acid is attached to the enzyme complexes in a single reaction catalysed by LplA (Cronan et al., 2005). Plants also possess a functional LplA-like protein, which is predicted to be mitochondrial but its importance *in vivo* has not yet been analysed (Kang

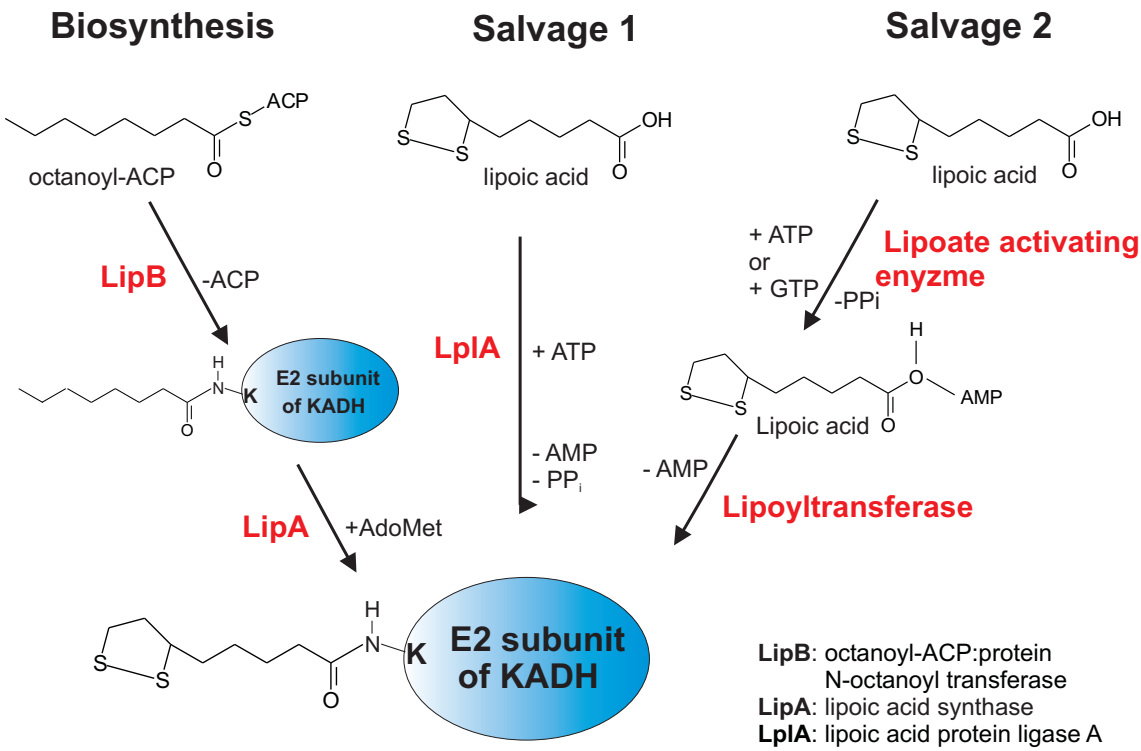

Figure 1.8.: Lipoic acid metabolism
Three lipoylation pathways are known. The biosynthesis pathway consists of octanoyl-ACP:protein N-octanoyl transferase (LipB), which attaches octanoyl-ACP to a specific lysine residue of the acyltransferase (E2) subunit of KADHs. Subsequently, lipoic acid synthase (LipA), a [Fe-S] cluster-containing, S-adenosylmethionine (AdoMet)-dependent enzyme, introduces two sulphurs into the octanoyl-moiety, resulting in protein bound lipoic acid. Salvage 1 consists of one enzyme, a lipoic acid protein ligase (LplA), which catalyses the attachment of scavenged lipoic acid to the E2 subunit in a single, ATP-dependent step. Salvage 2 consists of two enzymes that are responsible for the ligation of scavenged lipoic acid to the KADHs. First, lipoic acid activating enzyme activates lipoic acid using ATP or GTP and subsequently, activated lipoic acid is transferred to the E2 subunit by a lipoyltransferase.

et al., 2007).

1.7.3.1. Lipoic acid synthase

LipA catalyses the production of lipoic acid from octanoic acid, by inserting two sulphur atoms at position six and eight. The octanoic acid is provided by fatty acid biosynthesis in the form of octanoyl-ACP, and it was shown that LipA actually uses the protein-bound octanoyl-moiety as a substrate rather than free octanoyl-ACP (Miller et al., 2000, Zhao et al., 2003). LipA belongs to an enzyme superfamily that uses AdoMet and a specialised [4Fe-4S] cluster to cleave non-activated carbon-hydrogen (C-H) bonds (Wang and Frey,

2007). The [4Fe-4S] cluster is specialised in that three irons are ligated to conserved cysteine residues of the enzyme and one is ligated to AdoMet (Wang and Frey, 2007). The [4Fe-4S] cluster induces the reductive cleavage of the AdoMet C-S bond, generating methionine and 5'-deoxyadenosyl radical, which is required for the further reaction. It was shown that generation of one molecule of lipoic acid requires two molecules of AdoMet (Cicchillo et al., 2004a). Controversial is the source of sulfur used by LipA. The enzyme contains a second [4Fe-4S] cluster, which is distinct from the [4Fe-4S] AdoMet cluster (Cicchillo et al., 2004b). The enzyme forms a homo-dimer, and it was suggested that one of the additional [4Fe-4S] cluster supplies the two sulfur atoms, which are inserted into the C_8-chain (Cicchillo and Booker, 2005). It was hypothesised that both the C6 and C8 alkyl radicals, which are generated by removing the hydrogen atom from the respective C-H bond by the 5'-deoxyadenosyl radical, attack a sulphur atom of this [4Fe-4S] cluster with subsequent reduction of Fe^{3+} to Fe^{2+} and formation of the C-S bond (Booker et al., 2007).

LipA shares some mechanistic features with biotin synthase. Generally, lipoic acid metabolism and biotin metabolism are closely related in terms of reaction mechanisms carried out by the respective enzymes (Perham, 2000, Reche, 2000). Biotin is an essential cofactor of several enzyme complexes including acetyl-CoA carboxylase and pyruvate carboxylase (Pacheco-Alvarez et al., 2002, Nikolau et al., 2003). Bacteria, plants and some fungi are able to synthesise biotin in contrast to mammals, which rely on the uptake of this vitamin. Like LipA, biotin synthase belongs to the AdoMet radical superfamily and catalyses the generation of biotin from desthiobiotin. During this reaction, two C-H bonds are cleaved and one sulfur atom is inserted. Like LipA, biotin synthase forms a homo-dimer and requires two AdoMet molecules to form one molecule of biotin (Shaw et al., 1998). The protein also contains a second [Fe-S] cluster, which is thought to provide the inserted sulfur atom, but in contrast to LipA, this is a [2Fe-2S] cluster rather than a [4Fe-4S] cluster (Ugulava et al., 2001, Lotierzo et al., 2005, Bui et al., 2006).

1.7.3.2. Lipoic acid ligases

As LipA, which shows mechanistic similarities to biotin synthase, the ligases LplA and LipB involved in lipoic acid metabolism possess a high degree of similarity to biotin protein ligase (BPL). LplA, LipB and BPL even belong to the same protein family (Perham, 2000, Reche, 2000). Although sequence conversation between these proteins is very poor, a single lysine residue is highly conserved. It was suggested that this lysine is involved in the transfer of lipoic acid/biotin to the ε-amino group of a lysine residue in the apo-

domain of the respective enzyme complex (Reche, 2000, Bagautdinov et al., 2005, Ma et al., 2006, McManus et al., 2006).
The reaction catalysed by LipB differs in several aspects from the reactions performed by LplA and also BPL. Firstly, bacterial LipB is not able to transfer free lipoic acid to a lipoyl-domain of an enzyme complex, it requires the ACP-bound form as substrate (Jordan and Cronan, 2002). LipB is able to transfer lipoyl-ACP as well as octanoyl-ACP, but keeping in mind that the substrate of LipA is protein-bound octanoate rather than free octanoyl-ACP, it is suggestive that the physiological substrate of LipB is octanoyl-ACP. Octanoyl-ACP is a product of fatty acid biosynthesis and as already explained in Chapter 1.5.1, two distinct fatty acid biosynthesis pathways exist. Generally, type I fatty acid biosynthesis results in the generation of palmitate (C_{16}), whereas type II fatty acid biosynthesis is capable of producing a variety of fatty acids differing in length, including octanoyl-ACP (White et al., 2005). In the transfer reaction catalysed by LipB, octanoyl-ACP is covalently attached to the enzyme as an acyl-intermediate before it is transferred to the apo-lipoyl-domain (Zhao et al., 2005). It was proposed that LipB functions in a two step reaction as a cysteine/lysine dyad acyltransferase (Ma et al., 2006). In the first step, the octanoyl-moiety forms a thioester with a conserved cysteine residue, while the conserved lysine of LipB activates the ε-amino group of the target lysine in the lipoyl-domain by deprotonation. The thioester between the octanoyl-chain and LipB is then cleaved by nucleophilic attack of the activated ε-amino group of the target lysine, and the amide linkage to the lipoyl-domain lysine is formed (Ma et al., 2006).

In contrast to LipB, LplA catalyses the attachment of scavenged lipoic acid to the apo-enzyme complexes. It was shown that LplA is able to use the ACP thioester forms of octanoic acid and lipoic acid as substrates, although only poorly in comparison to lipoic acid (Jordan and Cronan, 2002). Lipoic acid is the preferred substrate of LplA (Green et al., 1995), and it is thought that the transfer of lipoic acid happens in two steps. First, lipoic acid becomes activated by ATP, forming the reaction intermediate lipoyl-AMP and releasing pyrophosphate (PPi). The activated form then is ligated to the apo-lipoyl-domain in a second step (Fujiwara et al., 2005, Kim et al., 2005, McManus et al., 2006). Thus, ligation of exogenously scavenged lipoic acid to the enzyme complexes by the salvage 1 pathway comprising LplA, occurs in the same way as it is catalysed by the salvage 2 pathway (see Figure 1.8). Here, two enzymes are required for the post-translational lipoylation, first for activation using ATP or GTP (Fujiwara et al., 2001) and second for transfer to the apo-protein (Fujiwara et al., 1997, 1999, 2007). This reaction mechanism of LplA

is also analogous to the BPL reaction mechanism in which biotin is first activated by ATP and subsequently transferred to the target lysine residue of the apo-enzyme complex (Chapman-Smith et al., 2001). Structural analyses of the *Escherichia coli* and *Thermoplasma acidophilum* LplA, and the bovine lipoyltransferase helped to better understand the reaction mechanism performed by lipoic acid ligases and also showed structural similarities to BPL (Fujiwara et al., 2005, Kim et al., 2005, McManus et al., 2006, Fujiwara et al., 2007). Moreover, similarities between the three proteins, but also differences between LplA and lipoyltransferase, and between the LplA proteins themselves were highlighted. From the structural analyses it was concluded that two different size categories of LplA exist, comprising the short forms (∼260-270 amino acids in length) and the long forms (∼330-340 amino acids in length) (Kim et al., 2005, McManus et al., 2006). The archaebacterium *T. acidophilum* was shown to possess a short form LplA whereas *E. coli* possesses a long LplA (Kim et al., 2005, McManus et al., 2006). It was further suggested that LplA enzymes contain two domains, a large N-terminal domain responsible for lipoic acid binding and activation, and a smaller C-terminal domain, whose precise function is not known (Fujiwara et al., 2005, Kim et al., 2005, McManus et al., 2006). The structurally related BPL protein contains a similar C-terminal domain, which contributes to the interaction with ATP and protein substrate (Chapman-Smith et al., 2001) and thus a similar function of the C-terminal domain in LplA enzymes was suggested (McManus et al., 2006). Interestingly, the short form *T. acidophilum* LplA does not possess the C-terminal domain and McManus et al. (2006) suggested that a second enzyme is required for the transfer of activated lipoic acid since their recombinant expressed protein showed no activity. However, Kim et al. (2005) also used *T. acidophilum* LplA in their studies but did not mention whether their protein was active or not. The N-terminal domain of both *E. coli* and *T. acidophilum* LplA was shown to possess three highly conserved sequence motifs, which contain key residues involved in the formation of the lipoyl-AMP binding pocket (Fujiwara et al., 2005, Kim et al., 2005, McManus et al., 2006). Lipoic acid is bound in a hydrophobic cavity causing a U-shape formation of the lipoyl-AMP, and it is believed that the binding and activation of lipoic acid with ATP takes place at the same site, because (1) no large conformational changes were observed after lipoic acid binding and activation and (2) ATP was found in the same position as AMP (Fujiwara et al., 2005, Kim et al., 2005). Furthermore, a conserved lysine residue was present in both LplAs, which was shown to directly interact with the carboxy-group of lipoic acid (Fujiwara et al., 2005, Kim et al., 2005, McManus et al., 2006). This lysine residue is highly conserved in all members of this protein family including LipB and BPL (Reche,

2000). It was suggested that this residue also interacts with the apo-protein substrate and promotes the nucleophilic attack of the target lysine to form the amide linkage (Ma et al., 2006). Other structural similarities were observed between LplAs and *E. coli* BPL. Superimposing the LplA structures with BPL showed that biotin and lipoic acid are bound in the same position of the respective enzyme (Fujiwara et al., 2005, McManus et al., 2006). By comparing BPL with *T. acidophilum* LplA, areas in the LplA enzyme were identified, which might be involved in conferring substrate specificity to the enzyme. It is known that BPL enzymes contain four unstructured loops, of which two are potentially participating in biotin and/or ATP binding (Streaker and Beckett, 1999). One of these loops becomes ordered upon biotin binding and interacts with biotinyl-AMP. *T. acidophilum* LplA contains a similar unstructured loop and superposition showed that this loop is in the same position as the one of BPL (McManus et al., 2006). The loop contains highly conserved amino acids and it was already proposed that this region might be important for lipoic acid binding (Reed et al., 1994, Morris et al., 1995). Thus, superimposing *T. acidophilum* LplA with *E. coli* BPL further supports this theory (McManus et al., 2006).
The bovine lipoyltransferase also consists of a large N-terminal and a short C-terminal domain, with lipoyl-AMP being bound in a U-shaped conformation in the N-terminal domain (Fujiwara et al., 2007). Comparing the structure of *E. coli* LplA with the bovine lipoyltransferase shows that the N-terminal domains superimpose very well, whereas the C-terminal domains, although similarly folded, are rotated to each other by about 180°C (Fujiwara et al., 2007). As mentioned before, it was suggested that the C-terminal domain of LplA might be involved in ATP binding, and thus the different conformation found in the lipoyltransferase might prevent ATP binding. This could possibly be the reason why mammalian lipoyltransferases are not able to activate lipoic acid (Fujiwara et al., 2007). Another difference identified between *E. coli* LplA and bovine lipoyltransferase is the "adenylate binding loop" (Fujiwara et al., 2007). In contrast to the LplA enzymes, recombinant lipoyltransferase generated in a prokaryotic expression system, was purified with endogenous lipoyl-AMP bound, suggesting a stronger interaction with the lipoyl-mononucleotide in comparison to LplA (Fujiwara et al., 2007). The "adenylate binding loop" is thought to function as a lid in the lipoyltransferase, interacting with the ribose-ring and phosphate-group of lipoyl-AMP. This loop is also present in the *E. coli* enzyme, however, it is disordered and not obviously associated with the substrate binding site (Fujiwara et al., 2007).

Post-translational modification of enzyme complexes by LplA, LipB and also BPL occurs

at a highly conserved lysine residue. The target lysine for both lipoylation and biotinylation is found in a special domain, the lipoyl- or biotinyl-domain, of the respective enzyme complex. Despite low amino acid sequence similarity between lipoyl- and biotinyl-domains, both share a common structure (Brocklehurst and Perham, 1993). Both domains consist of two anti-parallel organised four-stranded β-sheets, with the conserved lysine residue at the tip of one β-turn (Perham, 2000). The exact positioning of lysine in the domain is crucial for the apo-domain to be recognised and to become post-translationally modified (Wallis and Perham, 1994, Reche et al., 1998). However, it was shown that replacing the DKA/V motif of a lipoyl-domain with the MKM motif of a biotinyl-domain was not sufficient to cause biotinylation of the domain (Wallis and Perham, 1994). Albeit replacing the MKM motif of a biotinyl-domain with the DKA/V motif of a lipoyl-domain was enough for this domain to be recognised by LplA and to become lipoylated, but only poorly (Reche et al., 1998). These findings suggest that not only the positioning of lysine, but also of surrounding amino acids in each domain are crucial for correct post-translational modification. It appears that small structural differences between the domains are responsible for specific lipoylation or biotinylation (Reche and Perham, 1999). Recently, it was shown that removal of several amino acids in a loop adjacent to the β-turn containing the lysine in a lipoyl-domain caused major structural changes and decreased the lipoylation efficiency, highlighting the importance of the lipoyl-domain structure for complete post-translational modification (Jones and Perham, 2007). The biotinyl-domain of the *E. coli* biotin carboxy carrier protein of the acetyl-CoA carboxylase possesses an additional loop ("protruding thumb"), which is thought to prevent this domain from lipoylation *in vivo* (Reche and Perham, 1999, Kim et al., 2005). However, this effect may be limited to only some proteins because this extra loop is not present in most other biotinyl-domains (Reddy et al., 1998). The negatively charged side chain of aspartate in the DKA/V lipoylation motif may prevent recognition and binding of BPL to this domain, and thus potentially prevents unspecific biotinylation of a lipoyl-domain (Reche and Perham, 1999).

1.7.4. Lipoic acid metabolism in apicomplexan parasites

Apicomplexan parasites like *T. gondii* and *P. falciparum* possess all KADHs and the GCV that require post-translational lipoylation for their activity. The BCDH, KGDH and the GCV are found in the mitochondrion, whereas only one copy of the PDH is present, which is located in the apicoplast of these parasites (Foth et al., 2005, Günther et al., 2005, McMillan et al., 2005, Salcedo et al., 2005). The lipoylation of these com-

plexes thus requires lipoylation pathways to be present in the mitochondrion and in the apicoplast. Indeed, it was shown that apicomplexan parasites possess organelle specific lipoylation pathways. Biosynthesis of lipoic acid catalysed by LipB and LipA occurs in the apicoplast, with fatty acid biosynthesis providing the precursor octanoyl-ACP. Scavenged lipoic acid is used in the mitochondrion and is covalently attached to the enzyme complexes by the salvage 1 pathway compromising LplA (Thomsen-Zieger et al., 2003, Wrenger and Müller, 2004). It appears that the two pathways act independently from each other as salvaged lipoic acid appears to only be used by the mitochondrial pathway, whereas lipoylation in the apicoplast solely relies on *de novo* biosynthesis using octanoyl-ACP as a precursor (Crawford et al., 2006, Mazumdar et al., 2006, Allary et al., 2007). Knock-down of ACP in *T. gondii* affects parasite growth and virulence, and also suggests that the main function of type II fatty acid biosynthesis in the apicoplast is to provide octanoyl-ACP for the lipoylation of PDH (Mazumdar et al., 2006). Additionally, salvage of lipoic acid in *P. falciparum* and *T. gondii* was shown to be crucial for parasite viability (Crawford et al., 2006, Allary et al., 2007). These data suggest that both pathways act independently and that both are required for parasite survival. However, a second gene coding for a LplA-like protein (LplA2) was identified in *P. falciparum* during the course of this thesis and I could show that it localises to both the mitochondrion and apicoplast (Allary et al., 2007, Günther et al., 2007). This raises the questions whether lipoic acid metabolism in *Plasmodium* is more complicated than the two independent pathways described above. Interestingly, *Listeria monocytogenes*, a Gram-positive intracellular pathogen, is a lipoic acid auxotroph but possesses two distinct genes both encoding LplAs (Glaser et al., 2001, O'Riordan et al., 2003). It was suggested that the two LplA proteins are non-redundant during intracellular growth, because a *lplA1* knock-out strain was not able to replicate intracellularly despite the presence of *lplA2* (O'Riordan et al., 2003). Recently it was shown, that indeed *L. monocytogenes* LplA1 is required for intracellular growth since only LplA1 and not LplA2 is able to scavenge degraded host lipoyl-proteins as a source of lipoic acid (Keeney et al., 2007). This suggests, that these bacteria are highly adapted to their host-cell and that host derived lipoic acid is essential for *Listeria* virulence. The presence of two LplAs in *Plasmodium* could also be an adaptation of the parasites to the different environments they are exposed to during the course of their life cycle, and could confer, for instance, substrate specificity and/or be important in different stages of parasite development.

1.8. Aims of this study

• Validation of LplA1 and LplA2 as potential drug targets by reverse genetic approaches in *P. falciparum* and the rodent malaria parasite *P. berghei*.

• Analyses of potential redundancy between the three ligases (LipB, LplA1 and LplA2).

• Confirmation of *P. falciparum* LplA2 functionality and determination of its localisation within the parasite.

• Biochemical characterisation of *P. falciparum* LplA1 and LplA2 by developing a spectrophotometric assay system for the determination of lipoic acid protein ligase activity.

This thesis is divided into three result chapters covering LplA1 (Chapter 3), LplA2 (Chapter 4) and the biochemical characterisation of both proteins (Chapter 5). The results presented in these chapters and their implications will be discussed in Chapter 6.

2. Material and methods

2.1. Biological and chemical reagents

General chemicals were either purchased from BDH, Fisher Scientific or VWR.

Abcam	anti-rat IgG (HRP conjugated)
Amaxa	Human T cell Nucleofector kit
BD Biosciences	anti-His-tag antibody
BDH	Giemsa stain, saponin
Bio-Rad	Precision plus all blue protein standards, Bradford protein assay reagent
Blood transfusion service	Human full blood
BOC	Malaria culture gas (5% CO_2, 1% O_2 and 94% N_2)
Braun	Heparin
Calbiochem	anti-Lipoic acid antibody
Eurogentec	Custom antibody production, oligonucleotides
Fermentas	GeneRuler 1 kb DNA ladder
Fisher Scientific	10x phosphate buffered saline (PBS)
GE Healthcare	Rainbow protein marker, Gene Images CDP-Star detection module, Gene Images Random Prime Labelling Module
IBA	anti-Strep-tag antibody, Strep-Tactin Sepharose, D-Desthiobiotin, Strep-tag regeneration buffer with 2-[4'-hydroxy-benzeneazo]benzoic acid (HABA)
ICN Biomedicals Inc.	Lipoic acid
Invitrogen	Accuprime *Pfx* SuperMix, PCR SuperMix, TOPO TA cloning kit, ZERO BLUNT PCR cloning kit, chemically competent *E. coli* TOP10 and DB3.1, RPMI 1640 (with 25 mM HEPES, L-glutamine, without $NaHCO_3$), Albumax II, gentamycin, dNTP mix, 20x MOPS buffer, Hanks'balanced salt solution (HBSS), SYBR safe (10000x stock), agarose, low melting point agarose, gentamycin

Jacobus pharmaceuticals	WR99210
Melford	Ampicillin, carbenicillin, isopropyl-β-D-thiogalactopyranoside (IPTG), adenosine triphosphate (ATP), dithiothreitol (DTT), proteinase K
Millipore	Immobilon Western blot detection kit
Molecular Probes	Mitotracker CMXRos, anti-rat IgG (Alexa fluor 488 conjugated), anti-rabbit IgG (Alexa fluor 594 conjugated)
New England Biolabs	All restriction endonucleases
Novagen	BugBuster protein extraction solution, benzonase, chemically competent *E. coli* BLR(DE3)
Pierce	Restore Western blot stripping buffer
Promega	1 kb DNA ladder, anti-mouse IgG (HRP conjugated), anti-rabbit IgG (HRP conjugated)
Qiagen	Qiaprep spin DNA miniprep kit, Hi-speed plasmid maxi kit, Qiaquick gel extraction kit, QIAamp DNA mini kit, QIAamp DNA blood mini kit, RNeasy mini kit, nickel-nitrilotriacetic acid (Ni-NTA) agarose, RNaseA
Roche	Rapid DNA ligation kit, Expand High Fidelity PCR system
Thermo electron	Oligonucleotides
Schleicher Schuell	Protran nitrocellulose, fibrous cellulose powder CF11
Sigma	Hypoxanthine, *E. coli* inorganic pyrophosphatase, ammonium molybdate, trizol, Ponceau S Solution, 4-aminobenzoic acid, Alsever's solution, glass beads, L-polylysine, sarkosyl, bovine serum albumin (BSA), lysozyme, phenylmethylsulfonylfluoride (PMSF), leupeptin, pepstatin-A, E-64, 1,10-phenantholine, xanthurenic acid, penicillin/streptomycin, 4',6-Diamidino-2-phenylindole dihydrochloride (DAPI), 1,4-Diazabicyclo[2.2.2]octane (DABCO^{TM})
Stratagene	Chemically competent *E. coli* XL10-Gold

2.1.1. Buffers, solutions and media

General buffers

1x PBS	140 mM NaCl, 3 mM KCl, 10 mM Na_2HPO_4, 1.8 mM KH_2PO_4, pH 7.4
1x TAE	40 mM Tris-Acetate, 1 mM EDTA pH 8.0
0.5x TBE	45 mM Tris-Borate, 1 mM EDTA pH 8.0
TE	10 mM Tris/HCl pH 8.0, 1 mM EDTA pH 8.0

DNA analyses

DNA loading dye	0.25% (w/v) bromophenol blue, 0.25% (w/v) orange-G, 40% (w/v) sucrose
Buffer A	100 mM Tris/HCL, 300 mM NaCl, pH 9.5
1x SSC	15 mM Tri-sodium citrate, 150 mM NaCl, pH 7-8
PFGE-lysis buffer	0.5 M EDTA, 10 mM Tris pH 8.0, 1% (v/v) sarkosyl, 2 mg/ml proteinase K (added fresh prior use)
PFGE-storage buffer	50 mM EDTA, 10 mM Tris pH 8.0

Protein analyses

6x loading buffer	62.5 mM Tris/HCl pH 6.8, 2% (w/v) SDS, 10% (v/v) glycerol, 0.001% (w/v) bromophenol blue, 5% (v/v) 2-mercaptoethanol
2x native loading buffer	62.5 mM Tris/HCl pH 6.8, 10% (v/v) glycerol, 0.001% (w/v) bromophenol blue
1x running buffer	25 mM Tris, 192 mM glycine, 0.1% (w/v) SDS
1x MOPS buffer	50 mM 3-[N-morpholino]propane sulphonic acid, 50 mM Tris, 3.5 mM SDS, 1 mM EDTA
1x native running buffer	25 mM Tris, 192 mM glycine
Coomassie stain	40% (v/v) methanol, 10% (v/v) acetic acid, 0.1% (w/v) Coomassie brilliant blue R-250
Destain	20% (v/v) methanol, 10% (v/v) acetic acid
Towbin buffer	25 mM Tris, 192 mM glycine, 20% (v/v) methanol

2D-lysis buffer	100 mM HEPES pH 7.4, 5 mM $MgCl_2$, 10 mM EDTA, 0.5% (v/v) Triton X-100, 5 μg/ml RNAse A, 1 mM PMSF, 1 mM benzamidine, 2 μg/ml leupeptin, 10 μM E-64, 2 mM 1,10-phenanthroline, 4 μM pepstatin A (protease inhibitors were added prior to use)

Bacteria culture

Luria-Bertani (LB) medium	10 g/L tryptone, 5 g/L yeast extract, 5 g/L NaCl (add 15 g/L agar for LB plates)
M9 minimal medium	10x M9 salt stock: 58 g/L Na_2HPO_4, 30 g/L KH_2PO_4, 5 g/L NaCl, 10 g/L NH_4Cl Working solution: 1x M9 salts, 0.2% (w/v) glucose, 1 mM $MgSO_4$, 0.001% (w/v) thiamine (add 15 g/L agar for M9 plates)
Ampicillin	100 mg/ml in ddH_2O; stored at -20°C
Carbenicillin	100 mg/ml in ddH_2O; stored at -20°C
Kanamycin	50 mg/ml in ddH_2O; stored at -20°C
Tetracycline	5 mg/ml in ethanol; stored at -20°C
Chloramphenicol	34 mg/ml in ethanol; stored at -20°C

***P. falciparum* culture**

Complete RPMI medium	15.9 g/L RPMI 1640 (containing 25 mM HEPES and L-glutamine), 0.1% (w/v) sodium bicarbonate, 10 mM glucose, 200 μM hypoxanthine, 20 μg/ml gentamycin, 0.5% (w/v) Albumax II, pH 7.4
Blood-wash medium	15.9 g/L RPMI 1640 (containing 25 mM HEPES and L-glutamine), 0.1% (w/v) sodium bicarbonate, 10 mM glucose, 200 μM hypoxanthine, 20 μg/ml gentamycin, pH 7.4
Cytomix	120 mM KCl, 0.15 mM $CaCl_2$, 2 mM EGTA, 5 mM $MgCl_2$, 10 mM K_2HPO_4/KH_2PO_4 pH 7.6, 25 mM Hepes pH 7.6
WR99210	Stock: 20 mM in dimethylsulphoxide (DMSO) stored at -80°C Working solution: 20 μM diluted in blood-wash medium
Blasticidin	10 mg/ml in blood-wash medium

Freezing solution	30% (v/v) glycerol in PBS
MACS buffer	0.5% (w/v) BSA, 2 mM EDTA pH 8.0 in PBS

***P. berghei* culture**

Transfection medium	20% (v/v) foetal calf serum (heat inactivated for 30 min at 56°C), 14 μg/ml gentamycin in RPMI 1640 (containing 25 mM HEPES and L-glutamine)
Freezing solution	10% (v/v) glycerol in Alsever's solution (Sigma)
Dissection medium	3% (w/v) BSA in RPMI 1640 (containing 25 mM HEPES and L-glutamine)
Nycodenz	Stock: 5 μM Tris pH 7.5, 3 mM KCl, 0.3 mM EDTA, 276 mg/ml Nycodenz Working solution: 55% (v/v) Nycodenz stock in PBS
Pyrimethamine	Stock: 7 mg/ml in DMSO stored at 4°C Working solution: 10 ml/L pyrimethamine stock in tap water, pH 3.5-5.5
Ookinete culture medium	25% (v/v) foetal calf serum (heat inactivated for 30 min at 56°C), 50 μM xanthurenic acid, 1% (v/v) penicillin/streptomycin in RPMI 1640 (containing 25 mM HEPES and L-glutamine)

Mosquito breeding

Breeding water	0.1% (w/v) sea salt in dH_2O
Sucrose solution	10% (w/v) sucrose, 0.2 μg/ml 4-aminobenzoic acid in dH_2O

2.1.2. Bacteria strains

XL10-Gold (Stratagene)
Tet^r △*(mcrA)183* △*(marc-hsdSMR-mrr)173 endA1 supE44 thi-1 recA1 gyrA96 relA1 lac* Hte [F' *proAB lacI^{q}Z*△*M15 Tn10* (Tet^r) Amy Cam^r]^a

TOP10 (Invitrogen)
F$^-$ *mcrA* △(*mrr-hsd*RMS-*mcr*BC) ϕ80*lac*Z△M15 △*lac*X74 *rec*A1 *arc*D139 △(*arc-leu*)7697 *gal*U *gal*K *rps*L (Str^R) *end*A1 *nub*G

DB3.1 (Invitrogen)
F$^-$ *gyr*A462 *end*A1 △(sr1-*rec*A) *mcr*B *mrr* *hsd*S20(r$_B$-, m$_B$-) *sup*E44 *ara*-14 *gal*K2 *lac*Y1 *pro*A2 *rps*L20(Sm^R) *xyl*-5 λ-*leu mtl*1

BLR(DE3) (Novagen)
F$^-$ *ompT hsdS$_B$*(r$_B$- m$_B$-) *gal dcm* (DE3) △(srl-recA)306::Tn*10* (Tet^R)

Ker184 (*lipB*$^-$) (Reed and Cronan, 1993)
rpsL lipB182::Tn*1000*dKn

Tm134 (*lplA*$^-$) (Morris et al., 1994)
rpsL lplA148::Tn*10*dTc

Tm136 (*lipB*$^-$/*lplA*$^-$) (Morris et al., 1995)
rpsL lipB182::Tn*1000*dKn *lplA48*::Tn*10*dTc

2.1.3. *Plasmodium falciparum* strains

3D7	The Netherlands
D10	Papua New Guinea

2.1.4. *Plasmodium berghei* strains

NK65	NYU, New York

2.1.5. Mice and rat strains

NMRI	Naval Medical Research Institute, outbred mice, Charles River Laboratory, Sulzfeld, Germany
C57BL/6	Inbred mice, Charles River Laboratory, Sulzfeld, Germany
SD	Sprague-Dawley, outbred rats, Charles River Laboratory, Sulzfeld, Germany

The animals were kept in Makrolon cages. Usually five mice or two rats were kept per cage. The cages were stored in the animal facility at constant temperature (22°C) and humidity of 50% to 60%. The light-dark cycle was constant with 12h.
Animals were fed with standard diet pellets (SSNIFF).

2.1.6. Mosquito strains

Anopheles stephensi	Nijmegen, The Netherlands
	EMBL, Heidelberg, Germany

2.1.7. Oligonucleotide primers

Oligonucleotide primers were designed to amplify genes for recombinant protein expression, knock-out studies and localisation studies. To allow sub-cloning of the PCR fragments into the relevant destination plasmids, oligonucleotide primers had a 5' extension including the appropriate restriction sites. The oligonucleotide primers used in this study are listed below.

Recombinant protein expression

H-protein-S	5-GCGC**CATATG** GAA TAT ATA AAA ATT GAG GAT GG-3 (NdeI)
H-protein-AS	5-GCGC**GGATCC** TTA TTT CCC CCC TTG CCC TTT ATT TTC-3 (BamHI)
pdhE2-lipoyl1-S	5-GCGC**CATATG** AGA AAA AAT GTT GTT TTT TCA AAA ATA G-3 (NdeI)
pdhE2-lipoyl1c-AS	5-GCGC**GGATCC** TTA GAC ATC TCC AAC ATT TGC TTC ACA TCC-3 (BamHI)
pdhE2-lipoyl2-S	5-GCGC**CATATG** AAG AAG CAT ATA AAT GAT GAT G-3 (NdeI)
pdhE2-lipoyl2-AS	5-GCGC**GGATCC** TTA CCT TAA ATT TTT TAA AAA CTT TCT TCC C-3 (BamHI)
PM 26	5- GCGC**CATATG** GAG GGA AAA TCA TTT AAA GGG-3 (NdeI)
bcdhE2-lipoyl-AS	5-GCGC**GGATCC** TTA CTC CTT TTC TAC TTC TTC TTC ATC TC-3 (BamHI)
kgdhE2-lipoyl-S	5-GCGC**CATATG** ATT AAA GTA CCT AGA CTT GG-3 (NdeI)
kgdhE2-lipoyl-AS	5-GCGC**GGATCC** TTA ATG TGC TTC ATC TTT AAT ATC TC-3 (BamHI)
PfLplA-NdeI-S	5-GCGC**CATATG** GAA AAA AGG ACA AAT GGA CCT TTG-3 (NdeI)

PfLplA-BamHI-AS	5-GCGC**GGATCC** CTA AAG TTC TTG TAA TAT CCA TGA ACG-3 (BamHI)
PfLplA2-FL-NdeI-S	5-GCGC**CATATG** AGA ATT ATA AAG TGC CTG GAT CAA ATA TTC AGG CC-3 (NdeI)
PfLplA2-S1-NdeI-S	5-GCGC**CATATG** AAA AAA ATA AAC ATT CTT TAT TTT ATT GAT GTC AGC-3 (NdeI)
PfLplA2-S2-NdeI-S	5-GCGC**CATATG** AAT GAG TCC AAA GGA AAC GAA TGC-3 (NdeI)
PfLplA2-BamHI-AS	5-GCGC**GGATCC** TTA TAG AAA ATA TGT TGG TAT ATC GTA ATA CC-3 (BamHI)
PfLplA2-IBA3-1-fwd	5-GCGCGC**GGTCTCGA** ATG AGA ATT ATA AAG TGC CTG GAT C-3 (BsaI)
PfLplA2-IBA3-2-fwd	5-GCGCGC**GGTCTCGA** ATG AAA AAA ATA AAC ATT CTT TAT TTT ATT GAT GTC AGC-3 (BsaI)
PfLplA2-IBA3-3-fwd	5-GCGCGC**GGTCTCGA** ATG AAT GAG TCC AAA GGA AAC GAA TGC-3 (BsaI)
PfLplA2-IBA3-rev	5-GCGCGC**GGTCTCAGC** GCT TAG AAA ATA TGT TGG TAT ATC GTA ATA CC-3 (BsaI)

KO studies in *P. falciparum* - cloning and analyses

Pf-LplA2-KO-pHH1-fwd	5-GCGC**AGATCT** GTC ATT GTA AAT AAT ACA TGT GAA GAA ATG-3 (BglII)
Pf-LplA2-KO-pHH1-rev	5-GCGC**CTCGAG** TTA GTG TTC CGA ATT TCT TAA TAT ATG ATC-3 (XhoI)
LplA-pHH1-rescue-fwd	5-GCGC**AGATCT** GGA GAA ATA ACC GAT CTA TAA TTA TAG G-3 (BglII)
LplA-KOkon-rev	5-GCGC**CTCGAG** CTA AAG TTC TTG TAA TAT CCA TGA ACG-3 (XhoI)
Pb-LplA-BglII-S	5-GCGC**AGATCT** ATG CCA GGT ATA TCC TGT TTT GTA AAA CGA TGT TAT GG-3 (BglII)
Pb-LplA-NotI-AS	5-GCGC**GCGGCCGC** TTA GAG TTC TTC TAA TAT CCA TGA AGT TAT TTC TTC TAA GG-3 (NotI)
LplA2-fwd	5-cacc ATG AGA ATT ATA AAG TGC CTG G-3
LplA2-rev	5-TAG AAA ATA TGT TGG TAT ATC GTA ATA CC-3
CAM5'-check-F	5-GCGC CCA ATA GAT AAA ATT TGT AGA G-3

PbDT3'-check-R	5-GCGC CGA ACA TTA AGC TGC CAT ATC C-3

KO studies in *P. berghei* - cloning and analyses

Pf-LplA-ORF-fwd	5-GCGC**CTCGAG** ATG AAA CGA ATA TTC AGG TTG GTA AG-3 (XhoI)
Pf-LplA-ORF-rev	5-GCGC**CTGCAG** CTA AAG TTC TTG TAA TAT CCA TGA ACG-3 (PstI)
Pf-LplA2-ORF-fwd	5-GCGC**CTCGAG** ATG AGA ATT ATA AAG TGC CTG GAT C-3 (XhoI)
Pf-LplA2-ORF-rev	5-GCGC**CTGCAG** TTA TAG AAA ATA TGT TGG TAT ATC G-3 (PstI)
Pb-LplA-5'-fwd	5-GCGC**GGTACC** TAC TAT ATA TTT AAT ATA TAA CAG GG-3 (KpnI)
Pb-LplA-5'-rev	5-GCGC**AAGCTT** CCA ACG ATA AAT TAA AGT AAA TAT TTT G-3 (HindIII)
Pb-LplA-3'-fwd	5-GCGC**GCGGCCGC** CCA ATA CTT TAA AAC ATT TAA CAA TC-3 (NotI)
Pb-LplA-3'-rev	5-GCGC**CCGCGG** GGA CAA GCA TAG CTT ATG CCC GAT C-3 (SacII)
Pb-LplA-int-fwd	5-GCGC**GGATCC** CAA AAT ATT TAC TTT AAT TTA TCG TTG G-3 (BamHI)
Pb-LplA-int1-rev	5-GCGC**CCGCGG** TTA GTC TAA TGC ATC TGA AAA AAC ATT TCC-3 (SacII)
Pb-LplA2-5'-fwd	5-GCGC**GGTACC** GAG CAT TGT ATT ATT AAT GAG CTC C-3 (KpnI)
Pb-LplA2-5'-rev	5-GCGC**AAGCTT** GTA TGT ATC ATT ATA AGT TTT AAA TGG-3 (HindIII)
Pb-LplA2-3'-fwd	5-GCGC**GCGGCCGC** GCA TGC ATT TAT TAG GTA CTT TTC CC-3 (NotI)
Pb-LplA2-3'-rev	5-GCGC**CCGCGG** CGA TGT GGT GGG CAG GGA AGG AAT TGG-3 (SacII)
Pb-LplA2-int-fwd	5-GCGC**GGATCC** CAT ATT TAT GAA CAA TTA TTA ATC G-3 (BamHI)
Pb-LplA2-int1-rev	5-GCGC**CCGCGG** TTA GTG ATC AAA TAT ATC ACA TGT ACT AAA TGG-3 (SacII)

Pb-LplA2-NdeI-fwd	5-**CATATG** GAT TTT GAA AAA GAA ACT AGA CTT TAT CC-3 (NdeI)
Pb-LplA2-NdeI-rev	5-**TCTAGA CATATG** GTT TGG AAG AAT AAA CGA AGT TAA TAT AC-3 (XbaI, NdeI)
PfCAM5'-F2	5-GCGC **GGTACC GGATCC** GCG AAT TAG CTA AGC ATG CAA GC-3 (KpnI, BamHI)
PfCAM5'-R1	5-GCGC**CTCGAG** CCT GAT ATA TTT CTA TTA GGT ATT TAT TAT TAT AAA ATA TAA ATC-3 (XhoI)
PfHRPII3'-F1	5-GCGC**CTGCAG** CCC GCC ATT AAA TTT ATT TAA TAA TAG-3 (PstI)
PfHRPII3'-R1	5-GCGC**GCGGCCGC** GTA CCT CTA GAT TTC TCT GCG G-3 (NotI)
Tg-for	5-CCC GCA CGG ACG AAT CCA GAT GG-3
b3D-rev	5-GCGC CGA CGT TGT AAA ACG ACG GCC-3
Tg-rev	5-CGC ATT ATA TGA GTT CAT TTT ACA CAA TCC-3
PbLplA1-test-fwd	5-GGA TAA TGT AAT AAA ATC TAG CCA TTT AAC TC-3
PbLplA1-test-rev	5-GTG TTG GTG TGT ATA TGA GAA ATT CC-3
Pb-LplA1-REP-rev	5-GCGC GTG TTG GTG TGT ATA TGA GAA ATT CC-3
LplA2-test-for	5-CTT AAT TTA TGC TTT TTT AAA GGC CCC G-3
LplA2-test-rev	5-GCA TTT GTT TTT CCA CAT GAT AGG GGC-3
Pb-LplA2-REP-rev	5-GCGC CGA AAT AAG CAA AGA CAT GCA TGG ATG-3

Localisation studies

LplA2-fwd	5-cacc ATG AGA ATT ATA AAG TGC CTG G-3 (for directional TOPO cloning)
LplA2-rev	5-TAG AAA ATA TGT TGG TAT ATC GTA ATA CC-3
H-protein-fwd	5-cacc ATG ATA AAT ATA AGA AAA GTG CTT C-3 (for directional TOPO cloning)
H-protein-rev	5-TTT CCC CCC TTG CCC TTT ATT TTC-3

2.1.8. Antibodies

Table 2.1.: Primary antibodies and their dilutions

	Western blot	IFA	Source
anti-His-tag (mouse)	1:10000		BD Biosciences
anti-Strep-tag (rabbit)	1:2000		IBA
anti-Lipoic acid (rabbit)	1:500 (parasite extract) 1:2000 (recombinant protein)		Calbiochem
anti-LplA1 (rabbit)	1:1000		Eurogentec
anti-LplA2 (rat)	1:500	1:500	Eurogentec
anti-BCDH E2 (rabbit)	1:5000		Eurogentec
anti-KGDH E2 (rat)	1:100		Eurogentec
anti-H-protein (rabbit)	1:2000		Eurogentec
anti-aE3 (rabbit)		1:200	Eurogentec
anti-TrxPx1[a] (rabbit)	1:5000		Eurogentec

[a] Akerman and Müller (2003)

Table 2.2.: Secondary antibodies and their dilutions

	Western blot	IFA	Source
anti-mouse IgG (H+L), HRP (goat)	1:5000		Promega
anti-rabbit IgG (H+L), HRP (goat)	1:10000		Promega
anti-rat IgG (H+L), HRP (goat)	1:5000		Abcam
anti-rat IgG (H+L), Alexa fluor 488 (chicken)		1:500	Molecular Probes
anti-rabbit IgG (H+L), Alexa fluor 594 (goat)		1:500	Molecular Probes

2.2. *P. falciparum* cell culture

2.2.1. Culturing of *P. falciparum* erythrocytic stages

Parasites were cultured in complete RPMI 1640 medium with 5% (v/v) human erythrocytes (Trager and Jensen, 1976). The cultures were maintained at 37°C under an atmosphere of reduced oxygen (5% CO_2, 1% O_2 and 94% N_2). The medium was changed daily, and the parasitemia was kept between 1-5%. If a higher parasitemia was required the medium was changed twice a day. Parasitemia was determined by counting the infected erythrocytes in Giemsa stained blood smears. Smears were fixed in methanol followed by staining in Giemsa diluted 1:10 in H_2O for 10-20 min. The stained blood smears were analysed by light microscopy with an objective magnification of 100 fold.

2.2.2. Synchronisation of parasite culture

Parasites were synchronised using sorbitol according to Lambros and Vanderberg (1979). Cultures with mainly parasites in the ring stage were used for synchronisation. The culture was centrifuged at 1500 rpm (Jouan CR3i centrifuge with T4 rotor), 25°C for 5 min and the supernatant was discarded. The pellet was resuspended in 5 pellet volumes of 5% (w/v) sorbitol (in 10 mM potassium phosphate pH 7.2), incubated at 37°C for 10 min and then centrifuged as above. The supernatant was discarded, and the pellet was resuspended in RPMI 1640 complete medium and cultured as described above (see 2.2.1).

2.2.3. Preparation of *P. falciparum* stabilates

Stabilates were generated of cultures containing approximately 3-5% ring stage parasites. The infected erythrocytes were pelleted by centrifugation at 1500 rpm (Jouan CR3i centrifuge with T4 rotor), 4°C for 5 min. The supernatant was aspirated and the pellet was resuspended in one pellet volume of complete RPMI 1640 medium, and two pellet volumes of freezing solution (30% (v/v) glycerol in PBS). 600 μl aliquots were transferred to 1 ml cryotubes (Nalgene), incubated on ice for 10 min and subsequently transferred to liquid nitrogen.

2.2.4. Thawing of *P. falciparum* stabilates

Stabilates were thawed by constant shaking in a 37°C waterbath. Once thawed, the stabilates were transferred to a 15 ml tube and placed on ice. Two volumes of cold 27% (w/v)

sorbitol (in 10 mM potassium phosphate buffer pH 7.2) were added drop-wise with constant shaking and incubation on ice. After 13 min, two volumes of cold 5% (w/v) sorbitol (in 10 mM potassium phosphate buffer pH 7.2) were added as before and incubated on ice for 10 min. The solution was centrifuged at 1500 rpm (Jouan CR3i centrifuge with T4 rotor), 4°C for 5 min and the supernatant was discarded. The pellet was carefully resuspended in 5 ml cold 5% (w/v) sorbitol (in 10 mM potassium phosphate buffer pH 7.2) and incubated for a further 8 min on ice. The resuspended cells were centrifuged as above and the supernatant was discarded. The pellet was washed twice with cold complete RPMI 1640 medium before it was resuspended in warm complete RPMI 1640 medium and taken into culture with an initial haematocrit of 2.5%. Once the culture had a parasitemia of 4%, the haematocrit was increased to 5% and the appropriate drug selection was applied when transfected parasite lines were thawed.

2.2.5. Parasite extraction from infected erythrocytes

Parasites were extracted from erythrocytes using saponin as described by Umlas and Fallon (1971). The infected erythrocytes were lysed by addition of 1/10 of the culture volume of saponin (2% (w/v) in PBS). The culture-saponin mixture was incubated on ice for 10 min and was then centrifuged for 10 min at 3500 rpm (Jouan CR3i centrifuge with T4 rotor) and 4°C. The supernatant was discarded and the parasite pellet was washed in cold PBS. After the wash step, the isolated parasites were centrifuged as above and the resulting pellet was resuspended in the appropriate buffer. To prepare DNA from the parasite pellet it was resuspended in 200 μl PBS, for RNA it was resuspended in 1 ml Trizol and for protein preparation the parasite pellet was resuspended in one pellet volume 2D-lysis buffer.

2.2.6. Genomic DNA (gDNA) preparation of parasites

After saponin lysis (see 2.2.5) of a 50 ml culture, the parasite pellet was resuspended in 200 μl PBS. The following gDNA preparation was carried out using the QIAamp DNA mini kit (Qiagen) according to manufacturer's instructions.

2.2.7. Protein preparation of parasites

A 50 ml parasite culture was saponin-lysed (see 2.2.5) and the pellet was resuspended in one pellet volume of 2D-lysis buffer. The resuspended parasite pellet was stored at -80°C. To prepare the protein extract, the resuspended parasite pellet was thawed at room tem-

perature and frozen again using dry ice. This was repeated three times. Afterwards, the resuspended pellet was sonicated in a sonicating waterbath for 5 min followed by centrifugation at 13000 rpm (Fisher Scientific accuSpin MicroR with 24-place rotor), at 4°C for 5 min. The supernatant was transferred into a fresh tube and its protein concentration was determined using Bradford reagent and a standard curve of known BSA concentrations (see 2.6.6).

2.2.8. Preparation of chromosome blocks

To resolve chromosomal DNA of *P. falciparum* by pulse field gel electrophoresis (PFGE, see 2.5.12), chromosomal DNA was embedded into agarose plugs. A 10 ml parasite culture containing 5-7% trophozoites was saponin-lysed (see 2.2.5) and the parasites were pelleted by centrifugation. To prepare the blocks, the parasite pellet was resuspended in three times the pellet volume of warm (50°C) PBS. The same volume of warm (50°C) 2% (w/v) low melting point agarose in PBS was added and the mixture was transferred into the plug molds (Bio-Rad) and allowed to set on ice. Once set, the blocks were transferred into PFGE-lysis buffer and incubated at 37°C for 48 hours. Chromosome blocks were stored in PFGE-storage buffer at 4°C for at least 7 months.

2.2.9. Gene knock-out in *P. falciparum*

For knock-out studies in *P. falciparum* the plasmid pHH1 was used (Reed et al., 2000) (Figure 2.1). The knock-out fragments were cloned into the plasmid using the restriction sites BglII and XhoI. The knock-out fragment was truncated at the N-terminus thus missing the ATG-start codon. The fragment was also truncated at the C-terminus and contained an artificial stop codon to ensure the disruption of the gene. Disruption of the gene was achieved by single cross-over recombination of the knock-out plasmid with the gene locus, which should result in the formation of two truncated, non-functional copies of the gene. The plasmid contains the human dihydrofolate reductase (hDHFR) gene which allowed for the selection of transfected parasites with WR99210 (Waterkeyn et al., 1999). To select this plasmid in bacteria it also contained the ampicillin resistance gene.

2.2.10. Transfection of *P. falciparum*

Two methods were used to transfect *P. falciparum*. The first method, according to Deitsch et al. (2001), included the transfection of uninfected erythrocytes and the spontaneous uptake of DNA by the parasites. 100 μg plasmid DNA were resuspended in 50 μl TE buffer

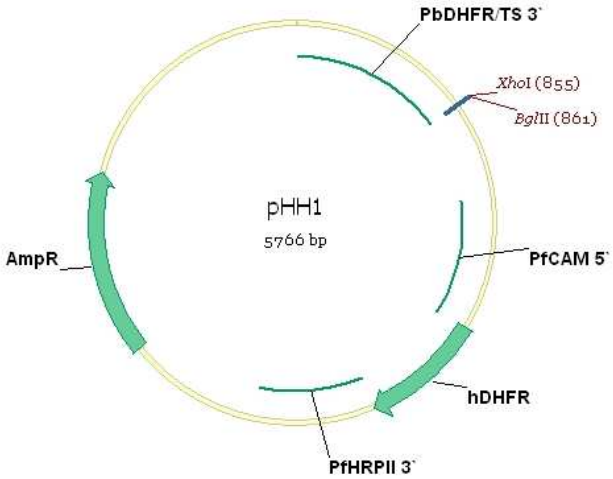

Figure 2.1.: Vector map of pHH1
This figure displays the important features of the pHH1 plasmid, which was used for knock-out studies in *P. falciparum*. The plasmid contains the ampicillin resistance cassette (AmpR; 861 bp) for selection in *E. coli* and the human dihydrofolate reductase gene (hDHFR; 569 bp) for selection in *P. falciparum*. The hDHFR is under control of the *P. falciparum* calmodulin promoter (PfCAM 5'; 631 bp) and flanked by the *P. falciparum* histidine-rich protein 2 3' UTR (PfHRPII 3'; 574 bp). The multiple cloning site consists of XhoI and BglII and is flanked by the *P. berghei* dihydrofolate reductase / thymilidate synthase 3' UTR (PbDHFR/TS 3'; 855 bp).

and were added to 450 μl uninfected erythrocytes that were previously washed with cytomix. The plasmid DNA was transfected by electroporation (310 V, 950 F; time constant should be about 30 ms) using the Gene Pulser Xcell electroporator (Bio-Rad). Subsequently, 10 ml complete RPMI 1640 medium and erythrocytes infected with schizonts were added to a final parasitemia of 1% and haematocrit of 5%. After 48 hours, the drug for selection of transfectants was added to the culture (either 5 nM WR99210 or 2 μg/ml blasticidin). After addition of the drug most parasites died and transfectants appeared three weeks to four months after the transfection.

Using the second transfection method, erythrocytes infected with *P. falciparum* ring stages of a parasitemia between 4-7% were transfected (Crabb and Cowman, 1996, Wu et al., 1996). For electroporation, 100 μg plasmid DNA were resuspended in 30 μl TE buffer and were mixed with 270 μl cytomix and 200 μl of the infected erythrocytes. After electroporation at 310 V and 950 μF (the time constant should be about 10 ms) the mixture was transferred into a culture flask and 200 μl uninfected erythrocytes were added. After 6 hours the medium was changed and the appropriate drug was added. Similarly, it took

three weeks to four months before transfected parasites were visible in Giemsa stained blood smears. Parasites used for transfection were either 3D7 (The Netherlands) or D10 (Papua New Guinea).

2.2.11. Cloning of *P. falciparum* by limiting dilution

Parasites were cloned according to Kirkman et al. (1996). The erythrocyte number of a culture with 3% parasitemia was determined and diluted in complete RPMI 1640 medium so that 10 ml contained 10^6 cells. 12.5 μl of these were transferred to 30 ml complete RPMI 1640 medium with 1% haematocrit. For cloning, 200 μl were transferred to each well of a 96 well plate which equals 0.25 parasites per well. After 5-6 days the medium was changed. After another 5-6 days the medium was changed again and was complemented with 1% (v/v) erythrocytes and the appropriate drug to select for transfectants. Following the third medium change 5-6 days later, the plates were monitored daily and wells in which the colour of the medium changed to yellow were transferred to a 12 well plate (2 ml cultures per well with 2% haematocrit and the appropriate drug). In the 12 well plate the cultures were monitored by blood smears and Giemsa staining until parasites were visible. These were transferred to 10 ml cultures with 5% haematocrit and were cultured for further analyses.

2.2.12. Growth rate assay

Cultures containing ring stage parasites were sorbitol-synchronised (see 2.2.2) twice within 4 hours and diluted to 1% parasitemia and 5% haematocrit. Progression through the intraerythrocytic developmental cycle was assessed by taking thin-smears every 8 hours over a 48 hour time course. The smears were stained with Giemsa and were analysed by light microscopy with an objective magnification of 100 fold.

2.2.13. MACS columns

MACS columns were used to obtain a highly synchronised culture of late stage parasites with parasitemias of $\sim$90%. These cultures were used to extract protein or to analyse the lipoic acid content of the parasites.
First, the CS-MACS column (Miltenyi Biotec) was assembled according to manufacturer's instruction using a blunt 0.8 mm needle. The column was placed in the VarioMACS separator (Miltenyi Biotec) and was equilibrated with MACS buffer (0.5% (w/v) BSA, 2 mM EDTA pH 8.0 in PBS) for 5 min at room temperature followed by washing

with 50 ml MACS buffer. The medium of a 50 ml culture containing mainly late stage parasites was removed and the blood was resuspended in 20 ml complete RPMI 1640. The 20 ml were applied to the column and were allowed to drop through the column slowly ($\sim$1.5 ml/min). During this process late stage parasites bound to the column due to the paramagnetic haemozoin in the food vacuole of the parasites. Once the whole culture had entered the column, it was washed with 50 ml MACS buffer. To elute the parasites, the column was removed from the VarioMACS separator, turned upside down and the late stage parasites were washed off with 30 ml MACS buffer. The elution fraction was centrifuged at room temperature, 1500 rpm (Jouan CR3i centrifuge with T4 rotor) for 10 min to pellet the infected erythrocytes. The supernatant was discarded and the pellet was taken up in 10 ml complete RPMI 1640 and incubated at 37°C for 30 min to allow the parasites to regenerate. After incubation the infected erythrocytes were saponin-lysed (see 2.2.5) and the parasite pellet was used for further analyses.

2.2.14. Immunofluorescence

Immunofluorescence analyses were carried out according to Tonkin et al. (2004). 10 μl of culture with 2.5% haematocrit was spotted into each well of Lab-Tek 8-well chamber slide (Nunc) previously treated with L-polylysine and allowed to dry. The cells were fixed with 4% (v/v) paraformaldehyde and 0.0075% (v/v) glutaraldehyde in PBS. After 30 min incubation, the cells were washed once with PBS and subsequently permeabilised in 0.1% (v/v) Triton X-100 in PBS for 10 min. The cells were washed again in PBS and incubated with 0.1 mg/ml sodium borohydride in PBS for further 10 min. Following another wash step with PBS cells were blocked overnight in 3% (w/v) BSA in PBS in a humidity chamber at 4°C. After blocking, the slide was washed three times with PBS containing 0.05% (v/v) Tween20. The primary antibodies were used at dilutions of 1:500 - 1:5000 in 3% (w/v) BSA in PBS (see Table 2.1). The first antibody was incubated for 1 hour at 4°C followed by three wash steps with PBS containing 0.05% (v/v) Tween20. The secondary antibody was applied at 1:500 dilution in 3% (w/v) BSA in PBS for one hour at 4°C. The second antibody was specific against the animal in which the first antibody was raised and was conjugated to either Alexa fluor 594 or 488 (see Table 2.2). Before the slide was washed, DAPI (final concentration of 0.5 μg/ml) was added for 5 min. After three wash steps with PBS containing 0.05% (v/v) Tween20 the plastic well divider was removed and the slide was mounted with mounting solution (2.5% (v/v) DABCO^{TM}, 50% (v/v) glycerol in PBS). The samples were analysed using an Axioskop-2 mot plus microscope (Zeiss) equipped with a Hamamatsu C4742-95 CCD camera.

2.2.15. Fluorescent microscopy

The subcellular localisation of parasite proteins was analysed either by immunofluorescence analyses (IFA), or by analysing live parasites expressing proteins fused to green fluorescent protein (GFP). The microscope used was an Axioskop-2 mot plus microscope (Zeiss) equipped with a Hamamatsu C4742-95 CCD camera.
Images were captured at 100 fold magnification using differential interference contrast (DIC) microscopy. The GFP-fusion proteins, as well as antibodies coupled with Alexa fluor 488, were observed using the fluorescent filter FITC (excitation at 494 nm and emission at 518 nm). In live cell imaging the mitochondrion was selectively stained using Mitotracker CMXRos (Molecular Probes), and was visualised using the fluorescent filter for rhodamine (excitation at 570 nm and emission at 590 nm). The same filter was used to visualise antibodies coupled with Alexa fluor 594.
Staining of the mitochondrion was performed by incubating 1 ml parasite culture (6% parasitemia, 5% haematocrit) with 25 nM Mitotracker CMXRos for 5 min at 37°C, before washing with 10 ml warm complete RPMI 1640. The culture was centrifuged at 1500 rpm (Jouan CR3i centrifuge with T4 rotor) for 10 min at 25°C, and the supernatant was discarded. The infected erythrocytes were resuspended in 1 ml warm complete RPMI 1640 medium before being analysed as described above.

2.3. *P. berghei* cell culture

2.3.1. *In vitro* culture of *P. berghei*

Parasites were maintained *in vitro* only for one developmental cycle to obtain mature schizonts for transfection. The culture was set up by collecting the blood of an infected rat by cardiac puncture at a parasitemia of 1-4%. The blood was transferred to 10 ml transfection medium containing 250 μl of the heparin stock solution (200 I.U./ml) and was centrifuged 10 min at 1000 rpm (Jouan CR3i centrifuge with T4 rotor). The supernatant was discarded, then the blood pellet was carefully resuspended in 25 ml transfection medium and transferred to a sterile 500 ml Erlenmeyer flask. 125 ml transfection medium was added without disturbing the blood layer at the bottom of the flask. The culture was incubated at 36.5°C with gentle shaking under an atmosphere of reduced oxygen (5% CO_2, 10% O_2 and 85% N_2), overnight. The following day the parasites had developed into mature schizonts, which were not released from their host cells *in vitro*.

2.3.2. Purification of mature *P. berghei* schizonts

A 55% Nycodenz working solution (in PBS) was used to purify mature schizonts. The 150 ml parasite culture (see 2.3.1) was split into five 50 ml tubes. 10 ml of 55% Nycodenz was carefully layered underneath the culture and centrifugation was performed at 1200 rpm (Jouan CR3i centrifuge with T4 rotor) for 30 min at room temperature without brake. During centrifugation, the uninfected erythrocytes moved through the Nycodenz to the bottom of the tube, whereas the mature schizonts assembled in a brown layer on top of the Nycodenz. The brown layer was collected with a Pasteur pipette and transferred to a fresh 50 ml tube. From a 150 ml culture 30-40 ml were collected. The Nycodenz was washed away by addition of transfection medium followed by centrifugation at 1000 rpm (Jouan CR3i centrifuge with T4 rotor) for 8 min at room temperature. The schizont pellet was resuspended in 15 ml transfection medium, and 1 ml aliquots were used for each transfection.

2.3.3. Transfection of *P. berghei*

Parasites were transfected according to Janse et al. (2006). Transfection was performed by electroporation using the Nucleofector II device and "Human T cell Nucleofector kit" from Amaxa biosystems. 5 μg of plasmid DNA was used per transfection. Before transfection, the plasmid was digested overnight to obtain linearised DNA. The digested DNA was ethanol precipitated (see 2.5.7) and resuspended in 10 μl ddH_2O. 100 μl of the Human T cell Nucleofector solution (Amaxa biosystems) were added to the DNA. The schizonts were pelleted by centrifugation at 13200 rpm in an Eppendorf microcentrifuge (F45-24-11 rotor) for 5 sec, and the parasite pellet was resuspended in the DNA-Nucleofector mixture. Electroporation was performed using the Nucleofector II device and protocol U33. 50 μl of culture medium were added to the cuvette and the transfected parasites were intravenously injected into a mouse. 24 hours later the drug selection started. The animals were provided with drinking water containing pyrimethamine (70 μg/ml), the drug used to select for the *Toxoplasma gondii* dihydrofolate reductase/thymilidate synthase (DHFR/TS). The parasitemia was assessed daily, and the parasites were collected for further analyses at a parasitemia of 1-5%.

2.3.4. Gene knock-out in *P. berghei*

For knock-out studies in *P. berghei* the plasmid b3D.DT^H.^D was used (kindly provided by A. P. Waters, Leiden University, The Netherlands) (Figure 2.2). The plasmid contained

the *T. gondii* DHFT/TS as a selectable marker referring resistance to pyrimethamine. The *Tg*DHFR/TS expression cassette was flanked by two multiple cloning sites (MCS), allowing knock-out of genes by either replacement (double cross-over recombination), or integration (single cross-over recombination). The plasmid backbone was based on the pBluescript plasmid (Stratagene) containing the beta-lactamase gene conferring resistance to ampicillin for selection in *E. coli*.

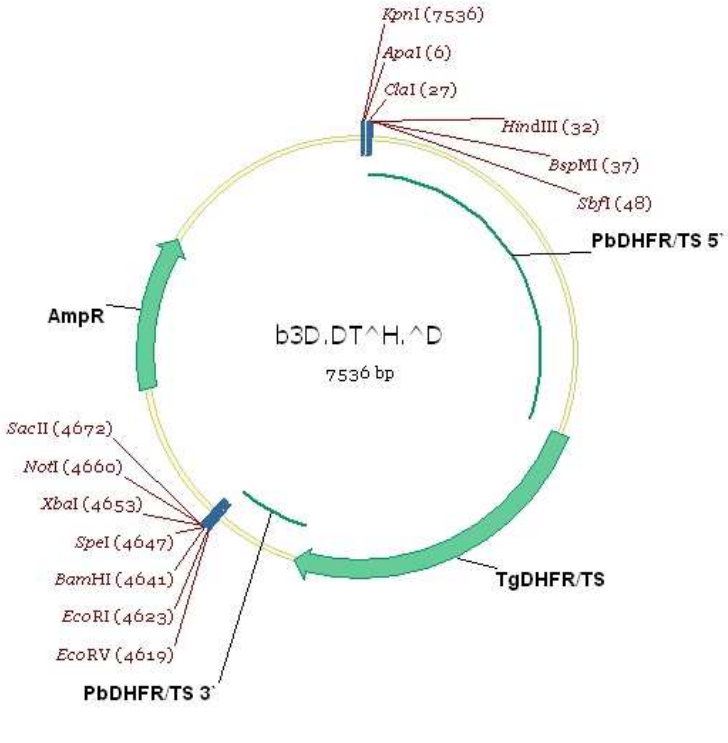

Figure 2.2.: Vector map of b3D.DT^H.^D
This figure displays the important features of the plasmid b3D.DT^H.^D, which was used for knock-out studies in *P. berghei*. The plasmid contains the ampicillin resistance cassette (AmpR; 861 bp) for selection in *E. coli*, and the *T. gondii* dihydrofolate reductase / thymilidate synthase expression cassette (*Tg*DHFR/TS (1803 bp) flanked by the *P. berghei* DHFR/TS 5' (2279 bp) and 3' UTR (481 bp)) for selection in *P. berghei*. Further, the plasmid contains two multiple cloning sites (KpnI-SbfI and EcoRV-SacII).

For the replacement strategy, 5' and 3' flanks (∼500 bp in size) of the gene of interest were amplified by PCR and cloned in the two MCSs. Prior to transfection, the plasmid was digested so that only the 5' flank, the *Tg*DHFT/TS expression cassette, and the 3' flank were used for transfection.

The integration strategy is similar to the method used to knock-out genes in *P. falciparum* (see 2.2.9). The knock-out fragments were amplified by PCR (∼1000 bp in size) and cloned into the second multiple cloning site using the restriction enzymes BamHI and SacII. The knock-out fragments were truncated at the N- and C-terminus. An artificial stop codon was introduced at the 3' end of the PCR product to ensure the disruption of the gene locus. Prior to transfection, the plasmid was linearised using a restriction enzyme which cut within the knock-out fragment.

2.3.5. Preparation of *P. berghei* stabilates

To prepare stabilates of *P. berghei* cultured in rats, 300 μl infected blood was added to 600 μl freezing solution (10% (v/v) glycerol in Alsever's solution (Sigma)). Stabilates prepared from mice were smaller. 100 μl infected blood was added to 200 μl freezing solution. The blood was gently mixed with the freezing solution and stored in liquid nitrogen immediately.

2.3.6. Extraction of *P. berghei* parasites from infected blood

The blood of an infected rat or mouse was collected by cardiac puncture at a parasitemia of 1-5%. To separate erythrocytes from lymphocytes and platelets, the blood was first purified using a cellulose column. For rats a 20 ml syringe, and for mice a 5 ml syringe was used as a column containing cotton, cellulose powder and glass beads. The glass beads removed platelets and the lymphocytes bound to the cellulose. The column was equilibrated with 10 ml PBS before the blood was applied. After the blood entered the column, it was washed with PBS and the eluate was collected once the first blood drop left the column. For rats 50 ml and for mice 14 ml were collected. The collected fraction was centrifuged at 1500 rpm (Jouan CR3i centrifuge with T4 rotor) for 8 min at room temperature and the supernatant was discarded. The pellet was resuspended in 0.2% (w/v) saponin (in PBS) and mixed by shaking until lysis of the erythrocytes was complete. The parasites were pelleted at 2800 rpm (Jouan CR3i centrifuge with T4 rotor) for 8 min at room temperature. The resulting parasite pellet was resuspended in 1 ml PBS, transferred into a 1.5 ml tube and centrifuged at 7000 rpm (Eppendorf microcentrifuge with F45-24-11 rotor) for 2 min at room temperature. The supernatant was discarded and the parasite pellet was resuspended in the appropriate buffer. For gDNA isolation the parasite pellet was resuspended in 200 μl PBS and stored at -20°C until gDNA was prepared. For protein analyses, the pellet was resuspended in the same volume of 2x SDS buffer (250 mM Tris pH 6.8, 6.6% (w/v) SDS, 24% (v/v) glycerol, 10 mM EDTA, 6%

(v/v) mercaptoethanol, bromophenolblue) and stored at -20°C. To prepare RNA, the pellet was resuspended in 350 μl lysis buffer of the RNeasy mini kit from Qiagen. The parasite pellet was homogenized by passing it through a 20-gauge needle at least five times before it was stored at -80°C until RNA was prepared according to manufacturer's guidelines.

2.3.7. Genomic DNA (gDNA) preparation from *P. berghei* parasites

Parasites were isolated from infected erythrocytes as described above (see 2.3.6) and the parasite pellet was resuspended in 200 μl PBS. gDNA was then extracted using the QIAamp DNA blood mini kit (Qiagen) according to manufacturer's guidelines.

2.3.8. Protein preparation from *P. berghei* parasites

Parasites, isolated by saponin lysis from erythrocytes (see 2.3.6), were resuspended in one pellet volume 2x SDS buffer (250 mM Tris pH 6.8, 6.6% (w/v) SDS, 24% (v/v) glycerol, 10 mM EDTA, 6% (v/v) mercaptoethanol, bromophenolblue). The resuspended parasites were boiled at 100°C for 5 min before being loaded onto a 12% SDS-polyacrylamide gel.

2.3.9. Cloning of *P. berghei* parasites

The blood of an infected mouse was collected by cardiac puncture at a parasitemia between 0.1 and 1%. The blood was diluted with RPMI 1640 (containing 25 mM HEPES and L-glutamine) so that 100 μl contained one parasite. These were then injected intravenously into 15 NMRI mice. After 7 days the parasitemia was monitored daily by Giemsa stained blood smears. Once the parasitemia was above 1%, the blood was collected by cardiac puncture. Stabilates and gDNA were made and the gDNA was analysed by PCR using primer sets diagnostic for integration, plasmid and wild-type.

2.3.10. Growth rate assay

The parasitemia of an infected mouse was determined and the blood was collected by cardiac puncture at a parasitemia between 0.1 and 1%. The blood was diluted with RPMI 1640 (containing 25 mM HEPES and L-glutamine) so that 100 μl contained 1000 parasites. These were injected intravenously into five NMRI mice. Parasitemia of the five mice was monitored and determined daily for eight days.

2.3.11. Transfer assay

To test whether a mutant parasite line showed a growth defect, the transfer assay was performed. The parasitemia of mice infected with mutant and wild-type parasites was determined and the blood was collected by cardiac puncture at a parasitemia between 0.1 and 1%. The infected blood was diluted with RPMI 1640 (containing 25 mM HEPES and L-glutamine) so that 100 μl contained 1000 mutant and 1000 wild-type parasites. These were injected intravenously into two NMRI mice. After three to four days, the blood of the mice was collected by cardiac puncture and 100 μl were transferred intraperitoneally into two naive mice. This was repeated five times. From the first and last two mice, parasites were extracted by saponin lysis (see 2.3.6) and gDNA was prepared (see 2.3.7). The gDNA was analysed by PCR using primer sets diagnostic for integration, plasmid and wild-type.

2.3.12. Exflagellation of *P. berghei* gametocytes

Exflagellation of male gametocytes in a parasite population was analysed before *Anopheles* mosquitoes were infected with *P. berghei*. Usually exflagellation occurs in the midgut of the mosquito and is the differentiation of a microgamont into four to eight microgametes. Among other things, this can be induced *in vitro* by a temperature drop of at least 2-5°C (Sinden and Croll, 1975).
A drop of blood was removed from an infected mouse by tale puncture and transferred to a slide covered with a cover slip. After 10 min the slide was checked microscopically for exflagellation. The temperature drop from 37°C to room temperature induces exflagellation. The slide was examined by phase contrast microscopy using an objective magnification of 40 fold. If four to six exflagellating microgamonts were visible in each field of view, the animal was used for a blood meal.

2.3.13. *In vitro* ookinete culture

Mice with a parasitemia above 1% were used for ookinete cultures. The exflagellation was examined (see 2.3.12) and animals with sufficient exflagellating parasites were bled by cardiac puncture. The blood was taken into culture using 10 ml of ookinete culture medium per 1 ml of fresh blood. The culture was incubated at 20°C for 20-24 hours. The ookinetes were purified using magnetic beads labeled with an antibody against the ookinete surface protein p28. The culture was centrifuged at 1700 rpm (Jouan CR3i centrifuge with T4 rotor) for 8 min at room temperature and the supernatant was discarded.

The blood pellet was resuspended in 500 μl PBS and transferred into a fresh 1.5 ml reaction tube. 3 μl anti-p28 labeled magnetic beads were added and gently mixed for 5 min. After mixing, the tube was placed into a magnetic rack and left for 2 min to allow the ookinetes bound to the magnetic beads to separate from the remaining blood and culture medium. The remaining blood and medium was removed and the ookinetes were washed twice with PBS. After the final wash step, the ookinetes were centrifuged at 7000 rpm (Eppendorf microcentrifuge with F45-24-11 rotor) for 2 min at room temperature. The supernatant was discarded and the ookinetes were resuspended in 100 μl HBSS (Hanks'balanced salt solution). To determine the number of ookinetes in the culture, they were counted using a hemocytometer and phase contrast microscopy (40 fold magnification).

2.3.14. Breeding of *A. stephensi*

Female mosquitoes require a blood meal before egg production. To feed mosquitoes, two mice or one rat were anaesthetised using ketamin/xylazinhydrochloride and placed on a cage containing two to seven days old mosquitoes. After 15 min the animals were removed. Four days later the oviposition took place. For that, a petridish filled with breeding water containing a fluted filter was placed in the cage. The eggs were removed and washed using the fluted filter with breeding water, followed by 70% (v/v) ethanol. The washed eggs were put in a larvae tank. Hatched larvae were washed every second day and diluted if required. They were fed daily using a third of a cat-food pellet. From day nine onwards the pupae were collected, placed in a petridish with breeding water and put into a mosquito cage to hatch.
Mosquitoes were fed daily using two pieces of cotton wool, one soaked with sucrose solution and the other soaked with breeding water. The mosquitoes were kept at 21°C (insectary) or 28°C (breeding room) and 80% humidity. The light-dark cycle was 14h to 10h.

2.3.15. Mosquito midgut infectivity with *P. berghei* oocysts

Midgut infectivity was screened at day 10-14 post blood feeding when oocysts were developed and contained either sporoblasts or sporozoites. A midgut was recorded as infected when at least one oocyst was detected. A minimum of 10 midguts were analysed, and the oocyst number in each midgut was determined. The mean total number of oocysts per midgut was then calculated from all separate counts of infected midguts. Midguts used were freshly dissected in dissection medium and were analysed by phase contrast

microscopy with 40 fold magnification.

2.4. Bioinformatics

2.4.1. Identifying genes in the *P. falciparum* genome

The *lplA2* gene was identified in the *P. falciparum* genome by TBlastN searching the *Plasmodium* genome database PlasmoDB (Bahl et al., 2003) with the *Arabidopsis thaliana* LplA sequence.

2.4.2. Multiple sequence alignments

Multiple protein alignments were performed using ClustalW (Thompson et al., 1994) with predicted *P. falciparum* protein sequences and sequences of orthologues proteins from other organisms. Orthologues were identified by BlastP searching the OrthoMCL database (Chen et al., 2006). Sequence similarities were determined based on the chemical properties of the amino acids using Vector NTI software (Invitrogen).

2.4.3. Subcellular localisation predictions

Subcellular localisation predictions using the predicted protein sequences were performed using MitoProt (Claros and Vincens, 1996), PATS (Zuegge et al., 2001), PlasMit (Bender et al., 2003), Predotar (Small et al., 2004) and SignalP (Nielsen et al., 1997).

2.5. Methods in molecular biology

2.5.1. Polymerase chain reaction (PCR)

Plasmodium genes were amplified from gDNA using the following PCR systems.

2.5.1.1. PCR SuperMix

The PCR SuperMix (Invitrogen) is a ready to use mix containing 1.65 mM $MgCl_2$, 220 μM dNTP and 22 U/ml *Taq* DNA polymerase. The SuperMix was mixed with 100 ng gDNA and 400 nM of each oligonucleotide to a final volume of 25 μl. The PCR was performed under the following conditions:

Initial Denaturation	94°C, 5 min
30 cycles of:	
Denaturation	94°C, 1 min
Annealing	oligonucleotide specific temperature, 1 min
Elongation	60°C, 1 min per kb to be amplified
Final Elongation	60°C, 10 min

The PCR products were analysed on a 1% agarose gel and fragments of the expected size were cloned into pCR 2.1-TOPO using the TOPO TA PCR cloning kit (see 2.5.2.1).

2.5.1.2. AccuPrime *Pfx* SuperMix

The AccuPrime *Pfx* SuperMix (Invitrogen) contained 1.1 mM $MgSO_4$, 330 μM dNTPs and 22 U/ml *Pfx* DNA polymerase. The PCR was set up using 100 ng gDNA and 400 nM of each oligonucleotide. The final volume per PCR reaction was 25 μl and PCR was performed under the following conditions:

Initial Denaturation	94°C, 5 min
30 cycles of:	
Denaturation	94°C, 1 min
Annealing	oligonucleotide specific temperature, 1 min
Elongation	68°C, 2 min per kb to be amplified
Final Elongation	68°C, 10 min

The PCR products were analysed on a 1% agarose gel and fragments of the expected size were cloned into pCR-BluntII-TOPO using the Zero Blunt TOPO PCR cloning kit (see 2.5.2.1).

2.5.1.3. Expand High Fidelity PCR kit

The Expand High Fidelity PCR kit (Roche) was set up in two master-mixes. The first mix contained 200 μM dNTPs, 400 nM of each oligonucleotide and 100 ng gDNA in a final volume of 12.5 μl. The second mix contained the reaction buffer with 1.5 mM $MgCl_2$ and 2.5 U of the Expand HiFiPLUS enzyme blend in a final volume of 12.5 μl. The enzyme

blend contained a *Taq* DNA polymerase and a thermostable proofreading protein without polymerase activity. The two master-mixes were mixed and the PCR was performed under the following conditions:

Initial Denaturation	94°C, 5 min
10 cycles of:	
Denaturation	94°C, 1 min
Annealing	oligonucleotide specific temperature, 1 min
Elongation	68°C, 2 min per kb to be amplified
20 cycles of:	
Denaturation	94°C, 1 min
Annealing	oligonucleotide specific temperature, 1 min
Elongation	68°C, 2 min per kb to be amplified + 5 sec per cycle
Final Elongation	68°C, 10 min

The PCR products were analysed on a 1% agarose gel and fragments of the expected size were cloned into pCR-BluntII-TOPO using the Zero Blunt TOPO PCR cloning kit (see 2.5.2.1).

2.5.2. Cloning techniques

2.5.2.1. TOPO cloning of PCR products

All PCR products amplified were initially cloned into the TOPO vectors (Invitrogen). Different types of TOPO vectors were used depending on the polymerase used in the PCR reaction. *Taq* polymerases produced adenine overhangs at the 3' ends of PCR products and required therefore the TOPO TA PCR cloning kit with the vector pCR 2.1-TOPO (Figure 2.3). PCR products amplified with a *Pfx*/*Pfu* polymerase had blunt ends and were therefore cloned using the Zero Blunt TOPO PCR cloning kit containing the vector pCR-BluntII-TOPO (Figure 2.4).

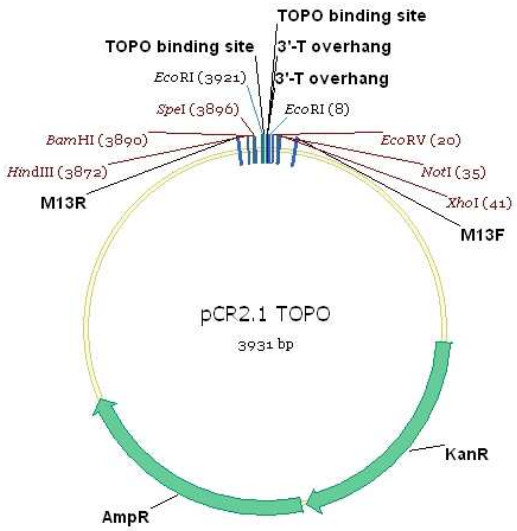

Figure 2.3.: Vector map of pCR2.1-TOPO
This figure displays the important features of the pCR2.1-TOPO plasmid (Invitrogen), which was used to clone PCR products amplified with *Taq* based polymerase. The plasmid contains the kanamycin (KanR; 795 bp) and ampicillin resistance cassette (AmpR; 861 bp) for selection in *E. coli*. The topoisomerase I is covalently bound to the TOPO binding sites. After cloning, the generated construct was analysed by diagnostic digests using the restriction sites shown, and the sequence of the cloned PCR product was verified by sequencing using the primers M13F and M13R.

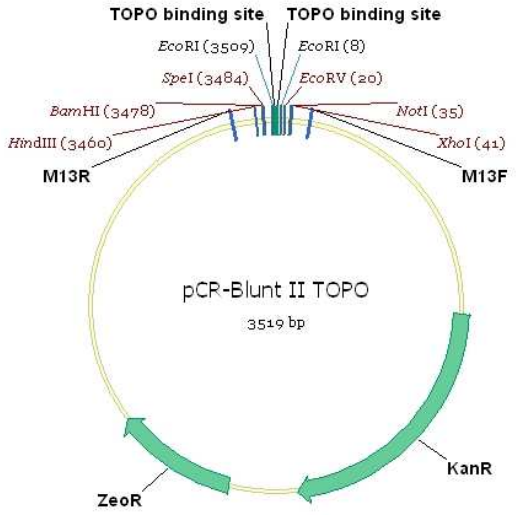

Figure 2.4.: Vector map of pCR-BluntII-TOPO
This figure displays the important features of the pCR-Blunt II-TOPO plasmid (Invitrogen), which was used to clone PCR products amplified with polymerases with proofreading abilities. The plasmid contains the kanamycin (KanR; 795 bp) and zeocin resistance cassette (ZeoR; 375 bp) for selection in *E. coli*. The topoisomerase I is covalently bound to the TOPO binding sites. After cloning, the generated construct was analysed by diagnostic digests using the restriction sites shown, and the sequence of the cloned PCR product was verified by sequencing using the primers M13F and M13R.

Directional TOPO cloning was performed if the amplified PCR product was used for Gateway cloning (see 2.5.2.3). The plasmid pENTR/D-TOPO (part of the pENTR/D-TOPO cloning kit) (Figure 2.5) was used, which contained a 5' directional GTGG overhang. Therefore, the PCR product was amplified with a forward oligonucleotide primer that introduced a CACC overhang to allow directional cloning.
The ligation reactions for all kits were performed as per manufacturer's instruction, were subsequently transformed into chemically competent *E. coli* TOP10 cells (Invitrogen) and were plated on LB-plates containing 50 μg/ml kanamycin. Single bacteria colonies were used to inoculate 3 ml LB-medium containing 50 μg/ml kanamycin and were grown overnight at 37°C. The following day the bacteria were pelleted, plasmid DNA was extracted (see 2.5.5) and analysed by digest with appropriate restriction enzymes (see 2.5.6). Before inserts were sub-cloned into a destination plasmid, the sequence was verified.

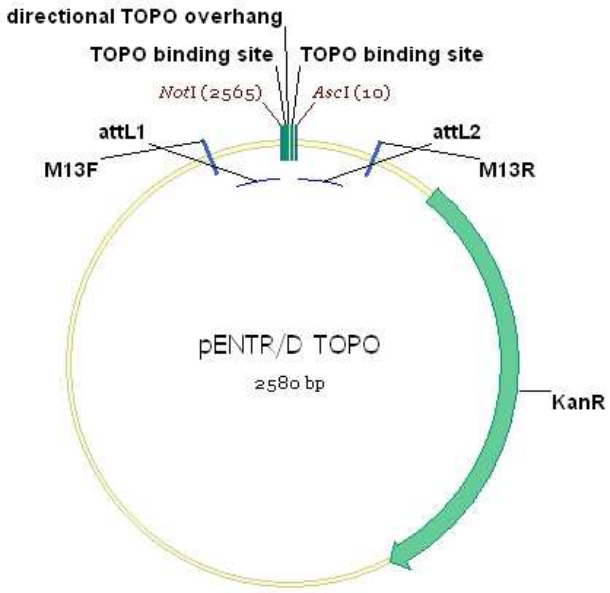

Figure 2.5.: Vector map of pENTR/D-TOPO
This figure displays the important features of the pENTR/D-TOPO plasmid (Invitrogen), in which PCR products were cloned directional. The plasmid contains the kanamycin resistance cassette (KanR; 810 bp) for selection in *E. coli*. The topoisomerase I is covalently bound to the TOPO binding sites and the directional TOPO overhang (GTGG) ensures that the PCR product is cloned directional. Further, the plasmid contains attL1 and attL2 sites for MultiSite Gateway LR recombination. After cloning, the generated construct was analysed by diagnostic digests using the restriction sites shown, and the sequence of the cloned PCR product was verified by sequencing using the primers M13F and M13R.

2.5.2.2. Sub-cloning into destination plasmids

Inserts of correct TOPO-clones were used and sub-cloned into the respective destination plasmid. The insert was isolated from the TOPO plasmid using the appropriate restriction endonucleases (see 2.5.6). The destination plasmid was linearised using the same restriction enzymes and the digests were separated by agarose gel electrophoresis (see 2.5.10). The insert and digested destination plasmid were excised from the gel and purified using the Qiagen Gel Extraction kit as per manufacturer's instructions. The DNA was eluted in 30 μl ddH_2O.
The insert was then ligated into the destination plasmid using the Rapid DNA Ligation kit (Roche). Molar vector to insert ratios from 1:3 to 1:10 were used in the ligation reactions which were performed as per manufacturer's instruction. 10 μl of the ligation reaction was subsequently transformed into chemically competent *E. coli* and plated on LB-plates containing the appropriate antibiotics. Single colonies were analysed by DNA miniprep (see 2.5.5) and restriction endonuclease digestion (see 2.5.6). Plasmids containing the correct insert size were analysed by DNA sequencing.

2.5.2.3. Gateway cloning

The Gateway cloning technology (Invitrogen) is based on the site-specific recombination system of phage l. The recombination occurs at the "att" sites which contain the binding sites for the proteins that mediate phage l recombination. Via the BP reaction, the prophage integrates into the genome of *E. coli* and via the LR reaction, the lambda-DNA is excised from the *E. coli* genome.
Only LR cloning reactions were carried out according to manufacturer's guidelines. SingleSite Gateway cloning was used to generate an over-expression plasmid of *P. berghei* LplA1. The entry plasmid pHGB and the destination plasmid pHrBI-1/2 with the blasticidin-S-deaminase (BSD) as a selectable marker were used (Tonkin et al., 2004) (Figure 2.6). *P. berghei lplA1* was amplified by PCR and directly cloned into the entry plasmid pHGB as described in 2.5.2.2 using the restriction endonucleases BglII and NotI. Once cloned into the entry vector the *lplA1* expression cassette (under control of the *P. falciparum* Hsp86 promotor) was cloned into pHrBI-1/2 by site specific recombination of the attL and attR sites.

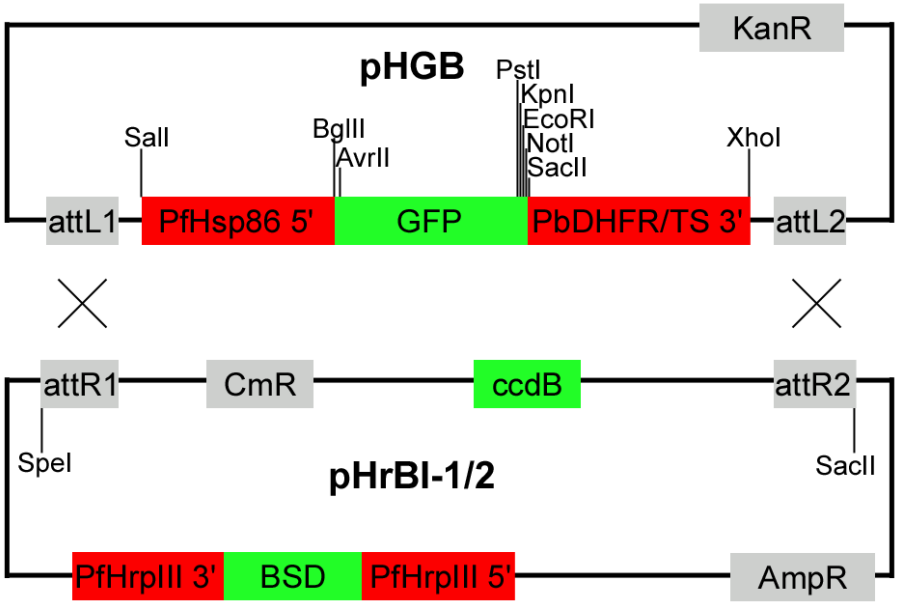

Figure 2.6.: Vector maps of pHGB and pHrBI-1/2
This figure displays the important features of the SingleSite gateway vectors pHGB and pHrBI (according to Tonkin et al. (2004)). The entry vector pHGB contains the kanamycin resistance cassette (KanR; 810 bp) for selection in *E. coli*. The attL1 and attL2 sites flank the expression cassette into which the gene of interest is cloned. The expression cassette is under control of the *P. falciparum* heat shock protein 86 promoter (PfHsp86 5'; 857 bp) and the *P. berghei* dihydrofolate reductase/thymilidate synthase 3' UTR (PbDHFR/TS 3'; 481 bp). The destination vector pHrBI-1/2 contains the ampicillin resistance cassette (AmpR; 861 bp) for selection in *E. coli* and the blasticidin-S-deaminase gene (BSD; 399 bp) for selection in *P. falciparum*. The blasticidin-S-deaminase is flanked by the UTR's of the *P. falciparum* histidine-rich protein 3 (PfHrpIII 5'/3'). pHrBI-1/2 contains attR1 and attR2 sites, which flank a selection cassette containing the ccdB death gene (306 bp) which interferes with DNA gyrase and thus allows negative selection in bacteria. A chloramphenicol resistance cassette is also present (CmR; 660 bp). After the recombination reaction the selection cassette is replaced with the expression cassette.

MultiSite gateway cloning was performed to generate GFP-tagged fusion cassettes. The PCR product of the gene of interest was cloned directionally into the plasmid pENTR/D-TOPO (see 2.5.2.1). The cloning of the constructs was performed as described by van Dooren et al. (2005). Two entry plasmids were used that introduced different promoters to the GFP-tagged fusion cassette. The PfHsp86 5'-pDONR4/1 contains the *P. falciparum* Hsp86 5' UTR and the PfCRT 5'-pDONR4/1 possesses the *P. falciparum* CRT 5' UTR (Figure 2.7). The C-terminal tag was provided by GFPmut2-pDONR2/3 (Figure 2.8).

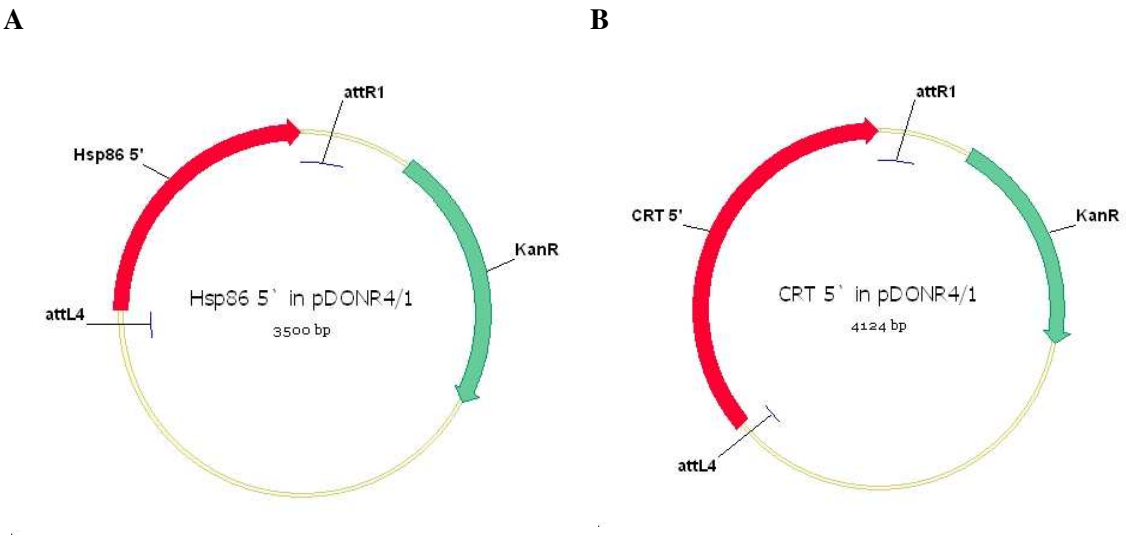

Figure 2.7.: Vector maps of PfHsp86 5'-pDONR4/1 and PfCRT 5'-pDONR4/1
This figure displays the important features of the 5' element entry vectors Hsp86 5'-pDONR4/1 (**Panel A**) and CRT 5'-pDONR4/1 (**Panel B**). Both contain the kanamycin resistance cassette (KanR; 810 bp) for selection in *E. coli*. The 5' elements, Hsp86 5' (857 bp) (A) and CRT 5' (1481 bp) (B), are flanked by the attL4 and attR1 recombination sites which fuse the 5' element in the LR recombination reaction at the N-terminus of the gene of interest.

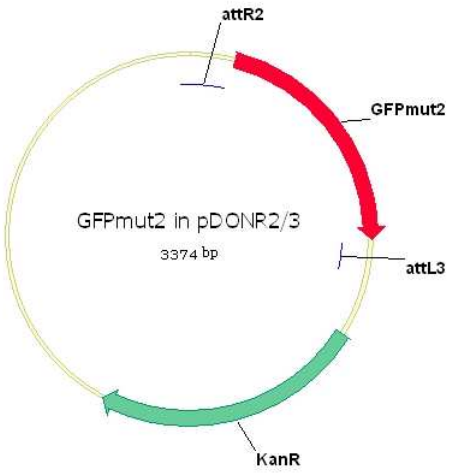

Figure 2.8.: Vector map of GFPmut2-pDONR2/3
This figure displays the important features of the 3' element entry vector GFPmut2 in pDONR2/3. It contains the kanamycin resistance cassette (KanR; 810 bp) for selection in *E. coli*. GFPmut2 (714 bp) is flanked by the attR2 and attL3 recombination sites which fuse the 3' element in the LR recombination reaction at the C-terminus of the gene of interest.

The destination plasmid used was pCHDR-3/4 which contains the human dihydrofolate reductase (hDHFR) as a selectable marker conferring resistance to WR99210 (Figure 2.9). Thus, four plasmids (either PfHsp86 5'-pDONR4/1 or PfCRT 5'-pDONR4/1, the gene of interest in pENTR/D-TOPO, GFP-pDONR2/3 and pCHDR-3/4) were incubated in the LR MultiSite cloning reaction according to manufacture's guidelines to generate the expression plasmid.

The Gateway cloning reactions were transformed into chemically competent *E. coli* TOP10 cells (Invitrogen) and were plated on LB-plates containing 100 μg/ml ampicillin. Single bacteria colonies were used to inoculate 3 ml LB-medium containing 100 μg/ml ampicillin and were grown overnight at 37°C. The bacteria were pelleted, plasmid DNA was extracted (see 2.5.5) and analysed by digestion with appropriate restriction enzymes (see 2.5.6). Plasmids with the expected insert size were analysed by DNA sequencing.

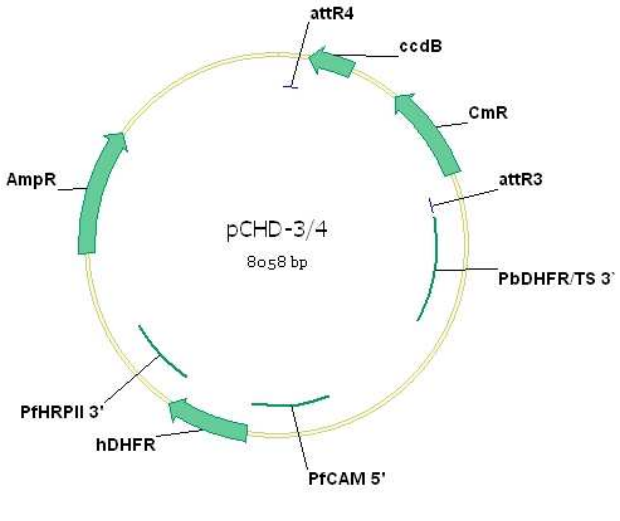

Figure 2.9.: Vector map of pCHD-3/4

This figure displays the important features of the pCHD-3/4 destination plasmid. These include the ampicillin resistance cassette (AmpR; 861 bp) for selection in *E. coli* and the human dihydrofolate reductase gene (hDHFR; 564 bp) for selection in *P. falciparum*. The hDHFR is under control of the *P. falciparum* calmodulin promoter (PfCAM 5'; 631 bp) and flanked by the *P. falciparum* histidine-rich protein 2 3' UTR (PfHRPII 3'; 574 bp). pCHD-3/4 contains attR4 and attR3 sites, which allow generation of an expression vector by recombining with three entry plasmids in a MultiSite Gateway LR reaction. The attR4 and attR3 site flank a selection cassette containing the ccdB death gene (306 bp) which interferes with DNA gyrase and thus allows negative selection in bacteria, and the chloramphenicol resistance cassette (CmR; 660 bp). After the recombination reaction, the selection cassette is replaced with the expression cassette flanked by the *P. berghei* dihydrofolate reductase / thymilidate synthase 3' UTR (PbDHFR/TS 3'; 853 bp).

2.5.3. *E. coli* transformation

Chemically competent *E. coli* were used to transform either plasmid DNA or ligation reactions. The DNA was added to the bacteria and incubated on ice for 30 min. The bacteria were then heat shocked at 42°C for 30-40 sec. To regenerate the bacteria, 500 μl LB-medium was added and they were incubated at 37°C for one hour in a shaking incubator before they were plated on LB-agar plates containing the appropriate antibiotics. The plates were incubated at 37°C overnight, and single colonies were analysed by miniprep DNA extraction (see 2.5.5) and restriction endonuclease digestion (see 2.5.6).

2.5.4. Preparing competent cells

Competent bacteria used during this work were either bought from Invitrogen, Novagen or Stratagene, or were made chemically competent using the following protocol.
A 5 ml overnight culture of the appropriate *E. coli* strain was used to inoculate 200 ml LB-medium without antibiotics. This culture was grown at 37°C and 220 rpm until OD_{600} reached 0.6. The culture was placed on ice for 10 min before it was centrifuged at 3000 rpm (Jouan CR3i centrifuge with T4 rotor), 4°C for 10 min. The supernatant was discarded and the pellet was placed back on ice and was resuspended in 50 ml cold 80 mM $CaCl_2$. The resuspended bacteria were incubated 30 min on ice before they were centrifuged as before. The pellet was resuspended in 10 ml cold 80 mM $CaCl_2$, 20% (v/v) glycerol and 200 μl aliquots of the bacteria were frozen using dry ice and stored at -80°C.

2.5.5. Plasmid DNA isolation from *E. coli*

Plasmid DNA was isolated from *E. coli* culture using two different methods depending on the required plasmid DNA amount.
For small scale isolations the Qiaprep Spin Miniprep kit from Qiagen was used. 3 ml LB-medium containing the appropriate antibiotics was inoculated with a single bacteria colony and grown overnight at 37°C in a shaking incubator (200 rpm). The bacteria were pelleted and plasmid DNA was extracted according to manufacture's guidelines. The plasmid DNA was eluted in 50 μl ddH_2O and was further analysed by digestion with the appropriate restriction endonucleases (see 2.5.6).
Large quantities of plasmid DNA were required of constructs that were used for transfection of *P. falciparum*. To prepare the plasmid DNA the Hi-Speed Plasmid Maxi kit from Quiagen was used. A 3 ml day culture was set up using a single bacteria colony and was grown at 37°C for 8 hours. This culture was used to inoculate 250 ml LB-medium

containing the appropriate antibiotics and was grown overnight at 37°C and 200 rpm. The following day, the bacteria were centrifuged at 3000 rpm (Sigma 6K15 centrifuge with 12500 rotor) at 4°C for 20 min. Plasmid DNA was then extracted following the manufacture's guidelines. Finally, the plasmid DNA was eluted in 500 μl ddH_2O and the DNA concentration was quantified by spectrophotometric analyses (see 2.5.8). Furthermore, the plasmid DNA was analysed by restriction endonuclease digestion (see 2.5.6).

2.5.6. Restriction endonuclease digestion

Plasmid DNA was routinely analysed by digestion with restriction endonucleases. Unless otherwise stated, 3 μl of plasmid DNA was added to 2 μl of the appropriate buffer, 0.2 μl BSA and 0.5 μl of each enzyme. ddH_2O was used to fill up the reaction mix to a final volume of 20 μl. The digestion took place at 37°C degree (or 50°C if BsaI was used) for 1-2 hours. 4 μl of 6x DNA loading dye was added, mixed, and then loaded onto a 1% (w/v) agarose gel.

2.5.7. Ethanol precipitation of genomic and plasmid DNA

To precipitate DNA, 1 μl glycogen and 0.1 volumes of 3 M NaAc pH 5.2 were added to the DNA solution before 2.5 volumes of cold 100% ethanol were added. The resulting mix was incubated at -20°C for at least one hour. The precipitated DNA was pelleted by centrifugation at 13000 rpm (Fisher Scientific accuSpin MicroR with 24-place rotor), 4°C for 30 min. The supernatant was discarded, and the DNA pellet was washed with cold 70% (v/v) ethanol and centrifuged as before. The supernatant was removed and the pellet air-dried before it was resuspended in the appropriate buffer.

2.5.8. Determining DNA and RNA concentration

The concentration of nucleic acid solutions was determined by measuring the OD_{260} of the solution using a UV-spectrophotometer (Shimadzu). An OD_{260} of 1 corresponded to a concentration of 50 μg/ml for double stranded DNA, 37 μg/ml for single stranded DNA and 40 μg/ml for RNA.

2.5.9. DNA sequencing

DNA sequencing was performed by The Sequencing Service, School of Life Sciences, University of Dundee (www.dnaseq.co.uk) using Applied Biosystems Big-Dye Ver 3.1 chemistry on an Applied Biosystems model 3730 automated capillary DNA sequencer.

The sequencing reaction required 200-300 ng of plasmid DNA and 3.2 pmoles of sequencing primer per reaction.

2.5.10. Agarose gel electrophoresis

The quality and quantity of DNA was routinely examined by agarose gel electrophoresis using the Sub-Cell GT system (Bio-Rad). 1% (w/v) agarose was dissolved in 1x TAE buffer by boiling the mixture in a microwave. Once the agarose cooled down to 50°C, SYBR safe (1:10000) (Invitrogen) was added and it was poured into gel trays with the appropriate size comb. The DNA samples were mixed with 6x DNA loading dye and electrophoresis was performed at 80-110 V for 30-60 min in 1x TAE buffer. 1 kb ladder (Promega) was run with DNA samples to allow the size determination of the bands visualised by UV illumination at 302 nm or 365 nm using the Gel Doc XR system (Bio-Rad).

2.5.11. Southern blot analysis

To analyse parasite DNA, digests with specific restriction enzymes led to a specific pattern of bands detectable on a Southern blot. 1-5 μg DNA was digested with the appropriate restriction enzymes at 37°C overnight. The following day the digested DNA was loaded onto a 0.8% (w/v) agarose gel and the gel was run at 15-20 V overnight. The DNA was then transferred to the positively charged nylon membrane Hybond-N+ (GE Healthcare). For the transfer the membrane was placed on the VacuGene XL apparatus (GE Healthcare) and was covered with 0.25 N HCl. The gel was put on top of the membrane and the vacuum pump was turned on (with the pressure between 50 and 60 mbar). The gel was covered with the depurination solution (0.25 N HCl) for 25 min until the colour of the loading dye changed from blue to yellow. The HCl was removed and the gel was covered with the denaturation solution (1.5 M NaCl and 0.5 M NaOH) for approximately 25 min until the loading dye colour changed back to blue. The denaturation solution was removed and 20x SSC was poured on the gel. The transfer took one hour during which the gel remained covered with 20x SSC. By using the UV crosslinker, the DNA was crosslinked with the membrane. To analyse the Southern blot the Gene Images CDP-Star detection module from GE Healthcare was used. The membrane was blocked with the pre-hybridisation buffer (5x SSC, 0.1% (w/v) SDS, 5% (w/v) dextran sulphate and 1:20 dilution of GI liquid block) for at least two hours at 60°C. The pre-hybridisation buffer was warmed to 60°C before it was added to the membrane. After pre-hybridising, a fluorescein-labelled probe was added. The probe of the gene of interest was synthesized using the Gene Images Random Prime Labelling Module from GE Healthcare. During

the PCR reaction fluorescein-11-dUTP partially replaced the dTTP so that a fluorescein-labelled probe was synthesized. 2 μl/ml hybridisation buffer of freshly made probe was added and was incubated with the membrane at 60°C overnight. Before adding to the membrane, the probe was denatured at 90°C for 5 min. After incubation with the probe the blot was washed twice for 10 min with 1x SSC + 0.1% SDS at 60°C and twice for 10 min with 0.5x SSC + 0.1% SDS at 60°C. After washing, the membrane was blocked in a 1:10 dilution of GI liquid block in buffer A (100 mM Tris/HCl, 300 mM NaCl, pH 9.5) for one hour at room temperature followed by incubation with the anti-fluorescein alkaline phosphatase (AP) conjugated antibody for at least one hour at room temperature. The antibody was diluted 1:5000 in buffer A with 0.5% (w/v) BSA. Then, the blot was washed three times for 30 min in buffer A with 0.3% (v/v) Tween20 and the detection reagent was added. The light produced in the reaction catalysed by the alkaline phosphatase (decomposition of the detection reagent) was detected on autoradiography film (Kodak).

2.5.12. Pulse field gel electrophoresis

To separate chromosomes from each other in an agarose gel, pulse field gel electrophoresis (PFGE) was performed using the CHEF-DR III Variable Angle System (Bio-Rad). Before the gel was run, the apparatus had to be washed and equilibrated. First, it was washed with 0.1% (w/v) SDS at room temperature overnight (pump setting: 60). The following day, the machine was washed twice with ddH_2O at 13°C followed by equilibration with 2 L of the appropriate running buffer (0.5x TBE for separation of chromosomes 1-10, or 1x TAE for separation of chromosomes 11-14) overnight at 13°C. The following day the running buffer was changed and the PFGE was performed. To prepare the gel, 1% (w/v) agarose was dissolved in 0.5x TBE (or 1x TAE for separation of chromosomes 11-14) and poured into a gel casting stand with the appropriate comb (Bio-Rad). Once set, the comb was removed and the equilibrated chromosome blocks (see 2.2.8) were loaded. The chromosome blocks were equilibrated for at least 30 min in the running buffer at room temperature before they were loaded on the gel. After loading, the wells were sealed with 1% (w/v) low melting point agarose in 0.5x TBE (or 1x TAE for separation of chromosomes 11-14) and the gel was run at the appropriate running conditions (see below). After the run was complete, the gel was removed and the apparatus was washed with ddH_2O, 0.1% (w/v) SDS and ddH_2O again. The gel was stained with SYBR safe (Invitrogen). DNA was visualised using the Gel Doc XR system (Bio-Rad) and analysed by Southern blotting as described in 2.5.11.

Conditions for resolution of chromosomes 1-5:
1% (w/v) agarose in 0.5x TBE, 60-120 sec pulse, 6 V/cm (200 volts), 24 hour run.
Conditions for resolution of chromosomes 1-10:
1% (w/v) agarose in 0.5x TBE, 225 sec pulse, 4.2 V/cm (140 volts), 60 hour run.
Conditions for resolution of chromosomes 11-14:
1% (w/v) agarose in 1x TAE, 360-800 sec pulse, 3 V/cm (100 volts), 96 hour run.

2.6. Methods in biochemistry

2.6.1. Sodium dodecyl sulphate polyacrylamide gel electrophoresis (SDS-PAGE)

Proteins were separated by polyacrylamide gel electrophoresis (PAGE) as described by Laemmli (1970). The NuPAGE electrophoresis system (Invitrogen) was used with either 4-12% Novex Bis/Tris pre-cast gels or self-made polyacrylamide gel. Gradient gels were utilised for the analyses of parasite extract whereas 15% and 12.5% polyacrylamide gels were used for examining purity of recombinant protein and enzyme assays. The running gel consisted of 6 ml running gel buffer (375 mM Tris pH 8.9, 0.1% (w/v) SDS, 12.5-15% (v/v) acrylamide) which was polymerised by addition of 5 μl N,N,N',N'-Tetramethylethylenediamine (TEMED) and 25 μl ammonium persulphate (APS) (10 mg/ml). The gel was poured into empty plastic cassettes (Invitrogen) and allowed to set. The stacking gel, consisting of 2 ml stacking gel buffer (122 mM Tris pH 6.7, 0.1% (w/v) SDS, 5% (v/v) acrylamide) was poured on top of the running gel and an appropriate comb was placed in the stacking gel. While the stacking gel was allowed to set protein samples were prepared. 15 μg parasite extract or 5 μg recombinant protein was mixed with 6x loading buffer and denatured at 100°C for 5 min. The samples were loaded and the self-made polyacrylamide gels were run in 1x running buffer and pre-cast gels in 1x MOPS buffer (Invitrogen) at 40 mA and 200 V. Following electrophoresis, gels were either stained with Coomassie blue (see 2.6.3), silver (see 2.6.4) or were analysed by western blotting (see 2.6.5).

2.6.2. Native polyacrylamide gel electrophoresis

For native PAGE, proteins were not denatured before or during electrophoresis and were therefore separated according to their charge. The NuPAGE electrophoresis system (Invitrogen) was used with 20% polyacrylamide gels. The running gel consisted of 6 ml native running buffer (125 mM Tris pH 8.9, 20% (v/v) acrylamide) and the stacking gel of 2 ml native stacking buffer (125 mM Tris pH 6.7, 5% (v/v) acrylamide). Samples

were prepared using 2x native loading buffer and were kept on ice until loading onto the gel. Gels were run in 1x native running buffer at 20 mA and 4°C until the loading buffer reached the bottom of the gel. The gel was removed from the cassette and either stained with Coomassie blue (see 2.6.3) or analysed by western blotting (see 2.6.5).

2.6.3. Coomassie blue staining of polyacrylamide gels

After electrophoresis, the gel was removed from the cassette and covered with Coomassie stain for at least 1h at room temperature. For destaining, the Coomassie blue solution was removed and the gel was incubated in destain for 2-3 hours.

2.6.4. Silver staining of polyacrylamide gels

Silver staining was performed according to Shevchenko et al. (1996). Following electrophoresis, the gel was taken out of the cassette and was fixed in 45% (v/v) methanol and 5% (v/v) acetic acid for 30 min. The gel was washed twice for 10 min in ddH_2O before it was treated with 0.02% (w/v) sodium thiosulphate for 1-2 min. After washing the gel twice in ddH_2O for 1 min, it was impregnated with 0.1% (w/v) silver nitrate at 4°C for 20-30 min. It was rinsed twice with ddH_2O and the developing solution (0.04% (v/v) formaldehyde, 2% (w/v) Na_2CO_3) was added until protein became visible. The color development was stopped by adding 5% (v/v) acetic acid, in which the gel was also stored.

2.6.5. Western blot analyses

By western blotting, proteins previously separated in a polyacrylamide gel were transferred to a nitrocellulose membrane (Schleicher & Schuell). Transfer was performed using the Trans-Blot SD Semi-Dry Electrophoretic Transfer Cell (Bio-Rad). The blot was built from the bottom to the top consisting of five layers of filter paper, nitrocellulose membrane, polyacrylamide gel and five layers of filter paper. Before set up, the filter paper, nitrocellulose membrane and the polyacrylamide gel were soaked in Towbin buffer. Transfer took place at 20 V for 35 min for one gel. Transfer of more than one gel increased the transfer time by 10 min for each additional gel. After transfer the membrane was stained with Ponceau S Solution (Sigma) which detected all proteins bound to the membrane. The blot was destained using PBS.
Western blots were analysed using the Immobilon Western kit from Millipore. First, the membrane was blocked in 5% (w/v) milk in PBS for at least two hours at room tem-

perature. After blocking the membrane was washed three times for 10 min with PBS containing 0.1% (v/v) Tween20 followed by incubation with the first antibody. The antibody was diluted in 1% or 2% (w/v) milk in PBS containing 0.1% (v/v) Tween20 and incubation took place for at least one hour at room temperature. The first antibodies and their dilutions used are listed in Table 2.1. After incubation, the membrane was washed as described above and the second antibody was added. The second antibodies used and their dilutions can be found in Table 2.2. The antibodies were diluted in 1% or 2% (w/v) milk in PBS containing 0.1% (v/v) Tween20 and the membrane was incubated for one hour at room temperature. The second antibody was specific against the animal in which the first antibody was raised and was conjugated to horseradish peroxidase (HRP). After incubation with the second antibody, the membrane was washed as described before and the detection reagents of the Immobilon Western blot detection kit (Millipore) were added. The kit contained two solutions; the HRP Substrate Peroxide Solution and the HRP Substrate Luminol Reagent. Equal volumes of both were mixed and added to the membrane. The reagents reacted with the HRP and produced a chemiluminescent signal with a maximum emission at 430 nm. The resulting light was detected on autoradiography film (Kodak).

2.6.6. Determining protein concentration

The protein concentration of parasite extract was determined by the Bradford assay (Bradford, 1976), using the Bio-Rad protein assay reagent. The absorbance of a protein solution mixed with Bradford reagent (Bio-Rad) was measured at 595 nm and the protein concentration was determined in reference to a standard curve of known BSA concentrations.
The concentration of purified recombinant protein was analysed by measuring the absorbance of the solution at 280 nm. The protein concentration was then calculated using a protein specific extinction coefficient that was calculated using Vector NTI software (Invitrogen).

2.6.7. Generation of polyclonal antibodies

Polyclonal antibodies were generated from purified recombinantly expressed proteins by Eurogentec (Belgium), following their standard immunisation protocols. 400 μg of recombinant LplA1 and H-protein, and 100 μg of recombinant LplA2 were separated by SDS-PAGE, cut out and sent to Eurogentec for immunisation of either rabbits or rats, respectively. Each bleed was tested on recombinant protein and parasite extract to test for specificity.

2.6.8. BugBuster Protein Extraction

To establish optimal expression conditions for a recombinant protein expression construct, the BugBuster protein extraction kit from Novagen was used. 100 ml LB-medium containing the appropriate antibiotics were inoculated with 1-5 ml of an overnight culture of bacteria transformed with the construct of interest. The bacteria were grown at 37°C until OD_{600} was 0.6 and were induced with 1 mM isopropyl-ß-D-thiogalactoside (IPTG) or 200 ng/ml anhydrotetracycline (AHT), depending on the plasmid used. Expression took place at different temperatures (37°C, 30°C, 23°C and 18°C). For protein extraction, 1 ml samples of each culture were taken before induction, each hour after induction and after overnight expression. For analyses, the samples were centrifuged for 1 min at 13200 rpm (Eppendorf microcentrifuge with F45-24-11 rotor), the supernatant was discarded and the pellet was resuspended in 100 μl BugBuster Protein Extraction Reagent. To digest bacterial DNA, 0.5 μl benzonase were added and the mixture was incubated at room temperature with constant shaking. After 15 min, the mixture was centrifuged for 15 min at 13000 rpm (Fisher Scientific accuSpin MicroR with 24-place rotor) and 4°C. The supernatant was transferred into a fresh tube, and the pellet was resuspended in 100 μl PBS. For analyses, 5 μl of the pellet fractions and 15 μl of the supernatant fractions were separated by SDS-PAGE (see 2.6.1) and evaluated by western blotting using specific antibodies against the protein or protein-tag (see 2.6.5).

2.6.9. Expression and purification of proteins with a His-tag

The plasmid pJC40 was used to attach a N-terminal $(His)_{10}$-tag to recombinantly expressed proteins (Figure 2.10) (Clos and Brandau, 1994). Proteins recombinantly expressed using this plasmid were *P. falciparum* LplA1 (see 5.2), *P. falciparum* LplA2 (see 5.3) and *P. falciparum* H-protein and the lipoyl-domains of the KADH-E2 subunits (see 5.5). For expression, 4x 500 ml LB-medium containing 100 μg/ml ampicillin were inoculated with 10-15 ml of a bacteria overnight culture. The bacteria were grown at 37°C and 220 rpm in a shaking incubator until OD_{600} was between 0.5 and 0.6 followed by induction of recombinant protein expression with 1 mM IPTG. The protein was expressed at optimal conditions, which were determined previously using the BugBuster protein extraction kit (see 2.6.8). After the optimal time of expression, the culture was centrifuged for 20 min at 3500 rpm (Sigma 6K15 centrifuge with 12500 rotor) and 4°C. The supernatant was discarded, and the pellet was resuspended in Tris-lysis buffer (50 mM Tris/HCl (pH 7.5), 300 mM NaCl, 10 mM imidazole and 1 mM DTT) or LplA-lysis buffer which contained in addition 10% (v/v) glycerol. The resuspended pellet was stored at -20°C.

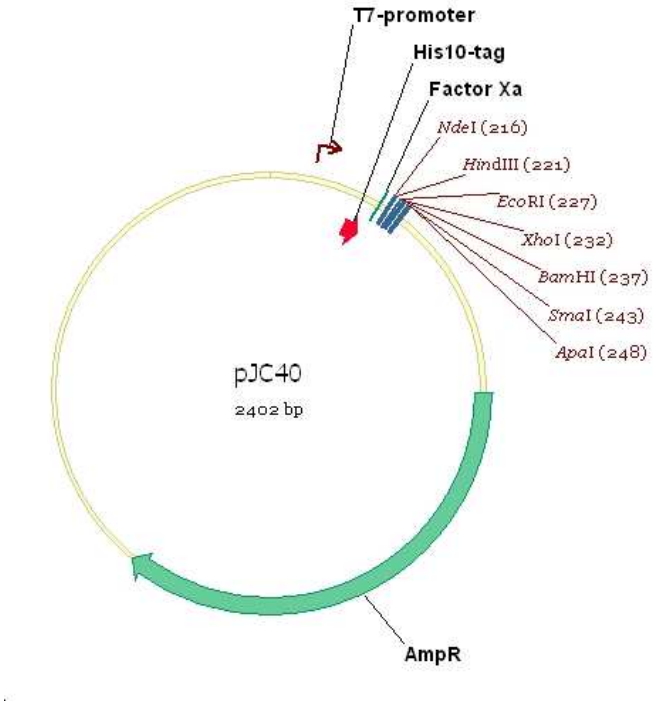

Figure 2.10.: Vector map of pJC40
This figure displays the important features of the pJC40 recombinant expression plasmid. These include the ampicillin resistance cassette (AmpR; 861 bp) and the multiple cloning site (NdeI-ApaI). Recombinant expression using this plasmid is under control of the T7 promoter and attaches a $(His)_{10}$-tag at the N-terminus of the recombinant protein which can be cleaved off with factor Xa.

For purification, the pellet was thawed and 50 μg/ml lysozyme was added. The pellet was incubated for 30 min on ice. Before the bacteria were disrupted the protease inhibitors phenylmethylsulfonylfluoride (PMSF, 1 mM), leupeptin (2 μg/ml) and pepstatin-A (1.5 μM) were added. To disrupt the bacteria they were either sonicated 5-10 times for 30 sec with 30 sec breaks or the one shot cell disrupter (Constant Systems) was used at 15 kpsi. Subsequently, the disrupted bacteria were centrifuged for 60 min at 20000 rpm (Beckman J2-H5 centrifuge with a JA-20 rotor) and 4°C, before the recombinant protein was purified by either batch nickel affinity chromatography (see 2.6.9.1), or FPLC nickel affinity chromatography (see 2.6.9.2).

2.6.9.1. Batch nickel affinity chromatography

After centrifugation, as described above, the supernatant was filtered through a 0.45 μm syringe filter (Sartorius). The following purification was performed using nickel-

nitrilotriacetic acid (Ni-NTA) agarose from Qiagen, which interacted with the His-tag. Approximately 5-10 mg of His-tagged protein bound to 1 ml Ni-NTA agarose. The supernatant of the centrifugation step was transferred onto Ni-NTA agarose, which was equilibrated with the appropriate lysis buffer before (Tris-lysis buffer contained 50 mM Tris/HCl (pH 7.5), 300 mM NaCl, 10 mM imidazole and 1 mM DTT; LplA-lysis buffer also contained 10% (v/v) glycerol). The binding was conducted at 4°C for one hour, rotating on a blood wheel, followed by centrifugation for 5 min at 600 rpm (Sigma 6K15 centrifuge with 11150 rotor) and 4°C. The pelleted Ni-NTA agarose beads with the bound protein were washed four times. Twice with the appropriate lysis buffer, followed by two wash steps with the appropriate wash buffer (50 mM Tris/HCl (pH 7.5), 300 mM NaCl, 20 mM imidazole and 1 mM DTT; LplA-wash buffer also contained 10% (v/v) glycerol). Each wash step was carried out at 4°C for 10 min, rotating on a blood wheel, followed by centrifugation as explained above. The last wash step was poured into a Econo-Pac column (Bio-Rad) and the resin was allowed to set. The protein was eluted from the agarose with elution buffer (50 mM Tris/HCl (pH 7.5), 300 mM NaCl, 500 mM imidazole and 1 mM DTT; LplA-elution buffer also contained 10% (v/v) glycerol). The elution volume varied depending on the recombinant protein and the amount of starting material. The volumes used were between 2 ml and 10 ml elution buffer. The protein concentration was determined by measuring the absorbance of the solution at 280 nm (see 2.6.6). Finally, SDS-PAGE (see 2.6.1) of all samples taken during the purification was carried out and was analysed by Coomassie blue staining (see 2.6.3) or western blotting (see 2.6.5).

2.6.9.2. FPLC nickel affinity chromatography

For FPLC nickel affinity chromatography, HiTrap chelating HP columns (1 ml; GE Healthcare) were used. HiTrap columns were washed sequentially with sterile filtered ddH_2O, 100 mM $NiSO_4$, ddH_2O and LplA-lysis buffer (50 mM Tris/HCl (pH 7.5), 300 mM NaCl, 10% (v/v) glycerol, 10 mM imidazole and 1 mM DTT), before protein samples were preloaded onto a HiTrap chelating column. The protein samples were filtered using a 0.2 μm syringe filter (Sartorius) before being loaded onto the column. The column was then attached to a BioLogic DuoFlow (Bio-Rad), washed with 10 column volumes of LplA-lysis buffer before the sample was eluted using a linear gradient of 10-500 mM imidazole. The linear gradient of imidazole was prepared by the BioLogic DuoFlow by mixing LplA-lysis buffer (10 mM imidazole) with LplA-elution buffer (500 mM imidazole). The elution profile of the proteins loaded onto the column was followed spectrally at 280 nm. Samples from OD_{280} peaks were analysed by SDS-PAGE (see 2.6.1) and western blotting

(see 2.6.5).

2.6.10. Expression and purification of proteins with a Strep-tag

The plasmid pASK-IBA3 (IBA) was used to attach a C-terminal Strep-tag to recombinantly expressed proteins (Figure 2.11). Proteins recombinantly expressed using this plasmid were *P. falciparum* LplA1 (see 5.2) and *P. falciparum* LplA2 (see 5.3).

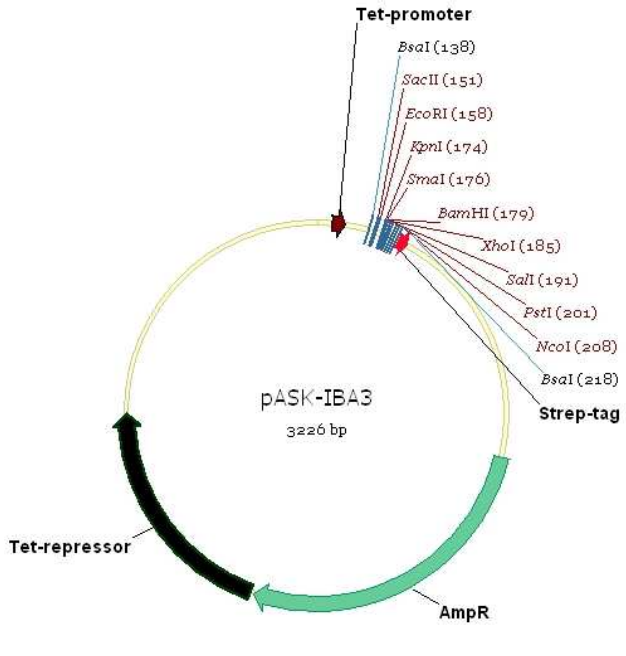

Figure 2.11.: Vector map of pASK-IBA3
This figure displays the important features of the pASK-IBA3 recombinant expression plasmid. These include the ampicillin resistance cassette (AmpR; 861 bp) and the multiple cloning site (BsaI-BsaI). Recombinant expression using this plasmid is under control of the Tet-promoter which is switched off by the Tet-repressor (624 bp) until induction. The Strep-tag is attached to the C-terminus of the recombinant protein.

For expression of recombinant protein, 500 ml LB-medium containing 100 μg/ml ampicillin were inoculated with 10 ml of overnight bacteria culture. The bacteria were grown at 37°C and 220 rpm in a shaking incubator until OD_{600} was between 0.5 and 0.6. The expression of the recombinant protein was induced by addition of 200 ng/ml AHT. The protein was expressed at optimal conditions, which were determined previously using the BugBuster protein extraction kit (see 2.6.8). After the optimal time of expression, the culture was centrifuged for 20 min at 3500 rpm (Sigma 6K15 centrifuge with 12500 rotor) and 4°C. The supernatant was discarded, and the pellet was resuspended in a small

volume of pre-cooled buffer W (100 mM Tris/HCl (pH 8.0), 150 mM NaCl). The resuspended pellet was stored at -20°C.
For purification, the pellet was thawed and 50 μg/ml lysozyme was added. The pellet was incubated for 30 min on ice. Before the bacteria were disrupted, the protease inhibitors PMSF (1 mM), leupeptin (2 μg/ml) and pepstatin-A (1.5 μM) were added. To disrupt the bacteria they were either sonicated 5-10 times for 30 sec with 30 sec breaks or the one shot cell disrupter (Constant Systems) was used at 15 kpsi. Subsequently, the disrupted bacteria were centrifuged for 60 min at 20000 rpm (Beckman J2-H5 centrifuge with a JA-20 rotor) and 4°C. The purification was accomplished using Strep Tactin Sepharose (IBA) in a column procedure. While the bacteria were centrifuged, the column was prepared. 500 μl of Strep Tactin Sepharose was transferred into a Econo-Pac column (Bio-Rad) and was equilibrated with buffer W. The bacterial supernatant was filtered through a 0.45 μm syringe filter (Sartorius) and added onto the Strep-Tactin Sepharose. Samples were taken from the pellet and the supernatant fraction for further analyses. After the supernatant had completely entered the resin by gravity-flow, it was washed with 10 column volumes of buffer W. Again, samples were taken for further analyses. For elution of the protein, 3 ml of elution buffer (buffer W with 2.5 mM desthiobiotin) were used. The eluate was collected in six tubes, each containing 0.5 ml of the elution fraction. The protein concentration of each elution fraction was determined by measuring the absorbance of each fraction at 280 nm (see 2.6.6). Finally, SDS-PAGE (see 2.6.1) of all samples taken during the purification and elution fractions was carried out and analysed by Coomassie blue staining (see 2.6.3) or western blotting (see 2.6.5).

2.7. Functionality and enzyme assays

2.7.1. Complementation assay to confirm *P. falciparum* LplA2 functionality

Three LplA2 expression constructs were generated using the plasmid pASK-IBA3 (see Figure 2.11). The constructs differed in length at their N-termini. The first construct was *lplA2* full length (base pairs 1-1152). Construct S1 consisted of base pairs 79-1152 and construct S2 of base pairs 235-1152. The constructs were transformed into the *lipB* deficient *E. coli* strain Ker184 (Reed and Cronan, 1993) and the *lipB/lplA* deficient *E. coli* strain Tm136 (Morris et al., 1995), to assess whether LplA2 can complement the growth defect of the bacterial lines when grown on minimal medium. The transformed Ker184 were plated on M9 minimal plates containing 100 μg/ml ampicillin, 50 μg/ml kanamycin and 200 ng/ml AHT to induce the expression. The transformed Tm136 were plated on

minimal plates containing the M9 minimal medium salts, 0.4% (w/v) glucose, 7.5 μ/ml $FeSO_4$, 1 μ/ml casein (vitamin free), 0.002% (w/v) thiamine, 1 mM $MgSO_4$, 100 μg/ml ampicillin, 50 μg/ml kanamycin, 15 μg/ml tetracycline and 200 ng/ml AHT. The bacteria were incubated at 37°C until growth was detected.

2.7.2. Lipoylation assay followed by PAGE and western blotting - "Gel assays"

Lipoate protein ligases (LplA) catalyse the attachment of lipoic acid to the lipoyl-domains of the KADH-E2 subunits and to the H-protein of the GCV using ATP and releasing AMP and inorganic pyrophosphate (PPi) as shown in the following equation:

$$\text{Lipoyl-domain} + \text{lipoic acid} + \text{ATP} \rightarrow \text{lipoylated-domain} + \text{AMP} + \text{PPi}$$

In this assay, LplA activity was qualitatively analysed by examining the lipoylation state of the protein substrate - the lipoyl-domain. In native PAGE, the lipoylated form of the protein migrates faster than the non-lipoylated form resulting in a shift of the protein band (Fujiwara et al., 1992). Using SDS-PAGE, the lipoylation state was determined by western blotting using an antibody against protein bound lipoic acid (see Table 2.1).
The lipoylation reaction was performed in a final volume of 30 μl containing 100 mM phosphate buffer (pH 7.4), 2 mM $MgCl_2$, 1 mM DTT, 2 mM ATP, 0.5 mM lipoic acid, 2-4.4 μM protein substrate and varying concentrations of recombinant LplA between 0-3.5 μM. The reaction was carried out at 37°C for 30 min for *E. coli* LplA, and for 60 min for *P. falciparum* LplA1.
If separated by native PAGE, the reaction was terminated by the addition of 2x native sample buffer and the reaction was transferred onto ice. Half of the reaction was separated by 20% native PAGE at 4°C overnight. If separated by SDS-PAGE, the reaction was terminated by the addition of 6x loading buffer. The samples were boiled for 5 min before half of the reaction was separated by 15% SDS-PAGE. The gel was analysed by western blotting using an antibody directed against protein-bound lipoic acid (see Table 2.1).

2.7.3. Spectrophotometric assay

Using the spectrophotometric assay to determine LplA activity, the release of PPi during the reaction was determined as a measure of LplA activity. As shown in Figure 2.12, the spectrophotometric assay is a coupled enzyme assay in which an inorganic pyrophosphatase converts the released PPi to inorganic phosphate (Pi^{2-}). The Pi^{2-} reacts with ammonium molybdate and forms a blue coloured complex which can be detected spec-

trophotometrically at 710 nm. After complex formation, a solution containing bismuth citrate is added to stabilise the formed complexes (Cariani et al., 2004).

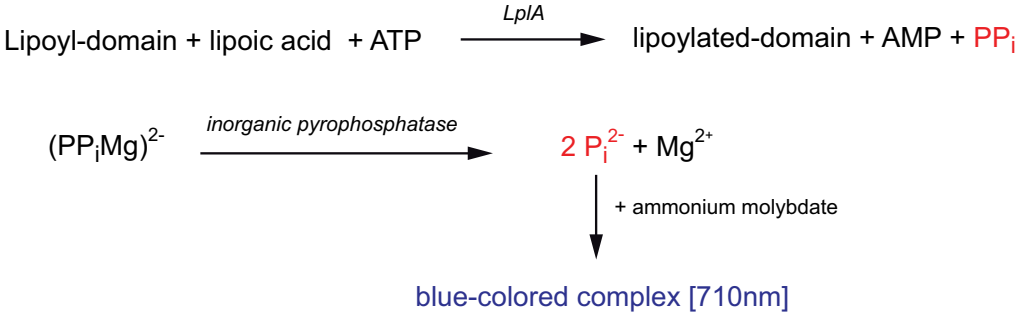

Figure 2.12.: Schematic diagram of spectrophotometric assay
The lipoyl-domains of the KADH-E2 subunits and the H-protein of the GCV are post-translationally lipoylated by LplA. During the LplA reaction ATP is used and AMP and pyrophosphate (PPi) are released. In the spectrophotometric assay, PPi is converted to 2 Pi^{2-} by an inorganic pyrophosphatase. The Pi^{2-} reacts with ammonium molybdate and forms a blue-coloured complex which can be detected spectrophotometrically at 710 nm.

Beside the actual LplA reaction mixture (see below), two solutions were required for this assay.

Solution 1: 3 g ascorbic acid was dissolved in 35 ml ddH_2O. 50 ml of 1 M HCl was added once the ascorbic acid was dissolved, and the solution was cooled down to 0°C on ice. 5 ml of 10% (w/v) ammonium molybdate and 15 ml of 20% (w/v) SDS were added whilst stirring continuously. The solution turned yellow. Kept on ice, solution 1 was stable for four hours.

Solution 2: 3.5 g bismuth citrate was dissolved in 100 ml 1 M HCl. 3.5 g sodium citrate was added. This solution was stable for one week, if protected from light.

To analyse the linearity of this assay and to quantify the released PPi during the LplA reaction, a standard curve of known Pi^{2-} concentrations was generated. A 1 mM K_2HPO_4 solution was used to make up solutions containing 0-30 nmol Pi^{2-} in 30 mM Tris/HCl (pH 7.5), 2 mM $MgCl_2$, 1 mM DTT and 0.5 mM lipoic acid in a final volume of 200 μl. To determine the Pi^{2-} concentration, 400 μl of solution 1 was added and the mixture was incubated on ice. After 10 min, 600 μl of solution 2 was added and the mixture was incubated for a further 10 min at 37°C. Absorbance at 710 nm was measured using a UV-2501PC (Shimadzu) after an additional 20 min at room temperature.

To determine LplA activity using the spectrophotometric assay, the reaction was carried out in a final volume of 200 μl containing 30 mM Tris/HCl (pH 7.5), 2 mM $MgCl_2$, 1 mM DTT, 2.5 U inorganic pyrophosphatase, 0.5 mM lipoic acid, 2 mM ATP and 0-40 μM of protein substrate. The reaction was started by addition of varying concentrations of LplA between 0-1.6 μM, and was incubated at 37°C for 30 min for *E. coli* LplA and 10 min - 30 min for *P. falciparum* LplA1. The reaction was stopped by addition of solution 1 and 2 as described above. Measured absorbance was first converted into Pi^{2-} using the standard curve and was than converted into released PPi. Data were analysed using Prism 3.0 (GraphPad software) and Grafit 5.0 (Erithacus software).

3. LplA1

3.1. Introduction

Apicomplexan parasites possess two machineries to lipoylate the KADH-E2 subunits and the H-protein of the GCV, which require the cofactor lipoic acid for their activity (Perham, 2000, Douce et al., 2001). The apicoplast contains a lipoic acid biosynthesis pathway and the mitochondrion a lipoic acid salvage pathway (Thomsen-Zieger et al., 2003, Wrenger and Müller, 2004). The biosynthesis of lipoic acid is catalysed by two proteins, a octanoyl-[acyl carrier protein]: protein N-octanoyltransferase (LipB) and a lipoic acid synthase (LipA) (Zhao et al., 2003, 2005). LipB attaches octanoyl-ACP provided by fatty acid biosynthesis to the E2 subunit of the PDH and LipA then catalyses the insertion of two sulphur atoms to form the lipoyl moiety. The salvage pathway consists of LplA, a functional lipoate protein ligase, which ligates scavenged lipoic acid to the H-protein and KADH-E2 subunits in the mitochondrion (Wrenger and Müller, 2004, Allary et al., 2007).
In this chapter, the role of LplA1 in *P. falciparum* and *P. berghei* is analysed, and it is assessed whether LplA1 is crucial for parasite survival by reverse genetic approaches.

3.2. Sequence considerations

Structural information about lipoate protein ligases is available from the *E. coli* and *T. acidophilum* proteins (Fujiwara et al., 2005, Kim et al., 2005, McManus et al., 2006). Comparison of *P. falciparum* and *P. berghei* LplA1 with the two bacterial proteins shows only modest sequence similarities to *T. acidophilum* LplA, but higher similarities to the *E. coli* protein (Table 3.1).

Table 3.1.: Sequence similarities of *P. falciparum* and *P. berghei* LplA1 with bacterial LplAs

	E. coli LplA	*T. acidophilum* LplA
P. falciparum LplA1	39.4%	25.5%
P. berghei LplA1	38.4%	23.8%

For further analysis, amino acid sequence alignment of *P. falciparum* and *P. berghei* LplA1 with the two bacterial proteins was performed. The alignment was carried out by combining ClustalW alignments of the bacterial proteins and the *Plasmodium* proteins using the program T-Coffee (Notredame et al., 2000, Poirot et al., 2003) (Figure 3.1). Three sequence motifs (highlighted in red), which are highly conserved in other LplAs, are also found in both *Plasmodium* LplA1s, highlighting the importance of these amino acids for LplA activity. It was shown that these motifs are involved in the formation of the lipoyl-AMP binding pocket, the reaction intermediate which is formed during the LplA reaction. The alignment also shows that the *Plasmodium* proteins possess an approximately 50 amino acid long insertion in comparison to the bacterial proteins. Further, both *Plasmodium* proteins contain an 18 amino acid long N-terminal extension which is likely responsible for targeting the proteins to the mitochondrion. Although 47% of the N-terminal extensions are identical, only the potential cleavage site of the targeting peptide for *P. falciparum* LplA1 can be predicted by MitoProt (indicated by arrow).

P. falciparum and *P. berghei* LplA1 are very similar to each other with 78% amino acid sequence similarity. Additionally, the gene loci are syntenic, except for three small hypothetical proteins in the *P. berghei lplA1* locus (Figure 3.2). These, however, could be a result of miss-annotation and they could actually be exons of the cop-coated vesicle membrane protein p24 precursor, *lplA1* or a conserved hypothetical protein. However, further investigations are required to determine whether these transcripts are present in *P. berghei* RNA.
The following experiments described in this chapter were all performed based using the annotated *lplA1* genes.

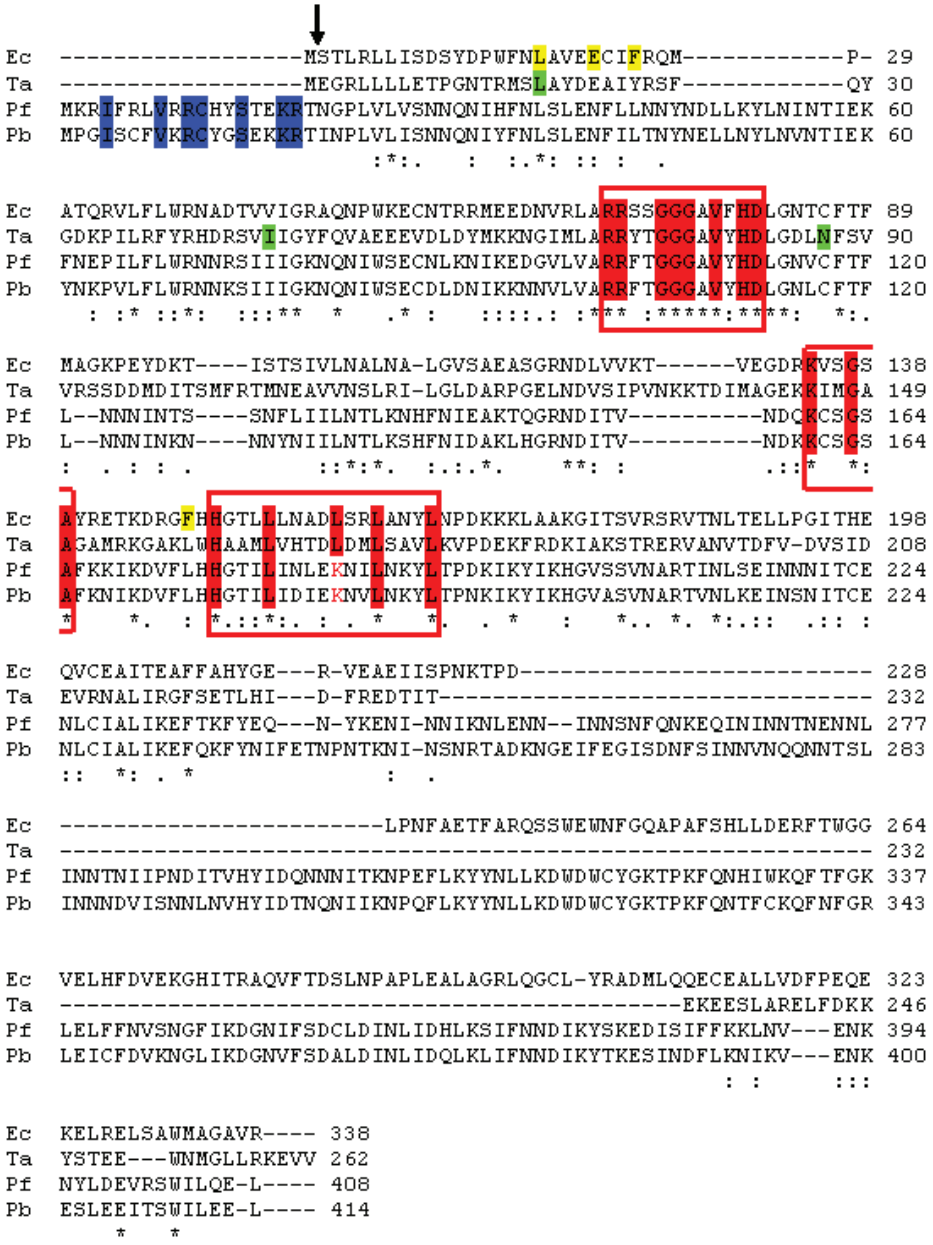

Figure 3.1.: Amino acid sequence alignment of *P. falciparum* and *P. berghei* LplA1 with bacterial LplA

Separate ClustalW alignments of *E. coli* (Ec) / *T. acidophilum* (Tc) LplA and *P. falciparum* (Pf) / *P. berghei* (Pb) LplA1 were combined using the program T-Coffee (Notredame et al., 2000, Poirot et al., 2003) showing (*) identical residues, (:) conserved residues and (.) homologous residues. Three highly conserved sequence motifs, which contain key residues involved in the formation of the lipoyl-AMP binding pocket, are highlighted in red. Residues outside these three motifs involved in lipoic acid binding are highlighted in yellow for the *E. coli* protein and green for the *T. acidophilum* protein. Both *Plasmodium* LplA1s possess a 18 amino acid extension of which 47% are identical residues (highlighted in blue). Both proteins are predicted to be mitochondrial, but a potential cleavage site can only be predicted for *P. falciparum* LplA1 by MitoProt (indicated by the arrow).

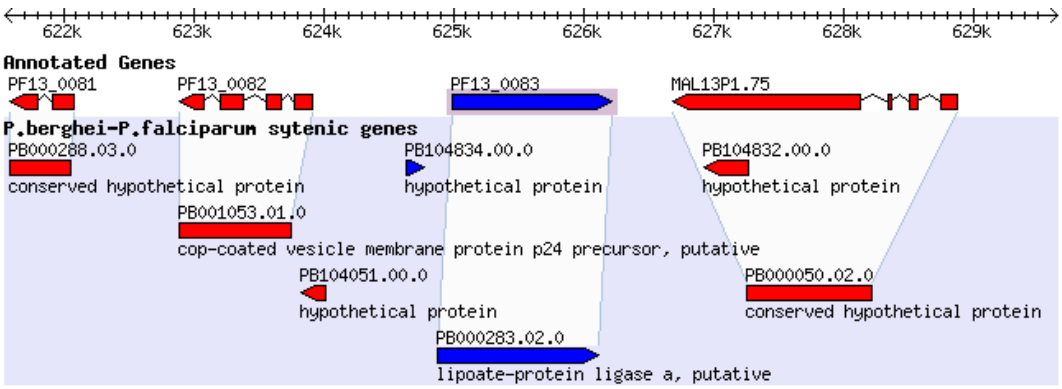

Figure 3.2.: Synteny map of *P. falciparum* and *P. berghei lplA1* gene loci
Synteny map of *lplA1* gene loci was taken from the PlasmoDB website (www.plasmodb.org). The map shows that the gene loci are syntenic except for three small proteins around the annotated *lplA1* gene in *P. berghei*. It is however possible, that they are miss-annotated and that they actually belong to the cop-coated vesicle membrane protein p24 precursor, *lplA1* and the hypothetical protein PB000050.02.0. One distinctive feature of both gene loci is that the *lplA1* coding sequence is on the opposite strand in comparison to the other genes present in the loci.

3.3. Lipoic acid dependent proteins in *P. falciparum*

To confirm that the lipoic acid biosynthesis and salvage pathways are active in *P. falciparum* blood stages, western blot analyses of parasite extract using an antibody directed against protein-bound lipoic acid was performed (Figure 3.3, lane 4). Four bands were detected by the anti-lipoic acid antibody likely corresponding to PDH-E2 (75 kDa), BCDH-E2 (50 kDa), KGDH-E2 (47 kDa) and H-protein (25 kDa). To further support this, western blot analyses were performed using antibodies raised against *P. falciparum* H-protein, BCDH-E2 and KGDH-E2 (Figure 3.3, lanes 1-3) (for antibody dilutions see Table 2.1). The apparent sizes of the proteins detected by the anti-H-protein (26 kDa; lane 1), anti-BCDH-E2 (50 kDa; lane 2) and anti-KGDH-E2 (47 kDa; lane 3) correlate nicely with the protein bands detected by the lipoic acid antibody, suggesting that indeed the mitochondrial KADHs and the H-protein are lipoylated in the erythrocytic stages of *P. falciparum*. It was shown previously that the 75 kDa band detected by the lipoic acid antibody corresponds to the PDH-E2 subunit (Allary et al., 2007).

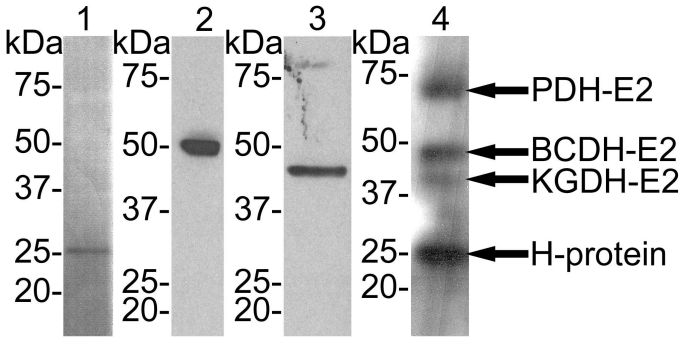

Figure 3.3.: Lipoylation pattern in wild-type parasites
Western blots of *P. falciparum* protein extract (15 μg) were separated on a 4-12% gradient gel and were analysed using four different antibodies: (lane 1) anti-H-protein recognising a 26 kDa band; (lane 2) anti BCDH-E2 recognising a 50 kDa band; (lane 3) anti KGDH-E2 recognising a 47 kDa band; (lane 4) anti-lipoic acid recognising four major protein bands corresponding to PDH-E2 (75 kDa), BCDH-E2 (50 kDa), KGDH-E2 (47 kDa) and H-protein (25 kDa).

Plasmodium PDH is solely found in the apicoplast, whereas the the BCDH and KGDH are present in the mitochondrion (Foth et al., 2005, Günther et al., 2005, McMillan et al., 2005). The H-protein is predicted to be in the mitochondrion as part of the GCV (Salcedo et al., 2005), but there is no experimental support for this prediction. Therefore, H-protein-GFP fusion proteins were generated to investigate H-protein localisation experimentally. Full length H-protein was amplified using the primers H-protein-fwd and H-protein-rev (see 2.1.7) and was cloned in frame with GFP using the MultiSite Gateway plasmids described in Chapter 2.5.2.3 (van Dooren et al., 2005). The destination plasmid pCHD-3/4 (see Figure 2.9) confers resistance to WR99210 and the expression of the fusion protein was controlled by either the *P. falciparum* Hsp86 or CRT promotor. Transfected parasites were analysed by fluorescence microscopy, and to visualise the mitochondrion the parasites were additionally stained with Mitotracker CMXRos (Molecular Probes). Merged images showed clearly that the H-protein is located in the mitochondrion supporting its predicted localisation (Figure 3.4, Panel A). Parasite lines expressing the bipartite leader sequence of the PDH-E2 (amino acids 1-166) cloned in frame with GFP (Panel B) and lines expressing the mitochondrial targeting sequence of the BCDH-E2 (amino acids 1-106) (Panel C) and KGDH-E2 (amino acids 1-114) (Panel D) cloned in frame with GFP were previously analysed in the laboratory (McMillan and Müller, unpublished data). Images of these parasites confirm localisation of the PDH-E2 to the apicoplast, and BCDH-E2 and KGDH-E2 to the mitochondrion.

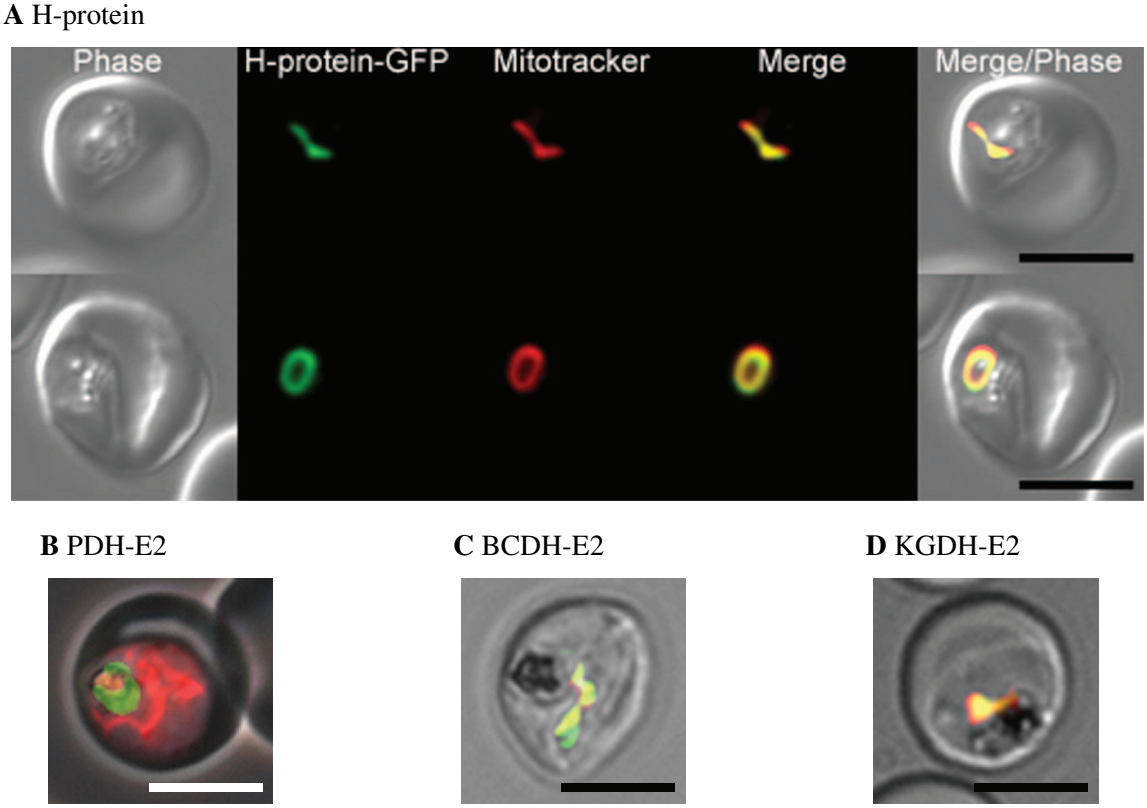

Figure 3.4.: Subcellular localisation of *P. falciparum* H-protein and KADH-E2 subunits (**Panel A**) The subcellular localisation of H-protein was investigated by expressing GFP fusion proteins in the erythrocytic stages of *P. falciparum*. Full length H-protein was cloned in frame with GFP and expression was controlled by either the Hsp86 or CRT promoter. Parasites mitochondria were selectively stained with Mitotracker CMXRos (Molecular Probes) and images of live cells were obtained by DIC microscopy (Phase) or in the FITC (H-protein-GFP) or rhodamine (Mitotracker) fluorescent channels. Overlays of the images are displayed to determine possible co-localisation (Merge). Merged images clearly show co-localisation of H-protein-GFP and Mitotracker, suggesting mitochondrial localisation of the protein. **Panels B-D** display merged images of parasites expressing the bipartite leader sequence of PDH-E2 (amino acids 1-166) in frame with GFP, the target peptide of BCDH-E2 (amino acids 1-106) in frame with GFP and the target peptide of KGDH-E2 (amino acids 1-114) in frame with GFP stained with Mitotracker CMXRos (McMillan and Müller, unpublished data). Scale bars equal 5 μm.

3.4. Knock-out studies in *P. falciparum*

3.4.1. Knock-out studies via single cross-over recombination

To analyse the role of *P. falciparum* LplA1 and to genetically assess it as a potential drug target, knock-out studies in *P. falciparum* were performed using the plasmid pHH1 (see Figure 2.1) (Reed et al., 2000). Using this plasmid, knock-out of the gene is achieved via single cross-over of the knock-out plasmid with the gene locus, which causes an interruption of the endogenous locus and should result ideally in two non-functional copies of the gene (Figure 3.5, Panel B). The plasmid was generated in the laboratory (Figure 3.5, Panel A) and was transfected into 3D7 wild-type parasites according to Deitsch et al. (2001). I took over the transfected parasites and "cycled" them with WR99210 to select for parasites where the transfected plasmid had targeted the *lplA1* gene locus. In the course of one cycle, parasites that were selected for the presence of the marker hDHFR with WR99210 were cultured without drug pressure for three weeks to encourage loss of episomal plasmid. Subsequently, drug pressure was applied again and only those parasites containing either plasmid or selectable marker integrated into their genome survived this treatment. It is believed that the "on-and-off" drug cycles help for a faster selection of stable transfectants. The parasites transfected with the *lplA1* knock-out plasmid were taken through three cycles and gDNA was analysed by Southern blotting to judge whether a disruption of the endogenous gene had occurred (Figure 3.5, Panel C). Probing the Southern blot with *P. falciparum lplA1* showed that no integration into the gene locus had occurred. Gene (1906 bp) and plasmid specific bands (6018 bp) were visible on the Southern blot suggesting that *P. falciparum lplA1* is either essential for parasite survival, and thus knock-out cannot be achieved, or the gene locus cannot be targeted.

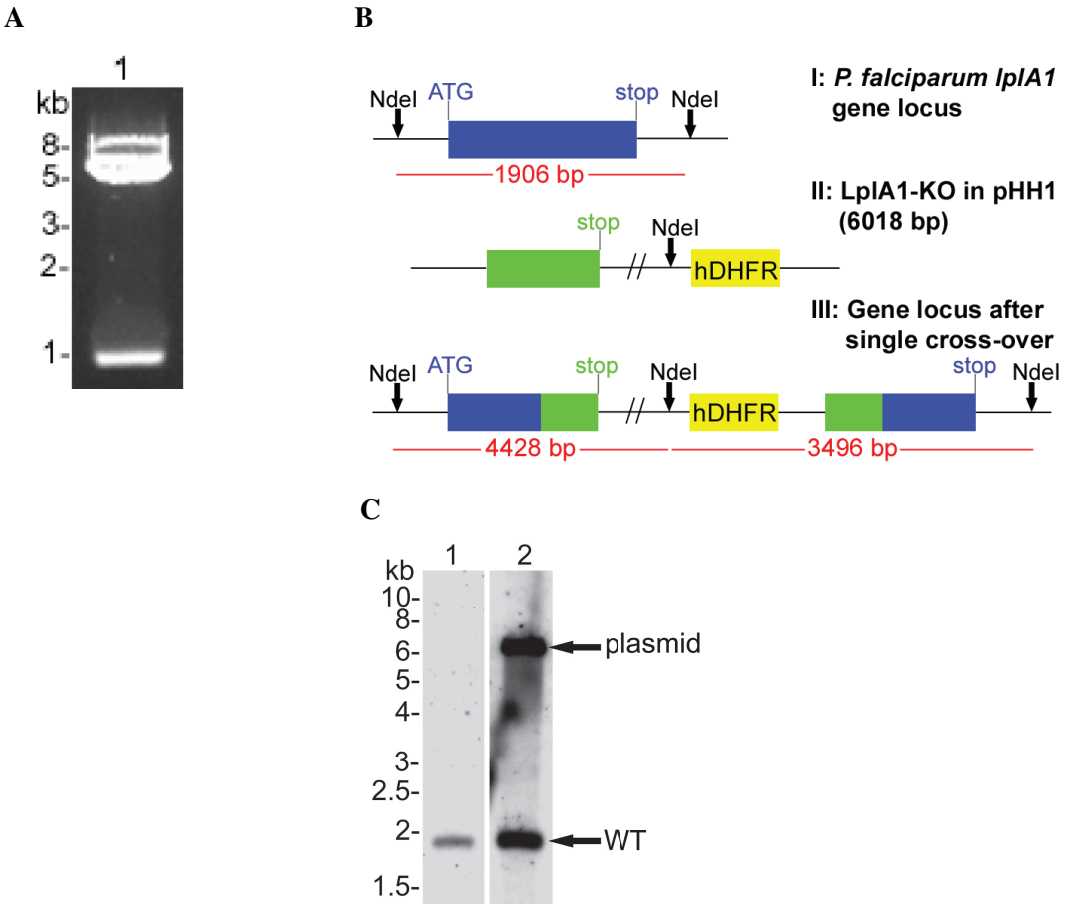

Figure 3.5.: Knock-out studies of *P. falciparum lplA1*
For knock-out studies the plasmid pHH1 was used. (**Panel A**) The 990 bp *lplA1* knock-out fragment was cloned into pHH1 (5760 bp) using the restriction enzymes BglII and XhoI. (**Panel B**) The *lplA1* knock-out fragment lacks the ATG-start codon and is truncated at the C-terminus where in addition an artificial stop-codon is introduced. Knock-out is achieved by single cross-over of this plasmid with the gene locus, which should result in an interruption of the locus generating two non-functional copies of the gene. Digest with the restriction enzyme NdeI results in a specific banding pattern on a Southern blot when probed with *P. falciparum lplA1* (WT: 1906 bp, plasmid: 6018 bp, integration 5': 4428 bp, integration 3': 3496 bp). **Panel C** displays a Southern blot of parasite gDNA digested with NdeI and probed with *P. falciparum lplA1*. Lane 1 contains 3D7 wild-type gDNA and lane 2 gDNA of parasites transfected with the knock-out construct taken through three cycles of WR99210 selection. Arrows indicate plasmid and wild-type bands visible on the Southern blot.

3.4.2. Complementation studies

To address the possibility that *P. falciparum* LplA1 is essential for parasite survival, the parasites already bearing the knock-out plasmid were transfected with a complementation construct carrying the *lplA1* gene from *P. berghei*, to overcome the lethal effect that might occur upon knock-out of the *lplA1* gene. The presence of the episomal copy of *P. berghei lplA1* should allow the knock-out of *P. falciparum lplA1* (Krnajski et al., 2002). *P. berghei lplA1* was amplified using the oligonucleotide primers Pb-LplA-BglII-S and Pb-LplA-NotI-AS (see 2.1.7), introducing a BglII and NotI site for cloning into the single side gateway entry vector pHGB (Tonkin et al., 2004). After sequence verification, *P. berghei lplA1* was sub-cloned into the destination plasmid pHrBI-1/2 which possesses a second selectable marker, the blasticidin-S-deaminase (BSD) conferring resistance to blasticidin (see 2.5.2.3) (Figure 3.6, Panel A). Using this plasmid, the expression of *P. berghei* LplA1 is controlled by the *P. falciparum* Hsp86 promotor, a strong promotor expressing throughout the blood stages (Wu et al., 1995, Militello et al., 2004). The over-expression plasmid was twice transfected into parasites carrying the knock-out plasmid (Crabb and Cowman, 1996, Wu et al., 1996), and the two independent parasite populations obtained were named KO+*Pb*-1 and KO+*Pb*-2. The populations were cultured in the presence of WR99210 and blasticidin to select for the two plasmids. Both parasite lines were taken through two WR99210 cycles with continuous blasticidin selection to maintain the episomal over-expression plasmid. gDNA was prepared and Southern blot analyses were performed for both parasite populations. Figure 3.6 (Panel B and C) show the Southern blots of KO+*Pb*-1 exemplary for both populations. Southern blot analyses revealed that the gene locus (1906 bp) was not targeted. Probing the blot with *P. falciparum lplA1* (Panel B) showed that after transfection (cycle 0), the parasites carried the knock-out plasmid (6018 bp) and over-expression plasmid (9000 bp) episomally (lane 2). However, after the first WR99210 cycle, the band corresponding to the knock-out plasmid disappeared and only the wild-type (1906 bp) and the band likely to correspond with the over-expression plasmid were visible (lane 3). This pattern did not change after the second cycle (lane 4). Probing a blot of wild-type, cycle 0 and cycle 1 gDNA with a hDHFR specific probe (Panel C) showed that the two plasmids apparently had recombined after transfection of the over-expression construct, because the 9000 bp band was also recognised by the hDHFR probe, although the selectable marker of the plasmid is the blasticidin-S-deaminase (BSD). Finally, both parasite populations were taken through a third cycle of drug selection in which both drugs (WR99210 and blasticidin) were removed in an attempt to loose the recombined plasmid and to select for parasites

that potentially had integrated the recombined plasmid. After six weeks, drug pressure (WR99210 and blasticidin) was applied again and parasites were analysed by Southern blotting (Panel B, lane 5). The Southern blots showed the same pattern as before, suggesting that despite the presence of an extra copy of *P. berghei* LplA1, the *P. falciparum lplA1* gene could not be disrupted.

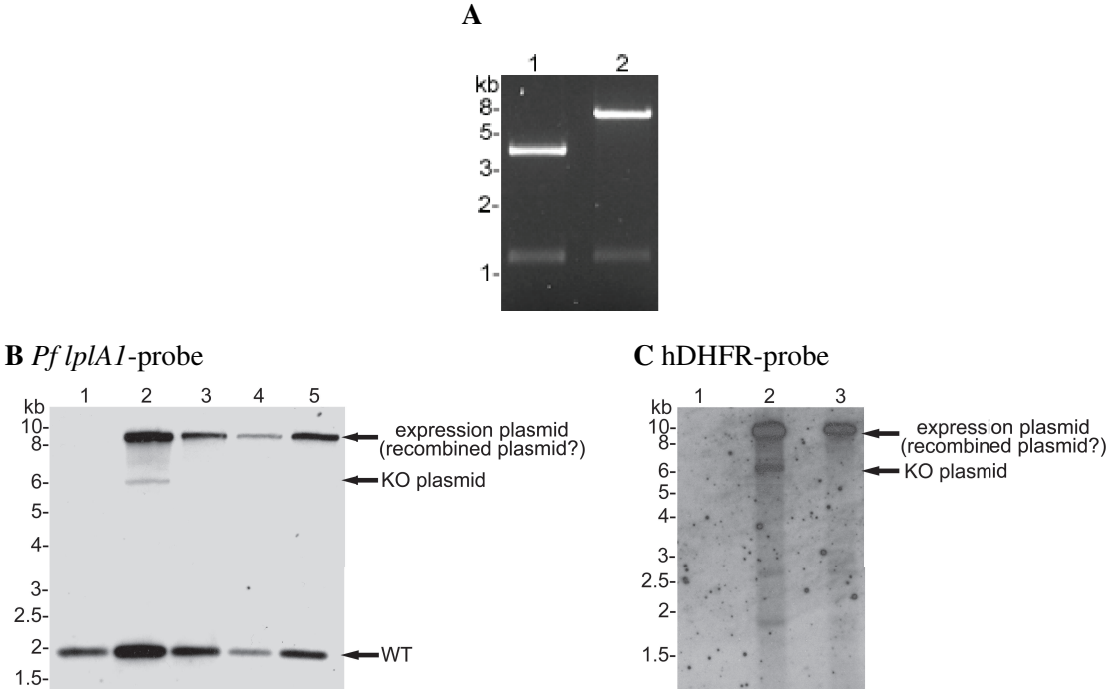

Figure 3.6.: Complementation studies to potentially allow knock-out of *P. falciparum lplA1*

To potentially allow the knock-out of *P. falciparum lplA1* a construct was designed which over-expresses *P. berghei* LplA1, to complement for the loss of *P. falciparum* LplA1 in case of an integration of the knock-out construct. **Panel A**, lane 1 displays full length *P. berghei lplA1* (1245 bp) cloned into the entry-plasmid pHGB (4000 bp) using the restriction enzymes BglII and NotI. Cloning into the destination plasmid pHrBI-1/2 (7800 bp) was performed by single side Gateway cloning (lane 2). **Panel B and C** display Southern blots of the parasite population KO+*Pb*-1. Lane 1 in both blots corresponds to 3D7 wild-type parasites, lane 2 to parasites after transfection of the over-expression plasmid (cycle 0) and lane 3 after the first WR99210 cycle. Lane 4 in Panel B corresponds to parasites after the second WR99210 cycle and lane 5 to parasites after a cycle in which WR99210 and blasticidin were removed (cycle 3). The Southern blot probed with *P. falciparum lplA1* shows that the endogenous *lplA1* gene is present after all cycles (1906 bp), showing that the gene locus was not targeted. The 6018 bp band corresponding to the knock-out plasmid is present after transfection in cycle 0 (lane 2), but disappears after cycle 1 (lanes 3-5). The over-expression plasmid (9000 bp) is present in all cycles (lanes 2-5). Probing the blot with the hDHFR suggests that the knock-out and over-expression plasmid recombined, because the over-expression plasmid was detected by the hDHFR probe. It was surprising that the recombined plasmid was still present after the third cycle in which WR99210 and blasticidin were removed. It suggests that maybe the band at 9000 bp corresponds to an unspecific integration event.

This was somewhat surprising because it was expected that parasites would lose any episomally carried recombined plasmid in the long "off-cycle", and that the third selection would specifically enrich parasites where the target locus was disrupted. Another possible explanation for the presence of the 9000 bp band could be, that the recombined knock-out and over-expression plasmid had integrated into the *P. falciparum* genome non-specifically, and that the observed restriction pattern in the Southern blot band corresponds to this unspecific integration event. To further analyse this possibility, PFGE analyses was performed using wild-type parasites and transfected parasites in cycle 1 and cycle 3 (Figure 3.7). The gene specific *P. falciparum lplA1* probe indicates the presence of the gene on chromosome 13 (Panel A). The hDHFR probe (the selectable marker of the knock-out plasmid) (Panel B) as well as the BSD probe (the selectable marker of the over-expression plasmid) (Panel C) did not detect chromosome 13, indicating that the plasmids had not integrated into the *lplA1* gene locus. However, bands at the bottom of the blot were detected with all three probes used. This is unusual, because episomal plasmids generally run off the gel during PFGE if chromosomes 11-14 are separated (see 2.5.12). The presence of this strong signal however suggests that unspecific integration somewhere on chromosomes <10 had occurred. It also supports recombination of the two plasmids prior to integration, since the hDHFR and BSD probes detect the same bands.

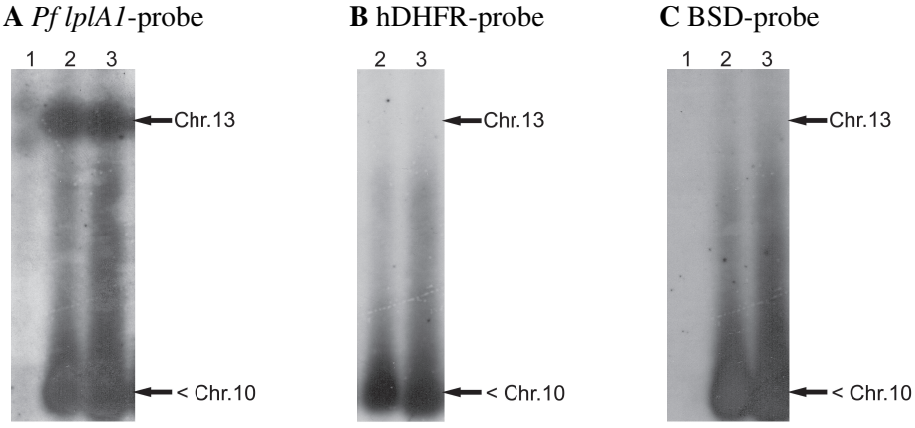

Figure 3.7.: PFGE of KO+*Pb*-1
PFGE of KO+*Pb*-1 parasite population was performed and analysed using *P. falciparum lplA1* (**Panel A**), hDHFR (**Panel B**) and BSD probes (**Panel C**). Lane 1 corresponds to wild-type parasites, lane 2 to KO+*Pb*-1 cycle 1 and lane 3 to KO+*Pb*-1 cycle 3. The *P. falciparum lplA1* probe detected *lplA1* on chromosome 13. The hDHFR and BSD probes did not detect chromosome 13 showing that no integration into the *lplA1* gene locus had occurred. However, additional bands were detected corresponding to chromosomes <10, suggesting that unspecific integration somewhere on these chromosomes had occurred.

There are two possible explanations as to why the recombined plasmid did not integrate into the *lplA1* gene locus. Either *P. berghei lplA1* was not expressed and thus did not complement the possible lethal effect of *P. falciparum lplA1* knock-out, or the gene locus could not be targeted. Therefore, it was first analysed whether *P. berghei* LplA1 was expressed to potentially complement for the loss of *P. falciparum* LplA1 in the event of integration. Western blot analyses of parasite extract using an antibody against *P. falciparum* LplA1 were performed. The predicted size of the annotated *P. falciparum* LplA1 is 45.5 kDa and slightly larger for *P. berghei* LplA1 with 45.8 kDa. Two protein bands were detected by the anti-LplA1 antibody in those parasite lines that harbour the *P. berghei* LplA1 over-expression plasmid whereas in wild-type parasites only the lower molecular weight band was detected (Figure 3.8, Panel A). The intensity of the bands are comparable, suggesting that the use of the heterologous promotor might not effect expression levels of the *P. berghei* protein. However, overall it appears that the parasites expressing both LplA1s − endogenous and *P. berghei* − contain ∼twice the normal amount of the protein which might result in some changes in lipoylation of mitochondrial KADH and H-protein. Therefore, total lipoic acid levels of KO+*Pb*-1 and KO+*Pb*-2 were determined in collaboration with Dr Terry K. Smith, University of Dundee, by gas chromatography-mass spectrometry (GC-MS) (Figure 3.8, Panel B). Analyses revealed that compared to wild-type parasites, there seems to be the tendency for a slight increase of the cofactor bound to protein. This could either be due to more lipoic acid bound to the mitochondrial complexes, or to lipoic acid sequestered by the LplA1 proteins themselves (see 5.6.2).

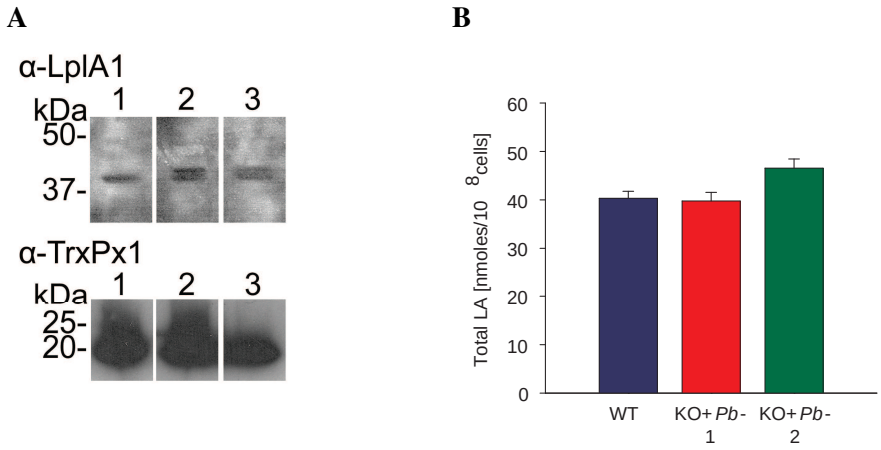

Figure 3.8.: Phenotypical analyses of parasites transfected with the knock-out and over-expression construct

Panel A displays western blots of parasite extract. Lane 1 corresponds to wild-type parasites, lane 2 to KO+*Pb*-1 and lane 3 to KO+*Pb*-2. The blots were probed with an antibody against *P. falciparum* LplA1. Western blot analyses revealed that *P. berghei* LplA1 is expressed in the parasites transfected with the over-expression plasmid. A doublet is visible in these blots (lane 2 and 3) in comparison to wild-type (lane 1) indicating that both *P. falciparum* LplA1 (expected size 45.5 kDa) and *P. berghei* LplA1 (expected size 45.8 kDa) are expressed. The blots were stripped and re-probed with anti-TrxPx1, a peroxiredoxin, as a loading control (Akerman and Müller, 2003). (**Panel B**) The lipoic acid (LA) content of the mutant parasite lines was analysed by GC-MS in collaboration with Dr Terry K. Smith, University of Dundee. Initial results suggest that there are slight variations between the independently transfected parasite lines. The lipoic acid level of KO+*Pb*-1 is comparable to the lipoic acid level determined for wild-type parasites (39.8 nmoles / 10^8 cells and 40 nmoles / 10^8 cells, respectively). The lipoic acid level in KO+*Pb*-2 is higher than that of wild-type parasites (47 nmoles / 10^8 cells). The data represent the mean $\pm$ standard error of three separate measurements on the same parasite batch.

3.4.3. Knock-out control studies

To investigate whether the *lplA1* gene locus could be targeted, a knock-out control construct was designed using the plasmid pHH1. The control construct was amplified using the oligonucleotide primers LplA-pHH1-rescue-fwd and LplA-KOkon-rev (see 2.1.7) introducing a BglII and XhoI site, respectively (Figure 3.9, Panel A). The construct was truncated at the N-terminus, but was full length at the C-terminus including the endogenous stop codon. Thus, integration of the control construct into the gene locus via single cross-over recombination should result in a functional copy of the gene (Figure 3.9, Panel B). 3D7 wild-type parasites were transfected twice with the control construct as described before (Crabb and Cowman, 1996, Wu et al., 1996), and the obtained parasite populations were taken through three WR99210 cycles to select for parasites that had the plasmid integrated into the correct gene locus. Transfectants were analysed by Southern blotting using gDNA that was digested with the restriction enzyme NdeI. Southern blots shown in Figure 3.9 (Panel C and D) were analysed using *P. falciparum lplA1* and hDHFR probes, and are exemplary for both transfected parasite populations. The blots show that the *lplA1* gene locus was not targeted by the knock-out control construct. Parasites after transfection (lane 2), after two WR99210 cycles (lane 3) and after three WR99210 cycles (lane 4) still contained the endogenous *lplA1* gene (1906 bp) (Panel C). A faint band corresponding to episomal plasmid was also detected (6050 bp). In addition, a band at 9000 bp was visible in parasites taken through two and three WR99210 cycles (lanes 3-4) when probed with either probe, and a band at 500 bp was visible in these parasites when probed with the hDHFR probe (Panel C). The presence of these bands and especially the 9000 bp band strongly suggested that the knock-out control construct integrated into the *P. falciparum* genome unspecifically possibly at the same position where integration had occurred of the knock-out/recombined plasmid described above. This was further analysed by PFGE (Figure 3.10). Probing with *P. falciparum lplA1* (Panel A) and hDHFR (Panel B) indeed showed that no integration into chromosome 13 had occurred. Moreover, a band was detected corresponding to chromosomes <10 suggesting unspecific integration of the knock-out control construct on one of these chromosomes.

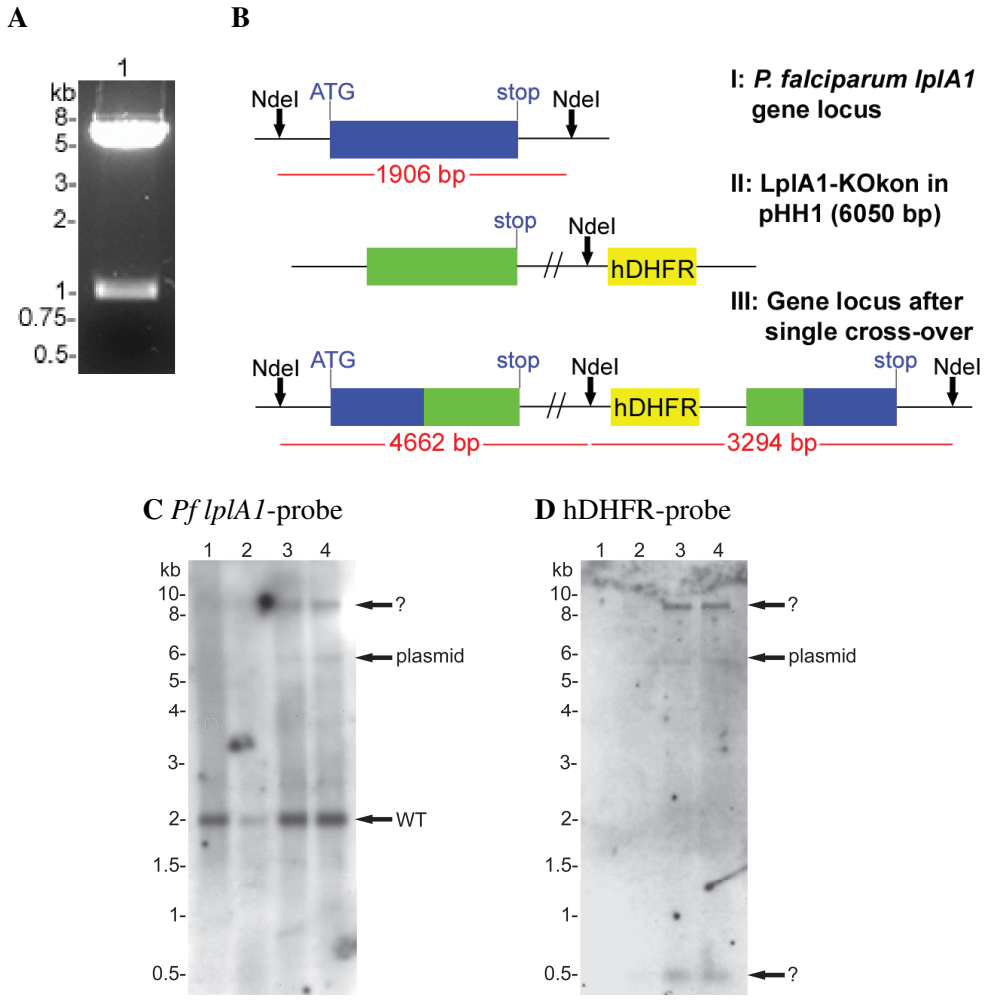

Figure 3.9.: Knock-out control studies of *P. falciparum lplA1*
Panel A shows the 1022 bp *lplA1* control fragment cloned into pHH1 (5760 bp) using the restriction enzymes BglII and XhoI. **Panel B** displays a schematic diagram of the *lplA1* knock-out control integration event. The control fragment is, like the knock-out construct truncated at the N-terminus, but is in contrast full length at the C-terminus retaining the endogenous stop codon. Integration of the knock-out control construct into the gene locus should thus result in the disruption of the locus generating a functional copy of the gene. Digest with the restriction enzyme NdeI results in a specific banding pattern on a Southern blot when probed with *P. falciparum lplA1* (WT: 1906 bp, plasmid: 6050 bp, integration 5': 4662 bp, integration 3': 3294 bp). **Panel C and D** display Southern blots of parasite gDNA digested with NdeI and probed with *P. falciparum lplA1* and hDHFR. Lane 1 in both blots contains 3D7 wild-type gDNA, lane 2 gDNA of parasites after transfection (cycle 0), lane 3 gDNA of transfected parasites in cycle 2 and lane 4 gDNA of transfected parasites in cycle 3. Arrows indicate the endogenous *lplA1* (1906 bp) and the plasmid specific band (6050 bp) showing that no integration into the *lplA1* gene locus had occurred. Additional bands at ∼9000 bp in both blots and at ∼500 bp in the hDHFR probed blot suggest that unspecific integration had occurred.

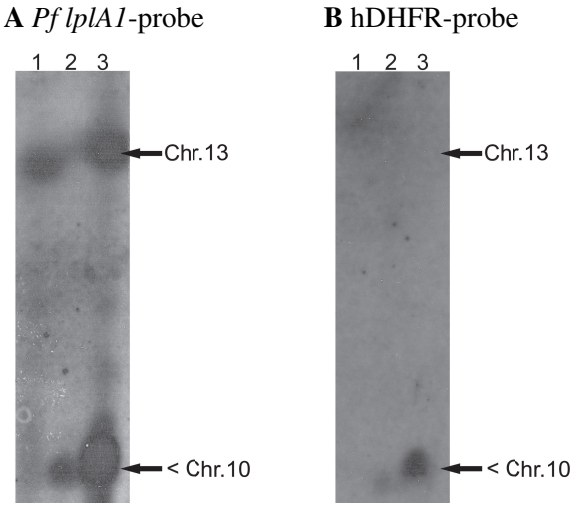

Figure 3.10.: PFGE of LplA1-KOkon-pHH1 transfected parasites
PFGE of parasites transfected with LplA1-KOkon-pHH1 was performed and analysed using *P. falciparum lplA1* (**Panel A**) and hDHFR probes (**Panel B**). Lane 1 corresponds to wild-type parasites, lane 2 to transfected parasites in cycle 0 and lane 3 to transfected parasites in cycle 3. The *P. falciparum lplA1* probe detected *lplA1* on chromosome 13. The hDHFR probe did not detect chromosome 13 showing that no integration into the *lplA1* gene locus had occurred. However, an additional band was detected corresponding to chromosomes <10, suggesting that unspecific integration somewhere on these chromosomes had occurred.

3.5. Over-expression of *P. berghei* LplA1

3.5.1. Genotypical analyses

D10 wild-type parasites were transfected with the *P. berghei lplA1* over-expression construct described in Chapter 3.4.2. Genotypical analyses of two independent transfected parasite populations named *Pb*LplA1-1 and *Pb*LplA1-2 were performed by Southern blotting, using *P. falciparum lplA1* and BSD specific probes (Figure 3.11). gDNA was digested with the restriction enzyme NdeI resulting in a *P. falciparum lplA1* gene specific band of 1906 bp and a plasmid specific band of 9000 bp. The Southern blot probed with the *P. falciparum lplA1* probe only detected the endogenous *P. falciparum lplA1* gene, but did not cross-react with the *P. berghei* gene in the over-expression plasmid (Panel A). The presence of plasmid in *Pb*LplA1-1 and *Pb*LplA1-2 was only shown by probing the blot with the BSD specific probe (Panel B).

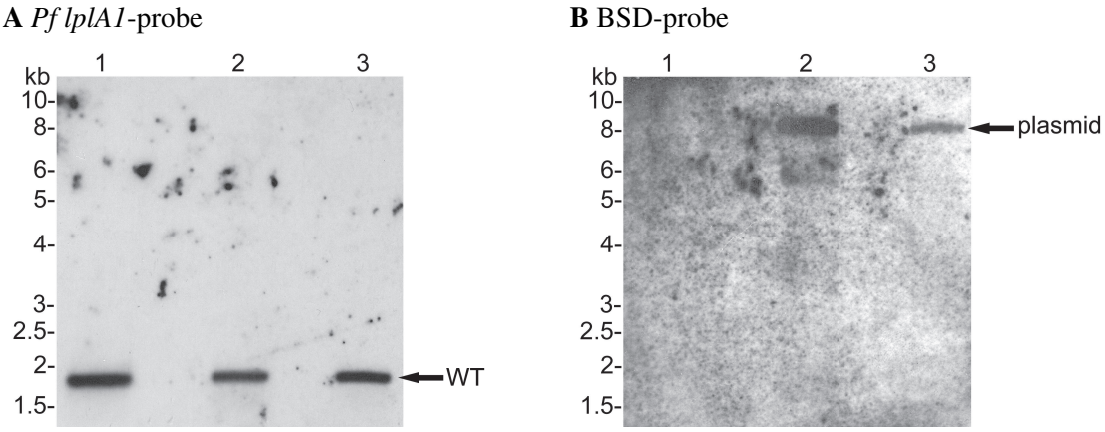

Figure 3.11.: Genotypical analyses of *P. berghei* LplA1 over-expressing parasites
D10 wild-type parasites were transfected with the *P. berghei* LplA1 over-expression plasmid and two independent parasite lines were obtained. The genotype of these lines was analysed by Southern blotting using *P. falciparum lplA1* (**Panel A**) and BSD (**Panel B**) probes. gDNA of wild-type (lane 1), *Pb*LplA1-1 (lane 2) and *Pb*LplA1-2 (lane 3) was digested using the restriction enzyme NdeI and analysed by Southern blotting. The *P. falciparum lplA1* probe did not cross-react with the *P. berghei lplA1* gene in the plasmid, thus only detecting endogenous *P. falciparum lplA1* (1906 bp). Using the BSD probe the over-expression plasmid (9000 bp) was detected.

3.5.2. Phenotypical analyses

For phenotypical analyses of parasites over-expressing *P. berghei* LplA1, the *Pb*LplA1-1 population was used. First, western blot analyses were performed using an antibody against *P. falciparum* LplA1 (Figure 3.12, Panel A). Western blotting confirmed that both LplA1s were expressed in the *Pb*LplA1-1 population, showing a doublet corresponding to *P. falciparum* LplA1 (45.5 kDa) and *P. berghei* LplA1 (45.8 kDa), in comparison to D10 wild-type parasites. Western blot analyses showed that both proteins are present in the parasites to equal amounts, suggesting that episomal "over-expression" of *P. berghei* LplA1 results in endogenous expression levels. Parasites over-expressing *P. berghei* LplA1 thus contain approximately double the amount of LplA1 proteins in comparison to wild-type parasites. This could have an effect on the lipoylation levels of mitochondrial KADH and/or H-protein. Thus, the lipoic acid content of *Pb*LplA1-1 was analysed by GC-MS in collaboration with Dr Terry K. Smith, University of Dundee (Figure 3.12, Panel B). Initial results suggest, that *Pb*LplA1-1 indeed contains more protein bound lipoic acid in comparison to wild-type parasites (54 nmoles/10^8 cells and 40 nmoles/10^8 cells, respectively). However, it is not clear whether this is due to higher lipoylation levels of the KADH-E2 subunits and H-protein or whether the lipoic acid is bound to the ligases themselves (see 5.6.2).

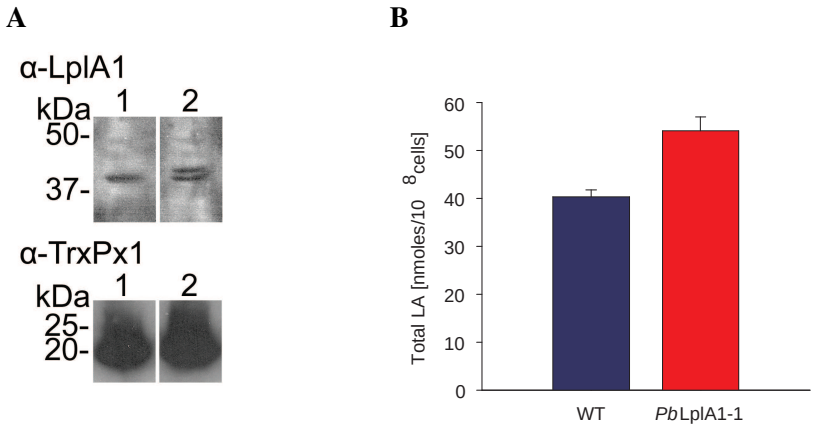

Figure 3.12.: Phenotypical analyses of *P. berghei* LplA1 over-expression parasites
Panel A displays western blots of parasite extract. Lane 1 corresponds to wild-type parasite and lane 2 to *Pb*LplA1-1. The blots were probed with an antibody against *P. falciparum* LplA1. Western blot analyses revealed that *P. berghei* LplA1 is expressed in the parasite line transfected with the over-expression plasmid. A doublet is visible in the blot (lane 2) in comparison to wild-type (lane 1) indicating that both *P. falciparum* LplA1 (expected size 45.5 kDa) and *P. berghei* LplA1 (expected size 45.8 kDa) are expressed. The blots were stripped and re-probed with anti-TrxPx1 as a loading control (Akerman and Müller, 2003). (**Panel B**) The lipoic acid (LA) content of the mutant parasite line was analysed by GC-MS in collaboration with Dr Terry K. Smith, University of Dundee. Initial results suggest that *Pb*LplA1-1 contains more lipoic acid than wild-type parasites (54 nmoles / 10^8 cells and 40 nmoles / 10^8 cells, respectively). The data represent the mean $\pm$ standard error of three separate measurements on the same parasite batch.

It was further investigated whether over-expression of *P. berghei* LplA1 had an effect on parasite growth. The progression through the intraerythrocytic developmental cycle was investigated. Thin-smears of highly synchronised *Pb*LplA1-1 and D10 wild-type parasites taken every 8 hours in the 48 hour developmental cycle were analysed by light microscopy (Figure 3.13). In the first 16 hours (Panel A-C), *Pb*LplA1-1 progression was slightly accelerated through the intraerythrocytic developmental cycle in comparison to D10, suggesting that the development from ring stage parasites to early trophozoites was not negatively affected by over-expression of *P. berghei* LplA1. However, after 24 hours (Panel D), all D10 parasites were in the trophozoite stage, whereas 7% of *Pb*LplA1-1 were still in the ring stage, suggesting that a small proportion of the over-expressing parasites were slowed down in their progression through the developmental cycle. The second half of the developmental cycle (from trophozoite to schizont) seemed to be more affected and was slowed down to some extend. After 32 hours (Panel E), 53% of the D10 parasites were already schizonts whereas only 32% of the over-expresser were in this developmen-

tal stage. The decelerated progression is particulary obvious after 48 hours (Panel G), where 85% of the D10 parasites had re-invaded erythrocytes and were in the ring stage. Only 46% of the parasites analysed of the *Pb*LplA1-1 population were at this time in the ring stage, suggesting that over-expression of LplA1 had a modest negative effect on the intraerythrocytic developmental cycle in these parasites lines. These observations suggest that the correct concentration of LplA1 in the blood stages is important for their development.

A 0h

I

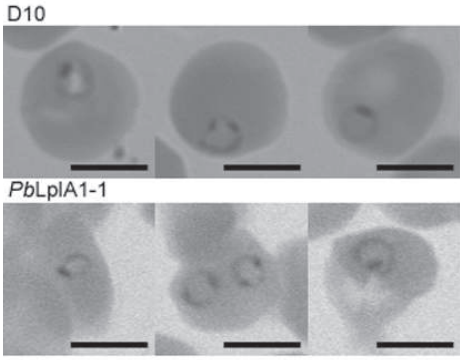

II

	ring	trophozoite	schizont
D10 (n=11)	100%	-	-
***Pb*LplA1-1** (n=12)	100%	-	-

B 8h

I

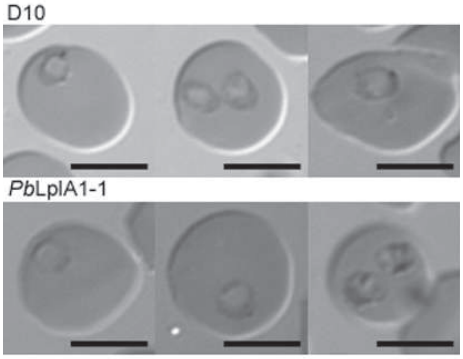

II

	ring	trophozoite	schizont
D10 (n=10)	80%	20%	-
***Pb*LplA1-1** (n=9)	67%	33%	-

C 16h

I

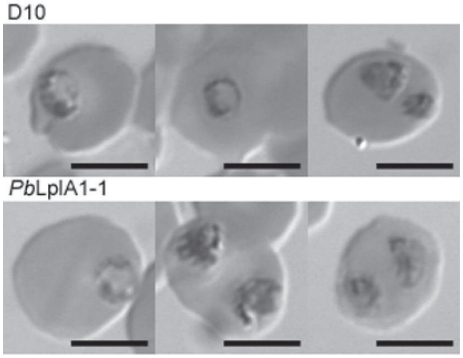

II

	ring	trophozoite	schizont
D10 (n=15)	47%	53%	-
***Pb*LplA1-1** (n=13)	31%	69%	-

D 24h

I

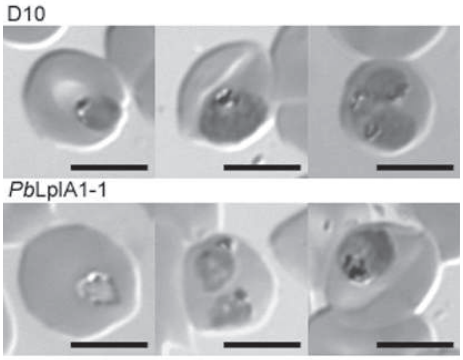

II

	ring	trophozoite	schizont
D10 (n=22)	-	100%	-
***Pb*LplA1-1** (n=14)	7%	93%	-

E 32h

I

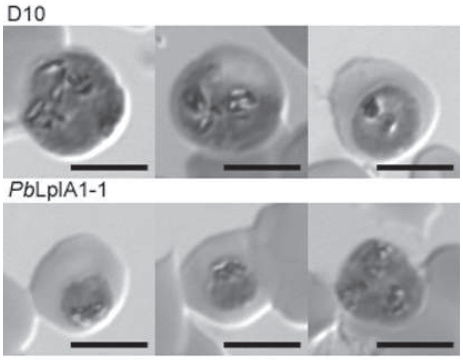

II

	ring	trophozoite	schizont
D10 (n=15)	-	47%	53%
***Pb*LplA1-1** (n=22)	4%	64%	32%

F 40h

I

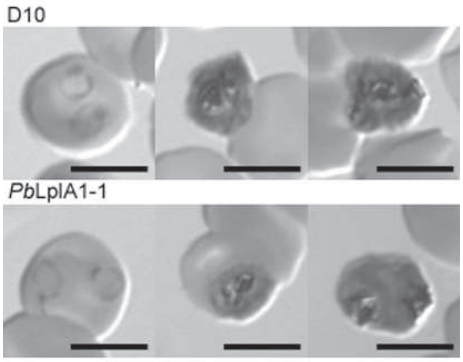

II

	ring	trophozoite	schizont
D10 (n=21)	38%	-	62%
***Pb*LplA1-1** (n=16)	37%	19%	44%

G 48h

I

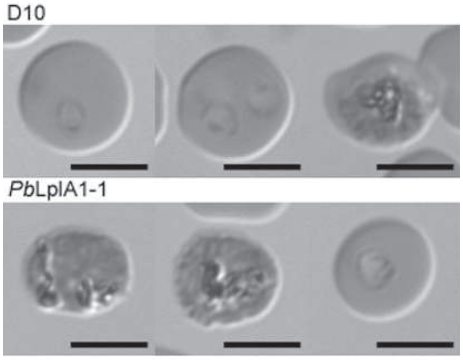

II

	ring	trophozoite	schizont
D10 (n=20)	85%	-	15%
***Pb*LplA1-1** (n=13)	46%	-	54%

Figure 3.13.: *Pb*LplA1-1 development through the intraerythrocytic cell cycle
Progression through the intraerythrocytic developmental cycle was assessed by taking thin-smears of highly synchronised cultures which were analysed by light microscopy. The photographs (I) show Giemsa stained blood smears from *Pb*LplA1-1 and D10 wild-type parasites taken every 8 hours over the 48 hour time course (**Panel A-G**). (II) gives the percentile portion of the three different intraerythrocytic developmental stages for each time point. During the first 16 hours of the intraerythrocytic developmental cycle, the *P. berghei* LplA1 over-expresser grow slightly faster than the D10 wild-type parasites (Panel A-C). However, decelerated growth was observed from 24 hours in the intraerythrocytic developmental cycle, when all wild-type parasites were in the trophozoite stage whereas *Pb*LplA1-1 still contained ring stage parasites (Panel D). This effect persisted until the end of the experiment (Panel E-G). Scale bars equal 5 μm.

3.6. Knock-out studies in *P. berghei*

Knock-out studies of *P. berghei lplA1* were performed in collaboration with Prof Kai Matuschewski, University of Heidelberg, Germany. Two different strategies were utilised to knock-out *lplA1*. For both, the plasmid b3D.DT^H.^D (see Figure 2.2) was used (kindly provided by A. P. Waters, Leiden University, The Netherlands). The first knock-out strategy equals the one described for *P. falciparum* gene knock-out and involves single cross-over recombination of the knock-out plasmid with the gene locus of interest. The second strategy involves double cross-over recombination of the knock-out plasmid with the gene locus, which should result in the replacement of the gene of interest with the selectable marker of the plasmid, the *T. gondii* DHFR/TS.

3.6.1. Knock-out studies via single cross-over recombination

For knock-out studies via single cross-over recombination, the plasmid *Pb*LplA1-KO-b3D was designed. Similar to knock-out studies in *P. falciparum*, a 1014 bp fragment corresponding to nucleotides 88-1098 of *P. berghei lplA1* was amplified using the primers Pb-LplA-int-fwd and Pb-LplA-int1-rev (see 2.1.7). An artificial stop codon was introduced at the 3' end of the PCR product and the fragment was cloned into the second multiple cloning site of b3D.DT^H.^D using the restriction enzymes BamHI and SacII (Figure 3.14, Panel A). Integration of *Pb*LplA1-KO-b3D into the *lplA1* locus should disrupt the locus resulting in two non-functional copies of the gene (Figure 3.14, Panel B). For transfection, *Pb*LplA1-KO-b3D was linearised using the restriction enzyme HpaI which cuts within the *P. berghei lplA1* knock-out fragment (Figure 3.14, Panel A). Linearised *Pb*LplA1-KO-b3D was transfected three times into NK65 wild-type parasites according to Janse et al. (2006), and after pyrimethamine selection in mice, the obtained parasite populations were analysed by PCR, using the gene locus specific primers PbLplA1-test-fwd and Pb-LplA-REP-rev (black arrows), and the plasmid specific primers Tg-for and b3D-rev (red arrows). Combinations of these primers were used to amplify 3' and 5' specific integration fragments (Figure 3.14, Panel B) (see 2.1.7). gDNA was prepared of the three independent parasite populations and Figure 3.14 (Panel C) shows the results of one parasite population exemplary for all three. *Pb*LplA1-KO-b3D had not integrated into the gene locus. I was not able to amplify either the 3' integration specific PCR product (2375 bp; lane 1) or the 5' integration specific PCR product (1727 bp; lane 2). However, recombined plasmid (1628 bp; lane 3) and wild-type *P. berghei lplA1* (2479 bp; lane 4) were present in the parasite populations. These data suggest that either a knock-out of *P. berghei lplA1* is not possible because LplA1 might be essential for *P. berghei* blood-stages, or the gene locus is refractory to integration, as it might be the case in *P. falciparum*.

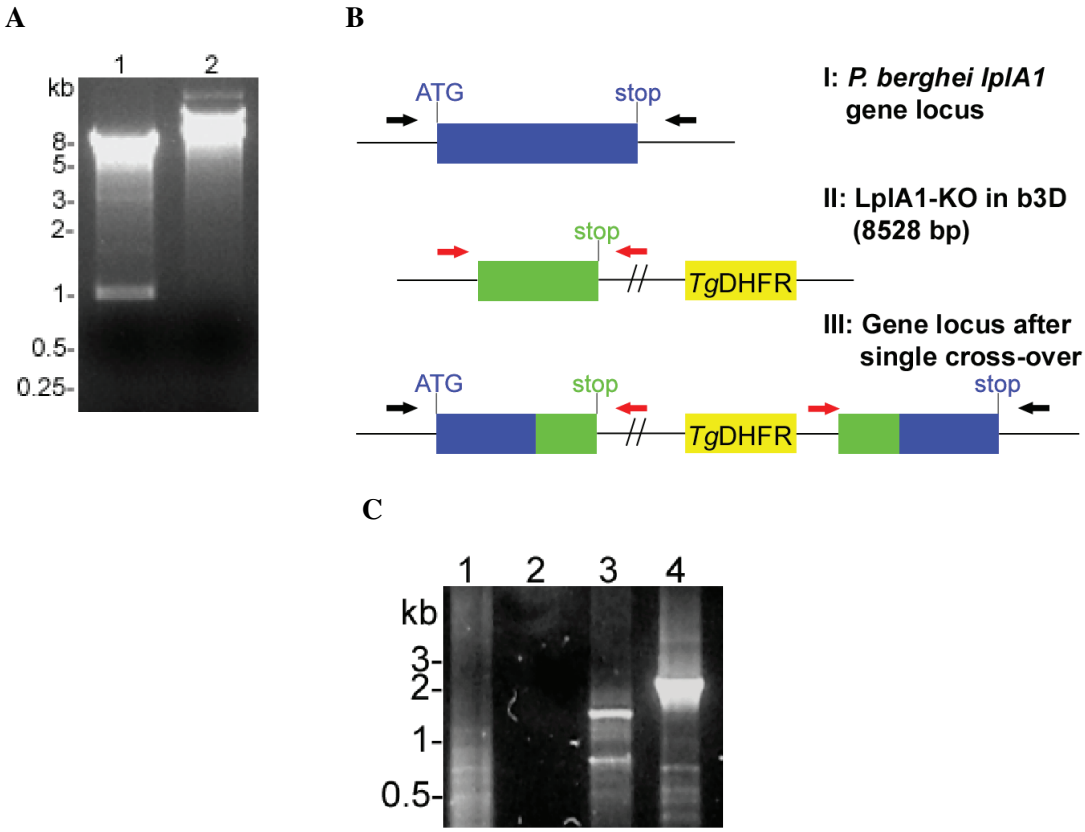

Figure 3.14.: Knock-out studies of *P. berghei lplA1* using the integration strategy (**Panel A**) The 1014 bp knock-out fragment was amplified from the *P. berghei* gDNA and was cloned into b3D.DT^H.^D (7514 bp) using the restriction enzymes BamHI and SacII (lane 1). Before transfection, *Pb*LplA1-KO-b3D was linearised using HpaI, resulting in a 8528 bp fragment (lane 2). **Panel B** is a schematic diagram of the integration of *Pb*LplA1-KO-b3D. Transfectants were analysed by PCR using gene locus specific primers (black arrows) and plasmid specific primers (red arrows). **Panel C** displays the PCR analyses of transfected parasites. Lane 1 shows the 3' integration specific PCR (2375 bp), lane 2 the 5' integration specific PCR (1727 bp), lane 3 the plasmid specific PCR (1628 bp) and lane 4 the wild-type specific PCR (2479 bp). The knock-out plasmid did not integrate into the gene locus. The plasmid was present as an episome.

3.6.2. Knock-out control studies via single cross-over recombination

To assess whether the *P. berghei lplA1* gene locus is refractory to integration, a control construct was generated which was named *Pb*LplA1-KOkon-b3D. The control fragment was amplified using the oligonucleotide primer Pb-LplA-int-fwd and Pb-LplA-3'-rev, resulting in a 1734 bp PCR fragment that was cloned directionally into the second multiple cloning site of b3D.DT^H.^D using the restriction enzymes BamHI and SacII (Figure 3.15, Panel A). The control fragment was truncated at the N-terminus therefore missing the ATG-start codon, but was full length at the C-terminus including the endogenous stop codon and 3' UTR. Thus, integration of the control construct into the *lplA1* gene locus should result in a functional copy of the gene (Figure 3.15, Panel B). Prior transfection *Pb*LplA1-KOkon-b3D was linearised using the restriction enzyme HpaI (Figure 3.15, Panel A), and the linearised construct was transfected only once into NK65 wild-type parasites. After pyrimethamine selection, the obtained parasite population was analysed by PCR using the primers described above in Chapter 3.6.1 (Figure 3.15, Panel B). Figure 3.15 (Panel C) displays the results of the PCR analyses showing that *Pb*LplA1-KOkon-b3D had integrated into the gene locus. The 3' integration specific band (2375 bp; lane 1), which was also verified by sequencing, and the 5' integration specific PCR band (2447 bp; lane 2) were amplified. Recombined plasmid (2348 bp; lane 3) and wild-type *P. berghei lplA1* (2479 bp; lane 4) were also present showing that it was a mixed population. This clearly shows, that the *P. berghei lplA1* locus can be targeted in contrast to the *P. falciparum lplA1* gene locus. Furthermore, it suggests that LplA1 might be essential for *P. berghei* blood stages, because the knock-out construct described above did not target the *lplA1* locus after three independent transfections. To further investigate this possibility, knock-out studies via double cross-over recombination were carried out additionally.

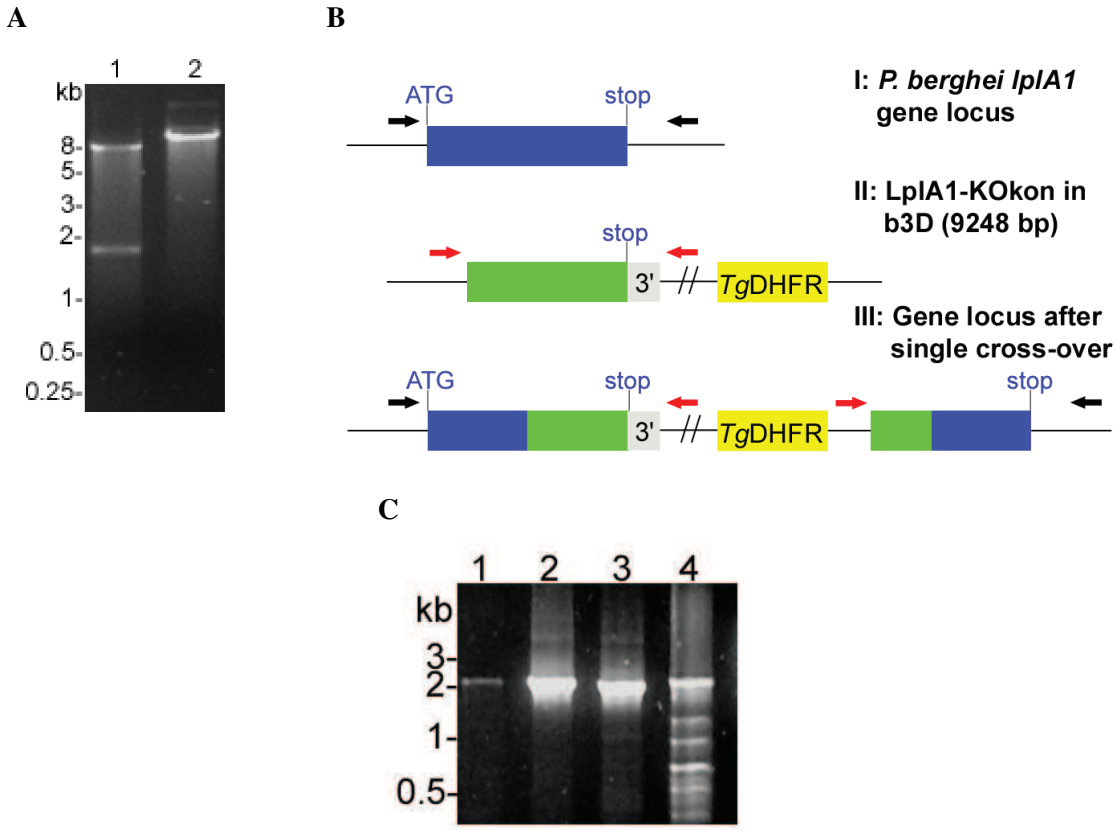

Figure 3.15.: Knock-out control studies of *P. berghei lplA1* using the integration strategy (**Panel A**) The 1734 bp knock-out control fragment was amplified from the *P. berghei* gDNA and was cloned into b3D.DT^H.^D (7514 bp) using the restriction enzymes BamHI and SacII (lane 1). Before transfection *Pb*LplA1-KOkon-b3D was linearised using HpaI resulting in a 9248 bp fragment (lane 2). **Panel B** is a schematic diagram of the integration of *Pb*LplA1-KOkon-b3D. Transfectants were analysed by PCR using gene locus specific primers (black arrows) and plasmid specific primers (red arrows). **Panel C** displays the PCR analyses of the transfectants. Lane 1 shows the 3' integration specific PCR (2375 bp), lane 2 the 5' integration specific PCR (2447 bp), lane 3 the plasmid specific PCR (2348 bp) and lane 4 the wild-type specific PCR (2479 bp). The knock-out control plasmid did integrate into the gene locus. However, the parasite population was mixed because episomal plasmid and wild-type *P. berghei lplA1* were also detected by PCR.

3.6.3. Knock-out studies via double cross-over recombination

Double cross-over of the knock-out plasmid with the gene locus should result in the replacement of the gene with the selectable marker of the plasmid, the *T. gondii* DHFR/TS. For this strategy, the 5' and 3' UTRs of *P. berghei lplA1* were amplified using the primer pairs Pb-LplA-5'-fwd / Pb-LplA-5'-rev and Pb-LplA-3'-fwd / Pb-LplA-3'-rev, respectively (see 2.1.7). The 480 bp 5' UTR fragment was amplified and cloned directionally into the first multiple cloning site of b3D.DT^H.^D, using the restriction enzymes KpnI and HindII. The PCR product amplified using the 3' UTR primer pair, was 516 bp in size and was cloned into the second multiple cloning site of the plasmid using NotI and SacII (Figure 3.16, Panel A). The resulting plasmid was named *Pb*LplA-REP-b3D. Transfection of this plasmid was performed as described by Janse et al. (2006). Before transfection, *Pb*LplA-REP-b3D was "linearised" with the restriction enzymes KpnI and SacII resulting in two fragments, a 5636 bp fragment containing the two *P. berghei lplA1* UTRs and the *T. gondii* DHFR/TS expression cassette, and a 2864 bp fragment containing the plasmid backbone (Figure 3.16, Panel A). Using this construct, knock-out is achieved by double cross-over of the 5' and 3' UTRs of *P. berghei lplA1*, which should result in the replacement of the gene with the selectable marker (Figure 3.16, Panel B). Digested *Pb*LplA-REP-b3D was transfected six times and parasite populations obtained after pyrimethamine selection in mice were analysed by PCR, using either the gene locus specific primer combination Pb-LplA-int-fwd / Pb-LplA-REP-rev (1837 bp) or PbLplA1-test-fwd / PbLplA1-test-rev (2479 bp) (black arrows) and the plasmid specific primers Tg-for, b3D-rev and Tg-rev (red arrows) (see 2.1.7). In five out of the six independent transfected lines, *Pb*LplA-REP-b3D had recombined and was amplified, suggesting that the DNA used for the transfection was not completely digested. If this is the case, the linearised DNA is lost quickly from the parasites, and the presence of pyrimethamine selects for the plasmid rather than the gene replacement. The sixth parasite population that was analysed revealed replacement of the *lplA1* locus, and the PCR results are shown in Figure 3.16 (Panel C). The replaced 3' UTR was amplified (1183 bp; lane 1) and sub-cloned to verify that the PCR product was specific for the replaced gene locus. However, the PCR fragment could only be obtained after two rounds of amplification, suggesting that only a minor proportion of the parasite population indeed contained the replaced *lplA1* gene locus. When the parasite population was transferred into a second mouse to generate more DNA for further analyses, the knock-out population was entirely lost (Figure 3.16, Panel D; lanes 1 and 2). Only endogenous *lplA1* (2479 bp; lane 4) and episomal *Pb*LplA-REP-b3D (1150 bp; lane 3) was amplified. This clearly suggests that the *lplA1* locus in

P. berghei can be targeted and that *lplA1*-replacement causes a severe defect on the viability of blood-stage *P. berghei*, which results in the selection of parasites that contain *Pb*LplA-REP-b3D episomally.

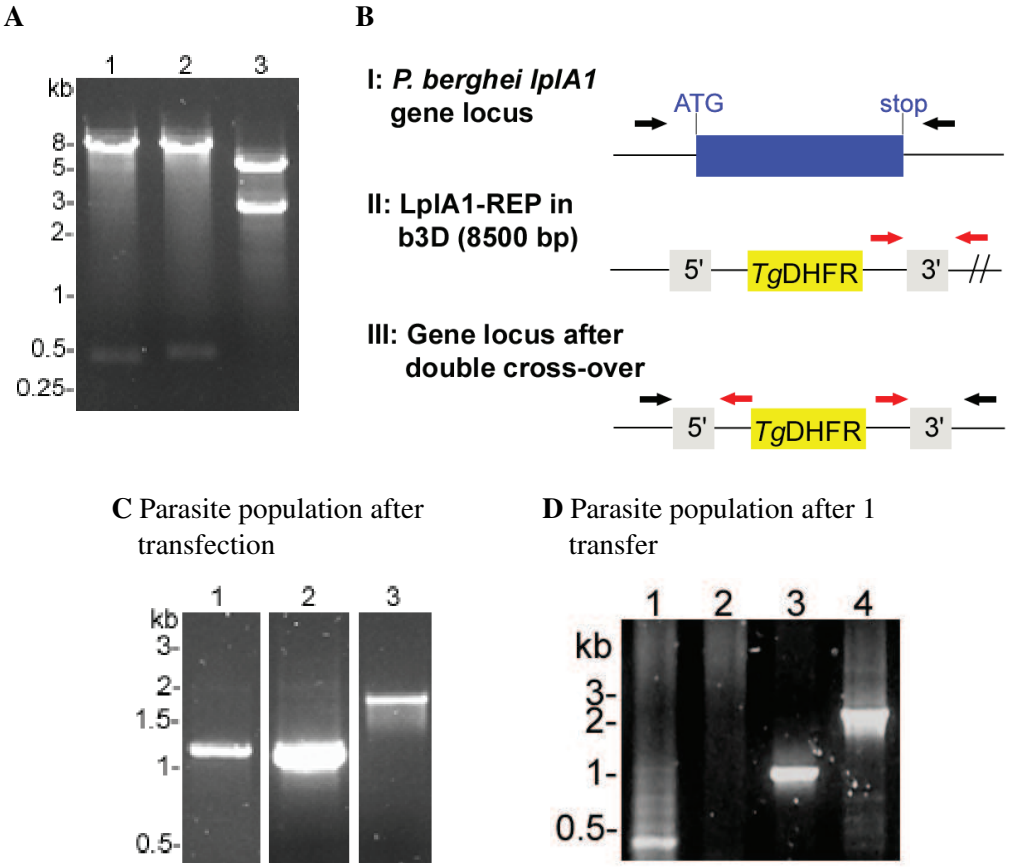

Figure 3.16.: Knock-out studies of *P. berghei lplA1* using the replacement strategy (**Panel A**) A 480 bp fragment was amplified as the *P. berghei lplA1* 5' UTR and was cloned into b3D.DT^H.^D (8020 bp), using the restriction enzymes KpnI and HindIII (lane 1). The 3' UTR PCR fragment (516 bp) was cloned into the plasmid using NotI and SacII (lane 2). Before transfection, *Pb*LplA1-REP-b3D was digested with KpnI and SacII, resulting in a 5636 bp fragment containing the two UTRs and the *T. gondii* DHFR/TS expression cassette, and a 2864 bp fragment containing the plasmid backbone (lane 3). **Panel B** is a schematic diagram of the replacement of *P. berghei lplA1*. Transfectants were analysed by PCR using gene locus specific primers (black arrows) and plasmid specific primers (red arrows). **Panel C** displays the PCR analyses of the parasite population directly after transfection. Lane 1 shows the 3' replacement specific PCR (1183 bp), lane 2 the plasmid specific PCR (1150 bp) and lane 3 the wild-type specific PCR (1837 bp). **Panel D** displays the PCR analyses of the parasite population after one transfer. Lane 1 shows the 3' replacement specific PCR (1183 bp), lane 2 the 5' replacement specific PCR (1015 bp), lane 3 the plasmid specific PCR (1150 bp) and lane 4 the wild-type specific PCR (2479 bp). The parasite population obtained after transfection contained parasites that had the plasmid integrated. However, this population was lost after transfer of the parasites into another mouse, indicating that the replacement of *lplA1* severely affected parasite growth.

3.6.4. Knock-out control studies via double cross-over recombination

To complement for the severe effects replacement of *P. berghei lplA1* seemed to have, the complementation plasmid *Pb*LplA1-comp-b3D was designed. The plasmid consisted of *Pb*LplA1-REP-b3D with an expression cassette of *P. falciparum* LplA1 cloned in front of the *P. berghei lplA1* 3' UTR. The expression cassette consisted of the *P. falciparum* calmodulin (CAM) promotor (amplified using PfCAM5'-F2 and PfCAM5'-R1), *P. falciparum lplA1* (amplified using Pf-LplA-ORF-fwd and Pf-LplA-ORF-rev) and the 3' UTR of *P. falciparum* histidine rich protein 2 (HRP2) (amplified using PfHRPII3'-F1 and PfHRPII3'-R1). For oligonucleotide sequences and introduced restriction sites see 2.1.7. The expression cassette was first generated in the plasmid pBluescript II SK (Stratagene) and was then sub-cloned into *Pb*LplA1-REP-b3D using the restriction enzymes BamHI and NotI (Figure 3.17, Panel A). Before transfection according to Janse et al. (2006), the plasmid was digested with KpnI and SacII, resulting in a 8114 bp fragment containing the two *P. berghei lplA1* UTRs, the *T. gondii* DHFR/TS and the *P. falciparum* LplA1 expression cassettes, and a 2864 bp fragment containing the plasmid backbone (Figure 3.17, Panel A). Digested *Pb*LplA1-comp-b3D was transfected only once, and the parasite population obtained after pyrimethamine selection was analysed by PCR using the gene locus specific primers Pb-LplA-int-fwd and Pb-LplA-REP-rev (black arrows), and plasmid primers PfHRPII3'-F1, b3D-rev and Pb-LplA-3'-fwd (red arrows) (Figure 3.17, Panel B) (see 2.1.7). Figure 3.17 (Panel C) shows the results of the PCRs after transfection. The 3' complementation specific band (1227 bp; lane 1) was amplified from the parasite population, and it was verified by sequencing. In addition, the presence of episomal plasmid (587 bp; lane 2) and wild-type *P. berghei lplA1* (1837 bp; lane 3) was shown. However, as for the replacement construct, the parasite population that had the complementation construct integrated into the gene locus was lost after transfer into another mouse (Figure 3.17, Panel D). This is somewhat surprising as the *P. falciparum lplA1* copy which was introduced into *P. berghei* should be able to complement for the loss of the endogenous gene. There are a number of potential reasons for this unsuccessful complementation experiment. First, it is possible that the over-expression of *P. falciparum* LplA1 is not entirely beneficial for *P. berghei*, given that the heterologous protein is not under the control of the *P. berghei lplA1* promoter, but is driven by the *P. falciparum* CAM promoter. Should this be the case, it can be postulated that the levels of LplA1 are crucial during parasite development. This hypothesis is in some ways supported by the data on *P. berghei* LplA1 over-expression in *P. falciparum*, which seems to have a slight negative effect on the parasites' progression through their life cycle (see 3.5.2). A second possibility is that

maybe *P. berghei* LplA1 and *P. falciparum* LplA1 cannot replace each other totally which might have a negative effect on the viability of transfected *P. berghei*. Finally, it needs to be considered that technical problems might have led to this result since the experiment was only performed once.

Taking all data of the knock-out studies in *P. berghei* together, they clearly show that the *P. berghei lplA1* gene locus can be targeted in contrast to the *P. falciparum lplA1* gene locus. Moreover, the data strongly suggest that knock-out of *lplA1* is likely not possible because of negative effects on blood stage parasite viability. It can also be concluded, that these negative effects are unlikely to be due to an alteration of the gene locus upon recombination, because integration of the knock-out control construct does not result in any obvious negative effect. The obtained data further allow to speculate that the level of LplA1 during erythrocytic development might be crucial, given that over-expression of *P. falciparum* LplA1 appears to be unable to compensate for *P. berghei lplA1* replacement with a selectable marker.

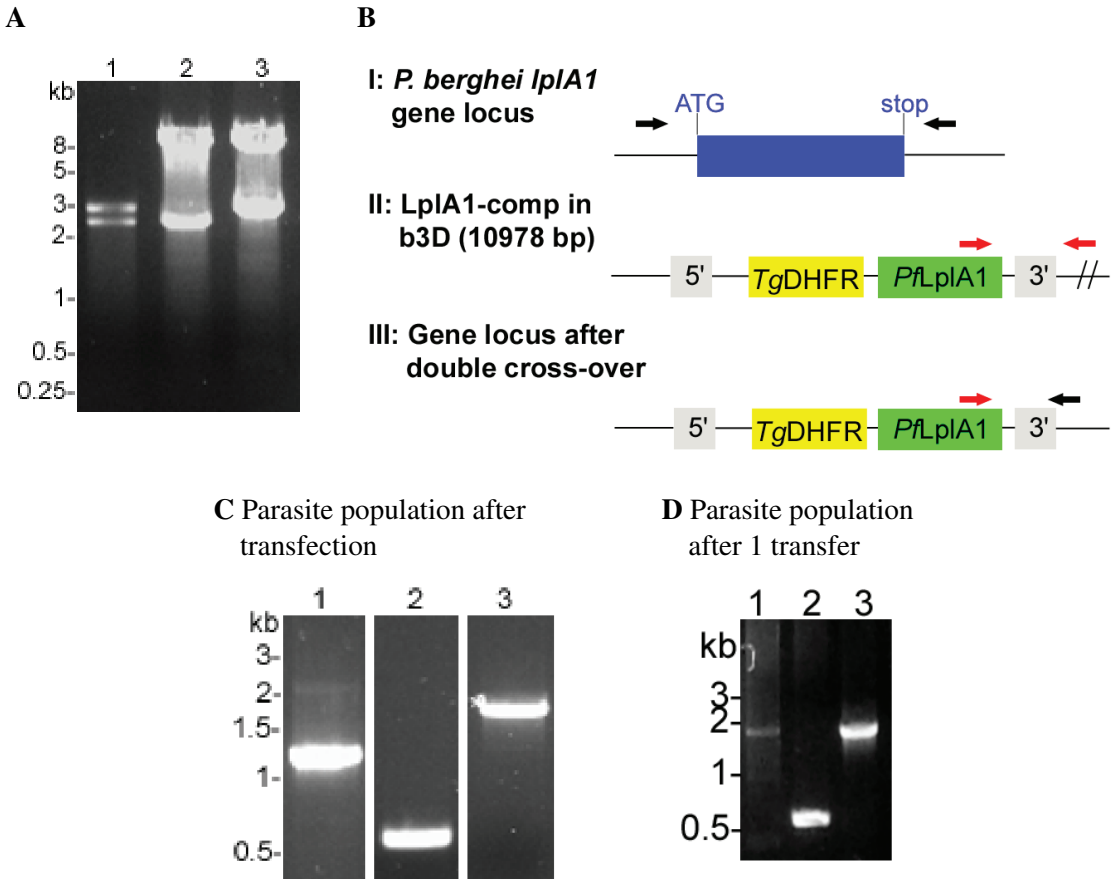

Figure 3.17.: Knock-out control studies of *P. berghei lplA1* using the replacement strategy (**Panel A**) For the control construct, a *P. falciparum* LplA1 expression cassette was cloned into *Pb*LplA1-REP-b3D. The expression cassette consisted of the *P. falciparum* CAM promoter, *lplA1* gene and HRP2 3' UTR. First, the expression cassette (2490 bp) was generated in the plasmid pBluescript II SK (3000 bp; Stratagene) (lane 1). Using the restriction enzymes BamHI and NotI, the expression cassette was cloned into *Pb*LplA1-REP-b3D (8500 bp) in front of the *P. berghei lplA1* 3' UTR resulting in the plasmid *Pb*LplA1-comp-b3D (lane 2). Before transfection, *Pb*LplA1-comp-b3D was digested with KpnI and SacII, resulting in a 8114 bp fragment containing the 5' and 3' *P. berghei lplA1* UTRs, the *T. gondii* DHFR/TS and the *P. falciparum* LplA1 expression cassettes, and a 2864 bp fragment containing the plasmid backbone (lane 3). **Panel B** is a schematic diagram of the complementation of *P. berghei lplA1* replacement. Transfectants were analysed by PCR using gene locus specific primers (black arrows) and plasmid specific primers (red arrows). **Panel C** displays the PCR analyses of the parasite population directly after transfection and **Panel D** of the parasite population after one transfer. Lane 1 shows the 3' replacement specific PCR (1227 bp), lane 2 the plasmid specific PCR (587 bp) and lane 3 the wild-type specific PCR (1837 bp). The parasite population obtained after transfection contained parasites that had the plasmid integrated. However, this population was lost after transfer of the parasites into another mouse, indicating that the complementation of *lplA1* replacement was not successful.

3.7. Summary

• *P. falciparum* and *P. berghei* LplA1 contain highly conserved sequence motifs required for LplA activity, and the two proteins share high sequence similarities (78%).

• *P. falciparum* possesses lipoylated H-protein and KADH-E2 subunits. The H-protein, as well as BCDH-E2 and KGDH-E2 are located in the mitochondrion whereas the PDH-E2 is found in the apicoplast.

• Attempting to knock-out *P. falciparum lplA1* by single cross-over recombination was unsuccessful. The knock-out plasmid was maintained episomally suggesting that *P. falciparum lplA1* is either essential for parasite survival or the gene locus cannot be targeted.

• A *P. berghei* LplA1 over-expression plasmid was designed and transfected into *P. falciparum* parasites already bearing the *lplA1* knock-out plasmid to complement for the loss of LplA1, thus potentially allowing the knock-out of *P. falciparum lplA1*. After transfection both plasmids were present episomally. However, the plasmids recombined and integrated non-specifically into the *P. falciparum* genome as shown by Southern blotting and PFGE. To confirm the presence of both LplA1s, western blot analyses were performed using an antibody against *P. falciparum* LplA1, showing that *P. falciparum* and *P. berghei* LplA1 were expressed. Preliminary determination of lipoic acid levels suggested no major changes in mutant parasites in comparison to wild-type.

• Knock-out control studies were performed to analyse whether the *P. falciparum lplA1* gene locus could be targeted by integration. According to the data obtained from two independent transfections, the *lplA1* locus was not targeted and thus might be refractory. The knock-out control fragment integrated non-specifically, possibly at the same position as the knock-out/recombined plasmid. Therefore, it cannot be concluded whether *P. falciparum* LplA1 is essential for parasite survival or not.

• *P. berghei* LplA1 was over-expressed episomally in *P. falciparum*. The presence of *P. berghei* LplA1 was confirmed by western blotting, and initial analyses of lipoic acid levels in these parasites showed that the transfectants contained slightly higher levels of lipoic acid than wild-type parasites. This seemed to negatively affect the parasites progression through the intraerythrocytic developmental cycle.

• Knock-out studies of *lplA1* in *P. berghei* using different strategies were performed. Knock-out via single cross-over integration was not achieved. Parasites maintained the knock-out plasmid episomally, but integration of the *Pb*LplA1-KOkon construct into the *P. berghei lplA1* gene locus showed that the locus was not refractory to integration. Replacement of *P. berghei lplA1* was achieved initially, but the parasite population that had the gene replaced with the *T. gondii* DHFR/TS was lost during attempts to enrich the population. The parasites were quickly overgrown by parasites still harbouring the endogenous *lplA1* gene and carrying the replacement plasmid episomally. This suggested that LplA1 plays an important role for blood stage viability. Complementation of the replacement using *P. falciparum* LplA1 was, however, also unsuccessful. This is possibly because the *P. falciparum* gene was not under the control of the endogenous *P. berghei lplA1* promotor, but was over-expressed, which seems to have a negative effect on parasite development as also observed by *P. berghei* LplA1 over-expression in *P. falciparum*.

• Analyses of the *P. falciparum lplA1* and *P. berghei lplA1* gene loci suggest that the two gene loci are syntenic, apart from three small annotated proteins present in the *P. berghei* gene locus. However, from the knock-out studies it seems that the *P. falciparum lplA1* gene locus is refractory to integration whereas the *P. berghei lplA1* gene locus is not.

4. LplA2

4.1. Introduction

The post-translational modification of KADH-E2 subunits and H-protein is performed by two independent lipoylation pathways present in apicomplexan parasites (Thomsen-Zieger et al., 2003, Wrenger and Müller, 2004). *De novo* biosynthesis of lipoic acid occurs in the apicoplast, consisting of LipB, the octanoyl-ACP transferase, and LipA, the lipoic acid synthase (Zhao et al., 2003, 2005). This pathway is responsible for lipoylation of the PDH-E2 subunit. Salvage of the cofactor occurs in the mitochondrion, and lipoate protein ligase A (LplA1) is responsible for lipoylation of the BCDH-E2, KGDH-E2 and the H-protein (Wrenger and Müller, 2004). However, analyses of the *P. falciparum* genome revealed the presence of a potential second lipoic acid protein ligase A named LplA2. This raises the question whether the different lipoic acid ligases present in *Plasmodium* (LipB, LplA1 and the newly identified LplA2) act independently or are redundant. In this chapter, this question was addressed by analysing the role of LplA2 in more detail. This chapter thus describes the identification of *lplA2*, analyses of its functionality, determination of its subcellular localisation and assessment of its potential function in *P. falciparum* and *P. berghei* by reverse genetic approaches.

4.2. Identification of *lplA2*

A second gene potentially encoding a lipoate protein ligase A was identified in *P. falciparum* by TBlastN searching the PlasmoDB database (Bahl et al., 2003) using the *Arabidopsis thaliana* LplA sequence. The hypothetical protein PFI1160w identified on chromosome 9 was designated LplA2. The sequence similarity of *P. falciparum* LplA2 to the *Arabidopsis* protein was modest with only 20.3% and was only marginally higher for *E. coli* LplA, *T. acidophilum* LplA and *P. falciparum* LplA1 (Table 4.1).

Table 4.1.: Sequence similarities of *P. falciparum* LplA2

	P. falciparum LplA1	*A. thaliana* LplA	*E. coli* LplA	*T. acidophilum* LplA
P. falciparum LplA2	27.2%	20.3%	23.5%	22.4%

Orthologues of LplA2 are present in other *Plasmodium* species (Table 4.2), and sequence alignment of the deduced amino acid sequence of *P. falciparum* and *P. berghei* LplA2 with *E. coli* and *T. acidophilum* LplA shows, that despite the modest sequence similarities of *P. falciparum* LplA2 with the bacterial proteins, three highly conserved sequence motifs involved in the formation of the lipoyl-AMP binding pocket are conserved in *Plasmodium* LplA2, suggesting that LplA2 is a functional protein ligase (Figure 4.1) (Fujiwara et al., 2005, Kim et al., 2005, McManus et al., 2006). The sequence alignment shows that the *Plasmodium* LplA2s contain several insertions in the N-terminal part of the protein in comparison to bacterial LplA. Additionally, they contain a 28 amino acid extension at the N-terminus. These extensions possibly correspond to targeting signals required for subcellular protein localisation and are described in more detail later (see below, Table 4.3). LplA2 orthologues are also found in *Theileria* and *Toxoplasma*, other apicomplexan parasites. Table 4.2 summarises the similarities of the deduced amino acid sequences of various apicomplexan LplA2s in comparison to *P. falciparum* LplA2.

Table 4.2.: Sequence similarities of *P. falciparum* LplA2 to apicomplexan LplA2s

	P. falciparum LplA2
Plasmodium berghei	57.7%
Plasmodium chabaudi	56.8%
Plasmodium knowlesi	55.1%
Plasmodium vivax	49.4%
Plasmodium yoelii	57.5%
Theileria annulata	37.0%
Theileria parva	39.0%
Toxoplasma gondii	17.8%

The potential *Theileria* protein, and the potential LplA2s of other *Plasmodium* spp. share a relatively high sequence similarity with *P. falciparum* LplA2 (between 37% and 57.7%). In contrast, the sequence similarity of the potential *T. gondii* LplA2 is lower with 17.8% when compared to the *P. falciparum* LplA2. Furthermore, analyses of the *T. gondii* sequence revealed that the first highly conserved sequence motif involved in lipoyl-AMP binding (see Figure 4.1) is absent in *T. gondii* LplA2, whereas it is present in all other apicomplexan LplA2 listed in Table 4.2 (Fujiwara et al., 2005, Kim et al., 2005, McManus et al., 2006). This suggests, that *T. gondii* LplA2 is likely not to be a functional lipoate protein ligase. No potential *lplA2* was identified in the genome of *Cryptosporidium*,

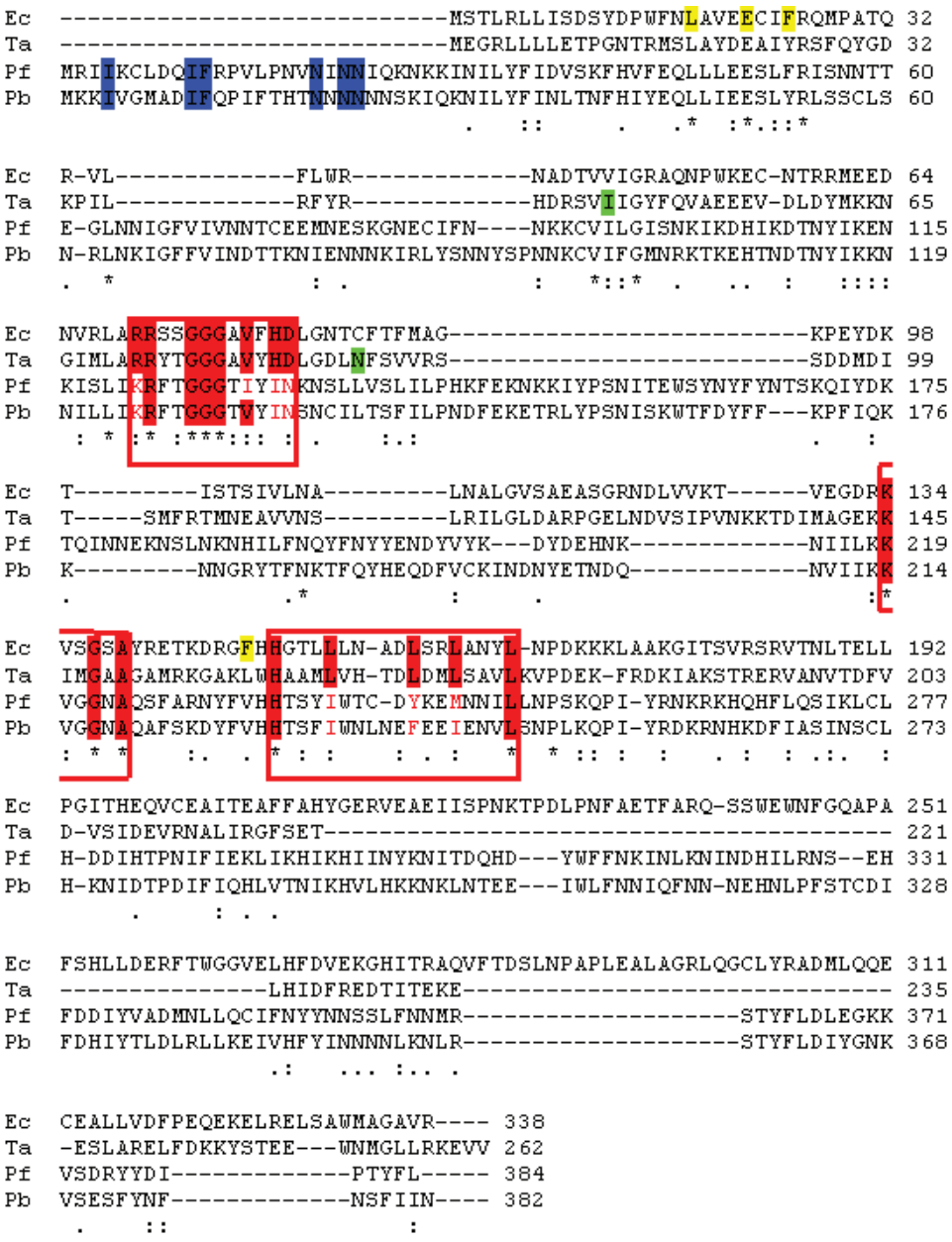

Figure 4.1.: Amino acid sequence alignment of *P. falciparum* and *P. berghei* LplA2 with bacterial LplA

Separate ClustalW alignments of *E. coli* (Ec) / *T. acidophilum* (Tc) LplA and *P. falciparum* (Pf) / *P. berghei* (Pb) LplA2 were combined using the program T-Coffee (Notredame et al., 2000, Poirot et al., 2003) showing (*) identical residues, (:) conserved residues and (.) homologous residues. Three highly conserved sequence motifs which contain key residues involved in the formation of the lipoyl-AMP binding pocket are highlighted in red. Residues outside these three motifs involved in lipoic acid binding are highlighted in yellow, for the *E. coli* protein, and green, for the *T. acidophilum* protein. Both *Plasmodium* LplA2s possess a 28 amino acid extension of which 29% are identical residues (highlighted in blue). This extension likely corresponds to a targeting sequence responsible for protein import into organelles and is explained later in more detail. In comparison to the bacterial proteins, *Plasmodium* LplA2 contain several amino acid insertions.

another apicomplexan parasite. The genomes of *Babesia* and *Eimeria* were also searched for a potential *lplA2* gene. However, their genomes are not annotated yet which makes it difficult to identify potential candidates.
While this study was performed, Allary and colleagues published the presence of LplA2 in *P. falciparum* and other *Plasmodium* spp. (Allary et al., 2007).

4.3. Functionality of LplA2

To experimentally confirm that *P. falciparum* LplA2 is a functional lipoate protein ligase, *lplA2* was used to complement the growth defect of the *lipB* deficient *E. coli* strain Ker184 and the *lipB*/*lplA* deficient *E. coli* strain Tm136 (Reed and Cronan, 1993, Morris et al., 1995). Three expression constructs of *P. falciparum lplA2* were generated using the plasmid pASK-IBA3 (see Figure 2.11). The first construct expressed full length (fl) LplA2, whereas the other two constructs produced N-terminal truncated forms of LplA2 (construct S1 equalled amino acids 27-385 and construct S2 equaled amino acids 79-385) (see Table 5.1). The different constructs were designed because of the N-terminal extension of *P. falciparum* LplA2 described above, which potentially corresponds to a N-terminal targeting sequence that possibly might interfere with protein expression and/or function of the recombinant protein in the prokaryotic expression system. Cloning of these constructs is described in Chapter 5.3.1. Bacteria were transformed with the expression constructs, and were incubated as described in material and methods (see 2.7.1) (Figure 4.2).

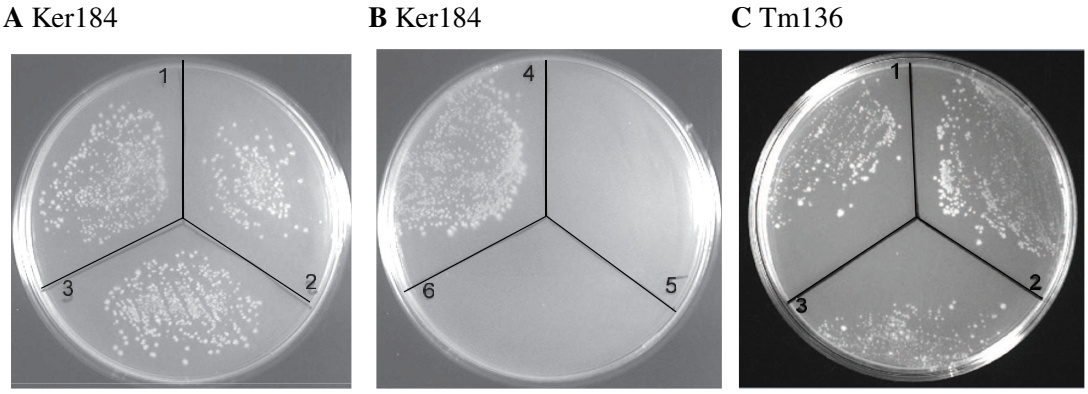

Figure 4.2.: Functionality of LplA2
Functionality of *P. falciparum* LplA2 was assessed by complementation studies of *lipB* deficient Ker184 (**Panel A and B**) and *lipB/lplA* deficient Tm136 (**Panel C**) (Reed and Cronan, 1993, Morris et al., 1995). 1 corresponds to LplA2-fl-pASK-IBA3, 2 to LplA2-S1-pASK-IBA3 and 3 to LplA2-S2-pASK-IBA3. 4, 5 and 6 are positive and negative controls, and are *P. falciparum* LplA1-pASK-IBA3 (4), pASK-IBA3 (5) and untransformed bacteria (6). All three LplA2 constructs (1-3) are able to complement the growth defect of Ker184 and Tm136.

Figure 4.2 shows that all three constructs were able to complement the growth defect of Ker184 and Tm136 when grown on minimal medium without lipoic acid. This suggests that *P. falciparum* LplA2 is indeed a functional lipoate protein ligase, able to complement for *E. coli* LplA and LipB. This is in contrast to Allary et al. (2007), who suggest that LplA2 can only complement LplA but not LipB activity. The different results obtained in the complementation studies may be explained by the different recombinant LplA2 expression constructs used, which differed at their C-termini.

4.4. Localisation of LplA2

The alignment in Figure 4.1 clearly shows that *P. falciparum* and *P. berghei* LplA2 possess a N-terminal extension in comparison to the bacterial proteins. This extension possibly corresponds to a targeting signal responsible for organellar targeting. Apicoplast targeting is achieved by a bipartite leader sequence consisting of a signal peptide responsible for entering the secretory pathway followed by a transit peptide for targeting to the apicoplast (Waller et al., 2000, Foth et al., 2003). Targeting to the mitochondrion is accomplished by a N-terminal mitochondrial transit peptide (Bender et al., 2003). Indeed, the enzyme complexes which require post-translational lipoylation for their activity are found in the apicoplast and mitochondrion of *P. falciparum* (Foth et al., 2005, Günther et al., 2005, McMillan et al., 2005, Salcedo et al., 2005) (see Figure 3.4). Thus, localisation of LplA2 to either of the organelles is likely. To investigate the localisation of LplA2, I first used the available prediction programs (listed in 2.4.3) to predict the potential subcellular localisation of this protein, and the results are summarised in Table 4.3.

Table 4.3.: Predicted LplA2 localisation of *Plasmodium* spp.

	MitoProt	PlasMit	Predotar	PATS	SignalP
P. falciparum	0.9328	non-mito 99%	0.03 mito 0.00 plastid	0.037	no signal peptide
P. berghei	0.4511	non-mito 99%	0.01 mito 0.01 plastid	0.025	0.003
P. chabaudi	0.4995	non-mito 99%	0.01 mito 0.01 plastid	0.023	no signal peptide
P. knowlesi	0.8879 CS[a]→34	non-mito 99%	0.38 mito 0.00 plastid	0.023	0.404
P. vivax	0.9895 CS[a]→28	non-mito 99%	0.87 mito 0.00 plastid	0	no signal peptide
P. yoelii	0.96	non-mito 99%	0.36 mito 0.00 plastid	0.657	no signal peptide

[a] predicted cleavage site

Predicting the subcellular localisation of LplA2 is ambiguous. The program MitoProt predicts *P. falciparum* LplA2 to be mitochondrial, however, it is predicted non-mitochondrial by PlasMit and Predotar. *P. knowlesi* and *P. yoelii* LplA2 are also predicted to be mitochondrial by MitroProt. The program even predicts a potential cleavage site of the transit peptide for *P. knowlesi* LplA2, but the results obtained by SignalP for the *P. knowlesi* protein and by PATS for the *P. yoelii* protein indicate a possible apicoplast targeting. The MitoProt predictions of the other LplA2s also suggest mitochondrial localisation, which is for *P. vivax* LplA2 further supported by Predotar. Overall, the localisation predictions do not fully agree with each other which makes it impossible to predict the localisation of LplA2 in the parasite.

4.4.1. Localisation analyses using GFP-fusion proteins

To further determine the subcellular localisation of *P. falciparum* LplA2, parasites expressing LplA2-GFP fusion proteins were generated and analysed. Full length *lplA2* was amplified from 3D7 gDNA using the oligonucleotide primers LplA2-fwd and LplA2-rev (see 2.1.7). The 1152 bp PCR fragment contained a CACC-overhang at the 5' end for directional cloning into the entry plasmid pENTR/D-TOPO (Invitrogen). Generation of the LplA2-GFP expression constructs was performed using MultiSite Gatway cloning described in Chapter 2.5.2.3 using the destination plasmid pCHD-3/4 (van Dooren et al., 2005). Two LplA2-GFP constructs were generated which differed in the promoter driving the expression of the fusion protein. One was controlled by the stronger *P. falciparum* Hsp86 promoter and the second construct was controlled by the weaker *P. falciparum* CRT promoter. Both constructs were transfected into D10 wild-type parasites, as described before (Crabb and Cowman, 1996, Wu et al., 1996), and obtained parasite populations were analysed by fluorescence microscopy (Figure 4.3). Regardless of the construct used, no differences in fluorescence were observed in the obtained parasite populations, and therefore images shown in Figure 4.3 are representative for both LplA2-GFP expression constructs. To visualise the mitochondria of the parasites, the parasites were treated with Mitotracker CMXRos (Molecular Probes), a dye to specifically stain mitochondria. The results suggest that LplA2 is present in two distinct organelles. One organelle is the mitochondrion since clear co-localisation with Mitotracker can be observed. The other organelle is distinct from the mitochondrion but closely associated with it, suggesting potential apicoplast localisation (van Dooren et al., 2005). Furthermore, parasites with dual targeting of LplA2 into both organelles were observed. Quantification of 50 parasites expressing the LplA2-GFP fusion protein revealed that in 68% LplA2-GFP was found in the mitochondrion, in 15% LplA2-GFP was present in the organelle distinct from the mitochondrion likely to be the apicoplast and in 18% it was dual targeted into both organelles. To experimentally confirm whether the second organelle really is the apicoplast, immunofluorescence analyses were carried out.

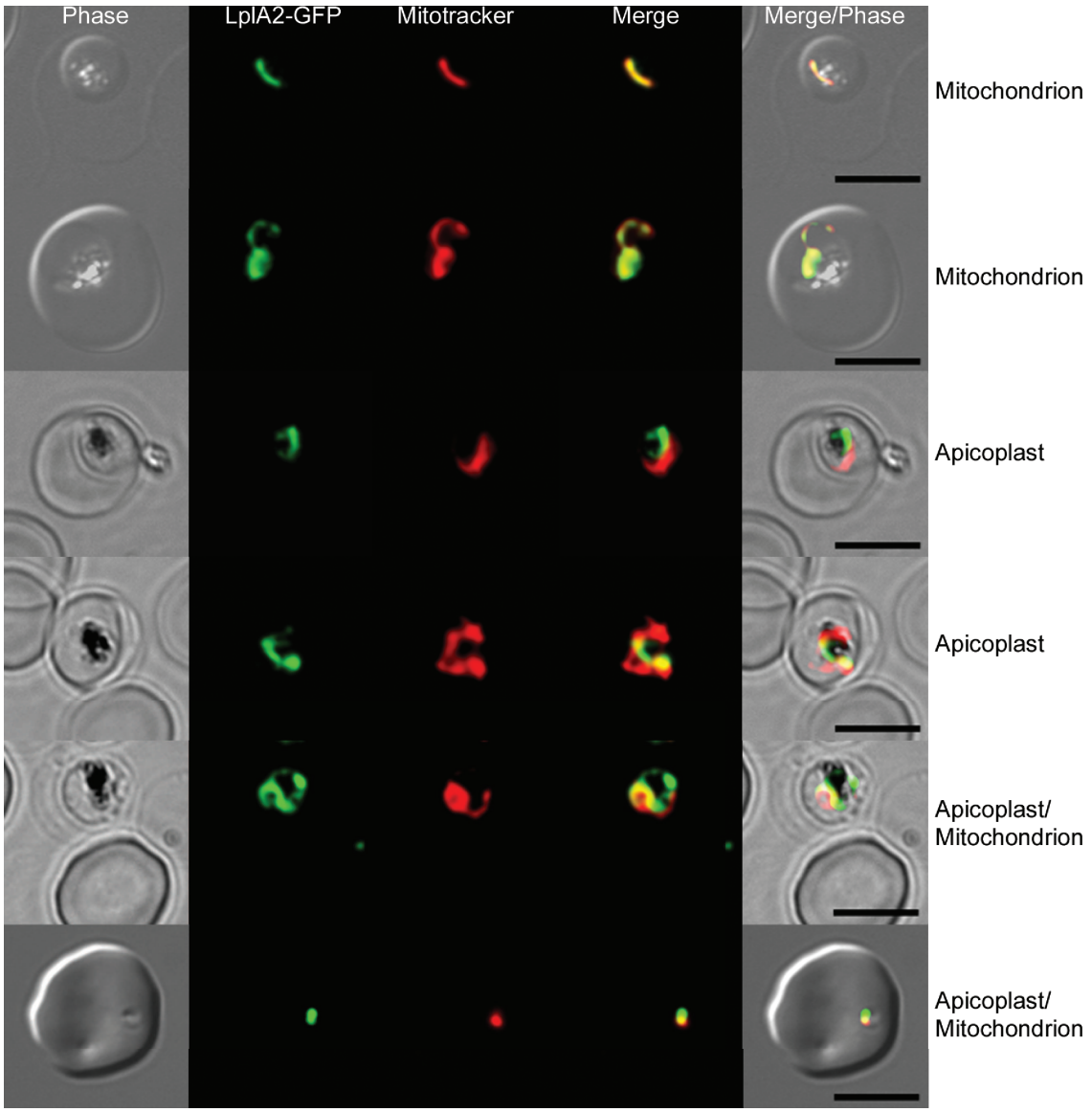

Figure 4.3.: Localisation of LplA2 using LplA2-GFP expressing parasites
The subcellular localisation of LplA2 was investigated by expressing GFP fusion proteins in the erythrocytic stages of *P. falciparum*. Full length LplA2 was cloned in frame with GFP and expression was controlled by either the Hsp86 or CRT promoter. Parasites mitochondria were selectively stained with Mitotracker CMXRos (Molecular Probes) and images of live cells were obtained by DIC microscopy (Phase) or in the FITC (LplA2-GFP) or rhodamine (Mitotracker) fluorescent channels. Overlays of the images are displayed to determine possible co-localisation (Merge). In the first two panels, LplA2-GFP clearly co-localises with the mitochondrion. In panel 3 and 4, the GFP fluorescence is not in the mitochondrion but in a different organelle closely associated with the mitochondrion, likely to be the apicoplast. The last two panels show parasites in which LplA2-GFP is present in two organelles, one being the mitochondrion and the other likely being the apicoplast. Scale bars equal 5 μm.

4.4.2. Immunofluorescence analyses

Immunofluorescence analyses using 3D7 wild-type parasites were performed to further investigate the localisation of LplA2. An antibody against apicoplast dihydrolipoamide dehydrogenase (aE3) which was available in the laboratory was used as an apicoplast marker (McMillan and Müller, unpublished) together with an antibody against *P. falciparum* LplA2 (Figure 4.4) (for antibody dilutions see Table 2.1). The results show that in some parasites the two proteins clearly co-localise, suggesting LplA2 localisation in the apicoplast. In addition, parasites were observed in which the two proteins did not co-localise, suggesting mitochondrial localisation of LplA2. As already observed in the LplA2-GFP expressing parasites, parasites with dual targeted LplA2 to both organelles were present. Analyses of LplA2 localisation by immunofluorescence in 46 parasites supported the distribution pattern observed in the LplA2-GFP expressing parasites, with 53% of LplA2 not co-localising with aE3 suggesting mitochondrial localisation, 19.6% of LplA2 co-localising with aE3 suggesting apicoplast localisation and 28% showing dual targeting of LplA2 to both organelles.

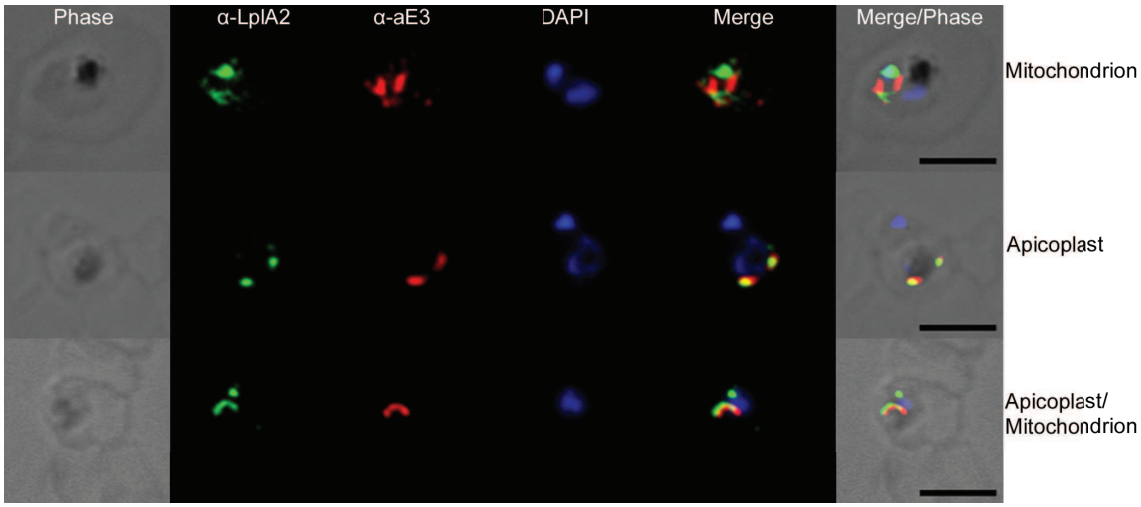

Figure 4.4.: Localisation of LplA2 by immunofluorescence analyses using anti-LplA2 and anti-aE3 antibodies

The subcellular localisation of LplA2 was investigated by immunofluorescence analyses using anti-LplA2 and anti-apicoplast localised dihydrolipoamide dehydrogenase (aE3) antibodies on 3D7 wild-type parasite. Images of cells were obtained by DIC microscopy (Phase), or in the FITC (α-LplA2), or rhodamine (α-aE3) fluorescent channels. DNA was stained with DAPI and overlays of all images taken are displayed to determine possible co-localisation (Merge). In the first panel, LplA2 does not co-localise with aE3 suggesting mitochondrial localisation. In the second panel, LplA2 clearly co-localises with aE3 supporting apicoplast localisation of LplA2. The last panel displays a parasite in which LplA2 is present in two organelles, one the apicoplast and the other likely the mitochondrion. Scale bars equal 5 μm.

These studies strongly suggest that LplA2 is dually targeted to the apicoplast and mitochondrion. However, the precise mechanism responsible for dual targeting for this protein is not known and requires further investigation.

4.5. Knock-out studies in *P. falciparum*

4.5.1. Knock-out studies via single cross-over recombination

To assess the potential role of LplA2 and to investigate a possible redundancy between the lipoic acid ligases present in *P. falciparum*, knock-out studies of *lplA2* were performed using the plasmid pHH1 (see Figure 2.1) (Reed et al., 2000). As described for LplA1 in Chapter 3.4.1, knock-out is achieved by single cross-over recombination of the knock-out plasmid with the gene locus (Figure 4.5, Panel B). The 792 bp knock-out fragment was amplified from 3D7 gDNA using the oligonucleotides Pf-LplA2-KO-pHH1-fwd and Pf-LplA2-KO-pHH1-rev (see 2.1.7). The knock-out fragment is truncated at the N- and C-terminus and corresponds to nucleotides 205-993 of *lplA2*. In addition, an artificial stop codon was introduced at the 3' end of the PCR product to ensure the disruption of the gene locus after integration. The PCR fragment was cloned directionally into pHH1 using the restriction enzymes BglII and XhoI (Figure 4.5, Panel A), and LplA2-KO-pHH1 was transfected into *P. falciparum* D10 wild-type parasites (Crabb and Cowman, 1996, Wu et al., 1996). The transfected parasite population was cycled with WR99210, to select for those parasites in which the knock-out plasmid had targeted the *lplA2* locus. After two cycles of drug selection, the parasite population was analysed by Southern blotting of NdeI digested DNA. The expected band for integration into the *lplA2* gene locus (4199 bp) was detected when probes specific for the hDHFR and the *P. falciparum* CAM 5' UTR were used (Figure 4.5, Panel D and E). Additionally, the PfCAM5' probe detected a weak band possibly corresponding to plasmid (5820 bp), and a band at 12.4 kb corresponding to the endogenous calmodulin gene locus. However, analyses of the LplA2-KO mutant parasites was not straightforward. Southern blot analyses using a gene specific probe did not produce a clear result (Panel C). Two bands at 5249 bp and 4199 bp were expected in case of integration of the knock-out plasmid into the *lplA2* gene locus. Only one band of approximately 4 kb was detected, however, precise size determination of this band was difficult due to the way the digested DNA ran through the gel.

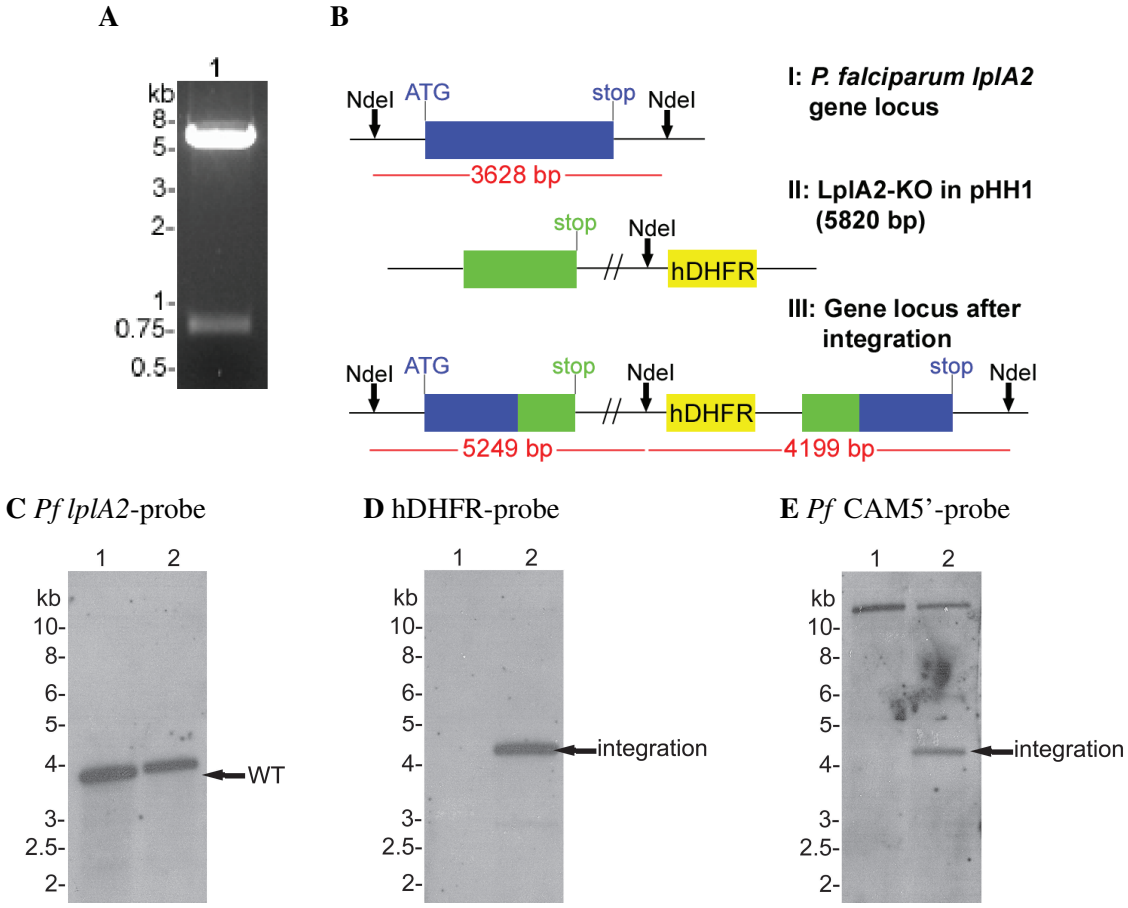

Figure 4.5.: Knock-out studies of *P. falciparum lplA2*
(**Panel A**) The 792 bp *lplA2* knock-out fragment was cloned into pHH1 (5760 bp) using the restriction enzymes BglII and XhoI. (**Panel B**) The *lplA2* knock-out fragment lacks the ATG-start codon and is truncated at the C-terminus, where in addition, an artificial stop-codon is introduced. Knock-out is achieved by single cross-over of this plasmid with the gene locus, which should result in an interruption of the locus generating two non-functional copies of the gene. For Southern blot analyses, the DNA was digested with the restriction enzyme NdeI. **Panel C-E** display Southern blots of parasite gDNA digested with NdeI and probed with *P. falciparum lplA2*, hDHFR and *P. falciparum* CAM5', respectively. In all blots, lane 1 contains D10 wild-type gDNA and lane 2 gDNA of parasites transfected with the knock-out construct taken through two cycles of WR99210 selection. Blots probed with hDHFR and PfCAM5' show the expected integration band (4199 bp), suggesting integration of the knock-out plasmid in the *lplA2* locus. The blot probed with *PflplA2* is ambiguous. Two bands are expected in the event of integration (5249 bp and 4199 bp). Only one band is detected and size determination of this band is not clearly possible because the band did not appear straight (although all three blots shown were separated on the same agarose gel).

To clarify the genotypical analyses of the parasites transfected with the *lplA2* knock-out plasmid, PCR was performed using the following primer pairs that were diagnostic for wild-type, plasmid and integration (Figure 4.6, Panel A). The gene locus specific primers

LplA2-fwd and LplA2-rev (black arrows) were used to amplify a *lplA2* specific band of 1152 bp, the plasmid specific primers CAM5'-check-F and PbDT3'-check-R (red arrows) were used to amplify a 1027 bp plasmid specific band and the integration specific bands (5' 1024 bp; 3' 1155 bp) were amplified by combining the above described primers (see 2.1.7). Figure 4.6 (Panel B) shows the result of the PCRs performed using the parasite population taken through two cycles of drug selection. A band of the correct size was amplified for 3' integration (lane 1) and wild-type *lplA2* (lane 4). No specific bands were amplified for either the 5' integration (lane 2) or plasmid (lane 3). The amplified 3' integration band was cloned into pCR 2.1-TOPO (see 2.5.2.1) and its sequence was verified. The sequencing result showed that no integration into the *lplA2* gene locus had occurred, because the band amplified did not match the expected sequence for integration.

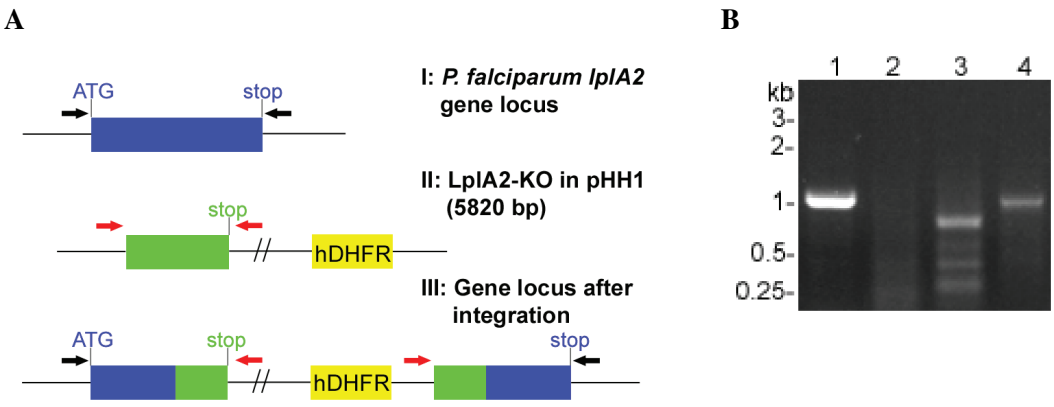

Figure 4.6.: PCR analyses of *P. falciparum lplA2* knock-out studies
Panel A is a schematic diagram of the integration of LplA2-KO-pHH1. Transfectants were analysed by PCR using gene locus specific primers (black arrows) and plasmid specific primers (red arrows). **Panel B** displays the PCR analyses of parasites transfected with the LplA2-KO-pHH1 construct and taken through two cycles of WR99210 selection. Lane 1 shows the 3' integration specific PCR (1155 bp), lane 2 the 5' integration specific PCR (1024 bp), lane 3 the plasmid specific PCR (1027 bp) and lane 4 the wild-type *lplA2* specific PCR (1152 bp). PCR showed that wild-type *lplA2* was present (lane 4), but the PCR specific for plasmid did not amplify a band of the correct size (lane 3). Nothing was amplified by the 5' integration specific PCR (lane 2), but a band of the expected size was amplified by the 3' integration specific PCR. However, sequencing of this PCR product revealed that no integration into the correct gene locus had occurred.

These results are somewhat puzzling because the *lplA2* gene is still present although Southern blot analyses using the hDHFR and CAM5' probes suggest that integration into the *lplA2* gene locus had occurred. A possible explanation for this is that the transfected

plasmid integrated non-specifically into the *P. falciparum* genome resulting in similar "integration" banding pattern when digested with NdeI. Although required, time constraints have prevented further analyses of the genotype of the "LplA2-KO" mutants.

4.6. Knock-out studies in *P. berghei*

As explained for LplA1, knock-out studies in *P. berghei* were carried out in collaboration with Prof Kai Matuschewski, University of Heidelberg, Germany using the plasmid b3D.DT^H.^D (see Figure 2.2) (kindly provided by A. P. Waters, Leiden University, The Netherlands). Knock-out studies were performed using single and double cross-over approaches.

4.6.1. Knock-out studies via single cross-over recombination

For single cross-over recombination, a knock-out fragment was generated which was truncated at the N- and C-terminus, and contained an artificial stop codon at the C-terminus to ensure the disruption of the gene locus after integration (Figure 4.7, Panel B). The knock-out fragment was first generated in the plasmid pBluescript II SK (Stratagene). Because linearised DNA is transfected in *P. berghei*, a NdeI site had to be introduced 331 bp into the knock-out fragment. This was achieved by amplifying two *lplA2* fragments and cloning them in pBluescript II SK. The primer pairs Pb-LplA2-int-fwd / Pb-LplA2-NdeI-rev and Pb-LplA2-NdeI-fwd / Pb-LplA2-int1-rev (see 2.1.7) were used. The first PCR product was cloned into pBluescript II SK using the restriction enzymes BamHI and XbaI, and the second PCR product was then cloned 3' using NdeI and SacII. Thus, a 882 bp knock-out fragment was generated containing an internal NdeI site, which was cloned directional into b3D.DT^H.^D using the restriction enzymes BamHI and SacII (Figure 4.7, Panel A). NdeI linearised *Pb*LplA2-KO-b3D was transfected twice according to Janse et al. (2006), and independent parasite populations obtained after pyrimethamine selection in mice were analysed by PCR using the gene specific primers Pb-LplA2-5'-fwd and Pb-LplA2-3'-rev (black arrows) and the plasmid specific primers Tg-for and b3D-rev (red arrows) (Figure 4.7, Panel B). gDNA of the parasite populations was made and was analysed by diagnostic PCRs. The results shown in Figure 4.7 (Panel C) are exemplary for both populations. Only recombined plasmid (1496 bp; lane 2) and *lplA2* wild-type (2577 bp; lane 3) were amplified in both parasite populations, but no 3' integration (2182 bp; lane 1) was detected. This indicated that *Pb*LplA2-KO-b3D had not integrated into the *lplA2* gene locus. There are several explanations as to why the construct did not integrate

into the *lplA2* gene locus. Either *lplA2* is essential for *P. berghei* intraerythrocytic stages, in which case knock-out is not possible, or the *lplA2* locus is refractory to integration. A third possibility is that technical problems are responsible for this result.

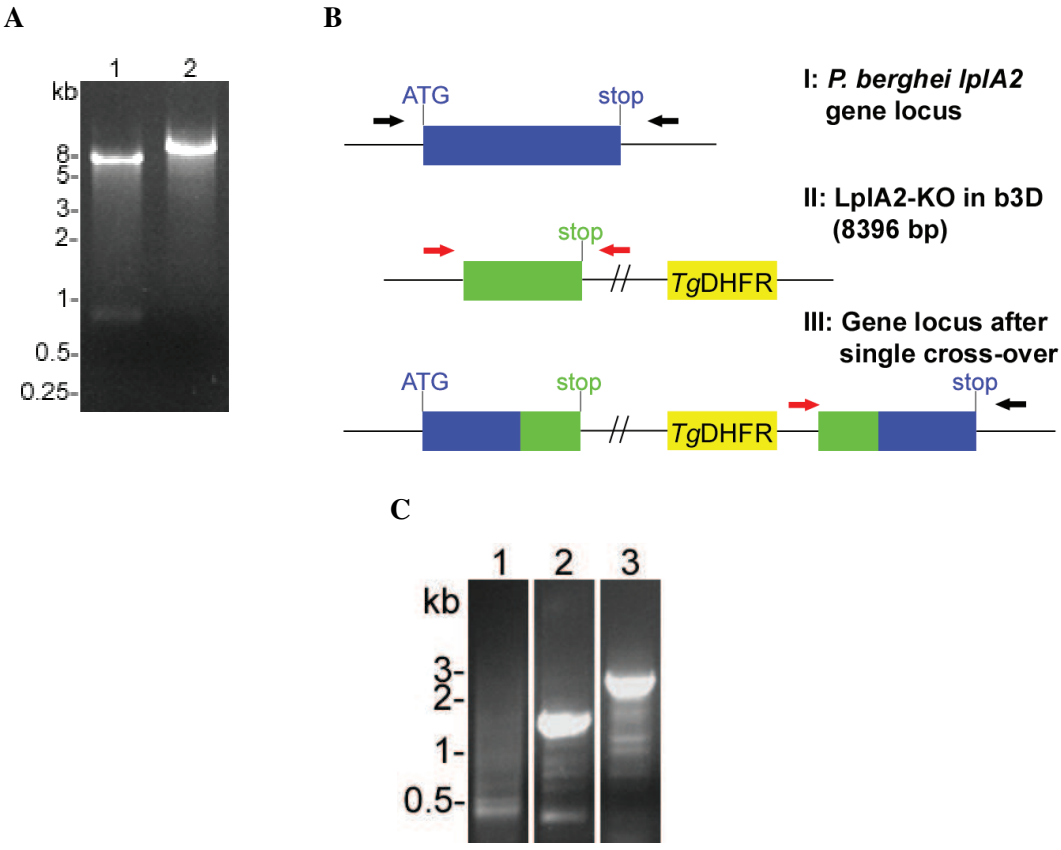

Figure 4.7.: Knock-out studies of *P. berghei lplA2* using the integration strategy
(**Panel A**) Two *lplA2* fragments were amplified by PCR and fused together in pBluescript II SK (Stratagene) to generate the 882 bp knock-out fragment which was cloned directionally into b3D.DT^H.^D (7514 bp) with BamHI and SacII (lane 1). Before transfection, *Pb*LplA2-KO-b3D was linearised using NdeI resulting in a 8396 bp fragment (lane 2). **Panel B** is a schematic diagram of the integration of *Pb*LplA2-KO-b3D. Transfectants were analysed by PCR using gene locus specific primers (black arrows) and plasmid specific primers (red arrows). **Panel C** displays the PCR analyses of transfected parasites. Lane 1 shows the 3' integration specific PCR (2182 bp), lane 2 the plasmid specific PCR (1496 bp) and lane 3 the wild-type specific PCR (2577 bp). The knock-out plasmid did not integrate into the gene locus. The plasmid was present as an episome.

4.6.2. Knock-out control studies via single cross-over recombination

To investigate whether the *lplA2* gene locus can be targeted by single cross-over recombination, a knock-out control construct was designed. As described for the knock-out construct, the knock-out control fragment was first generated in the plasmid pBluescript II SK (Stratagene) to introduce an internal NdeI site. The primers used were identical to the ones described previously (see 4.6.1) except for the antisense primer Pb-LplA2-int1-rev. Instead the primer Pb-LplA2-3'-rev was used (see 2.1.7), to include the endogenous *lplA2* stop codon and 3' UTR. The 1645 bp control fragment was then cloned directionally into b3D.DT^H.^D using the restriction enzymes BamHI and SacII, and prior to transfection of *Pb*LplA2-KOkon-b3D the plasmid was linearised using NdeI (Figure 4.8, Panel A). The control plasmid was transfected twice (Janse et al., 2006), and the two independent parasite populations obtained after pyrimethamine selection were analysed by PCR using the gene specific primers Pb-LplA2-5'-fwd and Pb-LplA2-REP-rev (black arrows), and the plasmid specific primers Tg-for and b3D-rev (red arrows) (Figure 4.8, Panel B). PCR analyses of both parasite populations revealed that *Pb*LplA2-KOkon-b3D had integrated into the gene locus. Figure 4.8 (Panel C) shows the PCR results of one parasite population exemplary for both. The 3' (2289 bp; lane 1) and 5' (2655 bp; lane 2) specific PCRs amplified bands of the expected size. Their sequence was verified by sequencing confirming the integration into the *lplA2* gene locus. This control experiment shows that the *lplA2* gene locus is not refractory to integration. It seems to be targeted very efficiently by *Pb*LplA2-KOkon-b3D since neither plasmid (2259 bp; lane 3) nor endogenous *lplA2* (2684 bp; lane 4) were detected by PCR. Therefore, it appears that *lplA2* is essential for intraerythrocytic stages as knock-out by single cross-over was not achieved. However, technical problems cannot be ruled out because the knock-out construct was only transfected twice.

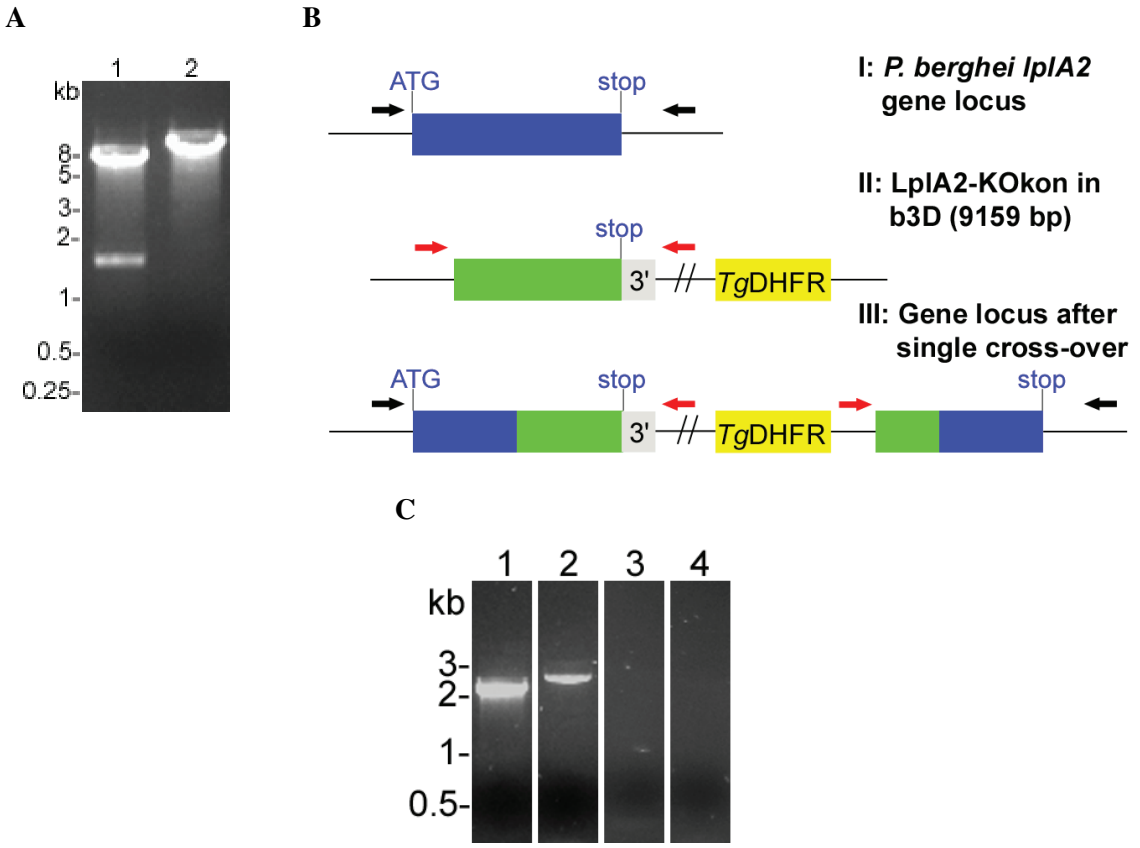

Figure 4.8.: Knock-out control studies of *P. berghei lplA2* using the integration strategy (**Panel A**) Two *lplA2* fragments were amplified by PCR and fused together in pBluescript II SK (Stratagene) to generate the 1645 bp knock-out control fragment which was cloned directionally into b3D.DT^H.^D (7514 bp) with BamHI and SacII (lane 1). Before transfection, *Pb*LplA2-KOkon-b3D was linearised using NdeI resulting in a 9159 bp fragment (lane 2). **Panel B** is a schematic diagram of the integration of *Pb*LplA2-KOkon-b3D. Transfectants were analysed by PCR using gene locus specific primers (black arrows) and plasmid specific primers (red arrows). **Panel C** displays the PCR analyses of the transfectants. Lane 1 shows the 3' integration specific PCR (2289 bp), lane 2 the 5' integration specific PCR (2655 bp), lane 3 the plasmid specific PCR (2259 bp) and lane 4 the wild-type specific PCR (2684 bp). The knock-out control plasmid did integrate into the gene locus. Even without cloning of the transfected parasite population, no plasmid or wild-type was detected by PCR, suggesting that the gene locus was very efficiently targeted.

4.6.3. Knock-out studies via double cross-over recombination

To further analyse whether *lplA2* is essential for *P. berghei* erythrocytic stages, knock-out studies via double cross-over recombination were performed. Using this strategy *lplA2* is replaced with the *T. gondii* DHFR/TS, the selectable marker of b3D.DT^H.^D. To achieve double cross-over recombination, the 5' and 3' UTR of *P. berghei lplA2* were amplified using Pb-LplA2-5'-fwd / Pb-LplA2-5'-rev and Pb-LplA2-3'-fwd / Pb-LplA2-3'-rev, respectively (see 2.1.7). The amplified 5' UTR (698 bp) was cloned directionally into the first multiple cloning site of b3D.DT^H.^D using KpnI and HindIII whereas the 3' UTR (581 bp) was cloned into the second multiple cloning site using NotI and SacII, generating the plasmid *Pb*LplA2-REP-b3D (Figure 4.9, Panel A). Before transfection according to Janse et al. (2006), the plasmid was digested using the restriction enzymes KpnI and SacII resulting in two fragments, the first containing the *lplA2* UTRs and the selectable marker (5919 bp), and the second containing the plasmid backbone (2864 bp) (Figure 4.9, Panel A). The digested plasmid was transfected twice, but only one transfection was successful resulting in a pyrimethamine resistant parasite population. This population was analysed by PCR using the gene specific primers LplA2-test-for and LplA2-test-rev (amplifying a 3008 bp band). For amplification of plasmid, the primers Tg-for and b3D-rev (red arrows) were used (amplifying a 1215 bp band) (Figure 4.9, Panel B). 3' integration specific PCRs were performed using either Tg-for / Pb-LplA2-REP-rev (amplifying a 1252 bp band) or Tg-for / LplA2-test-rev (amplifying a 1432 bp band), and 5' integration specific PCR was performed using LplA2-test-for / Tg-rev (amplifying a 1184 bp band). The PCR results shown in Figure 4.9 (Panel C) suggest that *Pb*LplA2-REP-b3D had replaced the *lplA2* gene locus. The 3' specific (1252 bp; lane 1) and 5' specific (1184 bp; lane 2) replacement PCRs resulted in the amplification of bands of the expected size and replacement was confirmed by sequencing of these PCR products. The parasite population also contained recombined plasmid (1215 bp; lane 3) and wild-type *lplA2* (3008 bp; lane 4), indicating that it was a mixed parasite population. These results suggest that *lplA2* is not essential for *P. berghei* intraerythrocytic stages, and that the failure to knock-out *lplA2* by single cross-over recombination is possibly be due to technical problems, like transfection of incompletely digested plasmid DNA.

To further analyse the potential effects of *lplA2* replacement, the mixed population was cloned as described in material and methods (see 2.3.9). After three cloning attempts, 12 independent clones were obtained of which the three clones shown in Figure 4.10 (clone II-1, II-5 and III-5) were used for further analyses (see below).

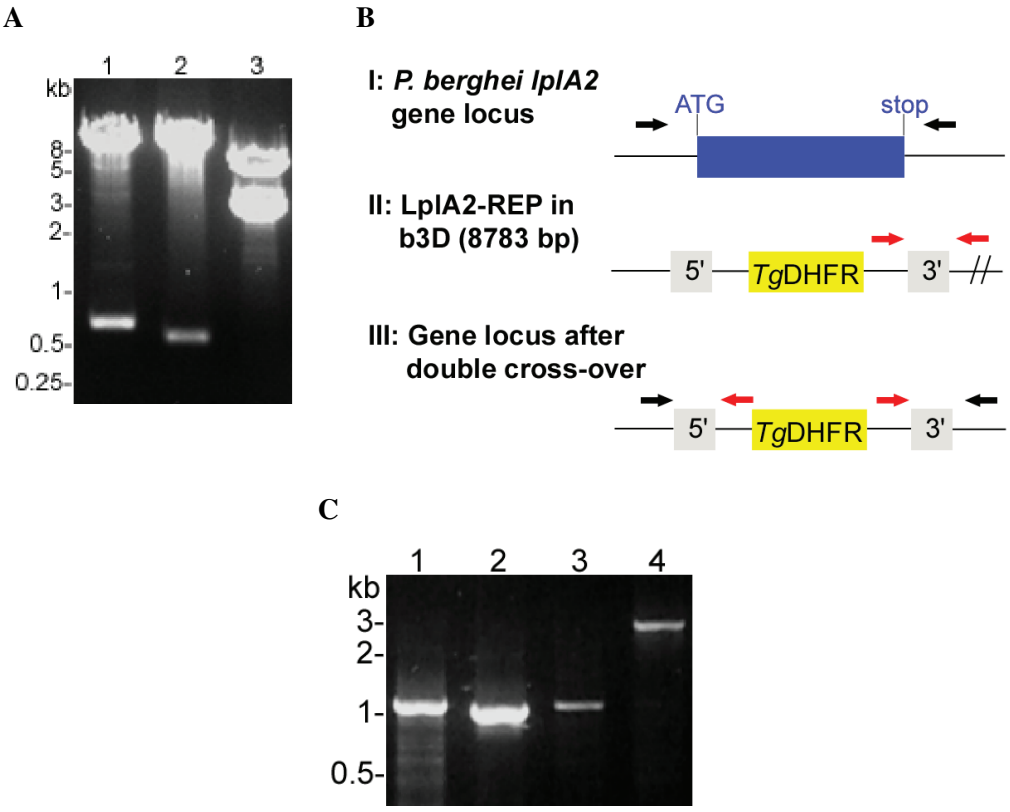

Figure 4.9.: Knock-out studies of *P. berghei lplA2* using the replacement strategy (**Panel A**) A 698 bp fragment was amplified as the *P. berghei lplA2* 5' UTR and was cloned into b3D.DT^H.^D (8020 bp) using the restriction enzymes KpnI and HindIII (lane 1). The 3' UTR PCR fragment (581 bp) was cloned into the plasmid using NotI and SacII (lane 2). Before transfection, *Pb*LplA2-REP-b3D was digested with KpnI and SacII resulting in a 5919 bp fragment containing the two UTRs and the *T. gondii* DHFR/TS expression cassette, and a 2864 bp fragment containing the plasmid backbone (lane 3). **Panel B** is a schematic diagram of the replacement of *P. berghei lplA2*. Transfectants were analysed by PCR using gene locus specific primers (black arrows) and plasmid specific primers (red arrows). **Panel C** displays the PCR analyses of transfected parasites. Lane 1 shows the 3' replacement specific PCR (1252 bp), lane 2 the 5' replacement specific PCR (1184 bp), lane 3 the plasmid specific PCR (1215 bp) and lane 4 the wild-type specific PCRs (3008 bp). The parasite population obtained after transfection was mixed, containing parasites that had the *lplA2* gene locus replaced and others which carried the plasmid episomally.

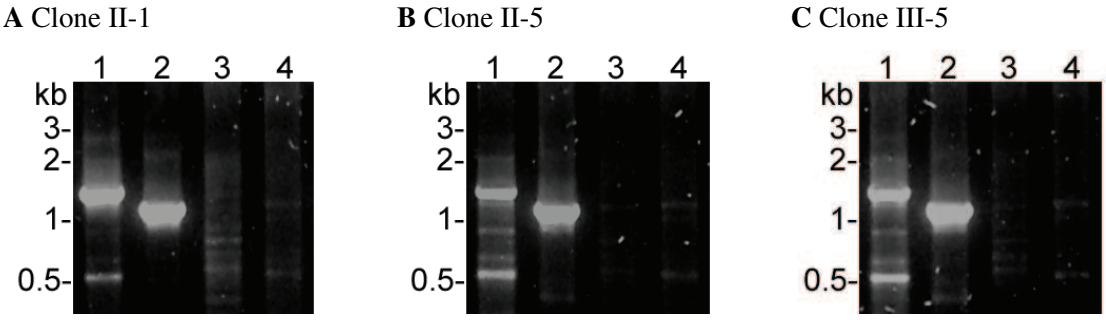

Figure 4.10.: PCR analyses of *P. berghei lplA2* knock-out clones
The mixed parasite population was cloned and obtained clones were analysed by PCR (**Panel A-C**). Lane 1 shows the 3' replacement specific PCR (1432 bp), lane 2 the 5' replacement specific PCR (1184 bp), lane 3 the plasmid specific PCR (1215 bp) and lane 4 the wild-type specific PCRs (3008 bp).

4.6.4. Knock-out control studies via double cross-over recombination

Knock-out control studies via double cross-over recombination were also carried out. The control plasmid contained an expression cassette of *P. falciparum* LplA2 to complement effects that the loss of *P. berghei lplA2*, after replacement, might induce. As described for LplA1 (see 3.6.4), the *P. falciparum* LplA2 expression cassette consisted of the *P. falciparum* CAM promotor (amplified using PfCAM5'-F2 and PfCAM5'-R1), *P. falciparum lplA2* (amplified using Pf-LplA2-ORF-fwd and Pf-LplA2-ORF-rev) and the 3' UTR of *P. falciparum* histidine rich protein 2 (HRP2) (amplified using PfHRPII3'-F1 and PfHRPII3'-R1) (see 2.1.7). The expression cassette was first generated in the plasmid pBluescript II SK (Stratagene) followed by sub-cloning into *Pb*LplA2-REP-b3D using the restriction sites BamHI and NotI (Figure 4.11, Panel A). The resulting plasmid was named *Pb*LplA2-comp-b3D which was digested with the restriction enzymes KpnI and SacII, before it was transfected four times into wild-type parasites (Janse et al., 2006). Three of the four transfections were successful, resulting in parasite populations after pyrimethamine selection in mice which were analysed by PCRs diagnostic for wild-type, plasmid and integration. The gene specific primers Pb-LplA2-int-fwd and Pb-LplA2-REP-rev (amplifying a 1744 bp band) (black arrows) were used to amplify endogenous *lplA2*, and the primers Pb-LplA2-3'-fwd and b3D-rev were used to amplify recombined plasmid (amplifying a 652 bp band) (red arrows). The 3' integration specific PCR was set up using the primers PfHRPII3'-F1 and Pb-LplA2-REP-rev (amplifying a 1296 bp band) (Figure 4.11, Panel B). The results shown in Figure 4.11 (Panel C) are exemplary for the three

parasite populations. *Pb*LplA2-comp-b3D did not integrate into the *lplA2* gene locus. No 3' replacement specific PCR band (1296 bp; lane 1) was amplified, but recombined plasmid (651 bp; lane 2) and wild-type *lplA2* (1744 bp; lane 3) were present. These data suggest that the complementation construct had not replaced the endogenous gene locus, which is surprising given that a knock-out of *lplA2* by double cross-over recombination was possible. These results could have several explanations. Firstly, the *P. falciparum* gene is not driven by its endogenous or the *P. berghei lplA2* promoter, but by the strong *P. falciparum* calmodulin promoter, which might lead to untimely over-expression of the protein. This may have a negative effect on parasite development, which possibly could explain my findings. However, technical problems could also be the cause of these results.

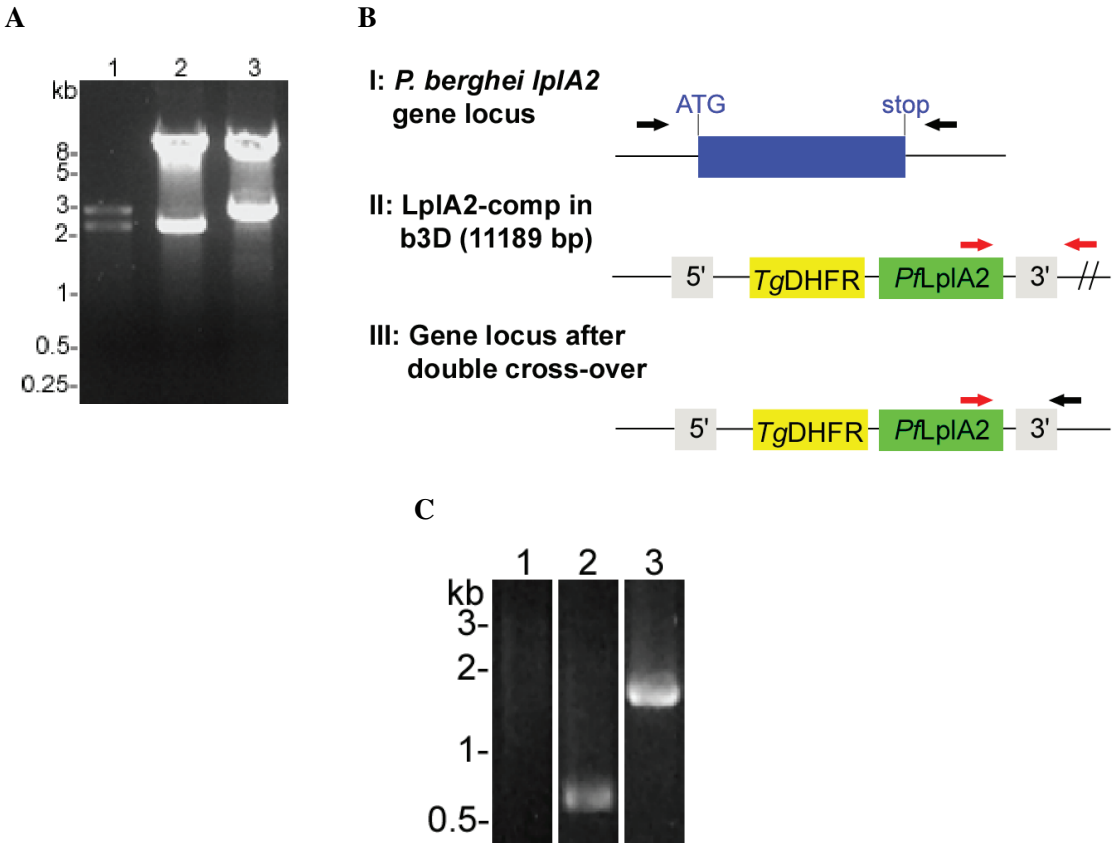

Figure 4.11.: Knock-out control studies of *P. berghei lplA2* using the replacement strategy (**Panel A**) For the control construct, a *P. falciparum* LplA2 expression cassette was cloned into *Pb*LplA2-REP-b3D. The expression cassette consisted of the *P. falciparum* CAM promoter, *lplA2* gene and HRP2 3' UTR. First, the expression cassette (2418 bp) was generated in the plasmid pBluescript II SK (3000 bp; Stratagene) (lane 1). Using the restriction enzymes BamHI and NotI the expression cassette was cloned into *Pb*LplA2-REP-b3D (8783 bp) in front of the *P. berghei lplA2* 3' UTR, resulting in the plasmid *Pb*LplA2-comp-b3D (lane 2). Before transfection, *Pb*LplA2-comp-b3D was digested with KpnI and SacII resulting in a 8325 bp fragment containing the 5' and 3' *P. berghei lplA2* UTRs, the *T. gondii* DHFR/TS and the *P. falciparum* LplA2 expression cassettes, and a 2864 bp fragment containing the plasmid backbone (lane 3). **Panel B** is a schematic diagram of the complementation of *P. berghei lplA2* replacement. Transfectants were analysed by PCR using gene locus specific primers (black arrows) and plasmid specific primers (red arrows). **Panel C** displays the PCR analyses of transfected parasites. Lane 1 shows the 3' replacement specific PCR (1296 bp), lane 2 the plasmid specific PCR (651 bp) and lane 3 the wild-type specific PCR (1744 bp). *Pb*LplA2-comp-b3D did not integrate into the *lplA2* gene locus, indicating that the complementation of *lplA2* replacement was not successful.

4.6.5. Phenotypical analyses of *lplA2* replacement mutants

4.6.5.1. Analyses of *P. berghei* erythrocytic stages

To analyse potential effects of *lplA2* knock-out, the intraerythrocytic stages of *P. berghei* were analysed first. Initial western blot analyses were performed on parasite extract using an antibody against protein bound lipoic acid, to assess whether knock-out of *lplA2* affects the lipoylation state of the KADH-E2 subunits and the H-protein (Figure 4.12, Panel A). The expected size of *P. berghei* PDH-E2 is 69.1 kDa, of BCDH-E2 50 kDa, of KGDH-E2 46.6 kDa and of H-protein 14 kDa. The anti-lipoic acid antibody detected two bands in the NK65 wild-type extract (lane 1), probably corresponding to PDH-E2 and BCDH-E2. KGDH-E2 and H-protein were not detected by the antibody. Western blot analyses of the *lplA2* mutant clones II-1 (lane 2) and III-5 (lane 4) showed in comparison to wild-type parasites no major differences in the lipoylation pattern observed. No loading control was used which makes it impossible to finally conclude whether lipoylation intensities changed in the LplA2-KO parasite clones. However, Ponceau staining of the membrane after transfer (see 2.6.5) did not show obvious differential loading of clones II-1 and III-5 in comparison to wild-type (not shown). Western blot analysis of clone II-5 (lane 3) suggested that the KADH-E2 subunits were less lipoylated than in wild-type parasites. This, however, is more likely due to different loading, which I observed after transfer with Ponceau staining of the membrane for this clone (not shown). Thus, initial western blotting suggests that *lplA2* knock-out does not reduce lipoylation of the enzyme complexes in comparison to wild-type parasites. Rather, it seems that the complexes are slightly stronger lipoylated which could be due to an up-regulation of the other ligases present in *Plasmodium*. This, however, needs to be further investigated by western and northern blotting of the LplA2-KO mutants.

Furthermore, it was analysed whether knock-out of *lplA2* affected the growth of *P. berghei* blood stages *in vivo*. Growth rate assays (see 2.3.10) were set up for the LplA2-KO mutant clones II-1, II-5 and III-5 monitoring growth of each clone in five mice for eight days. Growth rate assays for NK65 wild-type parasites were set up twice thus monitoring growth of NK65 in ten mice (Figure 4.12, Panel B). The results show that clone II-1 and clone II-5 had a slightly decreased growth phenotype with constantly lower parasitemia each day. The differences in parasitemia were significant on day five and six. In contrast, clone III-5 showed significantly higher parasitemia on day five and equal parasitemia on day six in comparison to wild-type parasites, suggesting a moderately accelerated growth phenotype of this clone. However, the last two days monitored (day seven and eight) the

parasitemia of clone III-5 was lower in comparison to wild-type parasites. Overall, the experiment suggests that LplA2-KO affects the blood stage parasite growth only modestly, and the significant differences observed are likely to be due to the fact that this experiment was performed in animals *in vivo*. This is supported by the standard errors obtained and the general growth pattern observed, because once the parasitemia reaches a certain level ($>1\%$), the immune system of the animal kills parasites and generally keeps the parasitemia $\leq 1\%$.

To further analyse a possible effect of the LplA2 mutant parasites in the blood stages, a transfer assay (see 2.3.11) was set up using clone II-5 and NK65 wild-type parasites. Two naive mice were infected with 1000 mutant and 1000 wild-type parasites each. The obtained mixed parasite populations were transferred into new naive mice. This was repeated five times and the genotype of the first and the last obtained parasite populations were analysed by PCR using the diagnostic primer sets described in Figure 4.9 (Panel B). The PCR results of the transfer assay are shown in Figure 4.12 (Panel C). After infection of the first animals with equal numbers of mutant and wild-type parasites, the 3' (1252 bp; lanes 1) and 5' (1184 bp; lanes 2) replacement specific bands were amplified. No *lplA2* wild-type specific PCR was amplified (3008 bp; lanes 3), which could be explained by either technical PCR problems or that the number of wild-type parasites was too low to be detected by PCR. However, after five transfers *lplA2* wild-type is present in both animals (lanes 3). On the contrary, the 3' replacement specific band is not detected anymore in either of the two animals (lanes 1). The 5' replacement specific PCR still amplifies a band of the expected size (1184 bp; lanes 2), but in addition a second band at 900 bp is visible. These results suggest that wild-type parasites seem to grow better over longer periods, which is supported by the growth experiment described above (Figure 4.12, Panel B). Here, the LplA2-KO clone II-5 grew slightly slower in comparison to wild-type parasites. Over the eight day period this had only a small effect but in direct competition with wild-type parasites over a longer time period, the effects are likely to be more obvious. However, this experiment was only performed once and should be repeated not only by PCR, but by quantitative PCRs, Southern blotting and PFGE. Moreover, analyses of the the parasite populations obtained after the four transfers in between would possibly clarify after how many transfers the *lplA2* mutant parasites were outcompeted by wild-type parasites *in vivo*.

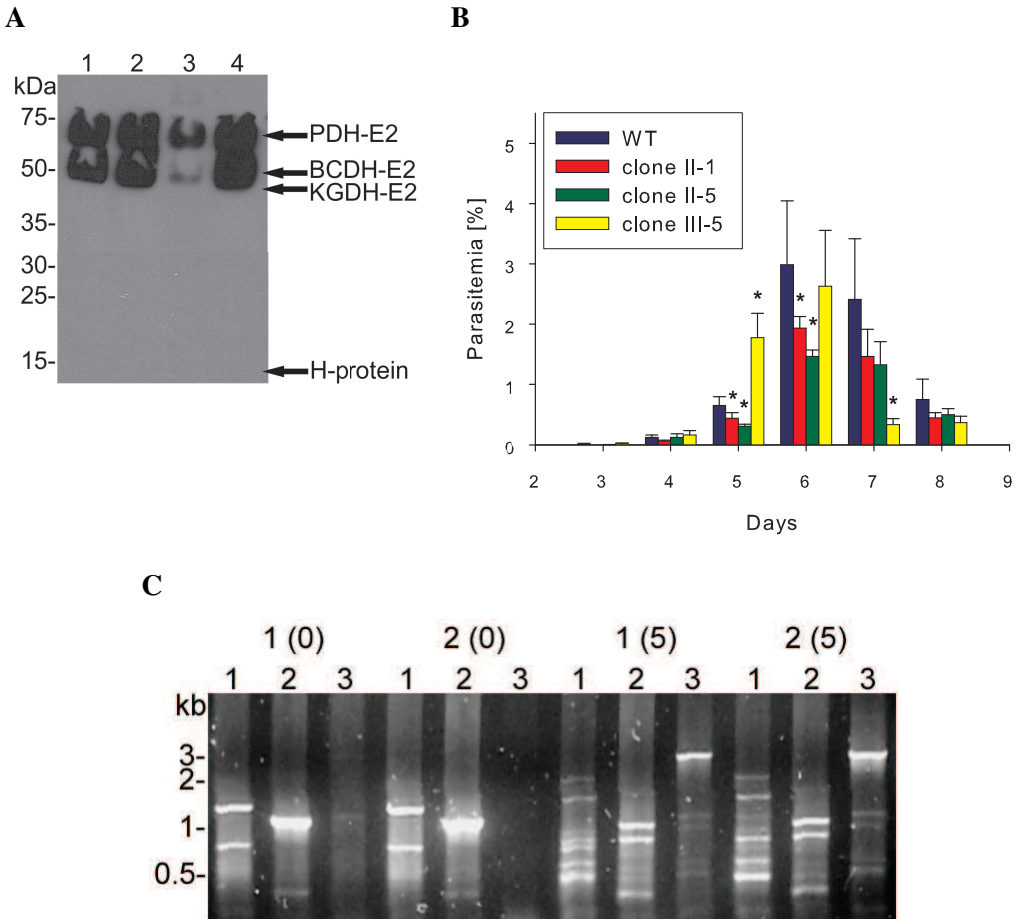

Figure 4.12.: Phenotypical analyses of *P. berghei* LplA2 mutant intraerythrocytic stages (**Panel A**) Western blot analysis was performed on parasite extract using an anti-lipoic acid antibody. Lane 1 contains wild-type parasites, lane 2 clone II-1, lane 3 clone II-5 and lane 4 clone III-5. Two bands were detected by the lipoic acid antibody likely corresponding to PDH-E2 (expected size 69.1 kDa) and BCDH-E2 (expected size 50 kDa). No major differences were observed in the clonal lines, except for clone II-5 where lipoylation seems to be less in comparison to wild-type. However, this is more likely due to different loading (not shown). The other two clones show no reduction in lipoylation. On the contrary, lipoylation of the enzyme complexes seems slightly stronger. **Panel B** displays growth of the LplA2-KO clones in comparison to wild-type (WT) parasites. Growth of NK65 wild-type in ten mice and in five mice for each clone was monitored for eight days. Each bar represents the mean $\pm$ standard error. Levels of significance were calculated by paired t-test using SigmaPlot 9.0 software (Systat). Differences were considered significant at $P<0.05$. Significant differences (*) in parasitemia of the clones in comparison to wild-type were observed on day five, six and seven. **Panel C** displays PCR results of animal 1 and 2 after the first infection (0) and after five transfers (5). Lane 1 shows the 3' replacement specific PCR (1184 bp), lane 2 the 5' replacement specific PCR (1184 bp) and lane 3 the wild-type specific PCR (3008 bp).

4.6.5.2. Analyses of *P. berghei* sexual developmental stages

To investigate potential effects of *lplA2* knock-out on the sexual development of *P. berghei* in the insect vector, clone II-5 was used for further analyses. Mosquitoes were infected via a blood-meal on infected mice, and 10-14 days after the blood-meal the presence of oocysts in the mosquitoes midgut was analysed. Midguts were dissected and were analysed microscopically for the presence of oocysts. The results are summarised in Table 4.4.

Table 4.4.: *In vitro* oocyst development of clone II-5 in the mosquitoes midgut

	Infected midguts	Oocysts per infected midgut	Re-infection of mice
WT	8/10	62.25	Yes
clone II-5 (1st feeding)	0/12	-	No
clone II-5 (2nd feeding)	0/10	-	No
clone II-5 (2mM LA)	0/10	-	No
clone II-5 + WT	3/10	7.67	Yes

In two independent experiments mosquitoes were infected with LplA2-KO clone II-5 and in both experiments no oocysts were detected in the midguts analysed. However, in mosquitoes infected with NK65 wild-type parasites, oocysts were detected in almost all midguts analysed. A third infection with clone II-5 was performed and mosquitoes were supplied with 2 mM lipoic acid via their food, but no infected midguts were observed. In another experiment, mosquitoes were infected with equal numbers of clone II-5 and wild-type parasites by letting them feed on a mouse, which was infected with equal numbers of knock-out clone and wild-type parasites. After 10-14 days, oocysts were detected in the midguts of the mosquitoes. Comparison to mosquitoes infected with wild-type parasites, however, revealed that less mosquitoes were infected, and that additionally the number of oocysts per infected midgut was drastically reduced. The mosquitoes listed in Table 4.4 were also used to infect naive mice. As expected, only mosquitoes infected with wild-type parasites, or mosquitoes infected with clone II-5 and wild-type, were able to re-infect mice.

Further analyses of the sexual developmental stages was carried out. In Giemsa stained blood smears of mice infected with LplA2-KO clone II-5, male as well as female gametocytes were observed suggesting that gametocytogenesis is not, or only modestly,

affected by *lplA2* knock-out. Moreover, exflagellation of male gametes was assessed before mosquito feedings (see 2.3.12) and was comparable to exflagellation of wild-type parasites, suggesting that knock-out of *lplA2* has no effect on male gametes. Thus, *in vitro* ookinete cultures were set up of NK65 wild-type parasites and clone II-5, to investigate whether the development of ookinetes is affected. Ookinetes were purified and their number was determined microscopically (see 2.3.13) (Table 4.5).

Table 4.5.: *In vitro* ookinete development of clone II-5

	Ookinetes per ml blood
WT	7,500,000
clone II-5	409,091

The formation of ookinetes is drastically reduced in the LplA2-KO clone II-5. The LplA2 mutant developed about 18 times less ookinetes in comparison to wild-type parasites. However, this experiment needs to be repeated since it was only performed once due to time constraints.
Overall, these data strongly suggest that the sexual development is severely affected. Future work will involve the analyses of gametocytogenesis and gametogenesis in more detail, and it will be analysed whether knock-out of *lplA2* causes a sex-specific defect.

4.7. Summary

• *Plasmodium* possess a second lipoic acid protein ligase like protein named LplA2. Orthologues were found in other apicomplexan parasites like *Theileria*, but probably not in *Toxoplasma*. The *Toxoplasma* predicted protein sequence misses amino acids crucial for functionality of LplA2, suggesting that the *Toxoplasma* LplA2 is not functional.

• *P. falciparum* LplA2 complements the growth defect of *lipB* deficient and *lipB*/*lplA* deficient bacteria, showing that it is a functional lipoic acid protein ligase.

• Prediction of LplA2 localisation within *Plasmodium* spp. using several prediction programs is not clearly possible.

• Localisation studies of LplA2-GFP expressing parasites suggested dual localisation of

LplA2 to mitochondrion and apicoplast. These data were experimentally supported by immunofluorescence analyses performed on wild-type parasites using antibodies against LplA2 and apicoplast localised lipoamide dehydrogenase (aE3).

• Knock-out studies of *P. falciparum lplA2* were attempted by single cross-over recombination and disruption of the gene locus using the plasmid pHH1. No disruption of the endogenous *lplA2* locus was obtained.

• Knock-out studies of *P. berghei lplA2* by single cross-over recombination appeared impossible. The 3' replacement construct did, however, target the *lplA2* gene locus.

• Knock-out studies of *P. berghei lplA2* by double cross-over recombination resulted in replacement of the *lplA2* gene. However, the control complementation construct did not replace the gene locus.

• Overall these studies show that (1) the *lplA2* locus can be targeted by both methods and (2) that it is difficult to conclude that a gene locus is essential simply because the gene locus is not targeted.

• Phenotypical analyses of the *lplA2* mutant parasites revealed that the erythrocytic stages were only modestly affected by the knock-out of *lplA2*. However, *lplA2* null mutants were unable to progress through the sexual developmental cycle. The formation of ookinetes is drastically reduced and consequently no oocysts are formed by the mutant parasites.

5. Biochemical characterisation of LplA1 and LplA2

5.1. Introduction

Lipoic acid is an essential cofactor of the acyltransferase (E2) subunit of the KADHs and the H-protein of the GCV (Perham, 2000, Douce et al., 2001). It is covalently attached to a conserved lysine residue of the lipoyl-domain of the E2 subunits and to the H-protein, which is structurally homologous to the lipoyl-domains (see Figure 1.6). Lipoate protein ligases (LplA) catalyse the attachment of lipoic acid to the lipoyl-domain using ATP, releasing AMP and inorganic pyrophosphate (PPi) as shown in the following equation:

Lipoyl-domain + lipoic acid + ATP $\rightarrow$ lipoylated-domain + AMP + PPi

During the reaction a lipoyl-AMP intermediate is formed which facilitates the transfer of lipoic acid to the lysine residue of the lipoyl-domain. This means that the activity of LplA can be assessed by determining the lipoylation state of the lipoyl-domain, which can be achieved in a variety of ways. Assay systems include the analyses of lipoylation of the KADH-E2 subunits and H-protein by native PAGE (Ali and Guest, 1990, Fujiwara et al., 1992). This allows distinction between lipoylated and non-lipoylated proteins due to a shift in their mobility, induced by a charge difference between the modified and non-modified proteins (Fujiwara et al., 1992). Other methods monitor the increase of enzymatic activity of H-protein (Walker and Oliver, 1986, Fujiwara et al., 1992), PDH or KGDH (Jordan and Cronan, 1997) as a measure of lipoylation. The latter assay systems, however, rely on the availability of a number of additional protein components, which are usually not commercially available and therefore need to be generated in addition to LplA and the apo-E2 domains that are required for the analyses of the transferase activity.
Therefore, in this study I attempted to establish and validate an enzyme assay for LplA which detects the release of PPi, the product of the first part of the LplA reaction. This, however, did not allow the analyses of the final product of the reaction - the lipoylated protein. Therefore, I also analysed the lipoylation state of H-protein and E2 lipoyl-domains of the three KADH by western blotting with an antibody directed against protein-bound lipoic acid.

This chapter thus describes the initial biochemical characterisation of *P. falciparum* LplA1

and LplA2. As a positive control, *E. coli* LplA was used (Green et al., 1995, Fujiwara et al., 2005) to establish and validate both assay systems used. The protein substrates that were used for the characterisation of the LplAs were the *P. falciparum* H-protein and the lipoyl-domains of the PDH, BCDH and KGDH, rather than the entire apo-E2-subunits of the enzyme complexes. Previous studies have shown that the lipoyl-domains in isolation can be recombinantly expressed and used for lipoylation experiments (Ali and Guest, 1990, Dardel et al., 1990, Quinn et al., 1993).

5.2. *P. falciparum* LplA1 - Recombinant protein expression and purification

5.2.1. Cloning of *P. falciparum* LplA1 expression constructs

For the recombinant expression of LplA1, the coding region of the gene was cloned into the two expression plasmids pJC40 (see Figure 2.10) and pASK-IBA3 (see Figure 2.11). pJC40 attached a $(His)_{10}$-tag at the N-terminus of the recombinant protein whereas pASK-IBA3 attached a Strep-tag at the C-terminus. For cloning into pJC40, *lplA1* was amplified from *P. falciparum* 3D7 gDNA using AccuPrime *Pfx* Supermix (Invitrogen). The oligonucleotide primers PfLplA-NdeI-S and PfLplA-BamHI-AS (see 2.1.7), used to amplify the gene, introduced a NdeI and BamHI site at the 5' and 3' end of the PCR product, respectively. The 1182 bp PCR fragment was equivalent to nucleotides 46-1227. The gene was truncated at the 5' end to remove the N-terminal mitochondrial targeting sequence of the protein (Wrenger and Müller, 2004) (see 3.2), that potentially could interfere with protein's solubility in the prokaryotic expression system. The PCR product was initially cloned into the TOPO-Blunt PCR cloning vector (Invitrogen) and its sequence was verified, before it was sub-cloned into the expression plasmid pJC40 using the NdeI and BamHI restriction sites (Figure 5.1, Panel A). The second expression construct, LplA1 in pASK-IBA3, was available in the laboratory (Wrenger and Müller, 2004) (Figure 5.1, Panel A). The two constructs were named LplA1-pJC40 and LplA1-pASK-IBA3.

5.2.2. Recombinant expression of *P. falciparum* LplA1

Test expressions of LplA1-pJC40 and LplA1-pASK-IBA3 were carried out to optimise expression conditions for both constructs. Expression of LplA1-pJC40 was tested in *E. coli* BLR(DE3) (Novagen) at three different temperatures (37°C, 30°C and 18°C) and for varying lengths of time after induction with 1 mM IPTG. Samples were taken before

induction and hourly after induction. The bacteria were harvested at the respective time points, and the pellets were lysed using the BugBuster protein extraction kit (Novagen). Soluble and insoluble protein fractions were analysed for recombinant LplA1 expression by western blotting using an anti-His-tag antibody (dilutions given in Table 2.1). Figure 5.1 (Panel B) shows the western blot analysis of the test expressions performed at 37°C. The expression pattern did not change at different temperatures. A band was detected on the western blot of the expected size of $(His)_{10}$-tagged LplA1 (48.3 kDa) and was expressed at similar levels throughout the experiment. For large-scale expressions it was decided to express the protein for two to three hours at 37°C to obtain a high bacteria density.

Figure 5.1 (Panel C) shows the western blot analysis of Strep-tagged LplA1 test expressions using an anti-Strep-tag antibody (dilutions given in Table 2.1). The construct was transformed into *E. coli* BLR(DE3) (Novagen), Ker184 (Reed and Cronan, 1993) and Tm134 (Morris et al., 1994), and recombinant expression was tested at 37°C, 30°C and 18°C for varying lengths of expression after induction with 200 ng/ml AHT. Samples were taken before induction, hourly after induction and after overnight expression. The bacteria were harvested and lysed as described above, and the recombinant expression of the 47.3 kDa protein was analysed by western blotting using an antibody against the Strep-tag. Strep-tagged LplA1 was not expressed in detectable amounts in BLR(DE3) and Ker184. In Tm134, the expression pattern observed was independent of temperature and thus only the western blot of the test expression performed at 37°C is shown (Figure 5.1, Panel C). The expression level of recombinant Strep-tagged LplA1 was similar in all hourly samples analysed, and decreased overnight. Therefore, large-scale expressions for purification were performed at 37°C for two to three hours.

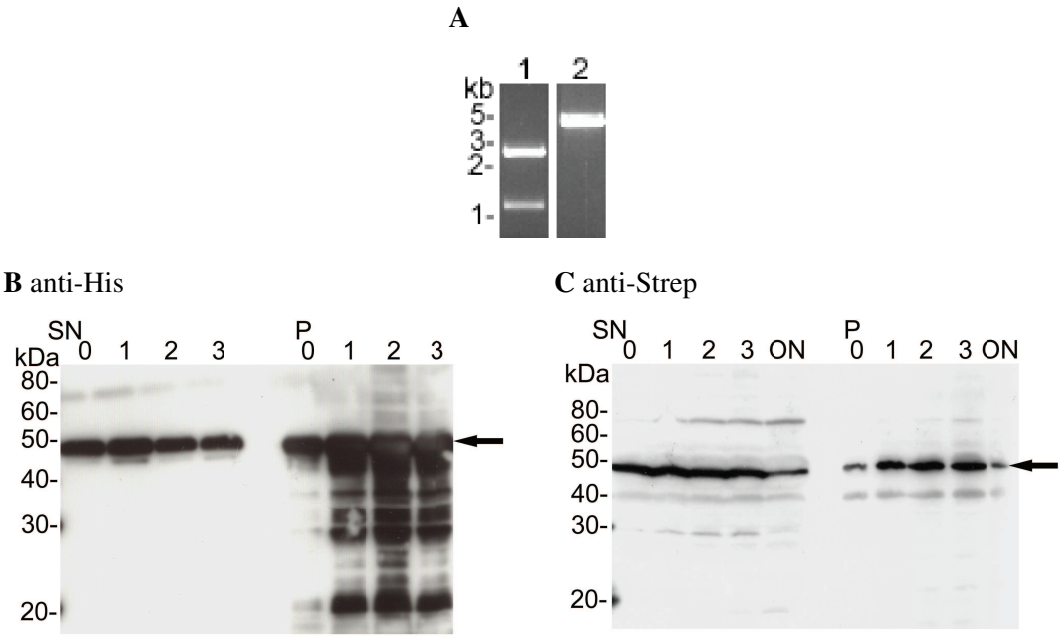

Figure 5.1.: Cloning of *P. falciparum* LplA1 expression constructs and western blot analyses of test expressions of *P. falciparum* LplA1 constructs
LplA1 was cloned into the two expression plasmids pJC40 and pASK-IBA3. **Panel A** shows the digests of the expression plasmids. LplA1 cloned into pJC40 (lane 1) was digested using the restriction enzymes NdeI and BamHI, resulting in two bands corresponding to *lplA1* (1187 bp) and pJC40 (2381 bp). The pASK-IBA3 construct (lane 2) was linearised using the restriction enzyme XbaI resulting in a 4334 bp band. Test expressions of both constructs were analysed by western blotting (**Panel B and C**) using anti-His-tag and anti-Strep-tag antibodies, respectively (for dilutions see Table 2.1). The blots show the protein in the supernatant fractions (SN) and pellet fractions (P) before induction (0), 1 to 3 hours after induction (1-3) and after overnight expression (ON). The expected size of the His-tagged LplA1 (**Panel B**) was 48.6 kDa and 47.3 kDa for the Strep-tagged LplA1 (**Panel C**). The expression of both constructs shown here was performed at 37°C, but was also tested at 30°C and 18°C. The expression pattern did not change at different temperatures. The expression of LplA1-pJC40 was tested in *E. coli* BLR(DE3). The expression of LplA1-pASK-IBA3 was tested in various *E. coli* cells. Expression in Tm134 is shown here.

5.2.3. Purification of *P. falciparum* LplA1

For purification of both recombinant LplA1 forms, large-scale expressions at 37°C were set up for each construct. The bacteria were harvested and the recombinant proteins were purified by batch nickel affinity chromatography (see 2.6.9.1) of the $(His)_{10}$-tagged LplA1 and Strep-Tactin column affinity chromatography (see 2.6.10) of the Strep-tagged LplA1. Generally, 2L expression cultures resulted in ∼2 mg $(His)_{10}$-tagged and ∼3 mg Strep-tagged LplA1. Figure 5.2 shows the recombinant proteins after purification. 5 μg of the elution fraction was separated by 12.5% SDS-PAGE, and was analysed by Coomassie

staining (Panel A) and western blotting (Panel B) using anti-His-tag and anti-Strep-tag antibodies, respectively. $(His)_{10}$-tagged LplA1 appeared to be less stable than Strep-tagged LplA1, as demonstrated by the presence of degradation products of the recombinant protein in the elution fraction. These were particulary obvious in the western blot (Figure 5.2, Panel B).

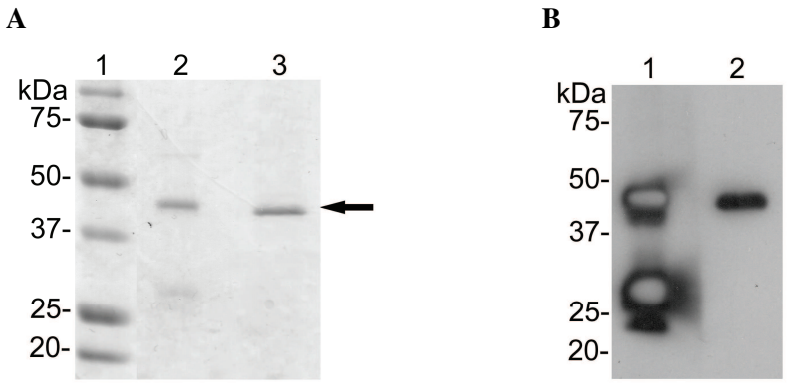

Figure 5.2.: Purification of recombinant expressed *P. falciparum* LplA1s
Panel A displays 5 μg of recombinantly expressed LplA1 with an N-terminal $(His)_{10}$-tag (48.6 kDa) (lane 2) and a C-terminal Strep-tag (47.3 kDa) (lane 3), separated on 12.5% SDS-PAGE stained with Coomassie. **Panel B** shows the equivalent western blot of His-tagged LplA1 (lane 1) using anti-His-tag antibody, and of Strep-tagged LplA1 (lane 2) using anti-Strep-tag antibody.

5.3. *P. falciparum* LplA2 - Recombinant protein expression and purification

5.3.1. Cloning of *P. falciparum* LplA2 expression constructs

For the recombinant protein expression of *P. falciparum* LplA2, the plasmids pJC40 (see Figure 2.10) and pASK-IBA3 (see Figure 2.11) were also used. Three expression constructs were generated and cloned into each plasmid. The sizes of the three constructs are summarised in Table 5.1. The constructs varied in length at their N-termini because of a possible, but not predictable, targeting sequence at the N-terminus of the predicted protein (see Table 4.3).

Table 5.1.: Sizes of *P. falciparum* LplA2 constructs

Construct	Length in bp	Length in aa
*Pf*LplA2-full length (fl)	1-1155	1-385
*Pf*LplA2-short 1 (S1)	79-1155	27-385
*Pf*LplA2-short 2 (S2)	235-1155	79-385

For cloning into pJC40, the antisense oligonucleotide primer PfLplA2-BamHI-AS was used for all three constructs introducing a BamHI site. The full length construct was amplified using the sense oligonucleotide PfLplA2-FL-NdeI-S, resulting in a 1155 bp PCR fragment. PfLplA2-S1-NdeI-S was used to amplify the S1 construct (1077 bp) and PfLplA2-S2-NdeI-S was used to amplify the S2 construct (921 bp). The sense primers introduced a NdeI site which then allowed directional cloning into pJC40 (Figure 5.3, Panel A) (for primer sequences see 2.1.7).
For cloning into pASK-IBA3, the antisense primer PfLplA2-IBA3-rev was used to amplify all three constructs. The primer had no stop codon so that the Strep-tag was attached at the C-terminus of the recombinant protein. In combination with the sense primer PfLplA2-IBA3-1-fwd, the full length fragment was amplified. The sense primer PfLplA2-IBA3-2-fwd generated the S1 fragment from nucleotide 79-1152. The third fragment (S2) was amplified using PfLplA2-IBA3-3-fwd corresponding to nucleotide 235-1152. All primers contained a BsaI restriction site which allowed directional cloning into pASK-IBA3 (Figure 5.3, Panel B) (for primer sequences see 2.1.7).

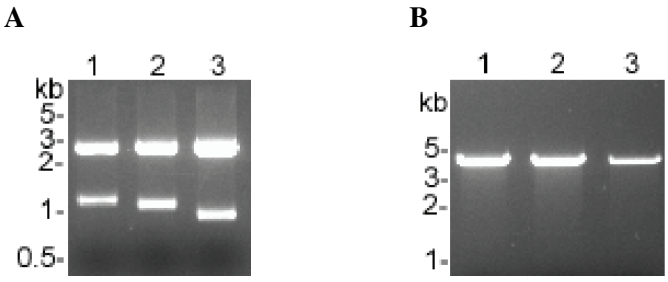

Figure 5.3.: Cloning of *P. falciparum* LplA2 expression constructs
For recombinant protein expression, the expression plasmids pJC40 and pASK-IBA3 were used. **Panel A** displays the three LplA2 expression constructs in pJC40. They were digested using the restriction enzymes NdeI and BamHI, resulting in a 2383 bp band corresponding to pJC40 (lane 1-3), a 1155 bp band corresponding to the LplA2-full length construct (lane 1), a 1077 bp band corresponding to the LplA2-S1 construct (lane 2) and a 921 bp band corresponding to the LplA2-S2 construct (lane 3). **Panel B** shows the LplA2 expression constructs in pASK-IBA3 linearised using the restriction enzyme XbaI. The linearised full length construct (lane 1) resulted in a 4305 bp band, the S1 construct (lane 2) in a 4229 bp band and the S2 construct (lane 3) resulted in a 4073 bp band.

5.3.2. Recombinant expression of *P. falciparum* LplA2

To find optimal expression conditions for each of the constructs, small-scale test expressions were set up. The three pJC40 constructs were transformed into *E. coli* BLR(DE3) (Novagen), and expression of the recombinant protein was monitored at different temperatures (37°C, 30°C, 23°C and 18°C) for varying expression times after induction with 1 mM IPTG, similar to the test expressions described for LplA1 (see 5.2.2). Figure 5.4, Panel A shows the western blots of the test expressions of the LplA2-fl construct (expected size 48.6 kDa) and Panel B displays the western blots of the test expressions of the LplA2-S1 construct (expected size 45.7 kDa). Regardless of the temperature used after induction of recombinant protein expression, both constructs were not solubly expressed. The recombinant proteins were only detected in the pellet fractions. The LplA2-S2 construct (expected size 39.6 kDa) was expressed in a small amount in the soluble fraction (Figure 5.4, Panel C). The expression level of the recombinant protein was constant in the first two hours after induction, but disappeared after overnight expression. Further, degradation of the recombinant protein was detected and it was decided that expression at 30°C, rather than 37°C, for two hours were the best conditions for large-scale expressions of the $(His)_{10}$-tagged LplA2-S2 construct. Expression at 30°C resulted in a high bacteria density, but was more gentle in terms of protein degradation in comparison to expression at 37°C.

A LplA2-fl-pJC40

I) 37°C

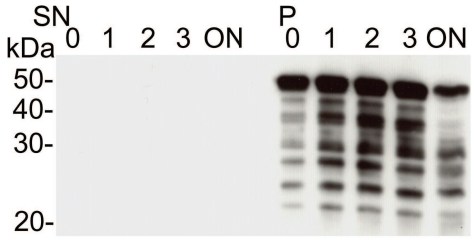

II) 30°C

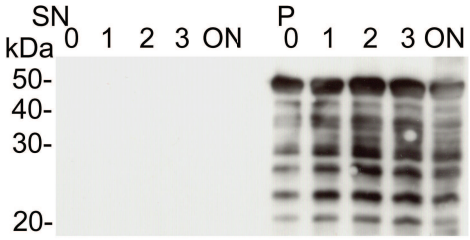

III) 23°C

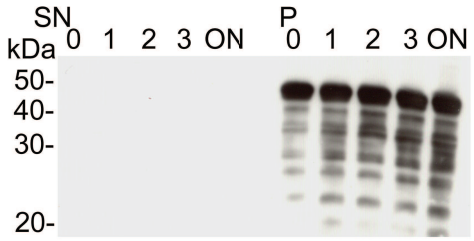

IV) 18°C

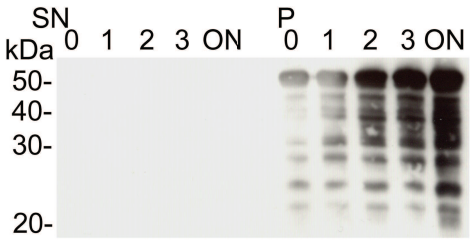

B LplA2-S1-pJC40

I) 37°C

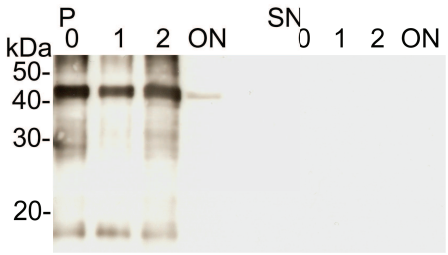

II) 30°C

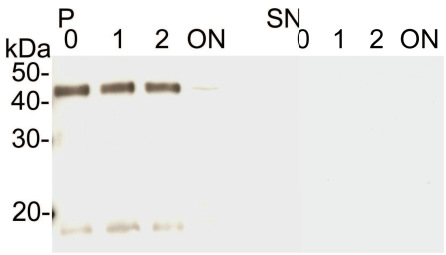

III) 23°C

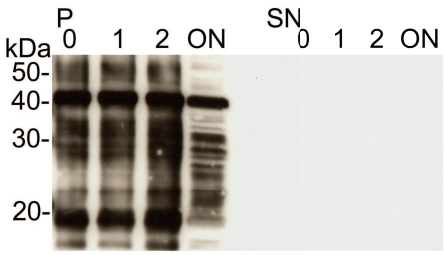

IV) 18°C

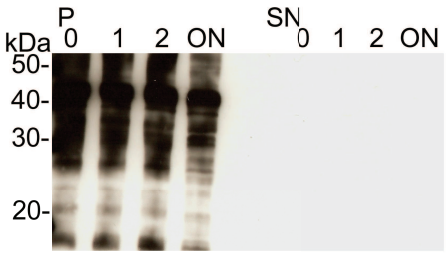

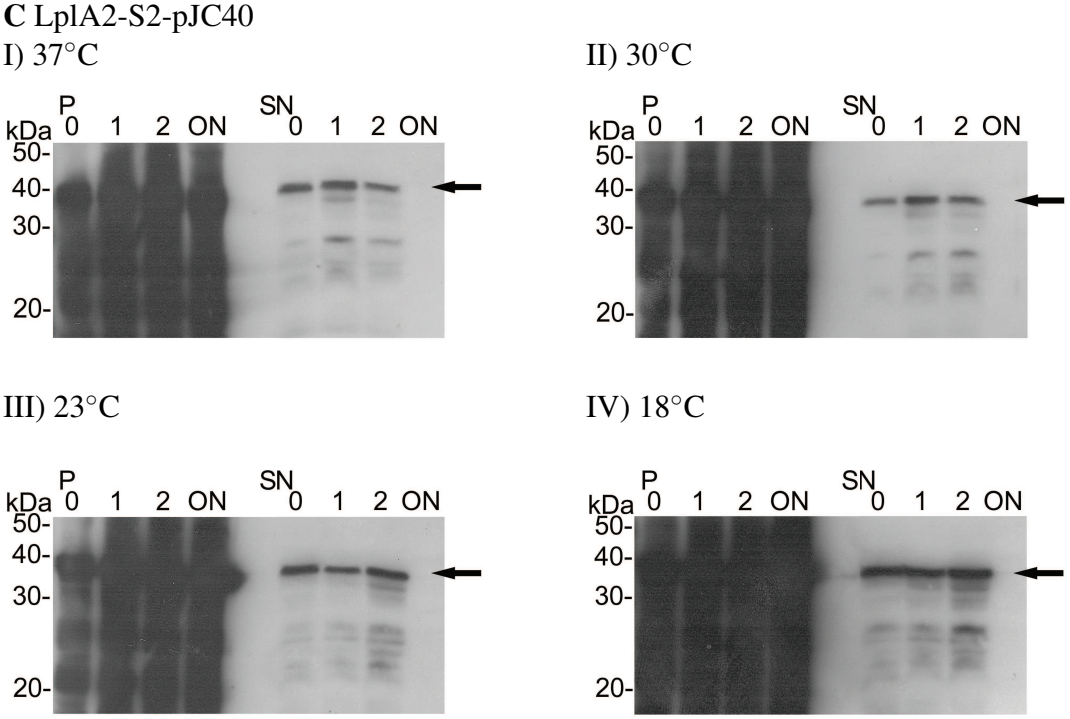

Figure 5.4.: Western blot analyses of test expressions of *P. falciparum* LplA2-pJC40 constructs in *E. coli* BLR(DE3)
Test expressions of LplA2-pJC40 constructs were performed in *E. coli* BLR(DE3) at (I) 37°C, (II) 30°C, (III) 23°C and (IV) 18°C each and were analysed by western blotting using an anti-His-tag antibody. **Panel A** displays test expressions of the full length construct (expected size 48.6 kDa), **Panel B** of the S1 construct (expected size 45.7 kDa), and **Panel C** of the S2 construct (expected size 39.6 kDa). The blots show the protein in the pellet fractions (P) and supernatant fractions (SN) before induction (0), 1 to 3 hours after induction and after overnight expression (ON). The full length and S1 construct were not expressed in soluble form and only a small amount of LplA2-S2 was expressed in the soluble fraction (arrow). However, degradation products of the recombinant protein were also detected by the antibody. Degradation seemed to be worse if expression was carried out at lower temperatures.

The pASK-IBA3 constructs were transformed into *E. coli* BLR(DE3) (Novagen), Ker184 (Reed and Cronan, 1993) and Tm134 (Morris et al., 1994), and recombinant expression was tested at 37°C, 30°C, 23°C and 18°C for varying lengths of time after induction with 200 ng/ml AHT. As described above, samples were taken before induction, hourly after induction and after overnight expression, and were analysed using the BugBuster protein expression kit (Novagen) followed by western blotting with an anti-Strep-tag antibody. All three constructs, LplA2-fl (expected size 47.3 kDa), LplA2-S1 (expected size 44.3 kDa) and LplA2-S2 (expected size 38.3 kDa) were not solubly expressed in any of the bacteria tested (Figure 5.5). The western blots shown here display the recombinant protein test expressions performed in Tm134.

A LplA2-fl-pASK-IBA3

I) 37°C

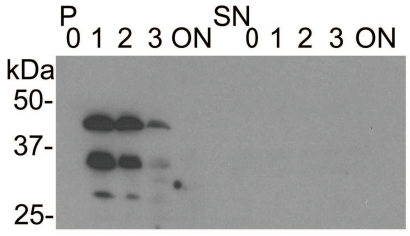

II) 30°C

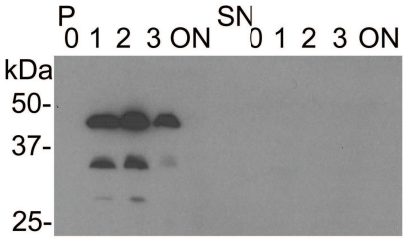

III) 23°C

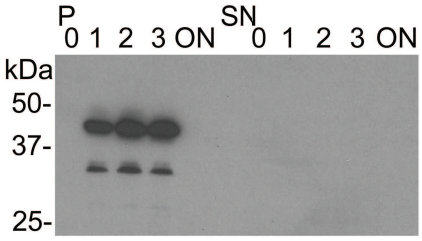

IV) 18°C

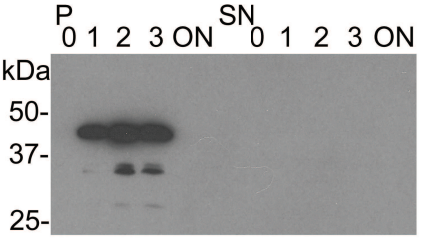

B LplA2-S1-pASK-IBA3

I) 37°C

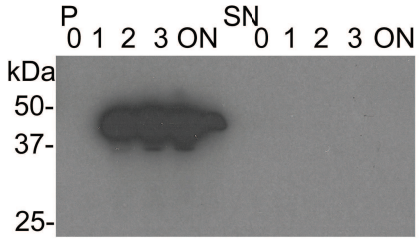

II) 30°C

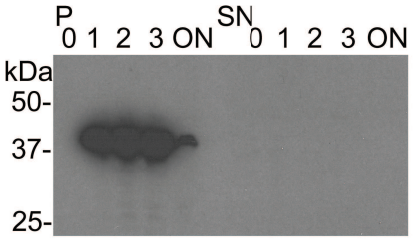

III) 23°C

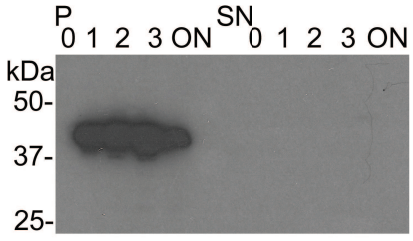

IV) 18°C

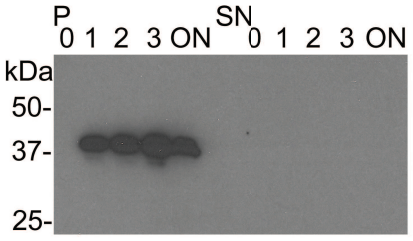

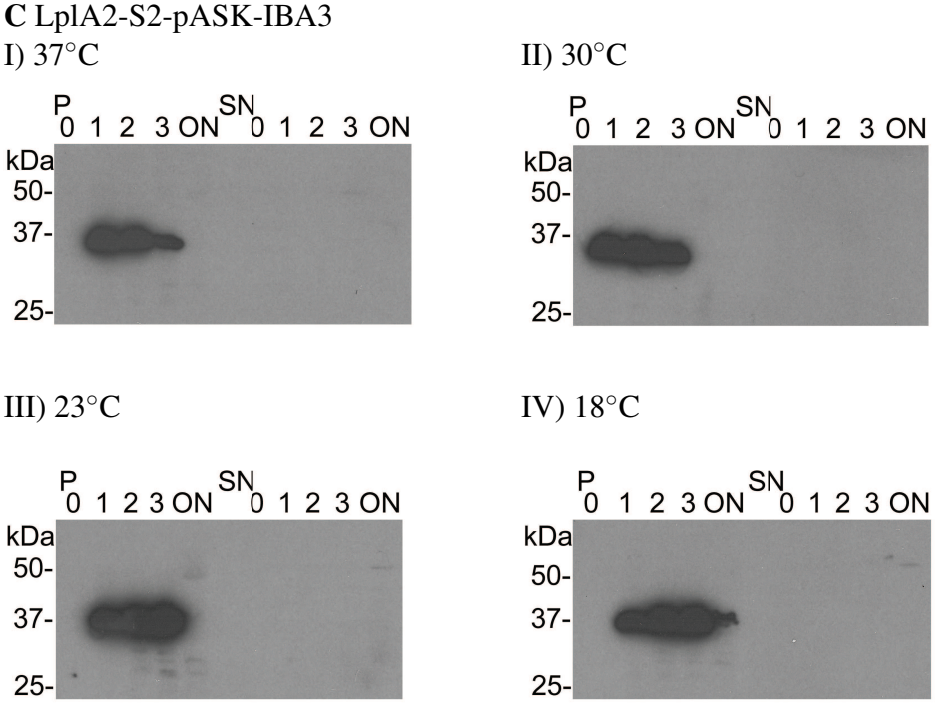

Figure 5.5.: Western blot analyses of test expressions of *P. falciparum* LplA2-pASK-IBA3 constructs in *E. coli* Tm134

Test expressions of LplA2-pASK-IBA3 constructs were performed in *E. coli* Tm134 at (I) 37°C, (II) 30°C, (III) 23°C and (IV) 18°C each and were analysed by western blotting using an anti-Strep-tag antibody. **Panel A** displays test expressions of the full length construct (expected size 47.3 kDa), **Panel B** of the S1 construct (expected size 44.3 kDa), and **Panel C** of the S2 construct (expected size 38.3 kDa). The blots show the protein in the pellet fractions (P) and supernatant fractions (SN) before induction (0), 1 to 3 hours after induction and after overnight expression (ON). Regardless of the construct and of the temperature used after induction of recombinant LplA2 expression, the protein was not expressed in soluble form. It was only detected in the pellet fractions.

5.3.3. Purification of *P. falciparum* LplA2

Only the $(His)_{10}$-tagged LplA2-S2 construct was expressed in soluble form and was therefore used for large-scale expressions and purification. The construct was expressed at 30°C for two hours before the bacteria were harvested and the recombinant protein was purified by batch nickel affinity chromatography (see 2.6.9.1). Figure 5.6 shows 5 μg of the elution fraction after purification of LplA2-S2 separated by 12.5% SDS-PAGE and stained with Coomassie (Panel A, lane 2), or analysed by western blotting (Panel B, lane 1) using an anti-His-tag antibody. The Coomassie stained gel showed the presence of several protein bands, three of them between 50 and 75 kDa, a faint protein band at 36 kDa and bands at 27 kDa and 22 kDa. Western blot analyses using the anti-His-tag antibody

confirmed that LplA2-S2 corresponded to the 36 kDa band. The 27 kDa band was also detected by the anti-His-tag antibody, possibly being a degradation product of the recombinant protein. This suggests that LplA2-S2 was co-purified with non-His-tagged proteins present in the *E. coli* extract, leading to the conclusion that recombinantly expressed LplA2-S2 may form complexes during expression with *E. coli* proteins which were not broken up using this purification method. It is known that recombinantly expressed proteins, if not folded properly, may form complexes with bacterial chaperones to enhance their solubility (Goloubinoff et al., 1989, Georgiou and Valax, 1996, Keresztessy et al., 1996). To analyse which proteins co-purified with LplA2-S2, the three proteins were analysed by tandem mass spectrometry (LC-MS/MS). The analyses was performed by Dr Richard Burchmore of the Sir Henry Wellcome Functional Genomics Facility based at the University of Glasgow. The proteins were identified as GroEL (gi|18028158), chaperonin Cpn60 (gi|119366229) and a nucleoside-diphosphate-sugar epimerase (gi|75187041) from *E. coli*. These data strongly suggest that LplA2-S2 indeed needs assistance during recombinant protein expression in the *E. coli* system.

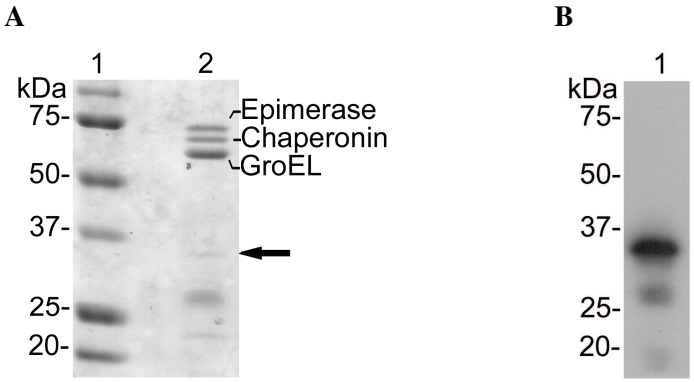

Figure 5.6.: Purification of His_{10}-tagged *P. falciparum* LplA2-S2
Panel A and B display LplA2-S2 purified by batch nickel affinity chromatography. 5 μg of the elution fraction was separated by 12.5% SDS-PAGE followed by Coomassie staining (**Panel A**) or western blot analyses (**Panel B**) using an anti-His-tag antibody. The expected protein size was 39.6 kDa. Several protein bands were detected in the elution fraction and western blot analysis confirmed that LplA2-S2 corresponds to the faint protein band at 36 kDa. It also showed degradation products of LplA2-S2 in the elution fraction. The three prominent bands between 50 and 75 kDa were analysed by tandem mass spectrometry and were identified as *E. coli* nucleoside-diphosphate-sugar epimerase (74.2 kDa), chaperonin Cpn60 (57.4 kDa) and GroEL (52 kDa), strongly suggesting that LplA2-S2 has folding problems during recombinant expression in *E. coli*.

Furthermore, I tested whether purification by FPLC nickel affinity chromatography (see 2.6.9.2) was able to separate the *E. coli* proteins from the recombinant LplA2-S2. However, it was not possible to separate the *E. coli* proteins from the recombinant protein. During FPLC, the recombinant LplA2-S2 and its degradation products eluted together with the *E. coli* proteins in the same peak (data not shown).

Unfortunately, it was not possible for me to continue with the optimisation of expression and purification of the LplA2 constructs due to time constraints. LplA2-S2 was also not tested in any activity assay (described below) since the quality of the purified recombinant protein was too poor. Only $\leq$10% of the elution fraction corresponded to the recombinant protein.

5.4. *E. coli* LplA - Recombinant protein expression and purification

The construct used for recombinant expression of *E. coli* LplA was kindly provided by John E. Cronan, Jr., University of Illinois at Urbana-Champaign, USA. The construct contained the full length *E. coli lplA* coding region cloned into the expression plasmid pQE-2, which attaches a $(His)_6$-tag to the N-terminus of the recombinant protein. Before testing the construct, it was analysed by restriction digest using the restriction enzymes NdeI and HindIII (Figure 5.7, Panel A).

To optimise the expression conditions of the *E. coli* LplA construct, a small-scale test expression at 37°C was set up. The construct was transformed into *E. coli* BLR(DE3) (Novagen), and recombinant protein expression was induced using 1 mM IPTG. Samples were analysed by using the BugBuster protein extraction kit (Novagen) followed by western blotting with an anti-His-tag antibody. Recombinant *E. coli* LplA (expected size 39.1 kDa) was highly expressed and it was decided that expression for three hours at 37°C is sufficient for further protein purification of large-scale expressions (Figure 5.7, Panel B). Recombinant *E. coli* LplA was purified by batch nickel affinity chromatography (see 2.6.9.1). Figure 5.7 (Panel C) displays a Coomassie stained SDS-PAGE of samples taken during the batch purification (lanes 2-8) and of the elution fraction (lane 9). 5 μg of the elution fraction was loaded onto the gel showing purified *E. coli* LplA of the expected size. Generally, a 100 ml culture used for recombinant protein expression resulted in $\sim$30 mg of recombinant *E. coli* LplA.

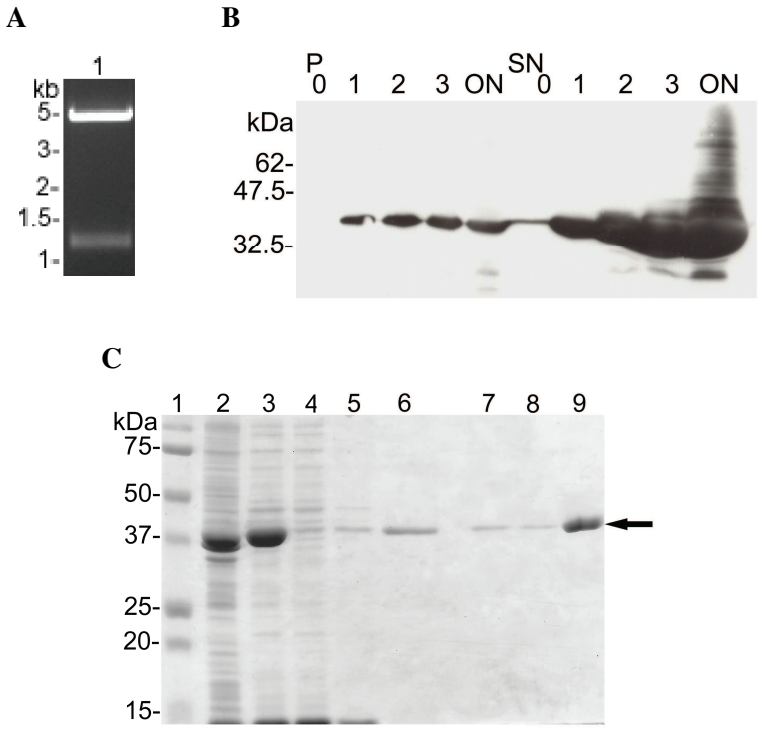

Figure 5.7.: Cloning, expression and purification of *E. coli* LplA in pQE-2

E. coli LplA in pQE-2 was kindly provided by John E. Cronan, Jr., University of Illinois at Urbana-Champaign, USA. **Panel A** shows a digest of the expression plasmid using the restriction enzymes NdeI and HindIII, resulting in a 1183 bp band (*E. coli lplA*) and a 4704 bp band (pQE-2). The optimal expression conditions were determined by western blot analysis of test expressions using an anti-His-tag antibody (**Panel B**). The recombinant protein (39.1 kDa) was expressed in *E. coli* BLR(DE3) cells at 37°C. The blot shows the protein in the pellet fractions (P) and supernatant fractions (SN) before induction (0), hours after induction (1-3) and after overnight expression (ON). **Panel C** displays the purification of recombinant *E. coli* LplA by batch nickel affinity chromatography, run on a 12.5% SDS-PAGE and stained with Coomassie for analysis. The gel was loaded with samples taken during the purification. Lane 2 shows the insoluble pellet fraction, lane 3 the supernatant fraction, lane 4 the flow through, lanes 5-8 the wash fractions and lane 9 the elution fraction of which 5 μg was loaded.

5.5. *P. falciparum* H-protein and lipoyl-domains - Recombinant protein expression and purification

5.5.1. Cloning and recombinant expression of *P. falciparum* H-protein and lipoyl-domains

The lipoyl-domains are part of the E2 subunits of the KADHs. Like the H-protein of the GCV, these domains are recognised by LplA and lipoic acid is covalently attached to them post-translationally. For *in vitro* LplA activity assays, expression constructs for the lipoyl-domains of the *P. falciparum* KADH-E2 subunits and for the H-protein were generated. The lipoyl-domains are located at the N-terminus of the E2 subunits (Reed and Hackert, 1990) and for expression of the domains, the constructs were truncated at the N-terminus to remove their subcellular targeting sequences (Foth et al., 2005, Günther et al., 2005, McMillan et al., 2005, Salcedo et al., 2005). The *Plasmodium* PDH-E2 subunit has two lipoyl-domains, whereas the BCDH-E2 and KGDH-E2 subunits have only one lipoyl-domain (see Figure 1.6). The sizes of the domains and their position within the E2 subunits, and the size and position of the H-protein used for cloning/expression are summarised in Table 5.2.

Table 5.2.: Sizes of *P. falciparum* H-protein and lipoyl-domain constructs

Lipoyl domain (LD)	Length in bp	Length in aa
1. H-protein	103-603	35-201
2. PDH-E2-LD1	82-315	28-105
3. PDH-E2-LD2	466-873	156-291
4. BCDH-E2-LD	40-372	14-124
5. KGDH-E2-LD	52-390	18-130

The H-protein and the lipoyl-domains of BCDH-E2 and KGDH-E2 as well as both PDH-E2 lipoyl-domains, were PCR amplified using the oligonucleotide primers specified in 2.1.7. The primers introduced NdeI and BamHI restriction sites at the 5' and 3' ends of the PCR products for directional cloning into pJC40 (Figure 5.8).

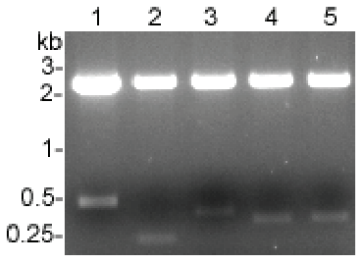

Figure 5.8.: Cloning of *P. falciparum* H-protein and lipoyl-domains in pJC40
For recombinant expression of the H-protein and the lipoyl-domains, the expression plasmid pJC40 was used. The expression constructs were digested using the restriction enzymes NdeI and BamHI resulting in a 2383 bp band corresponding to pJC40 (lanes 1-5), a 501 bp band corresponding to the H-protein (lane 1), a 234 bp band corresponding to PDH-E2-LD1 (lane 2), a 407 bp band corresponding to PDH-E2-LD2 (lane 3), a 333 bp band corresponding to BCDH-E2-LD (lane 4) and a 339 bp band corresponding to KGDH-E2-LD (lane 5).

The optimal expression conditions for each construct were determined by small-scale test expressions as described above for the LplAs. Table 5.3 summarises the results of the test expressions and shows the optimal expression conditions for each construct.

Table 5.3.: Optimal expression condition of *P. falciparum* H-protein and lipoyl-domains expressed in *E. coli* BLR(DE3)

Construct	Temperature	Time
H-protein-pJC40	37°C	2-3 hours
PDH-E2-LD1-pJC40	18°C	overnight
PDH-E2-LD2-pJC40	18°C	overnight
BCDH-E2-LD-pJC40	23°C	2-3 hours
KGDH-E2-LD-pJC40	37°C	2-3 hours

5.5.2. Purification of *P. falciparum* H-protein and lipoyl-domains

Large-scale expressions of recombinant H-protein and lipoyl-domains were set up for purification at the respective temperature and for the respective time. The bacteria were harvested and the recombinant proteins were purified by batch nickel affinity chromatography (see 2.6.9.1). Figure 5.9 shows 5 μg of each elution fraction loaded onto a 15% SDS-PAGE and analysed by Coomassie staining. 5 μg of H-protein elution fraction (expected size of 21.1 kDa) was separated in lane 1, PDH-E2-LD1 (expected size of 11.3

kDa) in lane 2, PDH-E2-LD2 (expected size of 18.9 kDa) in lane 3, BCDH-E2-LD (expected size of 15.4 kDa) in lane 4 and KGDH-E2-LD (expected size of 15.1 kDa) in lane 5. The expected sizes were calculated using Vector NTI software (Invitrogen) and were confirmed by MALDI-TOF mass spectrometry (performed by the Fingerprints proteomics facility, University of Dundee), although in the SDS-PAGE most of the domains had a higher apparent mass. It is not unusual that the apparent mass of a protein in a SDS-PAGE varies slightly from its original mass and ∼5 kDa is within the tolerable range. Post-translational modifications like glycosylation can, for example, affect the electrophoretic mobility of a protein, but also hydrophobic areas within a protein itself can affect the mobility (Banker and Cotman, 1972, Müller et al., 2007). Generally, 2L cultures used for recombinant protein expression resulted in ∼3.8 mg H-protein, ∼7 mg PDH-E2-LD1, ∼47 mg PDH-E2-LD2, ∼8 mg BCDH-E2-LD and ∼46 mg KGDH-E2-LD.

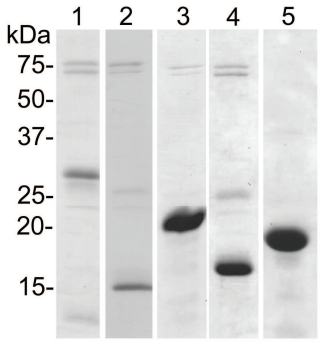

Figure 5.9.: Purification of *P. falciparum* H-protein and lipoyl-domains
The recombinant H-protein and lipoyl-domains were purified by batch nickel affinity chromatography. 5 μg of each elution fraction was separated on a 15% SDS-PAGE and was analysed by Coomassie staining. Lane 1 corresponds to purified H-protein (expected size 21.7 kDa), lane 2 corresponds to PDH-E2-LD1 (expected size 11.3 kDa), lane 3 corresponds to PDH-E2-LD2 (expected size 18.9 kDa), lane 4 corresponds to BCDH-E2-LD (expected size 15.4 kDa) and lane 5 corresponds to KGDH-E2-LD (expected size 15.1 kDa). Lanes 1-4 contain additional proteins which co-purified with the domains. It is hypothesised that these either correspond to multimers of the domains, or that they maybe correspond to chaperones of *E. coli*, because the sizes are similar to the proteins co-purified with LplA2-S2 (see 5.3.3).

5.5.3. Circular dichroism (CD) analysis of recombinant H-protein and lipoyl-domains

The CD spectra of recombinantly expressed H-protein and lipoyl-domains were analysed at far UV (Figure 5.10, Panel A) and near UV/visible ranges (Figure 5.10, Panel B) in order to investigate the secondary structures of the H-protein and lipoyl-domains. This was examined to analyse whether all recombinant expressed domains were potential protein substrates for LplA activity assays, or whether some were likely to be not accepted by LplA due to improper folding after recombinant expression. The experiments were carried out by Dr Sharon Kelly of the protein characterisation facility, Institute of Biomedical and Life Sciences, University of Glasgow. The obtained data were analysed using the online server DICHROWEB (Lobley et al., 2002, Whitmore and Wallace, 2004). Standard algorithms and datasets for secondary structure comparison were used to analyse the CD data and the "goodness of fit" parameter NRMSD was obtained for each recombinant protein. The parameter measures how good the experimental data fit with the theoretical CD spectrum back-calculated from the obtained secondary structure (Kelly et al., 2005). NRMSD values range from 0 (perfect fit) to 1 (no fit). Data above 0.25 are not reliable whereas data $\leq$0.05 are considered reliable. NRMSD obtained for the recombinant proteins were as follows: 0.03 for fresh purified H-protein (shown in blue in the spectra), 0.055 for H-protein stored one month at 4°C (shown in red in the spectra), 0.061 for PDH-E2-LD1 (shown in green in the spectra), 0.021 for PDH-E2-LD2 (shown in black in the spectra), 0.487 for BCDH-E2-LD (shown in pink in the spectra) and 0.042 for KGDH-E2-LD (shown in purple in the spectra). The data suggested that the BCDH-E2-LD and potentially the PDH-E2-LD1 were not folded properly after recombinant protein expression.

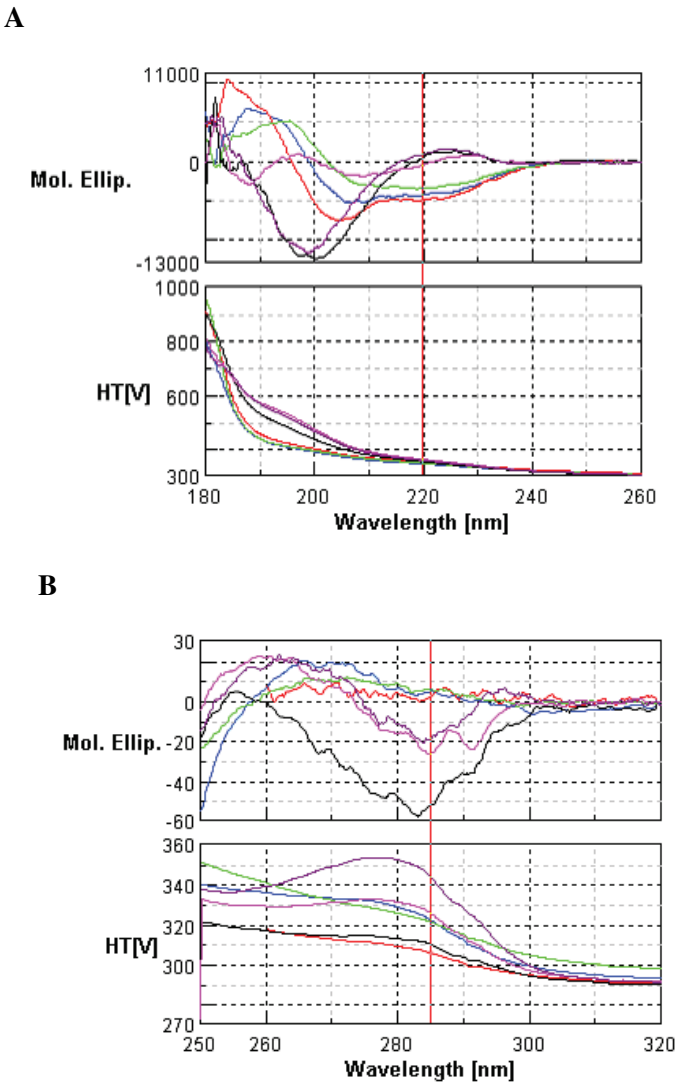

Figure 5.10.: Circular dichroism (CD) analysis of recombinant H-protein and lipoyl-domains

The CD spectra of recombinantly expressed H-protein and lipoyl-domains were analysed at far UV and near UV/visible wavelengths in order to investigate the secondary structure of the H-protein and lipoyl-domains. The experiments were carried out by Dr Sharon Kelly of the protein characterisation facility, Institute of Biomedical and Life Sciences, University of Glasgow. Data were collected in a JASCO J-180 instrument with protein samples at 0.5 mg/ml. **Panel A** displays a comparison of far UV CD spectra and **Panel B** of near UV CD spectra of fresh purified H-protein (blue), H-protein stored one month at 4°C (red), PDH-E2-LD1 (green), PDH-E2-LD2 (black), BCDH-E2-LD (pink) and KGDH-E2-LD (purple). The upper graph in Panel A and B represents the CD spectra and the lower graph the High Tension voltage traces.

5.6. "Gel assays"

LplA activity can be determined by analysing the lipoylation state of the protein substrate in the "gel assay" (Ali and Guest, 1990, Fujiwara et al., 1992). The attachment of lipoic acid to a conserved lysine residue of the lipoyl-domains of the KADH-E2 subunits and of the H-protein of the GCV results in the neutralization of a positive charge and enhances therefore the mobility of the lipoylated protein in a native PAGE. Thus, the lipoylated form of a protein migrates faster in native PAGE in comparison to the non-lipoylated form of the protein, and results in a shift of the protein band (Fujiwara et al., 1992).

The lipoylation reaction catalysed by LplAs was set up in a general reaction buffer containing 100 mM phosphate buffer (pH 7.5), 2 mM $MgCl_2$, 2 mM ATP, 0.5 mM lipoic acid and 1 mM DTT in a final volume of 30 μl. The concentration of the protein substrate varied between 2-4.4 μM and of LplA between 0-3.5 μM in each assay.

The assay shown in Figure 5.11 was performed using 4.4 μM KGDH-E2-LD and an increasing concentration of *E. coli* LplA (0-3.4 μM). The reaction mix was incubated at 37°C for 30 min before half of it was separated on a 20% native PAGE. Panel A shows the Coomassie stained native PAGE in which the band shift of KGDH-E2-LD is visible. The protein migrated faster in the native PAGE the more lipoylated it had become during the reaction. Panel B displays the native PAGE analysed by western blotting using an antibody that detects lipoic acid bound to proteins (for dilutions see Table 2.1). It is obvious that even the lowest concentration of *E. coli* LplA used in this assay (0.04 μM; lane 4) lipoylated the KGDH-E2-LD, although only to a small degree. The lipoylation level was so low that it was not detected in the Coomassie stained gel (Panel A, lane 4). Further, it can be seen that under the conditions used this lipoylation reaction reached saturating levels when 0.9 μM or more *E. coli* LplA were used (lanes 8-10), which is not surprising because only 4.4 μM of the protein substrate were used.

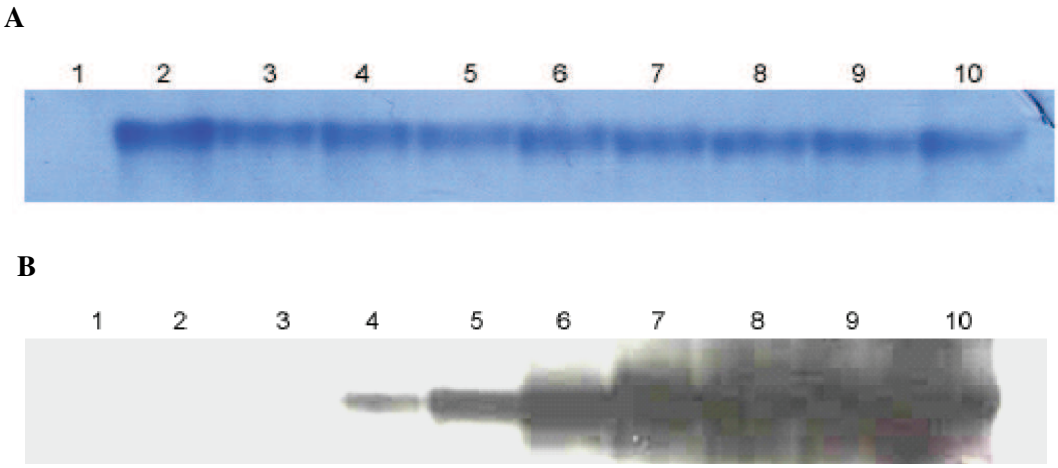

Figure 5.11.: Analyses of *E. coli* LplA lipoylation assay using native PAGE followed by (A) Coomassie staining or (B) western blotting
The lipoylation reaction was carried out in a final volume of 30 μl containing 100 mM phosphate buffer (pH 7.5), 2 mM $MgCl_2$, 2 mM ATP, 0.5 mM lipoic acid, 1 mM DTT and 4.4 μM KGDH-E2-LD. The reaction was started by addition of varying concentrations of *E. coli* LplA. Lane 1 and 2 were controls to determine the possible lipoylation state of *E. coli* LplA and KGDH-E2-LD after purification and contained 3.4 μM *E. coli* LplA (lane 1) and 4.4 μM KGDH-E2-LD (lane 2) not incubated in the reaction mix. Lane 3 contained 0 μM, lane 4 contained 0.04 μM, lane 5 contained 0.09 μM, lane 6 contained 0.2 μM, lane 7 contained 0.4 μM, lane 8 contained 0.9 μM, lane 9 contained 1.7 μM and lane 10 contained 3.4 μM *E. coli* LplA. The reaction was incubated at 37°C and after 30 min half of the reaction (15 μl) was loaded onto a 20% native PAGE and was analysed by Coomassie staining (**Panel A**) and western blotting (**Panel B**) using an anti-lipoic acid antibody that detects lipoic acid bound to proteins.

Using the anti-lipoic acid antibody had several advantages over the Coomassie staining in analysing LplA activity. As can be seen in Figure 5.11, the sensitivity and clarity in detecting lipoylated protein was markedly increased with the antibody. Further, the shift observed in the Coomassie stained gel was not very clear and densitometric analyses would be difficult and probably not very reliable using this method. In contrast, the antibody gave a strong signal which would allow densitometric quantification. Moreover, analysing the lipoylation reaction by western blotting using the anti-lipoic acid antibody allowed the separation of the lipoylation reaction by SDS-PAGE, which was quicker and easier to handle in comparison to a native PAGE. However, using the antibody for analyses brought up different problems. The signal produced from the anti-lipoic acid antibody differed in intensity when using different antibody batches. Therefore, the batches were always mixed in order to achieve uniformity, but there were never more than two batches available to be mixed at any one time. Thus, this method was not used for kinetic analyses of LplAs and was only used to assess LplA activity qualitatively.

5.6.1. *E. coli* LplA

Using *E. coli* LplA, I first analysed whether the enzyme distinguished between the recombinant *P. falciparum* H-protein and the different lipoyl-domains as substrates (Figure 5.12). The assays were set up in the general reaction buffer containing 3 μM H-protein (Panel A), 4.4 μM PDH-E2-LD1 (Panel B), 2.7 μM PDH-E2-LD2 (Panel C), 3.3 μM BCDH-E2-LD (Panel D) and 3.3 μM KGDH-E2-LD (Panel E). Three different concentrations of *E. coli* LplA were used in each assay (0 μM, 0.06 μM and 0.6 μM). The reaction was incubated at 37°C for 30 min and half of the reaction was analysed using a 15% SDS-PAGE followed by western blotting using anti-lipoic acid antibody. The western blots in Figure 5.12 show that *E. coli* LplA indeed accepts the H-protein and the lipoyl-domains as substrates but discriminates between them. It seems that H-protein was the best substrate since 0.06 μM *E. coli* LplA were sufficient to lipoylate H-protein (Panel A). A further increase of H-protein lipoylation was observed when the LplA concentration was elevated. The other lipoyl-domains were also accepted by *E. coli* LplA as substrates especially PDH-E2-LD2 (Panel C) and KGDH-E2-LD (Panel E), which were strongly lipoylated at higher concentrations of *E. coli* LplA, whereas at 0.06 μM LplA no discernable difference compared to the ground-level lipoylation was observed (lane 1). Ground-level lipoylation is the lipoylation of the domain after purification. Since the H-protein and the domains were not expressed in lipoylation deficient bacteria, it is possible that the domains are partly lipoylated by the *E. coli* lipoylation pathways during expression. To determine the ground-level lipoylation for each assay, a control assay was set up in parallel which contained no LplA. PDH-E2-LD1 (Panel B) and BCDH-E2-LD (Panel D) were only poorly lipoylated. Only a very slight increase in lipoylation was observed at high concentrations of *E. coli* LplA. These results suggest that at low concentrations of *E. coli* LplA, H-protein is the best substrate and that PDH-E2-LD2 and KGDH-E2-LD require a higher enzyme concentration to become lipoylated. The reason for the virtual lack of lipoylation of the BCDH-E2-LD and PDH-E2-LD1 might be explained by their improper/poor folding as shown by the CD analyses (see 5.5.3). It could also be that *E. coli* LplA possesses substrate specificity and is thus not able to use these two domains as substrates. According to these data, only the H-protein, PDH-E2-LD2 and KGDH-E2-LD were used as substrates in the following assays.

Additional bands at 75 kDa and 50 kDa were detected in the western blots by the anti-lipoic acid antibody suggesting that these proteins also have lipoic acid bound to them. One possible explanation is that these bands correspond to lipoylated multimers of the

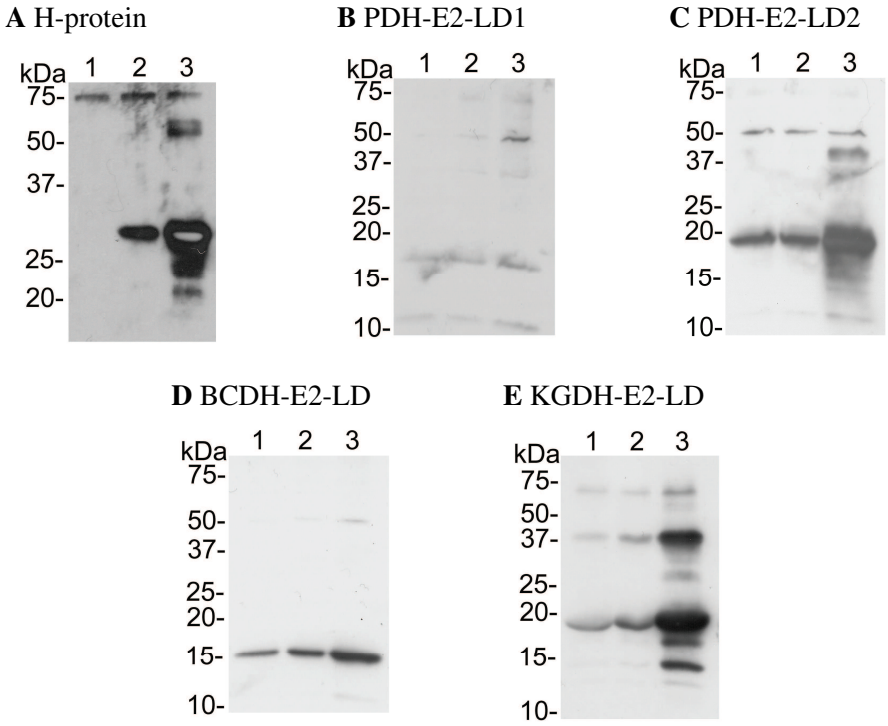

Figure 5.12.: Western blot analyses of *E. coli* LplA lipoylation assays using *P. falciparum* H-protein and lipoyl-domains

The lipoylation reactions were carried out in a final volume of 30 μl containing 100 mM phosphate buffer (pH 7.5), 2 mM $MgCl_2$, 2 mM ATP, 0.5 mM lipoic acid, 1 mM DTT and 3 μM H-protein (**Panel A**), 4.4 μM PDH-E2-LD1 (**Panel B**), 2.7 μM PDH-E2-LD2 (**Panel C**), 3.3 μM BCDH-E2-LD (**Panel D**) and 3.3 μM KGDH-E2-LD (**Panel E**). The reaction was started by addition of varying concentrations of *E. coli* LplA. Lane 1 contained 0 μM *E. coli* LplA, lane 2 contained 0.06 μM *E. coli* LplA and lane 3 contained 0.6 μM *E. coli* LplA. The reaction was incubated at 37°C and after 30 min half of the reaction (15 μl) was loaded onto a 15% SDS-PAGE, and was analysed by western blotting using anti-lipoic acid antibody. It seemed that *E. coli* LplA discriminated between the H-protein and lipoyl-domains as substrates. H-protein was the best accepted substrate. Small concentrations of *E. coli* LplA were enough to lipoylate the protein (Panel A). Also well accepted were PDH-E2-LD2 (Panel C) and KGDH-E2-LD (Panel E). Only poorly lipoylated were the PDH-E2-LD1 (Panel B) and BCDH-E2-LD (Panel D), which could be due to improper folding of these recombinant proteins.

H-protein and domains. It is known that the E2 subunits form large multimers (Reed and Hackert, 1990). The H-protein is generally present in the monomeric form (Oliver et al., 1990), however, recently it was shown that recombinantly expressed H-protein of the cyanobacterium *Synechocystis* forms dimers (Hasse et al., 2007). Another band at ~37 kDa appeared in Panel C and E which possibly corresponds to "lipoylated" *E. coli* LplA, which contains the reaction intermediate lipoyl-AMP tightly (although non-covalently)

bound to it (Kim et al., 2005, McManus et al., 2006). Further evidence for this speculation will be provided below.

To optimise the reaction conditions of *E. coli* LplA, the lipoylation reaction was performed at different temperatures and different incubation times. The assays were carried out in the general reaction buffer containing 3 μM H-protein in the presence of 0.03 μM *E. coli* LplA (Figure 5.13). The assays were incubated at 37°C (Panel A) and 30°C (Panel B), for 30 min (lane 2) or 1 hour (lane 3). Lane 1 in both assays contained the reaction mix without *E. coli* LplA to determine the ground-level lipoylation of the H-protein. Incubation at 37°C resulted in higher lipoylation levels than incubation at 30°C. The lipoylation level increased only slightly after 1 hour incubation at 37°C. At 30°C the lipoylation level of H-protein is markedly higher after 1 hour incubation, however, it is still less compared to incubation at 37°C.

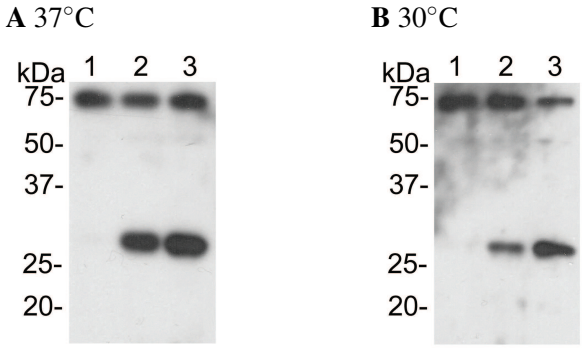

Figure 5.13.: Western blot analyses of *E. coli* LplA lipoylation assays to optimise reaction conditions

The lipoylation assays were carried out in a final volume of 30 μl containing 100 mM phosphate buffer (pH 7.5), 2 mM $MgCl_2$, 2 mM ATP, 0.5 mM lipoic acid, 1 mM DTT and 3 μM H-protein. The reactions were started by addition of 0.03 μM *E. coli* LplA. The assays were incubated at 37°C (**Panel A**) and 30°C (**Panel B**), for 30 min (lane 2) and 1 hour (lane 3). Lane 1 contained the reaction mix without LplA, and was incubated for 1 hour to analyse the ground-level lipoylation of the H-protein. After incubation, half of the reaction was analysed by SDS-PAGE, followed by western blotting using anti-lipoic acid antibody. Incubation at 37°C clearly resulted in higher lipoylation levels of the protein substrate in comparison to incubation at 30°C. The lipoylation increase from 30 min to 1 hour incubation is only marginal at 37°C, but clearly visible at 30°C.

Furthermore, it was investigated whether *E. coli* LplA accepts GTP as well as ATP as a substrate. It was shown that the mammalian lipoate activating enzyme accepts both, ATP and GTP, for the activation of lipoic acid (Fujiwara et al., 2001) (Figure 5.14). The

reaction was set up in the general reaction buffer but with either 5 mM ATP (Panel A) or 5 mM GTP (Panel B) containing 2.7 μM PDH-E2-LD2 as protein substrate. Varying concentrations of *E. coli* LplA (between 0 and 0.6 μM) were used to start the lipoylation reaction, which was incubated at 37°C for 30 min. Analysis revealed that both, ATP (Panel A) and GTP (Panel B), were used by *E. coli* LplA resulting in lipoylation of the PDH-E2-LD2, although lipoylation detected in the assay using ATP appeared to be slightly stronger than in the assay using GTP.

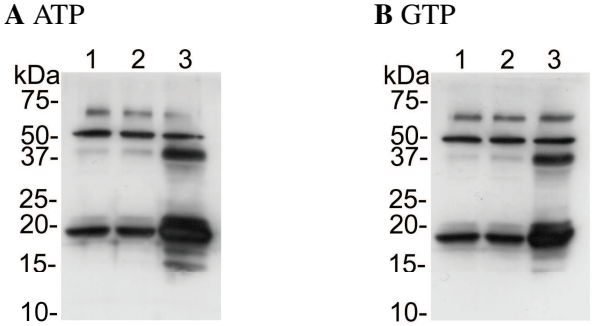

Figure 5.14.: Western blot analyses of *E. coli* LplA lipoylation assays using (A) ATP and (B) GTP as substrates
The lipoylation reactions were carried out in a final volume of 30 μl containing 100 mM phosphate buffer (pH 7.5), 2 mM $MgCl_2$, 0.5 mM lipoic acid, 1 mM DTT, 2.7 μM PDH-E2-LD2 and 5 mM ATP (**Panel A**) or 5 mM GTP (**Panel B**). The reactions were started by the addition of varying concentrations of *E. coli* LplA. Lane 1 contained 0 μM *E. coli* LplA, lane 2 contained 0.06 μM *E. coli* LplA and lane 3 contained 0.6 μM *E. coli* LplA. The reactions were incubated at 37°C and after 30 min half of the reaction was analysed by SDS-PAGE, followed by western blotting using anti-lipoic acid antibody.

5.6.2. *P. falciparum* LplA1

The activity of the N-terminal and C-terminal tagged forms of *P. falciparum* LplA1 was qualitatively analysed using the "gel assay" (Figure 5.15). The lipoylation activity was tested using 3.1 μM H-protein as protein substrate in the general reaction buffer. The reaction was started by addition of recombinant *P. falciparum* LplA1 with the N-terminal $(His)_{10}$-tag (Panel A) or the C-terminal Strep-tag (Panel B), with concentrations varying between 0 and 3.5 μM. The reactions were carried out at 37°C for 1 hour to initially determine whether the recombinant proteins were active. The reactions were terminated by addition of 6x loading buffer and boiling of the reaction mix. Half of the reaction was analysed by SDS-PAGE, followed by western blotting using anti-lipoic acid antibody.

Both recombinant *P. falciparum* LplA1s were able to lipoylate H-protein, but it appeared that the Strep-tagged protein (Panel B) was more active than the $(His)_{10}$-tagged protein (Panel A). A possible explanation could be that the N-terminal $(His)_{10}$-tag interfered with the catalytic sites at the N-terminus of the protein that were shown to be important for lipoic acid binding and activation (Fujiwara et al., 2005, Kim et al., 2005, McManus et al., 2006). Comparison with *E. coli* LplA suggests that both *P. falciparum* recombinant proteins are much less active than the bacterial recombinant protein. In the assay shown in Figure 5.13 (Panel A), only 0.03 μM *E. coli* LplA was used with H-protein as the protein substrate. The resulting lipoylation level of H-protein in this assay is comparable to the lipoylation level of H-protein incubated with 3.5 μM $(His)_{10}$-tagged *P. falciparum* LplA1 (Panel A; lane 6) or 1.8 μM Strep-tagged *P. falciparum* LplA1 (Panel B; lane 5). Differences in the intensities of the detected bands could also be due to different antibody batches that were used in the *E. coli* and *P. falciparum* assays, which makes the direct comparison difficult. However, also taking the *E. coli* assay displayed in Figure 5.12 (Panel A) into account, the data strongly suggests that the *E. coli* protein is more active.

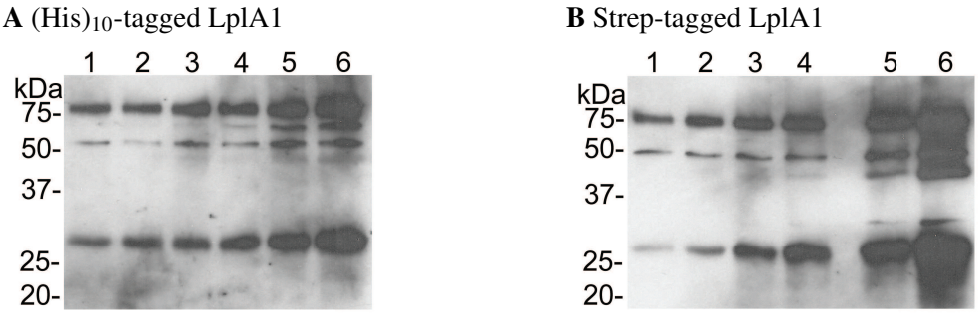

Figure 5.15.: Western blot analyses of lipoylation assays using recombinant *P. falciparum* LplA1 with (A) a N-terminal $(His)_{10}$-tag and (B) a C-terminal Strep-tag

The lipoylation reactions were carried out in a final volume of 30 μl containing 100 mM phosphate buffer (pH 7.5), 2 mM $MgCl_2$, 2 mM ATP, 0.5 mM lipoic acid, 1 mM DTT and 3.1 μM H-protein. The reactions were started by addition of varying concentrations of *P. falciparum* LplA1 with a N-terminal $(His)_{10}$-tag (**Panel A**) or a C-terminal Strep-tag (**Panel B**). Lane 1 contained 0 μM, lane 2 contained 0.07 μM, lane 3 contained 0.4 μM, lane 4 contained 0.7 μM, lane 5 contained 1.8 μM and lane 6 contained 3.5 μM of the respective recombinant LplA1. The reaction was incubated at 37°C for 1 hour. 15 μl of the reactions were separated on a 15% SDS-PAGE and analysed by western blotting using anti-lipoic acid antibody. Direct comparison of the two blots showed that *P. falciparum* LplA1 with the C-terminal Strep-tag was more active than the N-terminal $(His)_{10}$-tagged recombinant protein. Other protein bands beside the H-protein band above 25 kDa appeared on the western blots. It is believed that one of these bands corresponds to a dimer of H-protein (about 50 kDa) and another to a trimer of H-protein (about 75 kDa). A third band appearing with increasing concentration of *P. falciparum* LplA1 might correspond to *P. falciparum* LplA1 carrying activated lipoic acid.

In both western blots displayed in Figure 5.15, other protein bands in addition to H-protein were detected by the anti-lipoic acid antibody, suggesting these were also lipoylated. As already hypothesised above for the *E. coli* assays, the additional bands at 50 kDa and 75 kDa may correspond to multimers of the H-protein (Hasse et al., 2007). A band at 48 kDa which is detected with increasing concentration of *P. falciparum* LplA1 might correspond to LplA1 with lipoyl-AMP bound to it. To further test this hypothesis lipoylation assays were performed without any protein substrate (Figure 5.16). The assays were carried out in general reaction buffer with varying concentrations of Strep-tagged *P. falciparum* LplA1 (between 0 and 3.5 μM), at 37°C for 1 hour. Western blotting using the anti-lipoic acid antibody indeed detected lipoic acid bearing proteins in the assays containing the enzyme (lanes 2-4). The band at 48 kDa possibly corresponds to *P. falciparum* LplA1 with lipoyl-AMP bound to it, suggesting that the reaction intermediate is tightly bound and that SDS-PAGE is not able to break up this linkage. The nature of the 75 kDa band is unknown and is somewhat puzzling because the elution fraction of recombinant Strep-tagged *P. falciparum* LplA1 after purification is very pure and contains no other contaminating proteins (see Figure 5.2). It also seems that *P. falciparum* LplA1 without protein substrate is less "lipoylated" in comparison to the assay in Figure 5.15 (Panel B), where H-protein as protein substrate was present.

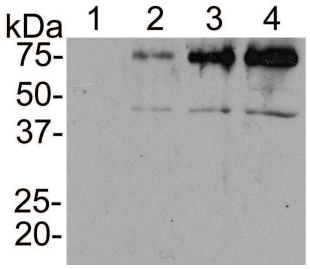

Figure 5.16.: Western blot analysis of *P. falciparum* LplA1 lipoylation assay without protein substrate

The lipoylation reactions were carried out in a final volume of 30 μl containing 100 mM phosphate buffer (pH 7.5), 2 mM $MgCl_2$, 2 mM ATP, 0.5 mM lipoic acid and 1 mM DTT. The reactions were started by addition of varying concentrations of Strep-tagged *P. falciparum* LplA1. Lane 1 contained 0 μM *P. falciparum* LplA1, lane 2 contained 0.7 μM *P. falciparum* LplA1, lane 3 contained 1.8 μM *P. falciparum* LplA1 and lane 4 contained 3.5 μM *P. falciparum* LplA1. The reaction was incubated at 37°C for 1 hour. 15 μl of the reactions were separated on a 15% SDS-PAGE and analysed by western blotting using anti-lipoic acid antibody. The 48 kDa band detected likely corresponds to *P. falciparum* LplA1 with lipoyl-AMP bound to it. The nature of the 75 kDa band is unknown.

Because *P. falciparum* LplA1 with the C-terminal Strep-tag appeared to be more active than the N-terminal $(His)_{10}$-tagged recombinant protein, the following assays were performed using only the Strep-tagged *P. falciparum* LplA1. The optimal reaction conditions were qualitatively identified by incubating the lipoylation reaction catalysed by *P. falciparum* LplA1 at different temperatures and different incubation times. The assay was carried out in the general reaction buffer using 3.1 μM H-protein as protein substrate and 3.5 μM Strep-tagged *P. falciparum* LplA1 (Figure 5.17). The assays were incubated at 37°C (Panel A), 30°C (Panel B) and 20°C (Panel C), for 30 min (lane 2) and 1 hour (lane 3). Lane 1 in each assay contained the reaction mix with 0 μM *P. falciparum* LplA1 to investigate the possible ground-lipoylation level of H-protein after purification. The assays were analysed by western blotting using anti-lipoic acid antibody. Highest lipoylation levels were obtained after 1 hour incubation at 37°C (Panel A, lane 3). *P. falciparum* LplA1 showed also activity at 30°C (Panel B) which was after 30 min comparable to incubation at 37°C. However, after 1 hour incubation at 30°C, the lipoylation level of H-protein was noticeably less when compared to 1 hour incubation at 37°C. The intensity of the detected band after 1 hour incubation at 37°C appears, however, less when compared to Figure 5.15 (Panel B; lane 6). This is possibly due to different antibody batches used for the two assays. At 20°C (Panel C) LplA1 showed no activity at all.

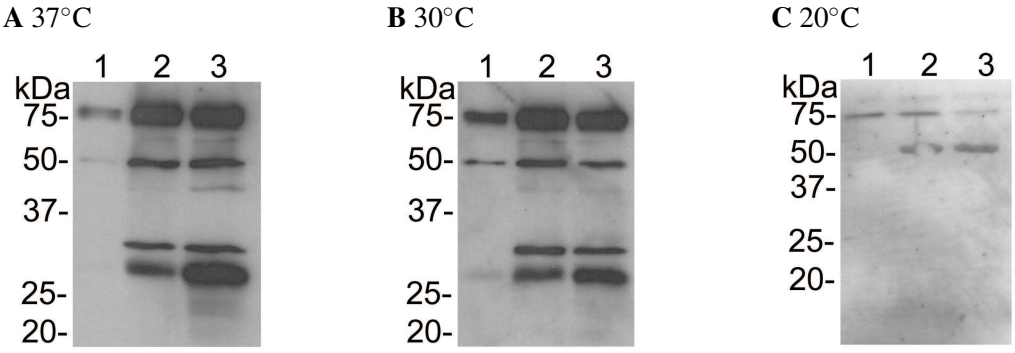

Figure 5.17.: Western blot analyses of *P. falciparum* LplA1 lipoylation assays to optimise the reaction conditions

The lipoylation assays were carried out in a final volume of 30 μl containing 100 mM phosphate buffer (pH 7.5), 2 mM $MgCl_2$, 2 mM ATP, 0.5 mM lipoic acid, 1 mM DTT and 3.1 μM H-protein. The reactions were started by addition of 3.5 μM Strep-tagged *P. falciparum* LplA1. The assays were incubated at 37°C (**Panel A**), 30°C (**Panel B**) and 20°C (**Panel C**), for 30 min (lane 2) and 1 hour (lane 3). Lane 1 contained the reaction mix without LplA1, and was incubated for 1 hour to analyse the lipoylation state of H-protein alone. After incubation, half of the reaction was analysed by SDS-PAGE followed by western blotting using anti-lipoic acid antibody. The best lipoylation result was obtained after 1 hour incubation at 37°C.

To investigate whether *P. falciparum* LplA1 uses the other lipoyl-domains as protein substrates *in vitro*, assays were performed containing the general reaction buffer, 3 μM of each domain and varying concentrations of *P. falciparum* LplA1 (between 0 and 1.8 μM). The reaction was incubated at 37°C for 1 hour, and half of the reaction mix was analysed by SDS-PAGE and western blotting using anti-lipoic acid antibody (Figure 5.18).

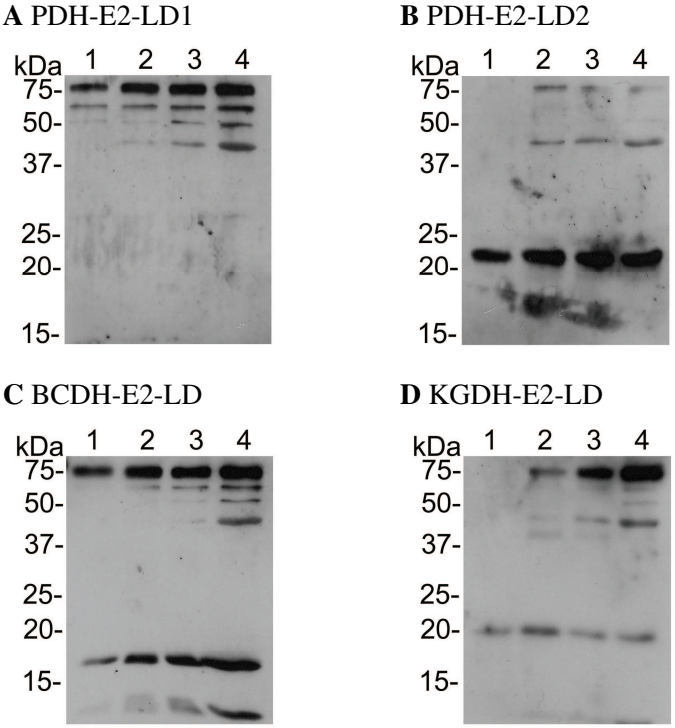

Figure 5.18.: Western blot analyses of *P. falciparum* LplA1 lipoylation assays using *P. falciparum* lipoyl-domains
The lipoylation reactions were carried out in a final volume of 30 μl containing 100 mM phosphate buffer (pH 7.5), 2 mM $MgCl_2$, 2 mM ATP, 0.5 mM lipoic acid, 1 mM DTT and 3 μM PDH-E2-LD1 (**Panel A**), PDH-E2-LD2 (**Panel B**), BCDH-E2-LD (**Panel C**) and KGDH-E2-LD (**Panel D**). The reaction was started by addition of varying concentrations of Strep-tagged *P. falciparum* LplA1. Lane 1 contained 0 μM, lane 2 contained 0.4 μM, lane 3 contained 0.7 μM and lane 4 contained 1.8 μM *P. falciparum* LplA1. The reaction was incubated at 37°C and after 1 hour, half of the reaction (15 μl) was loaded onto a 15% SDS-PAGE and analysed by western blotting using anti-lipoic acid antibody. Hardly any activity can be observed with either of these domains at the used conditions.

No activity is observed with the PDH-E2-LD1 (Panel A) and KGDH-E2-LD (Panel D) and only a marginal increase in lipoylation is detected using the PDH-E2-LD2 (Panel B) and BCDH-E2 (Panel C). The assay was repeated to analyse whether technical problems were the cause of these results. However, the second assays confirmed the data suggesting that *P. falciparum* LplA1 does not, or only very poorly, accept the recombinant

lipoyl-domains as protein substrates *in vitro* at the conditions used.

Further, the length of time that the Strep-tagged and $(His)_{10}$-tagged recombinant *P. falciparum* LplA1 remained stable for after purification, was also tested. Their activity was tested in lipoylation assays after storage at different temperatures for certain times. Aliquots of the purified recombinant proteins were stored at 4°C and -20°C and the activity was tested one week, two weeks and five weeks after purification (Figure 5.19). *P. falciparum* LplA1 activity was qualitatively investigated by using 3.5 μM of the recombinant LplA1 in the general reaction buffer, containing 3.1 μM H-protein. The assays were incubated at 37°C for 1 hour, and were analysed by western blotting using anti-lipoic acid antibody. After one week both recombinant *P. falciparum* LplA1s showed activity (Panel A). Strep-tagged LplA1 was more active when stored at 4°C rather than -20°C (lanes 1-3), whereas no obvious difference in activity of the $(His)_{10}$-tagged LplA1 stored at 4°C or -20°C was observed (lanes 4-6). After two weeks storage at -20°C and 4°C, *P. falciparum* LplA1 with the Strep-tag was able to lipoylate H-protein equally well (Panel B, lanes 1-3), while LplA1 with the $(His)_{10}$-tag showed reduced activity (Panel B, lanes 4-6). After five weeks of storage, the Strep-tagged recombinant protein still showed minor lipoylation activity (Panel C, lanes 1-3), but no activity was observed of the $(His)_{10}$-tagged LplA1 (Panel C, lanes 4-6). The strong lipoylation signals obtained in the western blot after two weeks of storage (Panel B) are the result of a different antibody batch which was used, rather than the result of an increase of LplA1 activity during storage.

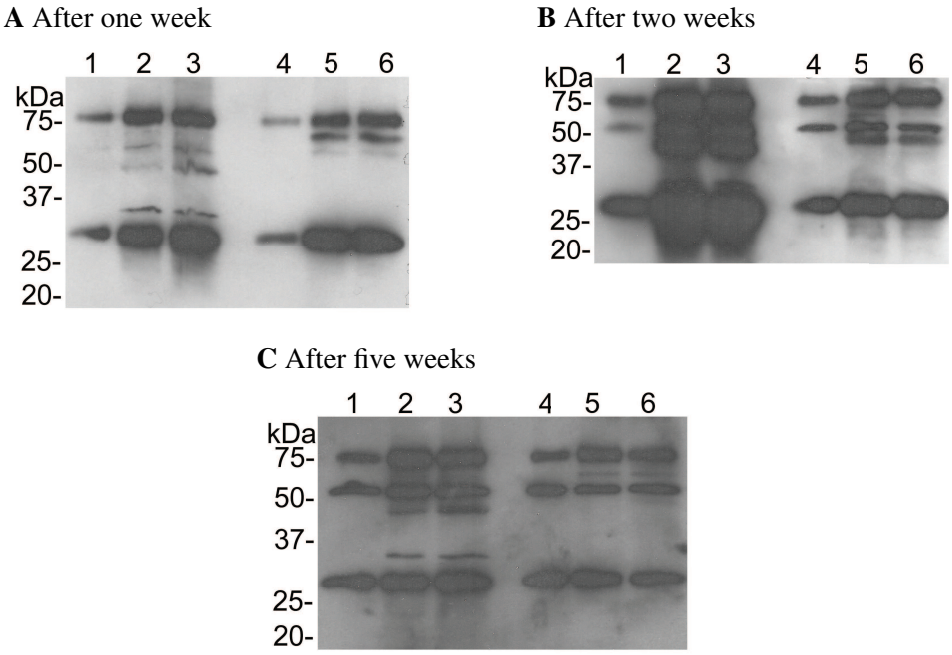

Figure 5.19.: Western blot analyses of lipoylation assays to investigate the stability of *P. falciparum* LplA1 recombinant proteins

The lipoylation assays were carried out in a final volume of 30 μl containing 100 mM phosphate buffer (pH 7.5), 2 mM $MgCl_2$, 2 mM ATP, 0.5 mM lipoic acid, 1 mM DTT and 3.1 μM H-protein. The reactions were started by addition of 3.5 μM *P. falciparum* LplA1 with a C-terminal Strep-tag (lanes 1-3) or a N-terminal $(His)_{10}$-tag (lanes 4-6). The assays were incubated at 37°C for 1 hour before they were analysed by western blotting using anti-lipoic acid antibody. **Panel A** displays assays carried out with recombinant *P. falciparum* LplA1 proteins stored for one week at -20°C (lanes 2 and 5) and at 4°C (lanes 3 and 6). **Panel B** shows activity of recombinant *P. falciparum* LplA1 proteins stored for two weeks at -20°C (lanes 2 and 5) and at 4°C (lanes 3 and 6) and **Panel C** displays lipoylation assays performed with recombinant *P. falciparum* LplA1 proteins stored for five weeks at -20°C (lanes 2 and 5) and at 4°C (lanes 3 and 6). Lanes 1 and 4 in each assay contained no recombinant LplA1, to analyse the ground-level lipoylation of H-protein. After one week, both recombinant proteins showed lipoylation activity. The Strep-tagged protein was more active when stored at 4°C in the first week. After two weeks, the recombinant LplA1 proteins were still able to lipoylate H-protein although the $(His)_{10}$-tagged LplA1 to a much lesser degree. After five weeks, only the Strep-tagged LplA1 showed minor lipoylation activity. Different antibody batches were used for the three blots resulting in the different relative signals.

5.7. Spectrophotometric assay

The "gel assays" described above were laborious and time consuming, and using different antibody batches to detect lipoylation made it difficult to directly compare different assays with each other. Therefore, a major aim was to establish a spectrophotometric

assay to determine LplA activity. Instead of analysing the lipoylation state of the protein substrate, this assay assessed the release of pyrophosphate (PPi) during the catalytic reaction as a measure of lipoylation. PPi is released during the LplA reaction through activation of lipoic acid with ATP to form the reaction intermediate lipoyl-AMP. In the assay, the released PPi was then converted to inorganic phosphate ($2Pi^{2-}$) by an inorganic pyrophosphatase in the presence of $MgCl_2$. The Pi^{2-} reacted with ammonium molybdate and formed a blue coloured complex which was detected spectrophotometrically at 710 nm (see Figure 2.12). Addition of bismuth citrate and sodium citrate stabilised the formed complex and prevented that more phosphate-molybdate were formed (Cariani et al., 2004).

Data obtained by the spectrophotometric assay were analysed using a standard curve of known Pi^{2-} concentrations. Known amounts of Pi^{2-} varying between 0 and 30 nmol were used for the standard curve, and were set up in a final volume of 200 μl containing 30 mM Tris/HCl (pH 7.5), 2 mM $MgCl_2$, 2 mM ATP, 0.5 mM lipoic acid and 1 mM DTT. The assay was carried out as described in material and methods (see 2.7.3), and the absorbance was determined at 710 nm (Figure 5.20).

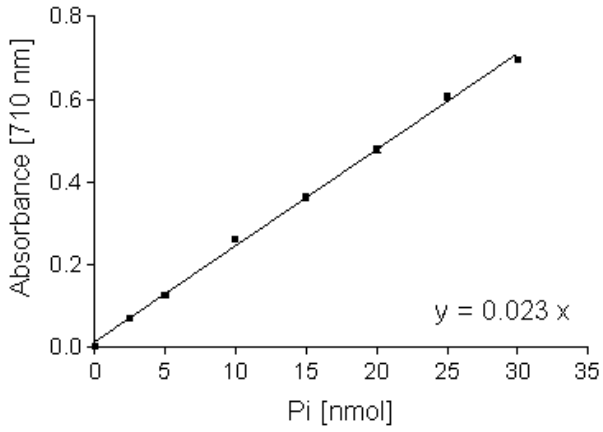

Figure 5.20.: Standard curve of spectrophotometric assay
The standard curve was set up using known concentrations of Pi^{2-}. 0-30 nmol of Pi^{2-} were used in the reaction buffer containing 30 mM Tris/HCl (pH 7.5), 2 mM $MgCl_2$, 2 mM ATP, 0.5 mM lipoic acid and 1 mM DTT in a final volume of 200 μl. After addition of solution 1 and 2 and incubation at the respective temperatures (see materials and methods), the absorbance was measured at 710 nm. Each assay was performed in duplicate. Shown here are two independent assays and each point represents the mean $\pm$ standard error.

To establish and validate whether this assay system is suitable to determine kinetic parameters of LplAs, *E. coli* LplA was used initially, and the results obtained were compared to published data that were obtained using a variety of other assay systems (summarised in Table 5.4) (Green et al., 1995, Fujiwara et al., 2005).

5.7.1. *E. coli* LplA

At first, I investigated whether an increase of *E. coli* LplA led to an increase of released PPi in the reaction in the new assay system. 5 μM of KGDH-E2-LD in a reaction mix containing 30 mM Tris/HCl (pH 7.5), 2 mM $MgCl_2$, 2 mM ATP, 0.5 mM lipoic acid and 2.5 U inorganic pyrophosphatase were used. The reaction was initiated with addition of 0-1 μM *E. coli* LplA and after 30 min incubation the absorbance at 710 nm was determined (Figure 5.21).

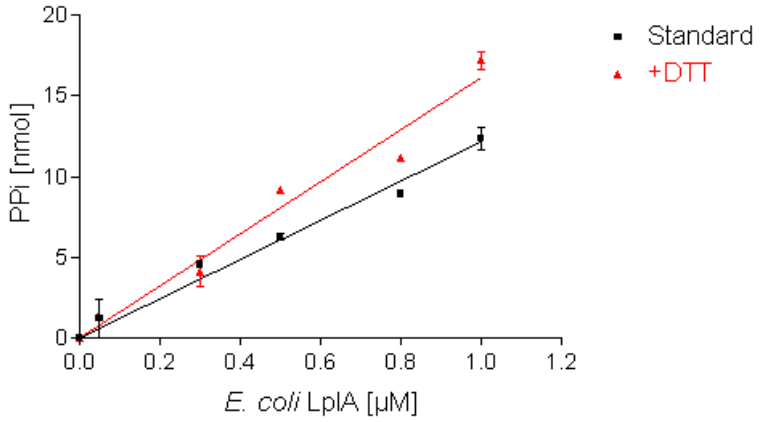

Figure 5.21.: Increase of *E. coli* LplA led to increase of PPi released and effect of DTT to the reaction
The standard lipoylation reactions were carried out in 200 μl final volume containing 5 μM KGDH-E2-LD, 30 mM Tris/HCl (pH 7.5), 2 mM $MgCl_2$, 2 mM ATP, 0.5 mM lipoic acid and 2.5 U inorganic pyrophosphatase (black). The DTT assays contained in addition 1 mM DTT (red). The assays were started by addition of *E. coli* LplA (0-1 μM) and were incubated at 37°C for 30 min. After addition of solution 1 and 2 and incubation at the respective temperatures (see materials and methods), the absorbance was measured at 710 nm. DTT enhanced the activity of *E. coli* LplA. The assays were performed in duplicate and each point represents the mean $\pm$ standard error.

Indeed, an increase of *E. coli* LplA led to an increase of PPi generated in the reaction (labeled as "Standard"). Further, the effect of DTT to the reaction was investigated by repeating the assay in the presence of 1 mM DTT (labeled as "+DTT"). It showed that

the activity of *E. coli* LplA was enhanced in the presence of DTT. Indeed Green and colleagues found, that the *E. coli* enzyme becomes inactive during oxidation containing at least one intramolecular disulphide bond, and that activity was restored upon incubation with DTT or β-mercaptoethanol (Green et al., 1995).

According to these data, the general reaction buffer for the spectrophotometric assay contained 30 mM Tris/HCl (pH 7.5), 2 mM $MgCl_2$, 2 mM ATP, 0.5 mM lipoic acid, 1 mM DTT and 2.5 U inorganic pyrophosphatase unless stated otherwise.

To analyse the dependence of the lipoylation reaction on the three substrates (lipoic acid, ATP and protein substrate) a standard assay was set up in general reaction buffer containing 5 μM of KGDH-E2-LD and 0-1 μM *E. coli* LplA (Figure 5.22). Beside the standard assay, five additional assays were carried out, the first without KGDH-E2-LD, the second without ATP and KGDH-E2-LD, the third without lipoic acid and KGDH-E2-LD, the fourth without lipoic acid and ATP and the last without all three substrates. In the second assay (without KGDH-E2-LD), PPi was released, however, slightly less compared to the standard reaction containing all assay components. The released PPi likely results from the activation of lipoic acid with ATP to form lipoyl-AMP and PPi. It supports the theory that the LplA reaction is a "two-step" reaction in which lipoic acid is first activated and then ligated to the apo-protein (Fujiwara et al., 2005). This is similar to what can be observed in biotin protein ligases (BPL) which first activate biotin with ATP to form biotin-AMP and then transfer the reaction intermediate to the apo-protein in a "two-step" reaction (Perham, 2000). The PPi released in the assay without KGDH-E2-LD was only marginally increased when the domain was present, suggesting that the transfer of activated lipoic acid to the lipoyl-domain might be the rate limiting part of the LplA reaction. However, it is not known whether PPi is firstly stoichiometrically released as lipoyl-AMP is formed, and secondly, whether PPi needs to be released before the apo-protein can bind to LplA. If the latter is the case, then it is possible that release of PPi is the rate limiting step. However, this remains unclear. Small amounts of PPi were also produced during the reaction without lipoic acid and KGDH-E2-LD. This was due to the ATP in the reaction mix which also contains some free Pi^{2-}. During the other three reactions, no PPi was measured showing the total dependence of the lipoylation reaction on lipoic acid and ATP.

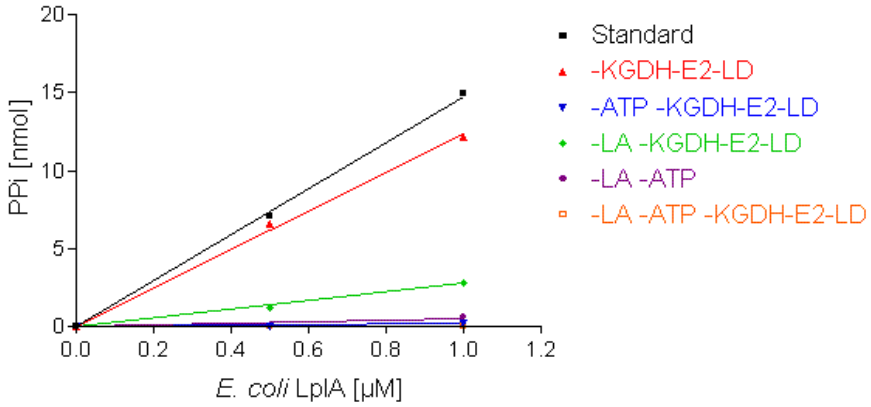

Figure 5.22.: Dependence of *E. coli* LplA lipoylation reaction on its substrates
The standard lipoylation reaction was carried out in 200 μl final volume containing 5 μM KGDH-E2-LD, 30 mM Tris/HCl (pH 7.5), 2 mM $MgCl_2$, 5 mM ATP, 0.5 mM lipoic acid, 2.5 U inorganic pyrophosphatase and 0-1 μM *E. coli* LplA (black). In red was the standard assay without KGDH-E2-LD, in blue without ATP and KGDH-E2-LD, in green without lipoic acid and KGDH-E2-LD, in purple without lipoic acid and ATP and in orange without all three substrates. The lipoylation reaction was incubated at 37°C for 30 min. After addition of solution 1 and 2 and incubation at the respective temperatures (see materials and methods), the absorbance was measured at 710 nm. In the reaction without KGDH-E2-LD (red) PPi was produced due to the activation of lipoic acid with ATP. This led to the conclusion that the reaction catalysed by LplA happened in two steps; first, activation of lipoic acid and second, transfer of activated lipoic acid to the protein substrate. These assays were performed only once with only one lipoyl-domain.

To analyse the time frame in which the *E. coli* LplA reaction was linear in the spectrophotometric assay, the lipoylation reaction was set up and was incubated for 5 to 60 min at 37°C. The assays were carried out using 0.9 μM H-protein as protein substrate in the general reaction buffer and 0.3 μM *E. coli* LplA to start the reaction (Figure 5.23). The reaction was linear up to 40 min incubation at 37°C before it slowly reached saturating levels.

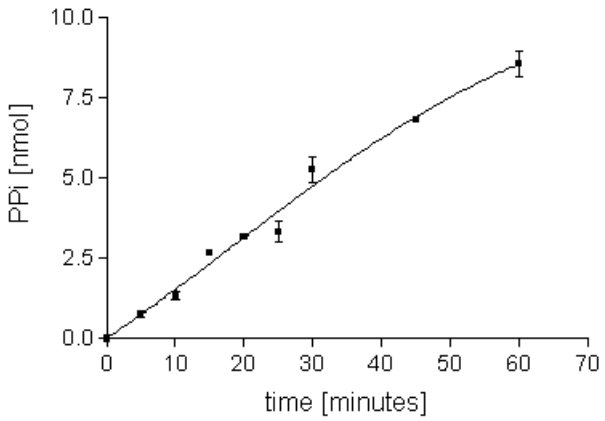

Figure 5.23.: Time dependence of *E. coli* LplA lipoylation reaction at 37°C in the spectrophotometric assay
The lipoylation reactions were carried out in 200 μl final volume containing 0.9 μM H-protein, 30 mM Tris/HCl (pH 7.5), 2 mM $MgCl_2$, 2 mM ATP, 0.5 mM lipoic acid, 1 mM DTT, 2.5 U inorganic pyrophosphatase and 0.3 μM *E. coli* LplA. The reactions were incubated 0 to 60 min before the reaction was stopped by addition of solution 1 and 2 (see materials and methods), and the absorbance was measured at 710 nm. The reaction was in the linear range for up to 40 min. The assay was measured in duplicate and each point represents the mean $\pm$ standard error.

Finally, I determined the apparent kinetic parameters of *E. coli* LplA using the spectrophotometric assay and compared them to published kinetic data of *E. coli* LplA which are summarised in Table 5.4 (Green et al., 1995, Fujiwara et al., 2005). Different assay systems were used to determine *E. coli* LplA activity. The "gel assay" used by Green et al. (1995) is similar to that described earlier using native PAGE. In this paper a radioactive method to determine LplA activity was also used in which the attachment of [^{3}H]-labelled lipoic acid to recombinant *E. coli* PDH-E2 lipoyl-domains was assessed. No information about the kinetic parameters of *E. coli* LplA for the *E. coli* PDH-E2 lipoyl-domains is given in this paper. Fujiwara and colleagues utilised the glycine-$^{14}CO_2$ exchange reaction as a measure for LplA activity (Fujiwara et al., 2005). Recombinant *E. coli* H-protein was used as protein substrate in a lipoylation reaction. After incubation for a certain time, the lipoylation reaction was terminated and used in the glycine-$^{14}CO_2$ exchange reaction (Fujiwara et al., 1992). Only the lipoylated H-protein was used by this assay and the amount of [^{14}C]-glycine formed was determined by liquid scintillation spectrometry as a measure of lipoylated H-protein.

Figure 5.24 displays the *E. coli* LplA apparent K_m and V_{max} determined using the spectrophotometric assay for lipoic acid in the absence of H-protein (Panel A) and in the

presence of 1.2 μM (Panel B) or 10 μM H-protein (Panel C).

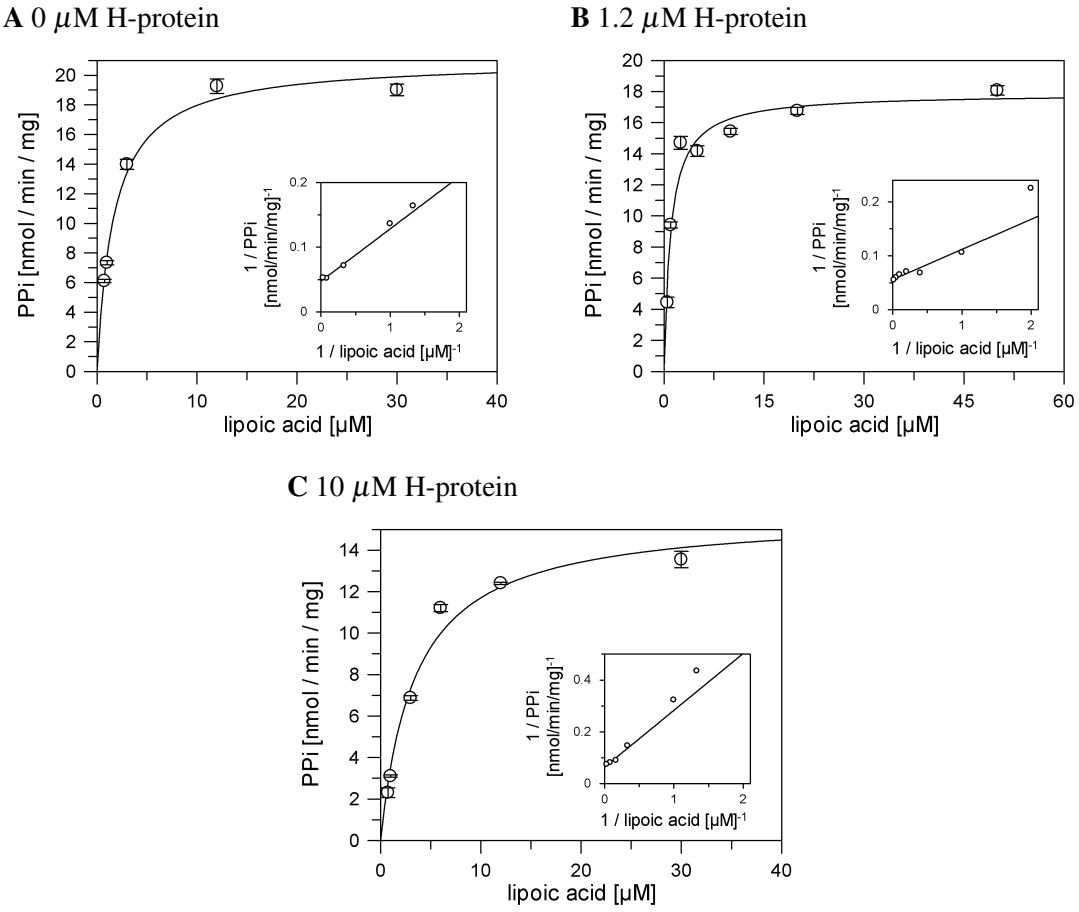

Figure 5.24.: Determining apparent kinetic parameters of *E. coli* LplA for lipoic acid
The apparent kinetic parameters of *E. coli* LplA for lipoic acid were determined at 37°C in 30 mM Tris/HCl (pH 7.5), 2 mM $MgCl_2$, 2 mM ATP, 1 mM DTT and 2.5 U inorganic pyrophosphatase. In addition, **Panel A** contained no H-protein, **Panel B** contained 1.2 μM H-protein and **Panel C** contained 10 μM H-protein. The lipoylation reaction was carried out with 1.6 μM *E. coli* LplA and varying concentrations of lipoic acid (0.5-50 μM). The production of PPi was measured after 30 min at 710 nm. Each point represents the mean $\pm$ standard error for two independent measurements, with apparent K_m and V_{max} determined using the Grafit 5.0 software (Erithacus software). Shown are the Michaelis-Menten and Lineweaver-Burke (double reciprocal) plots (insets) of the data obtained. The apparent K_m and V_{max} of *E. coli* LplA for lipoic acid without H-protein were determined to be 1.7 $\pm$ 0.2 μM and 21.0 $\pm$ 0.8 nmol/min/mg, respectively. In the presence of 1.2 μM H-protein the apparent K_m and V_{max} were determined to be 1.0 $\pm$ 0.2 μM and 17.9 $\pm$ 0.8 nmol/min/mg, respectively. With 10 μM H-protein in the lipoylation reaction the apparent K_m and V_{max} were determined to be 3.5 $\pm$ 0.7 μM and 15.7 $\pm$ 1.0 nmol/min/mg, respectively, indicating that the *P. falciparum* H-protein concentration does not affect the apparent kinetic parameters of *E. coli* LplA towards lipoic acid.

The assays were carried out in general reaction buffer containing 1.6 μM *E. coli* LplA, and different concentrations of lipoic acid varying between 0.5 and 50 μM. The production of PPi was measured after 30 min at 710 nm. The apparent K_m's and V_{max}'s obtained from these assays are listed in Table 5.4. Surprisingly, the H-protein concentration in the assays did not seem to affect the K_m and V_{max} of *E. coli* LplA for lipoic acid.

Similar results were obtained for the K_m and V_{max} determination of *E. coli* LplA for ATP (Figure 5.25). The assays were set up as described above but contained saturating levels of lipoic acid (0.5 mM) and variable concentrations of ATP (1-300 μM). The apparent K_m's and V_{max}'s determined are summarised in Table 5.4. As for lipoic acid, the H-protein concentration in the assays did not affect the K_m and V_{max} of *E. coli* LplA for ATP.

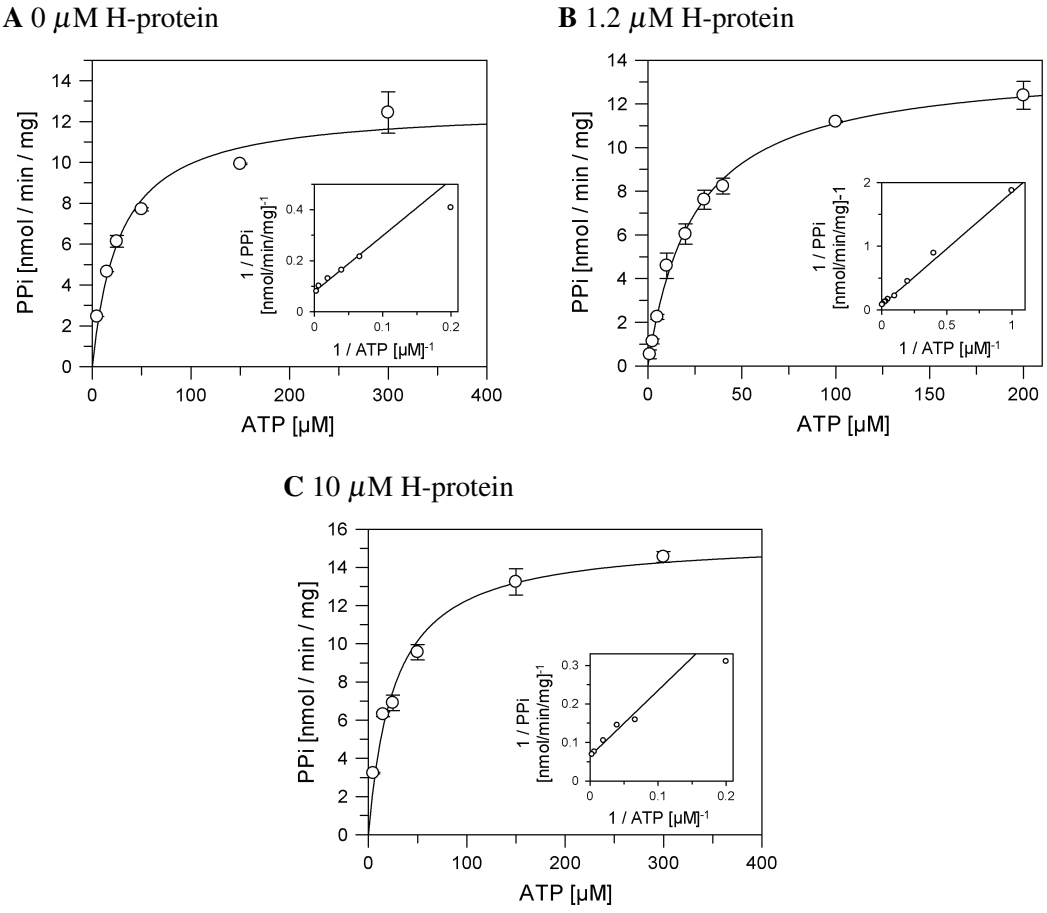

Figure 5.25.: Determining apparent kinetic parameters of *E. coli* LplA for ATP
The apparent kinetic parameters of *E. coli* LplA for ATP were determined at 37°C in 30 mM Tris/HCl (pH 7.5), 2 mM $MgCl_2$, 0.5 mM lipoic acid, 1 mM DTT and 2.5 U inorganic pyrophosphatase. In addition, **Panel A** contained no H-protein, **Panel B** contained 1.2 μM H-protein and **Panel C** contained 10 μM H-protein. The lipoylation reaction was carried out with 1.6 μM *E. coli* LplA and varying concentrations of ATP (1-300 μM). The production of PPi was measured after 30 min at 710 nm. Each point represents the mean $\pm$ standard error for two independent measurements, with apparent K_m and V_{max} determined using the Grafit 5.0 software (Erithacus software). Shown are the Michaelis-Menten and Lineweaver-Burke (double reciprocal) plots (insets) of the data obtained. The apparent K_m and V_{max} of *E. coli* LplA for ATP without H-protein were determined to be 27.9 $\pm$ 5.3 μM and 12.7 $\pm$ 0.7 nmol/min/mg, respectively. In the presence of 1.2 μM H-protein the apparent K_m and V_{max} were determined to be 24.6 $\pm$ 1.7 μM and 13.8 $\pm$ 0.3 nmol/min/mg, respectively. With 10 μM H-protein in the lipoylation reaction the apparent K_m and V_{max} were determined to be 26.4 $\pm$ 4.1 μM and 15.5 $\pm$ 0.7 nmol/min/mg, respectively, indicating that the H-protein concentration does not affect the apparent kinetic parameters of *E. coli* LplA towards ATP.

Determination of the kinetic parameters of *E. coli* LplA for *P. falciparum* H-protein as the protein substrate was not possible (Figure 5.26). The assay was set up in general

reaction buffer containing 0.1 μM *E. coli* LplA and varying concentrations of *P. falciparum* H-protein (0-40 μM). The lipoylation assays were incubated at 37°C for 30 min before the release of PPi was determined by measuring of the absorbance at 710 nm. The obtained data showed that the reaction with 40 μM *P. falciparum* H-protein was still in the linear range suggesting a very high K_m for the *P. falciparum* H-protein in contrast to the published data for *E. coli* H-protein. The published K_m of *E. coli* LplA for *E. coli* H-protein is 1.2 μM (Fujiwara et al., 2005). *P. falciparum* and *E. coli* H-protein share only modest sequence similarities with 32.2%, which may account for some differences in the K_m. Further, the glycine-$^{14}CO_2$ exchange reaction was inhibited when more than 5 μM H-protein were used (Fujiwara et al., 2005), concluding that the lipoylation reaction was not set up with saturating levels of H-protein as the protein substrate. This raises the question of the accuracy of the K_m determination of *E. coli* LplA for *E. coli* H-protein. Using higher H-protein concentrations in the spectrophotometric assay was impossible and resulted in precipitation of the proteins in the assay, pulling down the formed Pi^{2-}-molybdate complex. It was therefore impossible to determine the K_m and V_{max} of *E. coli* LplA for *P. falciparum* H-protein. It also meant that all reactions performed using the spectrophotometric assay were limited by the protein substrate, since the concentrations used were below the K_m.

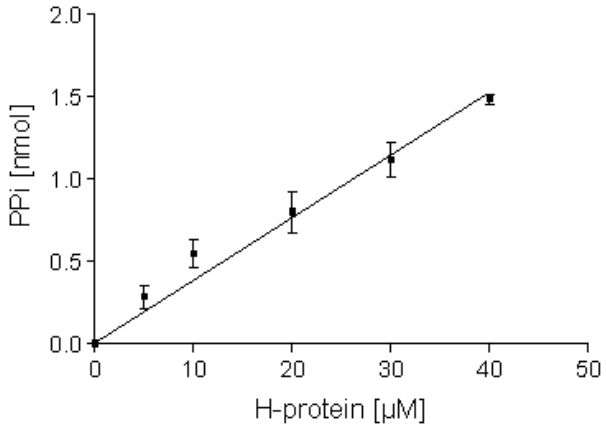

Figure 5.26.: *E. coli* LplA lipoylation reaction is limited by the protein substrate
The lipoylation reactions were carried out in 200 μl final volume containing 0-40 μM H-protein, 30 mM Tris/HCl (pH 7.5), 2 mM $MgCl_2$, 2 mM ATP, 0.5 mM lipoic acid, 1 mM DTT, 2.5 U inorganic pyrophosphatase and 0.1 μM *E. coli* LplA. The reactions were incubated at 37°C for 30 min before solution 1 and 2 (see materials and methods) were added. The absorbance was measured at 710 nm. The reaction was still in the linear range at high H-protein concentrations, suggesting that *E. coli* LplA has a high K_m for *P. falciparum* H-protein. The assay was performed in duplicate and each point represents the mean $\pm$ standard error.

The apparent K_m of *E. coli* LplA for lipoic acid and ATP obtained with the spectrophotometric assay correspond very nicely to the published data (Table 5.4). Large differences can be seen in the apparent V_{max} which might be explained by the different methods used to determine LplA activity.

Table 5.4.: Kinetic parameters of *E. coli* LplA

	K_m [μM]	V_{max} [nmol/min/mg]
Lipoic acid		
Gel assay[a]	1.7	2
Radioactive assay[a]	1.7	0.038
Glycine-$^{14}CO_2$ exchange reaction[b]	4.5	219
Spectrophotometric assay		
0 μM H-protein	1.7 ± 0.2	21.0 ± 0.8
1.2 μM H-protein	1.0 ± 0.2	17.9 ± 0.8
10 μM H-protein	3.5 ± 0.7	15.7 ± 1.0
ATP		
Gel assay[a]	1.9	40
Radioactive assay[a]	3	0.007
Glycine-$^{14}CO_2$ exchange reaction[b]	15.8	133
Spectrophotometric assay		
0 μM H-protein	27.9 ± 5.3	12.7 ± 0.7
1.2 μM H-protein	24.6 ± 1.7	13.8 ± 0.3
10 μM H-protein	26.4 ± 4.1	15.5 ± 0.7
H-protein		
Gel assay[a]	ND[c]	ND[c]
Radioactive assay[a]	ND[c]	ND[c]
Glycine-$^{14}CO_2$ exchange reaction[b]	1.2	258

[a] Green et al. (1995)
[b] Fujiwara et al. (2005)
[c] Not determined

I also determined the apparent K_m and V_{max} of *E. coli* LplA for octanoic acid. The assays were set up as before containing saturating levels of ATP (2 mM) but instead of lipoic acid, varying concentrations of octanoic acid (1-100 μM). After 30 min at 37°C, the PPi levels were determined by measuring the absorbance at 710 nm (Figure 5.27). The apparent K_m and V_{max} of *E. coli* LplA for octanoic acid were determined to be 75.1 ± 15.6 μM

and 49.1 ± 5.5 nmol/min/mg, respectively. This indicates that octanoic acid is used by *E. coli* LplA but only poorly, especially in comparison to lipoic acid, suggesting that under physiological conditions, only lipoic acid is used. However, the assay was only performed once in duplicate and therefore needs to be repeated to confirm the data obtained from the first assay.

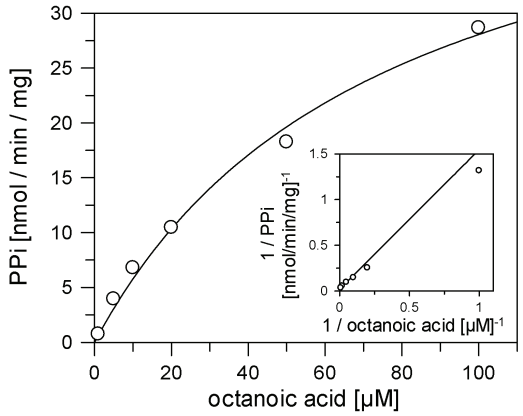

Figure 5.27.: Determining apparent kinetic parameters of *E. coli* LplA for octanoic acid
The apparent kinetic parameters of *E. coli* LplA for octanoic acid were determined at 37°C in 30 mM Tris/HCl (pH 7.5), 2 mM $MgCl_2$, 2 mM ATP, 1 mM DTT, 2.5 U inorganic pyrophosphatase and 1.2 μM H-protein. The lipoylation reaction was carried out with 1.6 μM *E. coli* LplA and varying concentrations of octanoic acid (1-100 μM). The production of PPi was measured after 30 min at 710 nm. Each point represents the mean ± standard error for two measurements, with apparent K_m and V_{max} determined using the Grafit 5.0 software (Erithacus software). Shown are the Michaelis-Menten and Lineweaver-Burke (double reciprocal) plots (insets) of the data obtained. The apparent K_m and V_{max} of *E. coli* LplA for octanoic acid were determined to be 75.1 ± 15.6 μM and 49.1 ± 5.5 nmol/min/mg, respectively.

5.7.2. *P. falciparum* LplA1

Initial assays for *P. falciparum* LplA1 were performed using the recombinant C-terminal Strep-tagged form. First, the time dependence of the *P. falciparum* LplA1 lipoylation reaction at 37°C was analysed. The lipoylation reaction containing 1.2 μM H-protein and 0.2 μM *P. falciparum* LplA1 was set up in general reaction buffer, and was incubated at 37°C for variable incubation times between 0 and 90 min (Figure 5.28). The reaction was linear for up to 10 min before it reached saturating levels.

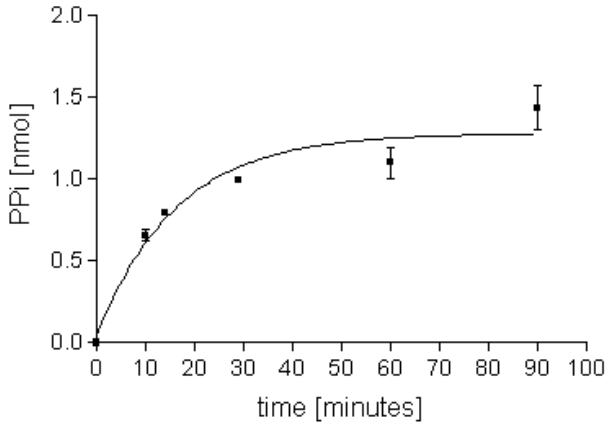

Figure 5.28.: Time dependence of *P. falciparum* LplA1 lipoylation reaction at 37°C in the spectrophotometric assay
The lipoylation reactions were carried out in 200 μl final volume containing 1.2 μM H-protein, 30 mM Tris/HCl (pH 7.5), 2 mM $MgCl_2$, 2 mM ATP, 0.5 mM lipoic acid, 1 mM DTT, 2.5 U inorganic pyrophosphatase and 0.2 μM *P. falciparum* LplA1. The reactions were incubated 0 to 90 min at 37°C before the reaction was stopped by adding solution 1 and 2 (see materials and methods), and the absorbance was measured at 710 nm. The reaction was in the linear range for up to 10 min before it reached saturation. The assay was measured in duplicate and each point represents the mean $\pm$ standard error.

The dependence of the *P. falciparum* LplA1 reaction on the H-protein was also initially analysed using the spectrophotometric assay. As for *E. coli* LplA, the determination of kinetic parameters for H-protein was not possible. The assay was incubated at 37°C and contained 0.1 μM *P. falciparum* LplA1 in general reaction buffer with variable H-protein concentrations between 0 and 20 μM. After 30 min incubation, the PPi level was analysed by measuring the absorbance at 710 nm (Figure 5.29). This was an end point determination, however, no saturating levels were reached with the highest H-protein concentrations used in the assay. The reaction was still in the linear range, indicating that the apparent K_m of *P. falciparum* LplA1 for H-protein is much higher than 20 μM.

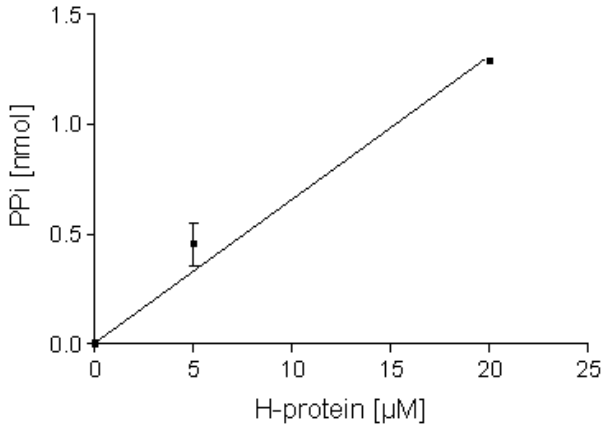

Figure 5.29.: *P. falciparum* LplA1 lipoylation reaction is limited by the protein substrate
The lipoylation reactions were carried out in 200 μl final volume containing 0-20 μM H-protein, 30 mM Tris/HCl (pH 7.5), 2 mM $MgCl_2$, 2 mM ATP, 0.5 mM lipoic acid, 1 mM DTT, 2.5 U inorganic pyrophosphatase and 0.1 μM *P. falciparum* LplA1. The reactions were incubated at 37°C for 30 min before solution 1 and 2 (see materials and methods) were added. The absorbance was measured at 710 nm. The reaction was still in the linear range at high H-protein concentrations, suggesting that *P. falciparum* LplA1 had a high K_m for *P. falciparum* H-protein. The assay was performed in duplicate and each point represents the mean $\pm$ standard error.

Both assays performed suggest that the *P. falciparum* protein behaves somewhat different in comparison to the *E. coli* protein. The reaction of *P. falciparum* LplA1 reaches saturating levels after 10 min incubation (see Figure 5.28), whereas the *E. coli* enzyme is in the linear range for up to 40 min, although more LplA enzyme and less H-protein substrate were used (see Figure 5.23). Further, using exactly the same reaction conditions, *P. falciparum* LplA1 releases more PPi than *E. coli* LplA (compare Figure 5.26 and Figure 5.29). However, the cause of this finding is not known and requires further investigation.

5.8. Summary

• Recombinant *P. falciparum* LplA1 was expressed and purified with either a N-terminal $(His)_{10}$-tag or a C-terminal Strep-tag.

• Of six *P. falciparum* LplA2 expression constructs generated, only LplA2-S2 with an N-terminal $(His)_{10}$-tag was expressed in soluble form. However, purification proved to be difficult because the recombinant protein was unstable and degradation products were present in the elution fraction. Further, the recombinant protein co-purified with *E. coli* proteins, including chaperons indicating that LplA2-S2 required folding assistance during recombinant protein expression. Because the LplA2-S2 elution fraction was contaminated with other proteins and thus only $\leq 10\%$ of the elution fraction actually corresponded to recombinant LplA2-S2, it was not tested for activity in either the "gel assay" or spectrophotometric assay.

• The lipoyl-domains of *P. falciparum* KADH-E2 subunits and the H-protein of the GCV were expressed and purified with N-terminal $(His)_{10}$-tags. CD analysis suggested that only three of the domains are adequately folded.

• Recombinant *E. coli* LplA was used in both the "gel assay" and spectrophotometric assay as a positive control for activity. The "gel assay" showed, that H-protein is the preferred substrate followed by PDH-E2-LD2 and KGDH-E2-LD. PDH-E2-LD1 and BCDH-E2-LD were not used as substrates by *E. coli* LplA likely because they were not folded properly as shown by CD analysis.

• Analysing Strep-tagged and $(His)_{10}$-tagged *P. falciparum* LplA1 showed that both enzymes were active although the C-terminally-tagged form had a higher enzymatic activity than the N-terminally-tagged version. The optimal reaction conditions for Strep-tagged LplA1 were at 37°C for 1 hour incubation.

• The "gel assays" suggested that recombinant *P. falciparum* LplA1 is less active than the recombinant *E. coli* LplA. Further it suggested, that *P. falciparum* LplA1 only uses H-protein as a protein substrate *in vitro*. "Gel assays" using the other four domains resulted in no lipoylation at the conditions used.

• A spectrophotometric assay system based on the detection of PPi release was estab-

lished.

• Using the spectrophotometric assay I could show for *E. coli* LplA that DTT enhances the activity of the enzyme. The spectrophotometric assay further supported that the LplA reaction is a "two-step" reaction in which firstly lipoic acid is activated forming lipoyl-AMP and secondly the activated lipoic acid is transferred to the apo-enzyme.

• Kinetic parameters for *E. coli* LplA were determined using the spectrophotometric assay, and the apparent K_m's and V_{max}'s determined were compared to published data. The apparent K_m's for lipoic acid and ATP were overall comparable to the published data, however, the apparent V_{max}'s were not. This is likely due to the different enzyme assays used, but could also be the result of the different protein substrates used. It was surprising that the determined kinetic parameters were not affected by the presence or absence of H-protein, suggesting that the release of PPi is only marginally affected by the protein substrate. It was not possible to determine kinetic parameters for *P. falciparum* H-protein. The data obtained by the spectrophotometric assay suggest that the K_m of *E. coli* LplA for *P. falciparum* H-protein is above 40 μM. Additionally, apparent K_m and V_{max} of *E. coli* LplA for octanoic acid were determined to be 75.1 $\pm$ 15.6 μM and 49.1 $\pm$ 5.5 nmol/min/mg, respectively.

• Initial tests were performed using Strep-tagged *P. falciparum* LplA1 in the spectrophotometric assay. Using this assay, the *P. falciparum* LplA1 reaction was in a linear range for up to 10 min. As for *E. coli* LplA, it was not possible to determine kinetic parameters for *P. falciparum* H-protein. The obtained data suggest that the apparent K_m of *P. falciparum* LplA1 for *P. falciparum* H-protein is above 20 μM.

• The spectrophotometric assay showed differences in the kinetic behaviour of *E. coli* LplA and the *Plasmodium* enzyme. However, this requires further investigation.

6. Discussion

The apicomplexan parasites *Plasmodium* and *Toxoplasma* possess two lipoylation pathways to post-translationally modify their KADHs and GCV. Biosynthesis of lipoic acid occurs in the apicoplast whereas scavenged lipoic acid is ligated to the enzyme complexes in the mitochondrion (Thomsen-Zieger et al., 2003, Wrenger and Müller, 2004). The distribution of the lipoylation pathways is in accordance with the subcellular localisation of the lipoic acid dependent enzyme complexes. The parasites possess a single PDH located in the apicoplast, and BCDH and KGDH complexes located in the mitochondrion (Foth et al., 2005, Günther et al., 2005, McMillan et al., 2005). The GCV is predicted to be mitochondrial (Salcedo et al., 2005), and indeed I could experimentally confirm that the H-protein, which is an integral part of the complex, is present in the mitochondrion of *P. falciparum* (see Figure 3.4). Lipoylation of these complexes is likely to be essential in most organisms and was also proposed to be crucial for *P. falciparum* and *T. gondii* viability (Crawford et al., 2006, Mazumdar et al., 2006, Allary et al., 2007). Salvage of lipoic acid in the mitochondrion of these parasites is achieved by LplA1, which attaches scavenged lipoic acid to the mitochondrial enzyme complexes (Wrenger and Müller, 2004, Crawford et al., 2006, Allary et al., 2007). It was shown that *P. falciparum* and *T. gondii* rely on the uptake of exogenous lipoic acid and it is believed that the scavenged lipoic acid is exclusively used for lipoylation in the mitochondrion, but not in the apicoplast (Crawford et al., 2006, Allary et al., 2007). Further, it is thought that biosynthesis of the cofactor solely occurs in the apicoplast by the action of LipB and LipA (Thomsen-Zieger et al., 2003, Wrenger and Müller, 2004). Octanoyl-ACP, the precursor which is attached to the apo-PDH-E2 by LipB, is provided by fatty acid biosynthesis in this organelle. Indeed, it appears that one of the main functions of fatty acid biosynthesis in the apicoplast is to provide the precursor for lipoylation, as knock-down of ACP in *T. gondii* abolished PDH lipoylation (Mazumdar et al., 2006). It seems that this finding also applies to mitochondria in plants and mammals, where one of the main products of fatty acid biosynthesis is octanoyl-ACP, believed to be used by the lipoylation machinery (Gueguen et al., 2000, Witkowski et al., 2007). Thus, the evidence to date suggests that lipoic acid metabolism in the apicomplexan parasites *P. falciparum* and *T. gondii* is carried out by two independent organelle-specific lipoylation pathways. However, a second gene encoding a lipoic acid protein ligase was identified during the course of this work, which was designated *lplA2* (Allary et al., 2007, Günther et al., 2007). The presence of a potential second LplA

raised the following questions about lipoic acid metabolism in *Plasmodium*, which I tried to address during my thesis:

1. Is LplA2 a functional ligase and when and where is it expressed?
2. Are the ligases essential for *Plasmodium* survival or are they redundant?
3. What are the biochemical properties of the two LplA proteins?

6.1. Identification of LplA2

LplA2 was identified by TBlastN searching the PlasmoDB database (Bahl et al., 2003) using *A. thaliana* LplA. Despite modest sequence similarities to the *A. thaliana* protein, bacterial LplAs and *P. falciparum* LplA1 (see Table 4.1), sequence analyses of the identified protein showed the presence of three highly conserved sequence motifs required for LplA activity (Fujiwara et al., 2005, Kim et al., 2005, McManus et al., 2006). This strongly suggests that LplA2 is a functional lipoic acid protein ligase and indeed complementation assays experimentally confirmed that LplA2 is functional, as it was able to replace LplA as well as LipB activity in deficient bacteria. The results of the functionality assays are in contrast to Allary et al. (2007), who suggested that LplA2 can only compensate LplA, but not LipB activity. The conflicting findings in both studies might be explained by the different expression constructs used to complement the growth defect of the *lipB/lplA* deficient bacterial strain. LplA2 expression constructs used by Allary et al. (2007) were truncated at the C-terminus, whereas I used constructs which were full length at the C-terminus. This difference is likely to account for the different results obtained and also implies that the C-terminal part missing in the LplA2 constructs used by Allary and colleagues is somehow required by the enzyme to use the ACP thioester bound form of octanoic acid as a substrate.

LplA2 is highly conserved in other *Plasmodium* spp. and also in *Theileria*. However, a potential orthologue in *T. gondii* appears not to be a functional lipoic acid protein ligase, because one highly conserved sequence motif (RRxxGGGxVxHD) required for lipoic acid binding and activation is absent in the deduced protein sequence. Thus, it appears that lipoic acid metabolism in the two apicomplexan parasites *Plasmodium* and *Toxoplasma* differs to some extent, although this hypothesis requires further investigation.

The discovery of the second LplA in *Plasmodium* spp. is particularly interesting with re-

gard to potential redundancy between the three ligases LplA1, LplA2 and LipB. In *E. coli* it is known that lipoic acid biosynthesis and salvage are redundant and can switch depending on the environmental situation (Cronan et al., 2005). This is in contrast to the bacterial pathogen *L. monocytogenes*, which also possesses two LplA-like proteins, but is not able to generate lipoic acid *de novo* and relies entirely on salvage of the cofactor (O'Riordan et al., 2003). It appears that LplA1 is absolutely required for intracellular growth and virulence of the pathogen despite the presence of LplA2. It was suggested that substrate specificity of LplA1 and LplA2 are the reason for this, as only LplA1 seems to be able to utilise degraded host cell lipoyl-protein as a source of lipoic acid (O'Riordan et al., 2003, Keeney et al., 2007). Thus, it appears that the two LplA-like proteins in *L. monocytogenes* are non-redundant because of their distinct substrate specificities. This is an interesting point regarding lipoic acid metabolism in *Plasmodium*, because the parasites possess four proteins that require the cofactor lipoic acid for their activity, and substrate specificities of the *Plasmodium* ligases will be further discussed below. Nevertheless, in *Plasmodium*, as opposed to *Listeria*, a crucial prerequisite for potential redundancy between the ligases is their subcellular localisation, and therefore the localisation of LplA2 was further investigated.

6.2. Localisation of LplA2

It was not possible to clearly predict the subcellular localisation of LplA2 and thus it was investigated *in vivo* by expressing full length LplA2 in frame with GFP in *P. falciparum*. Surprisingly, LplA2-GFP was targeted to two distinct, but closely associated organelles in the parasites, suggesting dual localisation of LplA2. One organelle was identified as the mitochondrion since LplA2-GFP fluorescence co-localised with Mitotracker-stained mitochondria. Because of the structure and close association of the second organelle with the mitochondrion, the apicoplast was suggestive (van Dooren et al., 2005). Immunofluorescence analyses were performed to further analyse this hypothesis. Wild-type parasites were analysed using antibodies against LplA2 and apicoplast localised dihydrolipoamide dehydrogenase (aE3) supporting that LplA2 is dually targeted to two organelles, one being the apicoplast. Together these data strongly suggest that LplA2 is targeted to both the mitochondrion and the apicoplast.

Recently, multiple protein targeting was observed in the two apicomplexan parasites *P. falciparum* and *T. gondii* (Pino et al., 2007, Ponpuak et al., 2007). In *P. falciparum*, the metalloprotease falcilysin was shown to be targeted to the food vacuole, apicoplast

and possibly mitochondrion (Ponpuak et al., 2007), however, the mechanism responsible for multiple targeting of this protein is not known. Several possibilities including post-translational modifications and alternative splicing were suggested (Ralph, 2007). In plants, multiple protein targeting has emerged to be an important process, but how it is regulated is poorly understood (Silva-Filho, 2003, Mackenzie, 2005, Millar et al., 2006). Many different mechanisms were shown to influence the localisation of a protein including post-translational modification, alternative splicing, different translation initiation sites or translation initiation from non-AUG codons, and thus it appears that multiple protein targeting can be achieved in a variety of different ways (Silva-Filho, 2003, Mackenzie, 2005). Often dual targeting is observed between the plastid and mitochondrion, possibly because of similar mechanisms of post-translational protein import into these organelles (Mackenzie, 2005), although some chloroplast proteins, like the α-carbonic anhydrase, were shown to be transported to the chloroplast via the secretory pathway (Villarejo et al., 2005). Furthermore, protein targeting to multiple destinations is not necessarily based on similar protein import mechanisms of these organelles. Indeed, dual targeting of plant proteins is also observed for destinations which either require entry into the secretory pathway (e.g. ER, Golgi, plasma membrane) or which facilitate protein import independently from the secretory system (e.g. mitochondrion, peroxisome, most chloroplast proteins) (Silva-Filho, 2003, Mackenzie, 2005). This is of particular interest in the light of multiple protein targeting in *Plasmodium* and *Toxoplasma*, especially concerning dual protein targeting of LplA2 to the apicoplast and mitochondrion. Mitochondrial protein import in these parasites occurs, like in plants and other organisms, post-translationally (van Dooren et al., 2006), but apicoplast targeting is exclusively via the ER from which apicoplast proteins are directly diverted to the apicoplast without entering the Golgi (DeRocher et al., 2005, Tonkin et al., 2006b). Pino and colleagues suggest that one of the main mechanisms for dual targeting to the apicoplast and mitochondrion in *T. gondii* is bimodal targeting by which an ambiguous targeting peptide is recognised by both protein import machineries (Pino et al., 2007). A critical step for this mechanism in apicoplast and mitochondrial targeting in these parasites is the entry into the ER mediated by the signal peptide. It suggests that proteins dually targeted to both organelles contain a week signal peptide which is only poorly recognised by the signal recognition particle (SRP), resulting in a proportion of the protein being targeted via the secretory system to the apicoplast, and another proportion being translated in the cytosol and imported to the mitochondrion (Pino et al., 2007). Interestingly, for the microsomal cytochrome P4502E1 (CYP2E1) protein in mammals it has been shown that bimodal

targeting to mitochondrion and ER (microsomes) is regulated by phosphorylation of an internal serine residue (Robin et al., 2002). It was shown that phosphorylation markedly increased binding of heat shock protein 70 (Hsp70) to CYP2E1. Subsequently, increased mitochondrial protein import was observed, suggesting that phosphorylation of the protein activated mitochondrial protein import (Robin et al., 2002).
The mechanism(s) involved in dual targeting of LplA2 are not yet understood and require further investigations. Bimodal targeting of LplA2 via the ambiguous N-terminal targeting peptide appears most likely. This is supported by the fact that the subcellular localisation of *Plasmodium* LplA2s was not reliably predictable, suggesting both, potential mitochondrial and apicoplast localisation (see Table 4.3). However, a second in frame methionine is found 78 amino acids downstream of the annotated start methionine (see Figure 4.1) and thus the use of two different translation initiation sites could also be responsible for dual targeting of LplA2. The latter, however, appears unlikely because the predicted subcellular localisation of the shorter LplA2 protein is neither mitochondrial nor apicoplast. However, how dual targeting of LplA2 is precisely achieved and moreover, how it is regulated remains elusive. If, for example, phosphorylation of LplA2 affects its subcellular localisation requires further investigation.

Multiple protein targeting to various destinations is generally observed of proteins that are required by the different organelles for their biological processes (Silva-Filho, 2003, Millar et al., 2006). The multiple targeted metalloprotease falcilysin in *P. falciparum* is known to participate in haemoglobin degradation in the food vacuole, and it has been suggested that in the apicoplast as well as in the mitochondrion it might be involved in transit peptide degradation (Ponpuak et al., 2007). The proteins shown to be dually targeted in *T. gondii* are involved in antioxidant defense and metabolic processes in both mitochondrion and apicoplast (Pino et al., 2007). Thus, dual localisation of LplA2 to the apicoplast and the mitochondrion suggests that the ligase participates in lipoic acid metabolism in both organelles. Allary et al. (2007) suggested that LplA2 possesses substrate specificity and showed that if expressed in lipoylation deficient *E. coli*, only the bacterial PDH-E2 is post-translationally modified by the *Plasmodium* enzyme. This further supports localisation of LplA2 to the apicoplast as PDH is only found in this organelle (Foth et al., 2005, McMillan et al., 2005). *E. coli* possesses three lipoic acid dependent enzyme complexes, namely the PDH, KGDH and the GCV (Cronan et al., 2005). Allary et al. (2007) clearly showed that bacterial KGDH-E2 is not a substrate of LplA2, but they did not clarify whether H-protein was lipoylated in the bacterial extract or not. Thus, H-protein and

BCDH-E2, which is absent in *E. coli*, could be other potential substrates of LplA2 in the mitochondrion of *P. falciparum* and this would support LplA2 localisation to the mitochondrion. The fact that LplA2 did not lipoylate *E. coli* KGDH-E2 points in the direction of substrate specificity, but certainly requires further investigation.

Recently, we showed that knock-out of *lipB*, the octanoyl-ACP transferase present in the apicoplast, is not lethal for the parasites (Günther et al., 2007). PDH lipoylation in these parasites was drastically reduced but not completely abolished, suggesting that dual targeted LplA2 can partially replace LipB. Reduced lipoylation of the PDH-E2 suggests that either only low levels of free lipoic acid are available in the apicoplast, or that LplA2 uses octanoyl-ACP, provided by fatty acid biosynthesis, for transfer. Bacterial LplA is able to use octanoyl-ACP as a substrate, although less efficient then free lipoic acid (Jordan and Cronan, 2002, Cronan et al., 2005). The fact that LplA2 complemented the growth defect of *lipB* deficient and *lipB/lplA* deficient bacteria in the absence of lipoic acid shows that LplA2 too can transfer octanoyl-ACP to the enzyme complexes, but like the bacterial enzyme less efficiently. Furthermore, previous studies in *P. falciparum* and *T. gondii* suggest that scavenged lipoic acid is exclusively used by the mitochondrial lipoylation machinery and not by the apicoplast (Crawford et al., 2006, Allary et al., 2007). The only source for lipoylation in the apicoplast was suggested to be octanoyl-ACP (Mazumdar et al., 2006). This would explain the reduction of PDH-E2 lipoylation in the *P. falciparum lipB* knock-out mutants, as LplA2 can use octanoyl-ACP albeit only poorly.

6.3. *LplA1* knock-out studies

Dual targeting of LplA2 potentially suggests that not only LipB but also LplA1 activity is redundant. This hypothesis was further investigated by knock-out studies of *lplA1* in *P. falciparum* and *P. berghei*. Knock-out of *lplA1* in *P. falciparum* by single cross-over recombination was not achieved. It was further attempted to knock-out the gene by providing the parasites with a copy of *P. berghei lplA1*. If the gene is essential for intraerythrocytic stages, knock-out of the gene should theoretically be possible if a second copy is provided and the protein it encodes is functionally expressed. This method was shown to be successful for knock-out of *P. falciparum* thioredoxin reductase (Krnajski et al., 2002). *P. berghei lplA1* was chosen to prevent recombination with the *P. falciparum* gene locus. But despite the presence of *P. berghei* LplA1, the *P. falciparum lplA1* gene locus was not targeted. Instead, non-specific integration of transfected plasmid into non-related gene loci occurred. The same phenomenon was also observed for the 3' replacement construct,

which did not target the *lplA1* gene locus, but seemed to integrate unspecifically into the *P. falciparum* genome. Thus, from the knock-out and knock-in studies in *P. falciparum*, it cannot be concluded whether *lplA1* is essential for intraerythrocytic stages of *P. falciparum* or whether LplA1 and LplA2 are redundant because the *lplA1* gene locus appeared to be refractory to single cross-over recombination.
Knock-out studies were also performed in *P. berghei*, the rodent malaria parasite. Knock-out of *lplA1* by single cross-over recombination was not achieved in three independent attempts, in contrast to the 3' replacement construct, which targeted the gene locus after only one transfection. This suggested that (1) *lplA1* is essential for parasite survival as knock-out appeared impossible and (2) the *lplA1* gene locus in *P. berghei* is easily targetable and not refractory as it appeared to be in *P. falciparum*. However, the *P. berghei lplA1* gene locus was also targeted by the replacement construct resulting in the replacement of *lplA1* with the *T. gondii* DHFR/TS, the selectable marker of the plasmid. But this parasite population was quickly overgrown by parasites containing the endogenous *lplA1* gene and carrying the selectable marker episomally, strongly suggesting that knock-out of *lplA1* has a severe effect on parasite viability. Complementation of *P. berghei lplA1* replacement by over-expression of the *P. falciparum* gene also resulted in the replacement of *lplA1*, but again the population was quickly overgrown by parasites with the endogenous *lplA1* gene and episomal selectable marker.

The results obtained by knock-out studies of *lplA1* in *P. falciparum* and *P. berghei* suggest that LplA1 is crucial for the intraerythrocytic stages, as knock-out of the gene appears impossible. This strongly suggests that LplA1 is required for parasite survival and further implies that LplA1 function cannot be replaced by LplA2, leading to the conclusion that LplA1 and LplA2 are not redundant. Substrate specificity of the two proteins could be a potential explanation for this finding, as was already suggested by Allary et al. (2007) and discussed above. Another potential explanation includes the stage specific expression of LplA1 and LplA2 in *Plasmodium* parasites during their developmental cycle. Analysis of the expression data available through the PlasmoDB database indeed implies that LplA1 is present throughout the intraerythrocytic development stages, whereas LplA2 is present in late trophozoites and mainly in gametocytes (Figure 6.1). Thus, substrate specificity and timing of protein expression may be the key components regulating the function of the two proteins in *Plasmodium* parasites.

A surprising and somewhat conflicting finding of the knock-out studies in *P. falciparum*

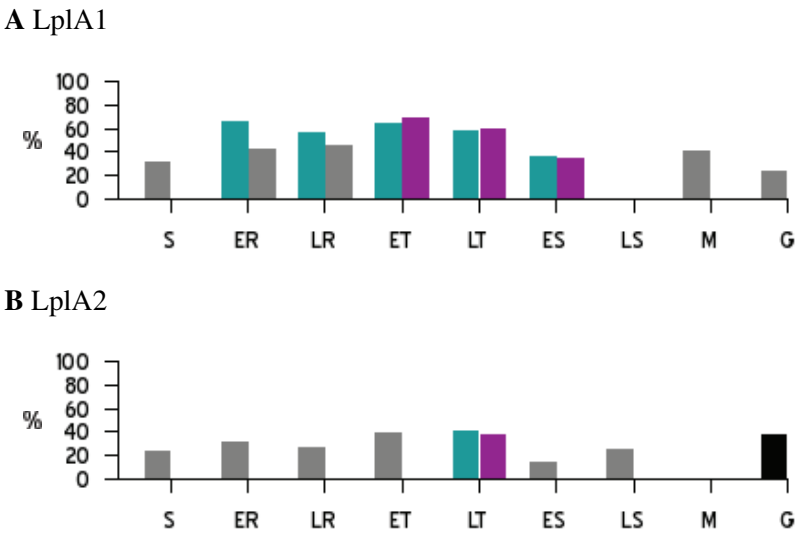

Figure 6.1.: Expression profile of (A) LplA1 and (B) LplA2
This figure displays the expression profile of *P. falciparum* LplA1 (**Panel A**) and *P. falciparum* LplA2 (**Panel B**) taken from the PlasmoDB website (www.plasmodb.org). Shown is the percentiled expression level of the respective gene relative to all other genes. Data in green are of parasites synchronised by sorbitol, in purple of parasites synchronised by temperature and in grey is data below the confidence threshold. Data for gametocytes were obtained by sorbitol synchronisation and sporozoite data represent an average of two replicates.
Abbreviations: S, sporozoite; ER, early ring; LR, late ring; ET, early trophozoite; LT, late trophozoite; ES, early schizont; LS, late schizont; M, merozoite; G, gametocyte

and *P. berghei* was that the *lplA1* gene locus in *P. berghei* was targeted by single and double cross-over recombination, whereas the gene locus on *P. falciparum* appeared refractory to integration. Given the high degree of synteny between the *P. falciparum* and *P. berghei lplA1* gene loci, it seemed highly unlikely that one locus can be targeted when the other cannot be targeted at least by the knock-in construct. It rather appears that the transfected plasmid in *P. falciparum* was rapidly lost after unspecific integration into the parasites genome and thus the possibility to address the *lplA1* gene locus never occurred.

Another unexpected result was that the complementation attempts in both, *P. falciparum* and *P. berghei* knock-out studies were unsuccessful giving reason to speculate as to why these attempts failed. A possible explanation is that *P. falciparum* LplA1 and *P. berghei* LplA1 are unable to compensate the function of the other protein. This, however, seems unlikely given the high degree of sequence similarity between the two proteins (78% amino acid sequence similarity). Technical problems might also be the reason for this outcome, because the constructs were only transfected once (in *P. berghei*) or twice (in *P.*

falciparum). A third possibility is that the intracellular concentration of LplA1 is important for the parasites. Over-expression of LplA1 might have a negative effect on parasite viability and this possibility will be further discussed below. Moreover, in the complementation studies, the subcellular localisation of the over-expressed LplA1 was never analysed in *P. falciparum* or in *P. berghei*. The localisation is, however, crucial for successful complementation of the potential loss of the endogenous copy. If, for instance, the over-expressed LplA1 copy has negative effects on parasite viability, it could, as a consequence, be transported to the food vacuole for degradation and thus complementation would not be possible. This, however, is only speculative and requires further analyses.

To investigate the effect of LplA1 over-expression further, mutant parasites were generated by transfecting wild-type *P. falciparum* with the *P. berghei* LplA1 over-expression construct. In this construct, *P. berghei lplA1* is not controlled by its endogenous or the *P. falciparum lplA1* promoter, but by the *P. falciparum* Hsp86 promoter, which is constitutively active throughout the erythrocytic development stages (Wu et al., 1995, Militello et al., 2004). The presence of *P. berghei* LplA1 was experimentally confirmed by western blotting and was further supported given that these parasites contained slightly elevated levels of protein bound lipoic acid in comparison to wild-type parasites. Interestingly, the parasites displayed a slight growth phenotype, progressing modestly slower through the intraerythrocytic development stages than wild-type parasites. These data suggest that indeed the concentration of LplA1 is important for the parasites viability. The increased levels of protein bound lipoic acid in these parasites could be due to an increased lipoylation of the enzyme complexes, however, it could also be the result of sequestration of lipoic acid to the ligases. In Chapter 5, I showed that lipoic acid is bound to the ligases strongly enough that the linkage is not broken up during SDS-PAGE. It is conceivable that strong sequestration of lipoic acid by the ligases results in inhibition of the enzymes, but it may also imply that lipoic acid fulfils other functions in the parasites. Mammalian cells contain very little free lipoic acid (Biewenga et al., 1997) and this is also found in *P. falciparum* (Günther et al., 2007). However, by over-expressing LplA1, the small amount of free lipoic acid that potentially is present in the parasites might be sequestered by the ligases and thus depletes sources of free lipoic acid which might be involved in other processes like for instance in antioxidant defense.

The *lplA1* gene loci of *P. falciparum* and *P. berghei* share a high degree of synteny apart from three small proteins in the *P. berghei* gene locus, that are not annotated in *P. fal-*

ciparum. However, one of these small annotated proteins could be an additional upstream exon of *P. berghei lplA1*. Indeed closer analysis of the genomic sequence of the *P. berghei* locus revealed potential splicing sites, and the predicted localisation of the resulting LplA1 would be the apicoplast (Table 6.1). Moreover, searching the *P. falciparum lplA1* gene locus for a similar exon also revealed the presence of a potential upstream exon. As for *P. berghei*, the potential localisation of the resulting protein was predicted using the available prediction programs (Table 6.1). The results obtained are ambiguous for the "long" *P. falciparum* LplA1, as it is predicted to be in the mitochondrion and apicoplast, depending on the program used.

Table 6.1.: Predicted localisations of potential "long" LplA1s

	MitoProt	PlasMit	Predotar	PATS	SignalP
P. falciparum	0.9916 CS[a]→74	non-mito 99%	0.01 mito 0.00 plastid	0.95	0.005
P. berghei	0.0193	non-mito 99%	0.04 mito 0.00 plastid	0.92	0.091

[a] predicted cleavage site

The presence of these potential transcripts in *P. falciparum* and *P. berghei* is currently being investigated by reverse transcriptase PCR. If these transcripts are really present in parasite RNA, it would suggest that LplA1, like LplA2, is potentially dually targeted to apicoplast and mitochondrion. This possibility is also currently analysed by immunofluorescence analyses in *P. falciparum* using anti-LplA1 antibodies and mitochondrial and apicoplast markers, respectively. If dual targeting also applies for LplA1 it would be another explanation why the complementation of *lplA1* knock-out failed. The localisation of the annotated LplA1 proteins in all *Plasmodium* spp. are predicted to be mitochondrial and thus, the proteins used in the complementation studies possibly only compensate for mitochondrial LplA1 loss and not that of the apicoplast. However, even if LplA1 was dually targeted, it can only be speculated whether apicoplast targeting is of any relevance as long as LipB is functional. The potential exons in *P. falciparum* and *P. berghei lplA1* were only identified while writing this thesis. At the time when the constructs for the knock-out studies in *P. falciparum* and *P. berghei* were designed, this information was not available.

6.4. *LplA2* knock-out studies

To analyse the potential function of LplA2 in the parasites, knock-out studies in *P. falciparum* and *P. berghei* were performed. Knock-out of *lplA2* in *P. falciparum* was attempted by single cross-over recombination, but integration into the *lplA2* gene locus was not achieved. The results obtained by Southern blot analyses were ambiguous, possibly suggesting unspecific integration of the knock-out construct into the *P. falciparum* genome, but this speculation requires further investigation by PFGE.
As for *lplA1*, knock-out of *lplA2* in *P. berghei* was attempted by single and double cross-over approaches. Knock-out of *lplA2* via integration was unsuccessful, although the 3' replacement construct integrated very efficiently into the *lplA2* gene locus. This demonstrated that the gene locus is not refractory, but it appeared that knock-out of *lplA2* by single cross-over is not possible. However, replacement of the gene was accomplished by double cross-over recombination and clonal *lplA2* knock-out mutants were generated. Surprisingly, the complementation construct by which *P. berghei lplA2* is replaced with *P. falciparum lplA2* did not target the gene locus. In this construct, *P. falciparum lplA2* is not under control of its endogenous or the *P. berghei lplA2* promoter. It is likely to be over-expressed as it is driven by the *P. falciparum* calmodulin promoter, which was shown to be strongly active throughout the intraerythrocytic stages (Crabb and Cowman, 1996), and this could potentially have negative effects on parasites viability as discussed above for LplA1. However, technical problems could also be the cause of this result. If, for instance, incomplete digested plasmid DNA was transfected, it could easily re-ligate and never target the gene locus.

The results obtained by the knock-out studies in *P. berghei* clearly show that LplA2 is not essential for intraerythrocytic development stages, as replacement of the gene with *T. gondii* DHFR/TS, the selectable marker, is possible. Phenotypical analyses of LplA2 mutant parasites revealed that asexual stages were only modestly affected by *lplA2* knock-out, growing slightly slower in comparison to wild-type parasites. In another experiment where *lplA2* mutants were mixed with wild-type parasites one to one, which were then taken through five mice, the mutant parasites were outcompeted over time by wild-type parasites, further supporting a mild growth defect in comparison to wild type parasites. However, a drastic effect was observed during the sexual development of LplA2 null mutants. The development of ookinetes was drastically reduced, suggesting a potential effect of *lplA2* knock-out in gametocytes, gametes and/or the zygote. Thin blood smears of the *lplA2* knock-out clones were analysed regularly to monitor parasitemia, and in

these blood smears male as well as female gametocytes were observed, thus potentially narrowing down the effect of *lplA2* knock-out to gametes and/or the zygote. The effect of *lplA2* knock-out, however, can possibly be further confined. Before the knock-out populations were used to feed mosquitoes or to set up ookinete cultures, exflagellation of male gametes was investigated. As exflagellation appeared to be comparable to wild-type parasites, it may allow potential exclusion of a direct effect of the knock-out on male gametes, leaving female gametes and the zygote as the sexual stages which are most likely affected in the LplA2 null mutants. However, this is speculative and definitively requires further analyses of these developmental stages to identify when, where and why *lplA2* knock-out causes its drastic effect on sexual development of the parasites.

The knock-out studies of both *lplA1* and *lplA2* strongly suggest that the two ligases are non-redundant. One major factor involved appears to be the stage specificity of both enzymes. As mentioned above, LplA1 is expressed throughout the asexual stages, whereas LplA2 is mainly expressed in gametocytes (see Figure 6.1). Additionally, it appears that the lipoic acid dependent enzyme complexes are up-regulated during gametocytogenesis and gametogenesis (Hall et al., 2005, Salcedo et al., 2005, Young et al., 2005). Analyses of the expression profile of the KADH complexes available through PlasmoDB implies that particularly the PDH and KGDH are important during sexual developmental of the parasites (Figure 6.2). In general, analyses of proteome and transcriptome of the rodent malaria parasites *P. chabaudi* and *P. berghei* revealed that mitochondrial enzymes involved in, for instance, the TCA cycle or oxidative phosphorylation were up-regulated in gametocytes, and were present at even higher levels in ookinetes in comparison to the asexual stages (Hall et al., 2005). In accordance, analysis of the *P. falciparum* transcriptome of sexual stages showed down-regulation of enzymes involved in glycolysis and up-regulation of enzymes which are part of the TCA cycle (Young et al., 2005), suggesting a different role of the mitochondrion in energy metabolism in these developmental stages. The fact that gametocytes contain multiple, cristate mitochondria in contrast to the asexual stages, which contain a single acristate mitochondrion, further supports the suggestion that the mitochondria in sexual stages fulfil a different role, as cristate mitochondria are generally associated with "active" mitochondria (Rudzinska, 1969, van Dooren et al., 2006). Further experiments on gametocyte mitochondria support the theory that these are more active than their asexual counterparts, as activity of the mitochondrial dihydroorotate dehydrogenase, cytochrome c reductase and cytochrome c oxidase appears to be about 8-10 times higher in gametocytes (Learngaramkul et al., 1999). Interestingly,

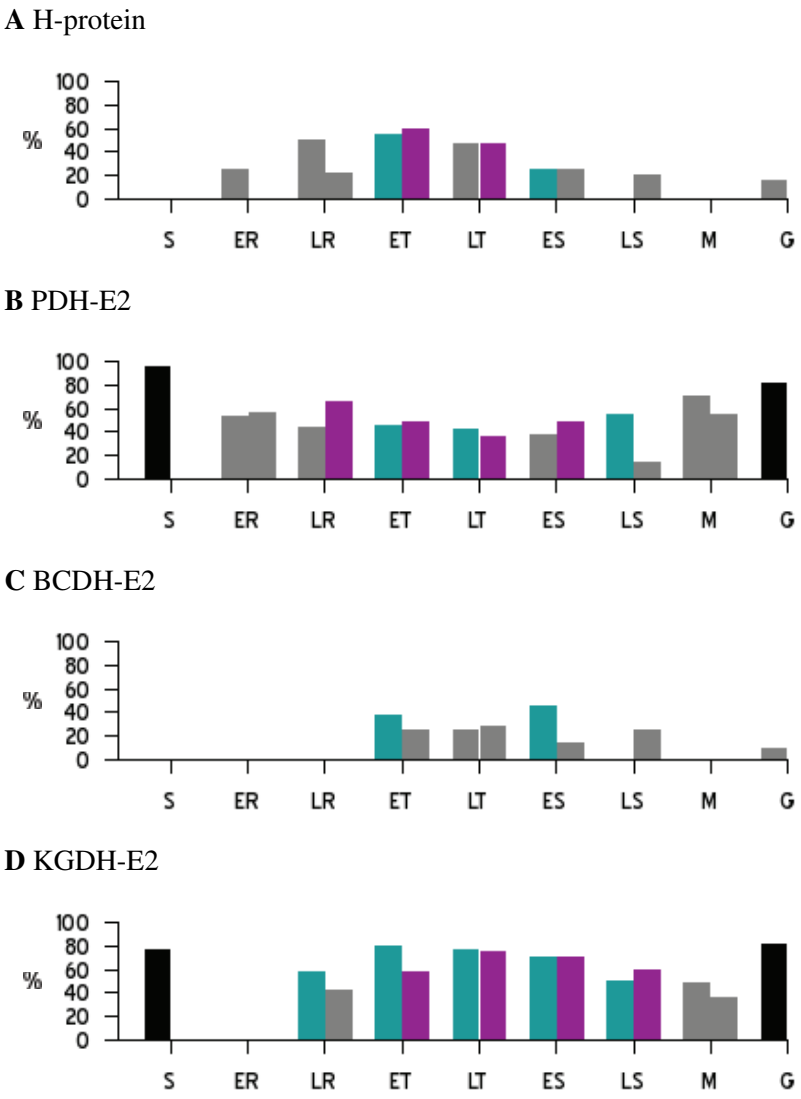

Figure 6.2.: Expression profile of lipoic acid dependent enzymes
This figure displays the expression profile of *P. falciparum* H-protein (**Panel A**), *P. falciparum* PDH-E2 (**Panel B**), *P. falciparum* BCDH-E2 (**Panel C**) and *P. falciparum* KGDH-E2 (**Panel D**) taken from the PlasmoDB website (www.plasmodb.org). Shown is the percentiled expression level of the respective gene relative to all other genes. Data in green are of parasites synchronised by sorbitol, in purple of parasites synchronised by temperature and in grey is data below the confidence threshold. Data for gametocytes were obtained by sorbitol synchronisation and sporozoite data represent an average of two replicates.
Abbreviations: S, sporozoite; ER, early ring; LR, late ring; ET, early trophozoite; LT, late trophozoite; ES, early schizont; LS, late schizont; M, merozoite; G, gametocyte

an up-regulation in gametocytes was also observed for δ-aminolevulinate synthase, porphobilinogen deaminase and uroporphyrinogen decarboxylase, which are all part of the haem biosynthesis pathway present in the mitochondrion, apicoplast and possibly cytosol

(Young et al., 2005). Given this background, it appears that the lipoic acid dependent enzyme complexes like KGDH, which produces succinyl-CoA required in the first step of haem biosynthesis, fulfil crucial metabolic functions in the sexual developmental stages, and potentially explains its strong expression in these stages. Indeed, PDH up-regulation was also observed in gametocytes together with gametocyte specific expression of LipA, the lipoic acid synthase (Young et al., 2005). These data strongly suggest that most of the lipoic acid dependent enzyme complexes display increased activity in the sexual stages and thus adequate lipoylation, possibly mediated by LplA2, is crucial in these stages. Interestingly, Khan et al. (2005) analysed for the first time the sex specific proteomes of *P. berghei* male and female gametocytes. The studies described above were all performed on mixed gametocytes populations, not allowing to distinguish between male and female specific processes. However, Khan et al. (2005) showed that only 69 proteins are shared by both male and female gametocytes. Intriguingly, mitochondrial proteins like BCDH-E2 and KGDH-E2 were more abundant in female gametocytes together with proteins involved in protein synthesis, whereas in the proteome of male gametocytes, proteins involved in DNA replication and axoneme formation were mainly expressed (Khan et al., 2005). This strongly suggests that the mitochondrion is particularly important in female gametocytes, further supporting my speculations that *lplA2* knock-out possibly affects female rather than male gamete development.

During the course of this thesis, knock-out studies were performed in the human and rodent malaria parasites *P. falciparum* and *P. berghei*. For the studies in *P. falciparum*, the plasmid pHH1 was used, targeting the gene of interest by single cross-over recombination which should result in the disruption of the gene (Reed et al., 2000). A common problem, not only observed during this study, but also during knock-out studies of several other genes performed in the laboratory was that the plasmid integrated unspecifically into the genome of *P. falciparum*. This is very unsatisfactory as it can hinder integration into the correct gene locus if the episomal plasmid is lost after this unspecific integration event. A better alternative to pHH1 are the transfection plasmids pHTK and pCC, which allow replacement of the gene of interest by double cross-over recombination (Duraisingh et al., 2002, Maier et al., 2006). The plasmids contain, in addition to the positive selection cassette, a negative selectable marker, which is either the thymidine kinase or cytosine deaminase. The possibility to select for parasites that contain the positive selectable marker but which have lost the negative selection cassette drastically decreases the time required to select for parasites that have integrated the plasmid. The pCC plasmids are particularly

useful as negative selection with the cytosine deaminase is more stringent and reliable in comparison to the thymidine kinase (Maier et al., 2006).

In *P. berghei* two techniques were carried out, as it was attempted to knock-out the genes of interest by single and double cross-over approaches. Generally, the *P. berghei* system has several advantages over *P. falciparum*. First of all, the transfection efficiency is much greater in *P. berghei* in comparison to *P. falciparum*, with 10^{-2}-10^{-3} in *P. berghei* and $\sim 10^{-6}$ in *P. falciparum* (O'Donnell et al., 2002, Janse et al., 2006). This allows more efficient transfection and thus allows the possibility of repeating transfections more often, whereas in *P. falciparum* the selection of parasites after transfection is a very lengthy process, particularly if the pHH1 plasmid is used, which restricts the amount of transfections due to practicality. Another advantage of knock-out studies in *P. berghei* is the fact that all life cycle stages can be investigated. Indeed, the whole *Plasmodium* life cycle can be analysed *in vivo*. There only remains the question how diverged *P. berghei* and *P. falciparum* are, or wether *P. berghei* can actually be used as a model system for *P. falciparum*. However, significant differences in the life cycle of both parasites can be observed. The intraerythrocytic development in *P. berghei* takes only 24 hours, whereas *P. falciparum* requires twice as long to complete this part of its development. Differences are even more obvious during gametocytogenesis in both parasites. Mature gametocytes emerge after only one day for *P. berghei*, whereas this process in *P. falciparum* takes $\sim$11 days (Alano, 2007). Moreover, recent knock-out studies suggest that orthologue proteins may fulfil different roles in *P. berghei* and *P. falciparum*. Knock-out studies of the mitogen-activated protein (MAP) kinase map-2 in *P. berghei* showed that the kinase is required for male gamete formation, but no obvious effects in the intraerythrocytic stages were observed (Khan et al., 2005, Rangarajan et al., 2005, Tewari et al., 2005). This is in contrast to *P. falciparum*, where knock-out studies implied that Pfmap-2 already fulfils essential functions in the asexual stages, as knock-out of the gene seemed impossible (Dorin-Semblat et al., 2007), suggesting that indeed differences between *P. falciparum* and *P. berghei* exist on the protein level. Thus, it is questionable whether *P. berghei* is a suitable model organism for *P. falciparum*, particularly in the quest of new potential drug targets. Rather, it seems that analyses in both organisms would be ideal to potentially also identify more exciting differences between these two parasites, which are reflected by differences in their biology and physiology.

6.5. Biochemical characterisation

6.5.1. Recombinant protein expression and purification

To analyse the biochemical properties of *P. falciparum* LplA1 and LplA2 *in vitro*, constructs for recombinant protein expression were designed. Both, LplA1 and LplA2, were expressed with either a N-terminal $(His)_{10}$-tag or a C-terminal Strep-tag. The LplA1 constructs were both truncated at the N-terminus and missed the first 15 amino acids, which are predicted to constitute mitochondrial targeting of the annotated LplA1. They were removed because the transit peptide, which is usually cleaved after import into the mitochondrion, could interfere with protein expression and solubility in the prokaryotic expression system. $(His)_{10}$- and Strep-tagged LplA1 were both expressed and purified, however, the Strep-tagged recombinant protein appeared more stable. Because a potential targeting peptide could not be predicted for LplA2, three different LplA2 constructs were generated differing in length at their N-termini. The first construct was full length at the N-terminus, whereas the second construct (S1) was truncated and missed the first 27 amino acids. The S1 construct thus starts where the bacterial LplAs align with the *P. falciparum* LplA2 sequence (see Figure 4.1). Furthermore, this starting site is in the same region of the predicted mitochondrial transit peptide cleavage sites of *P. knowlesi* and *P. vivax* LplA2 (see Table 4.3). The third construct (S2) is further truncated at the N-terminus and misses the first 79 amino acids. All three constructs complemented the growth defect of *lipB* and *lipB/lplA* deficient bacteria, suggesting that all three constructs produce functional enzymes. Thus, six LplA2 expression construct were generated, three containing a N-terminal $(His)_{10}$-tag and three a C-terminal Strep-tag. Of these only one, the $(His)_{10}$-tagged LplA2-S2 construct, was expressed in soluble form. The other constructs were not expressed solubly, despite different expression temperatures and bacterial strains used. Purification of LplA2-S2 via batch and FPLC nickel affinity chromatography proved difficult, as the recombinant protein was not very stable and degraded during expression. Moreover, the recombinant protein co-purified with bacterial chaperones, strongly suggesting that the protein had folding problems and required assistance during expression (Goloubinoff et al., 1989, Georgiou and Valax, 1996, Keresztessy et al., 1996). Interestingly, small scale test expression analyses of the other two $(His)_{10}$-tagged LplA2 constructs also showed degradation of the proteins during expression, whereas this was hardly observed for the Strep-tagged constructs. It appears that the N-terminal tag interferes with protein stability as also the LplA1 construct with the N-terminal $(His)_{10}$-tag was partially degraded after purification, whereas this was not observed with the C-terminal

Strep-tag. Interestingly, recombinant protein expression of *P. falciparum* Pfg27, a cytoplasmic protein crucial for gametocyte formation (Lobo et al., 1999), yielded a highly stable protein when a C-terminal extension was attached to the recombinant protein (Sati et al., 2002). Thus, it appears that the C-terminal Strep-tag may "protect" the recombinant *P. falciparum* proteins from degradation of bacterial proteases. However, the N-terminal $(His)_6$-tagged *E. coli* LplA recombinant protein, which was used as a positive control for LplA activity, was in contrast not degraded during expression. This could, however, simply be due to the fact that it is an *E. coli* protein, not alien to the bacteria expressing it, whereas it is known that *P. falciparum* displays a different codon usage in comparison to *E. coli*, which can be problematic for recombinant protein expression in the prokaryotic expression system (Sayers et al., 1995).

In addition to the LplAs, the lipoyl-domains of the *P. falciparum* KADHs and the H-protein of the *P. falciparum* GCV were recombinantly expressed and purified with N-terminal $(His)_{10}$-tags (see Figure 1.6 and Table 5.2). The four lipoyl-domains and the H-protein share between 25%-42% amino acid sequence similarity and all possess the highly conserved target lysine residue, which becomes post-translationally lipoylated, in the conserved DKA/V motif generally found in lipoyl-domains (Wallis and Perham, 1994, Reche and Perham, 1999). It was shown in previous studies that LplAs do not require the full length apo-enzyme complex, but that the lipoyl-domain itself is sufficient for lipoylation (Ali and Guest, 1990, Dardel et al., 1990, Quinn et al., 1993), although correct folding of these domains appears to be important (Reche and Perham, 1999). Therefore, the recombinantly expressed H-protein and lipoyl-domains were analysed by CD to investigate their secondary structures (Kelly et al., 2005), and the analysis revealed that only three of the five recombinant proteins are properly folded.

6.5.2. LplA enzyme assays

A variety of different enzyme assays can be employed to analyse LplA activity and to determine the kinetic parameters of these enzymes. All of these assays are based on the lipoylated protein substrate and thus determine LplA activity as a measure of lipoylation of the apo-protein substrate. The most frequently used assay is the "gel assay" which involves native PAGE (Ali and Guest, 1990, Fujiwara et al., 1992). In this assay, the lipoylated form of a protein can be distinguished from the non-lipoylated form by a shift of the protein band in the native gel. The attachment of lipoic acid to the ε-amino group of the target lysine residue neutralises a positive charge in the protein, and thus changes its

electrophoretic mobility in the native gel, causing it to run faster to the cathode (Fujiwara et al., 1992). This assay can be used with all possible protein substrates (the H-protein as well as the KADH-E2s) but its accuracy for determination of kinetic parameters is questionable. Other enzyme assays to determine LplA activity are specific for the protein substrate used and usually require other proteins which are part of the respective enzyme complex to be present. For example, the activity of apo-PDH-E2 or apo-KGDH-E2 can be determined after the lipoylation reaction as a measure of LplA activity, but require the respective E1 and E3 subunits to be present (Jordan and Cronan, 1997). Another possibility is to use the H-protein as protein substrate in the LplA reaction, and then use the lipoylated H-protein in the glycine-$^{14}CO_2$ exchange reaction by which [^{14}C]glycine is generated in the reverse reaction of the P- and H-protein (Walker and Oliver, 1986, Fujiwara et al., 1992). Finally, Gueguen et al. (1999) developed the dihydrolipoamide dehydrogenase / tris(2-carboxyethyl)phosphine (TCEP) assay to determine LplA activity. In this assay, TCEP reduces protein bound lipoic acid to dihydrolipoamide, which in turn is re-oxidised by LipDH with NAD^+ as the final electron acceptor. Thus, LplA activity can be determined spectrophotometrically by following the generation of NADH at 340 nm (Gueguen et al., 1999). A problem of these enzyme assays is that, as already mentioned above, other proteins, that are part of the respective enzyme complex, are required. Usually, these proteins are not commercially available and therefore need to be generated in addition to the ligase and apo-protein substrate. Thus, I aimed to establish a new spectrophotometric assay system, which, in contrast to the above described assays, is not based on the lipoylated substrate but on the PPi, which is produced during the lipoylation reaction. In this assay, the LplA reaction is coupled with an inorganic pyrophosphatase, converting the released PPi to Pi. Pi then reacts with acidified ammonium molybdate and forms a complex, which can be detected at 710 nm (Cariani et al., 2004). The colorimetric determination of Pi with ammonium molybdate was first described by Fiske and Subbarow (1925), and has been used since to determine activities of ATPases and phosphatases. It is a well established method, which is also very sensitive, detecting Pi in the low nmol range (Chifflet et al., 1988, Cariani et al., 2004). Using this assay to characterise *P. falciparum* LplAs has, in the long run, the advantage that the assay is suitable for high-throughput screening of potential inhibitors, as the assay volume can be scaled down to set it up in 96 well or even smaller plates. This is of particular interest as the knock-out studies of *lplA1* and *lplA2* revealed that both proteins fulfil crucial functions at different points in the parasites development. Inhibitors of LplA1 could potentially be used in chemotherapy as knock-out studies suggest that LplA1 is crucial for intraerythrocytic

development, whereas inhibitors against LplA2 may be used as transmission blockers as knock-out studies imply that LplA2 is essential for sexual development in the mosquito. However, a disadvantage of the spectrophotometric assay is that it is a coupled assay and LplA activity can only be measured via the inorganic pyrophosphatase. Therefore, substances that inhibit this assay either inhibit LplA activity or the activity of the inorganic pyrophosphatase.

The biochemical characteristics of recombinant *P. falciparum* LplA1 were investigated using a gel based assay and the new spectrophotometric assay. Recombinant *E. coli* LplA was used as a positive control. Unfortunately, activity of recombinantly expressed *P. falciparum* LplA2 was not tested due to the poor quality of the recombinant protein after purification. Initially, the "gel assay" was carried out as described above, using native PAGE. However, the protein shift caused by lipoylation was not very clear and also appeared not very reliable, so an antibody that specifically detects protein bound lipoic acid was used instead. Using the antibody also meant that normal SDS-PAGE could be performed, which is faster and easier to handle in comparison to native PAGE. Allary et al. (2007) also used this modified "gel assay" with the anti-lipoic acid antibody to show *in vitro* activity of *P. falciparum* LplA1 with *P. falciparum* H-protein as protein substrate. With this assay it was only possible to analyse the lipoylation reaction qualitatively, as the use of different antibody batches varied immensely in the signal they produced. Thus without standards, it is impossible to directly compare the assays or to quantify a reaction densitometrically. Currently, standards for this assay, consisting of different concentrations of fully lipoylated protein substrate, are being tested. This will allow the quantification of the results obtained with this assay in the future.
ATP is used by *E. coli* LplA for the activation of lipoic acid by which the reaction intermediate lipoyl-AMP is formed (Green et al., 1995, Fujiwara et al., 2005). The mammalian lipoic acid activating enzyme, however, appears to use GTP instead of ATP for the activation of lipoic acid, as the lipoyl-AMP reaction intermediate is not easily released from the enzyme in contrast to lipoyl-GMP (Fujiwara et al., 2001). Therefore, it was tested whether *E. coli* LplA specifically uses ATP or whether it could also use GTP instead. The "gel assay" showed that *E. coli* LplA is indeed able to use GTP for the activation and transfer reaction of lipoic acid, almost as efficiently as ATP. Thus, both nucleotide triphosphates may be used for the activation of lipoic acid *in vivo*, as ATP and GTP are both present in *E. coli* in the mM range with $\sim$3 mM and $\sim$1.5 mM, respectively (Buckstein et al., 2007). Whether *E. coli* LplA uses both ATP and GTP for lipoic acid activation, or whether one

nucleotide triphosphate is preferred is not known and requires additional investigations. Furthermore, the recombinantly expressed *P. falciparum* lipoyl-domains and H-protein were tested as substrates for *E. coli* LplA. H-protein was best accepted as low concentrations of *E. coli* LplA (0.06 μM) lipoylated *P. falciparum* H-protein. PDH-E2-LD2 and KGDH-E2-LD were also accepted as protein substrate whereas PDH-E2-LD1 and BCDH-E2-LD were hardly lipoylated by the enzyme. This supports the belief that a properly folded domain is required for adequate lipoylation (Reche and Perham, 1999), as the PDH-E2-LD1 and BCDH-E2-LD are the two domains suggested to be not properly folded by CD analyses. Interestingly, recombinant *P. falciparum* LplA1 also uses H-protein as a protein substrate, but lipoylation of the other domains is hardly observed, even at the highest LplA1 concentration used (1.8 μM). Generally, the activity of recombinant *P. falciparum* LplA1 appears to be lower in comparison to recombinant *E. coli* LplA, as much higher enzyme concentrations of the recombinant *Plasmodium* enzyme were required in the lipoylation assays. For instance, it seemed that 0.03 μM *E. coli* LplA lipoylated H-protein as efficient as 1.8 μM of the recombinant Strep-tagged LplA1. Thus, higher concentrations of the recombinant *Plasmodium* enzyme could be required for lipoylation of the other domains in the *in vitro* assay, since lipoylation of PDH-E2-LD2 and KGDH-E2-LD in the *E. coli* LplA assay were only observed at the highest *E. coli* LplA concentration (0.6 μM) used. However, this assay also potentially implies substrate specificity of LplA1. Distinct substrate specificity of *P. falciparum* LplA1 and LplA2 was previously suggested and shown to exist for LplA2, when expressed in lipoylation deficient *E. coli* (Allary et al., 2007). *P. falciparum* LplA1, however, was able to lipoylate bacterial PDH-E2 and KGDH-E2 when expressed in *E. coli* (Allary et al., 2007). Therefore, further analyses is required to elucidate which apo-enzyme complexes are lipoylated by *P. falciparum* LplA1 and LplA2 *in vivo*, keeping potential stage specificity and dual targeting to the apicoplast and mitochondrion in mind.

As already mentioned, the *Plasmodium* enzyme seemed less active in comparison to the *E. coli* protein. Moreover, the N-terminal $(His)_{10}$-tagged LplA1 showed even poorer activity and stability than the C-terminal Strep-tagged recombinant protein. It appears that the N-terminal $(His)_{10}$-tag does not only result in less stable recombinant protein, but it also seems to interfere with LplA activity. Lipoic acid binding and activation occurs in the N-terminal part of LplA proteins (Fujiwara et al., 2005, Kim et al., 2005, McManus et al., 2006), and it is therefore conceivable that the N-terminal $(His)_{10}$-tag interferes with these sites reducing LplA activity. However, surprisingly, the N-terminal $(His)_6$-tag of the recombinant *E. coli* protein does not seem to interfere with enzyme activity, suggesting

that maybe the ∼1 kDa difference between the $(His)_6$- and $(His)_{10}$-tag is responsible for this difference.
Another curious phenomenon observed in the gel assay for both, *P. falciparum* LplA1 and *E. coli* LplA, was that lipoic acid appeared to bind covalently to the enzyme. This was surprising as the linkage is believed to be non-covalent (Fujiwara et al., 2005, Kim et al., 2005, McManus et al., 2006). Recently, bovine lipoyltransferase was recombinantly expressed in the prokaryotic expression system for structural analyses, and purified enzyme had lipoyl-AMP tightly, but non-covalently, bound to it (Fujiwara et al., 2007). A loop in the lipoyltransferase structure was found to interact with lipoyl-AMP. This loop is also present in *E. coli* LplA, but it does not appear to interact with lipoyl-AMP (Fujiwara et al., 2007). However, other parts of the LplA protein may be involved in the strong interaction with the lipoyl-AMP reaction intermediate.

The new spectrophotometric assay was set up using *E. coli* LplA. Kinetic parameters of this protein were previously determined by two independent experiments using the "gel assay" involving native PAGE and the glycine-$^{14}CO_2$ exchange reaction (Green et al., 1995, Fujiwara et al., 2005). This allowed me to directly compare the apparent K_m's and V_{max}'s determined by the spectrophotometric assay with the published data. The apparent K_m's for ATP and lipoic acid are in accordance with the published data, however, the apparent V_{max}'s are not. But the V_{max} for ATP and lipoic acid vary not only between the published data and the spectrophotometric assay data, but also among the published data themselves. It is possible that the different assay systems used to determine the kinetic parameters of LplA affect the specific activity in the different reactions. Furthermore, different protein substrates were used in the different assays, which potentially affect the specific activity of *E. coli* LplA. Indeed, Green et al. (1995) mentioned that the specific activity of *E. coli* LplA for *E. coli* apo-PDH-lipoyl-domain is 11-fold higher compared to human mitochondrial PDH apo-domain. Thus, it appears that the different domains, although similarly folded, are differentially accepted by LplA, further supporting substrate specificity of these enzymes. Surprisingly, changing the concentration of *P. falciparum* H-protein in these assays did not influence the kinetic behaviour of *E. coli* LplA for ATP or lipoic acid, suggesting that the transfer reaction does not, or only marginally, influence the activation of lipoic acid. Trying to determine apparent K_m and V_{max} of *E. coli* LplA for *P. falciparum* H-protein was impossible because the reaction was still in the linear range at high H-protein concentrations (up to 40 μM), suggesting that the lipoylation reaction is limited by the protein substrate. This is in contrast to Fujiwara et al. (2005),

who determined the K_m of *E. coli* LplA for *E. coli* H-protein to be 1.2 μM. However, this determination was performed using the glycine-$^{14}CO_2$ exchange reaction, which is inhibited if more than 5 μM H-protein is used (Fujiwara et al., 2005), and thus the accuracy of their determined kinetic parameters for H-protein are questionable.
In an initial assay, it was also tested whether octanoic acid is used by *E. coli* LplA as a substrate. The apparent K_m and V_{max}, but especially the K_m, were much higher in comparison to lipoic acid, rendering it a "poor" substrate. In the physiological context, the preferred substrate is lipoic acid and its low K_m ensures that the low concentration of lipoic acid in the cell is utilised efficiently by LplA. Interestingly, Crawford et al. (2006) performed *in vivo* inhibition studies in *T. gondii* using octanoic acid. The parasites were grown in lipoic acid depleted medium and were incubated with octanoic acid. Only at 500 μM octanoic acid, a toxic effect on parasites was observed which was reversed in the presence of 1 μM lipoic acid, suggesting that indeed LplA has a very low affinity for octanoic acid and that the toxic effect is possibly due to post-translational modification of the enzyme complexes (Crawford et al., 2006). Additionally, in this study another lipoate analogue, 8-bromooctanoic acid, was used which affected *T. gondii* viability at much lower concentrations (10 μM). Again, the effect was reversed in the presence of 1 μM lipoic acid, suggesting a higher affinity of LplA for 8-bromooctanoic acid in comparison to octanoic acid, but a lower affinity in comparison to lipoic acid. However, further investigations using recombinant protein are required to clearly show that LplA and subsequently the lipoic acid dependent enzyme complexes are affected by these substances and are the cause for the results obtained by Crawford et al. (2006). Similar studies using 8-bromooctanoic acid were performed in *P. falciparum*, however, *P. falciparum* cannot be cultured in the absence of lipoic acid, since the parasites require serum/Albumax in the culture medium. Thus, in this study, high concentrations of 8-bromooctanoic acid were used and caused a growth defect at 400 μM and parasite death at 1 mM (Allary et al., 2007). However, how specific these effects can be ascribed to ligation of the substance to the enzyme complexes and thus their inhibition, requires further analyses. *In vitro* assays using recombinantly expressed enzyme should help to clarify these points.
Initial tests of *P. falciparum* LplA1, to determine the linearity of its reaction and its dependence on the protein substrate, were also performed using the spectrophotometric assay. Surprisingly, it appears that the *Plasmodium* enzyme behaves enzymatically different from the *E. coli* counterpart. In the same assay set up, *P. falciparum* LplA1 released more PPi during the reaction in comparison to *E. coli* LplA. If this is, however, due to a higher production of the reaction intermediate lipoyl-AMP with subsequent release of

PPi, or whether PPi formed is released more quickly from the *Plasmodium* enzyme in comparison to the *E. coli* protein is not known. Further analyses is required to identify the potential differences between the two proteins.

6.6. Conclusions and future directions

Lipoic acid is an essential cofactor of enzyme complexes that are integral to energy metabolism and amino acid degradation. In the malaria parasite *Plasmodium falciparum*, the cofactor is synthesised in the apicoplast, employing lipoic acid synthase (LipA) and octanoyl-ACP:protein N-octanoyl transferase (LipB), whereas the mitochondrion relies on salvage of lipoic acid using lipoic acid protein ligase 1 (LplA1). Previous studies have suggested that both pathways are strictly independent.

We showed that a recently identified second lipoic acid ligase (LplA2) compensates to some extent for the loss of LipB function, because the protein is dually targeted to both apicoplast and mitochondrion. This clearly suggests that salvage and biosynthesis are not entirely independent and that there exists some redundancy between the ligases present in both organelles. The situation could be even more flexible because scrutiny of the *lplA1* gene locus also suggests the possibility of dual targeting as outlined in the discussion of the thesis. However, the latter has to be verified experimentally and work towards this is currently underway.

Despite the finding of redundancy between the ligases, they also appear to have distinct functions during the parasites life cycle. Surprisingly, it was not possible to generate *lplA1* null mutants in *P. falciparum* and *P. berghei*, suggesting that LplA2 cannot replace the function of the mitochondrial ligase during erythrocytic development. Similarly, it was not possible for LplA1 to replace the functions of LplA2 during sexual development - the *lplA2* knock-out in *P. berghei* arrests parasite development before oocysts are generated. These results suggest that LplA1 and LplA2 firstly might have distinct substrate specificities, which is currently being analysed using recombinantly expressed proteins. In addition, these data support the hypothesis that the proteins might be differentially expressed during progression of the parasites through their developmental cycle. This suggestion is supported by data obtained from several transcriptome and proteome expression studies, and will be further analysed in the future.

Overall, my work suggests that LplA1 is essential for the survival of *Plasmodium* during

erythrocytic development whereas LplA2 is of crucial importance during sexual development in the insect host. The ligation of octanoyl-ACP in the apicoplast pathway appears to be of utmost importance since this reaction is at least carried out by LipB and LplA2, and potentially LplA1 to guarantee the functionality of the apicoplast-located pyruvate dehydrogenase complex. Figure 6.3 summarises these new findings and displays the resulting complexity of lipoic acid metabolism in *Plasmodium* spp.

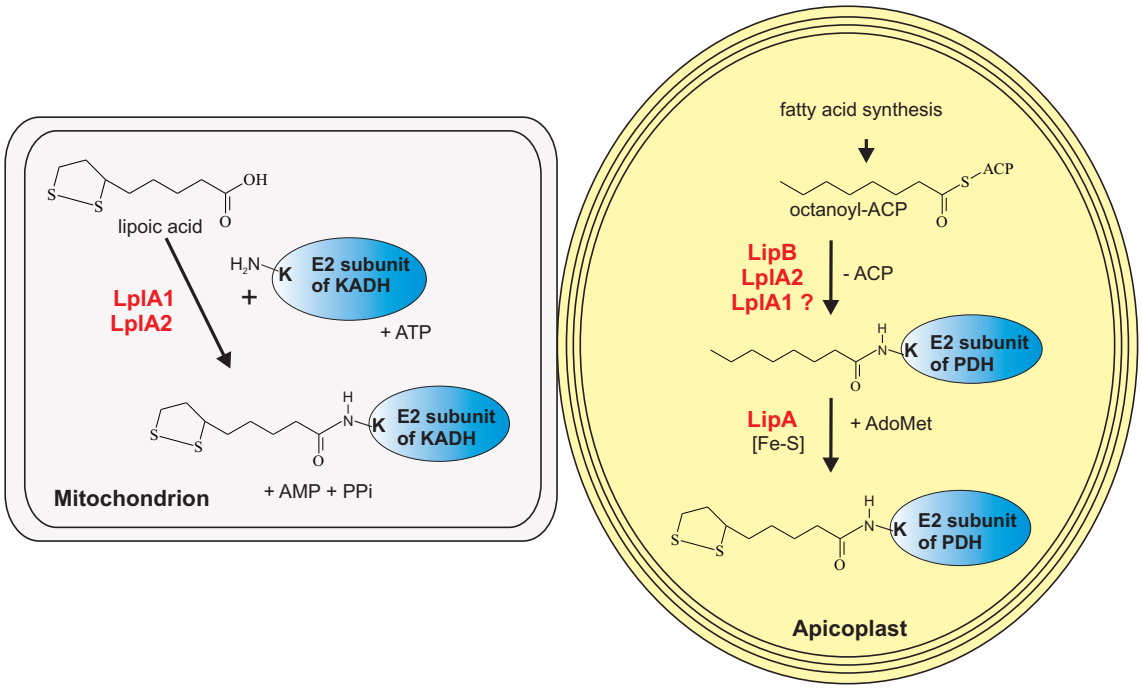

Figure 6.3.: Lipoic acid metabolism in *Plasmodium* spp. - revisited
Lipoic acid dependent enzyme complexes are found in the parasites mitochondrion and apicoplast and thus both organelles possess ways to post-translationally lipoylate these complexes. It appears that in the mitochondrion LplA1 as well was LplA2 are responsible for the attachment of scavenged lipoic acid to the enzyme complexes. LplA1 is present throughout the intraerythrocytic stages and it seems that LplA2 takes over in the sexual stages of the parasites life cycle. Lipoic acid biosynthesis occurs in the apicoplast by the action of LipB and LipA. However, it is believed that LipB function can be replaced by LplA2, which was shown to be dually targeted to mitochondrion and apicoplast. LplA1 might also be able to replace LipB function as it too is potentially dually targeted to the mitochondrion and apicoplast, but further analyses is required to support this hypothesis.

References

Adams, K. L. and Palmer, J. D. (2003). Evolution of mitochondrial gene content: gene loss and transfer to the nucleus. *Mol Phylogenet Evol* **29**, 380–395.

Aevarsson, A., Seger, K., Turley, S., Sokatch, J. R. and Hol, W. G. (1999). Crystal structure of 2-oxoisovalerate and dehydrogenase and the architecture of 2-oxo acid dehydrogenase multienzyme complexes. *Nat Struct Biol* **6**, 785–792.

Akerman, S. E. and Müller, S. (2003). 2-Cys peroxiredoxin PfTrx-Px1 is involved in the antioxidant defence of *Plasmodium falciparum*. *Mol Biochem Parasitol* **130**, 75–81.

Akerman, S. E. and Müller, S. (2005). Peroxiredoxin-linked detoxification of hydroperoxides in *Toxoplasma gondii*. *J Biol Chem* **280**, 564–570.

Alano, P. (2007). *Plasmodium falciparum* gametocytes: still many secrets of a hidden life. *Mol Microbiol* **66**, 291–302.

Ali, S. T. and Guest, J. R. (1990). Isolation and characterization of lipoylated and unlipoylated domains of the E2p subunit of the pyruvate dehydrogenase complex of *Escherichia coli*. *Biochem J* **271**, 139–145.

Allary, M., Lu, J. Z., Zhu, L. and Prigge, S. T. (2007). Scavenging of the cofactor lipoate is essential for the survival of the malaria parasite *Plasmodium falciparum*. *Mol Microbiol* **63**, 1331–1344.

Anderson, M. D., Che, P., Song, J., Nikolau, B. J. and Wurtele, E. S. (1998). 3-Methylcrotonyl-coenzyme A carboxylase is a component of the mitochondrial leucine catabolic pathway in plants. *Plant Physiol* **118**, 1127–1138.

Arnot, D. E. and Gull, K. (1998). The *Plasmodium* cell-cycle: facts and questions. *Ann Trop Med Parasitol* **92**, 361–365.

Bagautdinov, B., Kuroishi, C., Sugahara, M. and Kunishima, N. (2005). Crystal structures of biotin protein ligase from *Pyrococcus horikoshii* OT3 and its complexes: structural basis of biotin activation. *J Mol Biol* **353**, 322–333.

Bahl, A., Brunk, B., Crabtree, J., Fraunholz, M. J., Gajria, B., Grant, G. R., Ginsburg, H., Gupta, D., Kissinger, J. C., Labo, P., Li, L., Mailman, M. D., Milgram, A. J., Pearson, D. S., Roos, D. S., Schug, J., Stoeckert, C. J. and Whetzel, P. (2003). PlasmoDB: the *Plasmodium*

genome resource. A database integrating experimental and computational data. *Nucleic Acids Res* **31**, 212–215.

Baldi, D. L., Andrews, K. T., Waller, R. F., Roos, D. S., Howard, R. F., Crabb, B. S. and Cowman, A. F. (2000). RAP1 controls rhoptry targeting of RAP2 in the malaria parasite *Plasmodium falciparum*. *EMBO J* **19**, 2435–2443.

Baldwin, J., Michnoff, C. H., Malmquist, N. A., White, J., Roth, M. G., Rathod, P. K. and Phillips, M. A. (2005). High-throughput screening for potent and selective inhibitors of *Plasmodium falciparum* dihydroorotate dehydrogenase. *J Biol Chem* **280**, 21847–21853.

Banerjee, R., Liu, J., Beatty, W., Pelosof, L., Klemba, M. and Goldberg, D. E. (2002). Four plasmepsins are active in the *Plasmodium falciparum* food vacuole, including a protease with an active-site histidine. *Proc Natl Acad Sci U S A* **99**, 990–995.

Banker, G. A. and Cotman, C. W. (1972). Measurement of free electrophoretic mobility and retardation coefficient of protein-sodium dodecyl sulfate complexes by gel electrophoresis. A method to validate molecular weight estimates. *J Biol Chem* **247**, 5856–5861.

Bannister, L. H., Hopkins, J. M., Fowler, R. E., Krishna, S. and Mitchell, G. H. (2000). A brief illustrated guide to the ultrastructure of *Plasmodium falciparum* asexual blood stages. *Parasitol Today* **16**, 427–433.

Beitner, H. (2003). Randomized, placebo-controlled, double blind study on the clinical efficacy of a cream containing 5% alpha-lipoic acid related to photoageing of facial skin. *Br J Dermatol* **149**, 841–849.

Bender, A., van Dooren, G. G., Ralph, S. A., McFadden, G. I. and Schneider, G. (2003). Properties and prediction of mitochondrial transit peptides from *Plasmodium falciparum*. *Mol Biochem Parasitol* **132**, 59–66.

Biewenga, G. P., Haenen, G. R. and Bast, A. (1997). The pharmacology of the antioxidant lipoic acid. *Gen Pharmacol* **29**, 315–331.

Bilska, A. and Wlodek, L. (2005). Lipoic acid - the drug of the future? *Pharmacol Rep* **57**, 570–577.

Blisnick, T., Betoulle, M. E. M., Barale, J. C., Uzureau, P., Berry, L., Desroses, S., Fujioka, H., Mattei, D. and Breton, C. B. (2000). Pfsbp1, a Maurer's cleft *Plasmodium falciparum* protein, is associated with the erythrocyte skeleton. *Mol Biochem Parasitol* **111**, 107–121.

Booker, S. J., Cicchillo, R. M. and Grove, T. L. (2007). Self-sacrifice in radical S-adenosylmethionine proteins. *Curr Opin Chem Biol* **11**, 543–552.

Bourguignon, J., Merand, V., Rawsthorne, S., Forest, E. and Douce, R. (1996). Glycine decarboxylase and pyruvate dehydrogenase complexes share the same dihydrolipoamide dehydrogenase in pea leaf mitochondria: evidence from mass spectrometry and primary-structure analysis. *Biochem J* **313 (Pt 1)**, 229–234.

Bradford, M. M. (1976). A rapid and sensitive method for the quantitation of microgram quantities of protein utilizing the principle of protein-dye binding. *Anal Biochem* **72**, 248–254.

Bray, P. G., Ward, S. A. and O'Neill, P. M. (2005). Quinolines and artemisinin: chemistry, biology and history. *Curr Top Microbiol Immunol* **295**, 3–38.

Brocklehurst, S. M. and Perham, R. N. (1993). Prediction of the three-dimensional structures of the biotinylated domain from yeast pyruvate carboxylase and of the lipoylated H-protein from the pea leaf glycine cleavage system: a new automated method for the prediction of protein tertiary structure. *Protein Sci* **2**, 626–639.

Bryant, C., Voller, A. and Smith, M. J. (1964). The incorporation of radioactivity from ^{14}C-glucose into the soluble metabolic intermediates of malaria parasites. *Am J Trop Med Hyg* **13**, 515–519.

Bryk, R., Lima, C. D., Erdjument-Bromage, H., Tempst, P. and Nathan, C. (2002). Metabolic enzymes of mycobacteria linked to antioxidant defense by a thioredoxin-like protein. *Science* **295**, 1073–1077.

Buckstein, M. H., He, J. and Rubin, H. (2007). Characterization of nucleotide pools as a function of physiological state in *Escherichia coli*. *J Bacteriol* **[Epub ahead of print]**.

Bui, B. T. S., Mattioli, T. A., Florentin, D., Bolbach, G. and Marquet, A. (2006). *Escherichia coli* biotin synthase produces selenobiotin. Further evidence of the involvement of the [2Fe-2S]$^{2+}$ cluster in the sulfur insertion step. *Biochemistry* **45**, 3824–3834.

Camps, M., Arrizabalaga, G. and Boothroyd, J. (2002). An rRNA mutation identifies the apicoplast as the target for clindamycin in *Toxoplasma gondii*. *Mol Microbiol* **43**, 1309–1318.

Cariani, L., Thomas, L., Brito, J. and del Castillo, J. R. (2004). Bismuth citrate in the quantification of inorganic phosphate and its utility in the determination of membrane-bound phosphatases. *Anal Biochem* **324**, 79–83.

CDC (2007). Malaria - Treatment guidlines. www.cdc.gov/malaria/.

Chapman-Smith, A., Mulhern, T. D., Whelan, F., Cronan, J. E. and Wallace, J. C. (2001). The C-terminal domain of biotin protein ligase from *E. coli* is required for catalytic activity. *Protein Sci* **10**, 2608–2617.

Chen, F., Mackey, A. J., Stoeckert, C. J. and Roos, D. S. (2006). OrthoMCL-DB: querying a comprehensive multi-species collection of ortholog groups. *Nucleic Acids Res* **34**, D363–D368.

Chifflet, S., Torriglia, A., Chiesa, R. and Tolosa, S. (1988). A method for the determination of inorganic phosphate in the presence of labile organic phosphate and high concentrations of protein: application to lens ATPases. *Anal Biochem* **168**, 1–4.

Cicchillo, R. M. and Booker, S. J. (2005). Mechanistic investigations of lipoic acid biosynthesis in *Escherichia coli*: both sulfur atoms in lipoic acid are contributed by the same lipoyl synthase polypeptide. *J Am Chem Soc* **127**, 2860–2861.

Cicchillo, R. M., Iwig, D. F., Jones, A. D., Nesbitt, N. M., Baleanu-Gogonea, C., Souder, M. G., Tu, L. and Booker, S. J. (2004a). Lipoyl synthase requires two equivalents of S-adenosyl-L-methionine to synthesize one equivalent of lipoic acid. *Biochemistry* **43**, 6378–6386.

Cicchillo, R. M., Lee, K.-H., Baleanu-Gogonea, C., Nesbitt, N. M., Krebs, C. and Booker, S. J. (2004b). *Escherichia coli* lipoyl synthase binds two distinct [4Fe-4S] clusters per polypeptide. *Biochemistry* **43**, 11770–11781.

Claros, M. G. and Vincens, P. (1996). Computational method to predict mitochondrially imported proteins and their targeting sequences. *Eur J Biochem* **241**, 779–786.

Clos, J. and Brandau, S. (1994). pJC20 and pJC40–two high-copy-number vectors for T7 RNA polymerase-dependent expression of recombinant genes in *Escherichia coli*. *Protein Expr Purif* **5**, 133–137.

Cogswell, F. B. (1992). The hypnozoite and relapse in primate malaria. *Clin Microbiol Rev* **5**, 26–35.

Cook, G. C., ed. (1996). *Mansons Tropical Diseases*. Saunders.

Cowman, A. F. and Crabb, B. S. (2006). Invasion of red blood cells by malaria parasites. *Cell* **124**, 755–766.

Crabb, B. S., Cooke, B. M., Reeder, J. C., Waller, R. F., Caruana, S. R., Davern, K. M., Wickham, M. E., Brown, G. V., Coppel, R. L. and Cowman, A. F. (1997). Targeted gene disruption shows that knobs enable malaria-infected red cells to cytoadhere under physiological shear stress. *Cell* **89**, 287–296.

Crabb, B. S. and Cowman, A. F. (1996). Characterization of promoters and stable transfection by homologous and nonhomologous recombination in *Plasmodium falciparum*. *Proc Natl Acad Sci U S A* **93**, 7289–7294.

Crawford, M. J., Thomsen-Zieger, N., Ray, M., Schachtner, J., Roos, D. S. and Seeber, F. (2006). *Toxoplasma gondii* scavenges host-derived lipoic acid despite its *de novo* synthesis in the apicoplast. *EMBO J* **25**, 3214–3222.

Cristina, M. D., Spaccapelo, R., Soldati, D., Bistoni, F. and Crisanti, A. (2000). Two conserved amino acid motifs mediate protein targeting to the micronemes of the apicomplexan parasite *Toxoplasma gondii*. *Mol Cell Biol* **20**, 7332–7341.

Cronan, J. E., Zhao, X. and Jiang, Y. (2005). Function, attachment and synthesis of lipoic acid in *Escherichia coli*. *Adv Microb Physiol* **50**, 103–146.

Dahl, E. L., Shock, J. L., Shenai, B. R., Gut, J., DeRisi, J. L. and Rosenthal, P. J. (2006). Tetracyclines specifically target the apicoplast of the malaria parasite *Plasmodium falciparum*. *Antimicrob Agents Chemother* **50**, 3124–3131.

Dailey, T. A., Woodruff, J. H. and Dailey, H. A. (2005). Examination of mitochondrial protein targeting of haem synthetic enzymes: *in vivo* identification of three functional haem-responsive motifs in 5-aminolaevulinate synthase. *Biochem J* **386**, 381–386.

Dardel, F., Packman, L. C. and Perham, R. N. (1990). Expression in *Escherichia coli* of a subgene encoding the lipoyl domain of the pyruvate dehydrogenase complex of *Bacillus stearothermophilus*. *FEBS Lett* **264**, 206–210.

Dasaradhi, P. V. N., Korde, R., Thompson, J. K., Tanwar, C., Nag, T. C., Chauhan, V. S., Cowman, A. F., Mohmmed, A. and Malhotra, P. (2007). Food vacuole targeting and trafficking of falcipain-2, an important cysteine protease of human malaria parasite *Plasmodium falciparum*. *Mol Biochem Parasitol* **156**, 12–23.

Deitsch, K., Driskill, C. and Wellems, T. (2001). Transformation of malaria parasites by the spontaneous uptake and expression of DNA from human erythrocytes. *Nucleic Acids Res* **29**, 850–853.

DeRocher, A., Gilbert, B., Feagin, J. E. and Parsons, M. (2005). Dissection of brefeldin A-sensitive and -insensitive steps in apicoplast protein targeting. *J Cell Sci* **118**, 565–574.

Doerig, C., Chakrabarti, D., Kappes, B. and Matthews, K. (2000). The cell cycle in protozoan parasites. *Prog Cell Cycle Res* **4**, 163–183.

Dong, Y. and Vennerstrom, J. L. (2003). Mechanisms of *in situ* activation for peroxidic antimalarials. *Redox Rep* **8**, 284–288.

Dorin-Semblat, D., Quashie, N., Halbert, J., Sicard, A., Doerig, C., Peat, E., Ranford-Cartwright, L. and Doerig, C. (2007). Functional characterization of both MAP kinases of the human malaria parasite *Plasmodium falciparum* by reverse genetics. *Mol Microbiol* **65**, 1170–1180.

Douce, R., Bourguignon, J., Neuburger, M. and Rébeillé, F. (2001). The glycine decarboxylase system: a fascinating complex. *Trends Plant Sci* **6**, 167–176.

Duraisingh, M. T., Triglia, T. and Cowman, A. F. (2002). Negative selection of *Plasmodium falciparum* reveals targeted gene deletion by double crossover recombination. *Int J Parasitol* **32**, 81–89.

Eckstein-Ludwig, U., Webb, R. J., Goethem, I. D. A. V., East, J. M., Lee, A. G., Kimura, M., O'Neill, P. M., Bray, P. G., Ward, S. A. and Krishna, S. (2003). Artemisinins target the SERCA of *Plasmodium falciparum*. *Nature* **424**, 957–961.

Egan, T. J., Combrinck, J. M., Egan, J., Hearne, G. R., Marques, H. M., Ntenteni, S., Sewell, B. T., Smith, P. J., Taylor, D., van Schalkwyk, D. A. and Walden, J. C. (2002). Fate of haem iron in the malaria parasite *Plasmodium falciparum*. *Biochem J* **365**, 343–347.

Egan, T. J., Mavuso, W. W., Ross, D. C. and Marques, H. M. (1997). Thermodynamic factors controlling the interaction of quinoline antimalarial drugs with ferriprotoporphyrin IX. *J Inorg Biochem* **68**, 137–145.

Fichera, M. E., Bhopale, M. K. and Roos, D. S. (1995). *In vitro* assays elucidate peculiar kinetics of clindamycin action against *Toxoplasma gondii*. *Antimicrob Agents Chemother* **39**, 1530–1537.

Fiske, C. H. and Subbarow, Y. (1925). The colorimetric determination of phosphorus. *J Biol Chem* **66**, 375–400.

Flint, D. H., Emptage, M. H. and Guest, J. R. (1992). Fumarase A from *Escherichia coli*: Purification and characterization as an iron-sulfur cluster containing enzyme. *Biochemistry* **31**, 10331–10337.

Foley, M. and Tilley, L. (1998). Quinoline antimalarials: mechanisms of action and resistance and prospects for new agents. *Pharmacol Ther* **79**, 55–87.

Foth, B. J., Ralph, S. A., Tonkin, C. J., Struck, N. S., Fraunholz, M., Roos, D. S., Cowman, A. F. and McFadden, G. I. (2003). Dissecting apicoplast targeting in the malaria parasite *Plasmodium falciparum*. *Science* **299**, 705–708.

Foth, B. J., Stimmler, L. M., Handman, E., Crabb, B. S., Hodder, A. N. and McFadden, G. I. (2005). The malaria parasite *Plasmodium falciparum* has only one pyruvate dehydrogenase complex, which is located in the apicoplast. *Mol Microbiol* **55**, 39–53.

Fried, M. and Duffy, P. E. (1996). Adherence of *Plasmodium falciparum* to chondroitin sulfate A in the human placenta. *Science* **272**, 1502–1504.

Fujiwara, K., Hosaka, H., Matsuda, M., Okamura-Ikeda, K., Motokawa, Y., Suzuki, M., Nakagawa, A. and Taniguchi, H. (2007). Crystal structure of bovine lipoyltransferase in complex with lipoyl-AMP. *J Mol Biol* **371**, 222–234.

Fujiwara, K., Okamura-Ikeda, K. and Motokawa, Y. (1992). Expression of mature bovine H-protein of the glycine cleavage system in *Escherichia coli* and *in vitro* lipoylation of the apoform. *J Biol Chem* **267**, 20011–20016.

Fujiwara, K., Okamura-Ikeda, K. and Motokawa, Y. (1997). Cloning and expression of a cDNA encoding bovine lipoyltransferase. *J Biol Chem* **272**, 31974–31978.

Fujiwara, K., Suzuki, M., Okumachi, Y., Okamura-Ikeda, K., Fujiwara, T., Takahashi, E. and Motokawa, Y. (1999). Molecular cloning, structural characterization and chromosomal localization of human lipoyltransferase gene. *Eur J Biochem* **260**, 761–767.

Fujiwara, K., Takeuchi, S., Okamura-Ikeda, K. and Motokawa, Y. (2001). Purification, characterization, and cDNA cloning of lipoate-activating enzyme from bovine liver. *J Biol Chem* **276**, 28819–28823.

Fujiwara, K., Toma, S., Okamura-Ikeda, K., Motokawa, Y., Nakagawa, A. and Taniguchi, H. (2005). Crystal structure of lipoate-protein ligase A from *Escherichia coli*. Determination of the lipoic acid-binding site. *J Biol Chem* **280**, 33645–33651.

Galappaththy, G. N. L., Omari, A. A. A. and Tharyan, P. (2007). Primaquine for preventing relapses in people with *Plasmodium vivax* malaria. *Cochrane Database Syst Rev* , CD004389.

Gardner, M. J., Hall, N., Fung, E., White, O., Berriman, M., Hyman, R. W., Carlton, J. M., Pain, A., Nelson, K. E., Bowman, S., Paulsen, I. T., James, K., Eisen, J. A., Rutherford, K., Salzberg, S. L., Craig, A., Kyes, S., Chan, M.-S., Nene, V., Shallom, S. J., Suh, B., Peterson, J., Angiuoli, S., Pertea, M., Allen, J., Selengut, J., Haft, D., Mather, M. W., Vaidya, A. B., Martin, D. M. A., Fairlamb, A. H., Fraunholz, M. J., Roos, D. S., Ralph, S. A., McFadden, G. I., Cummings, L. M., Subramanian, G. M., Mungall, C., Venter, J. C., Carucci, D. J., Hoffman, S. L., Newbold, C., Davis, R. W., Fraser, C. M. and Barrell, B. (2002). Genome sequence of the human malaria parasite *Plasmodium falciparum*. *Nature* **419**, 498–511.

Gaur, D., Mayer, D. C. G. and Miller, L. H. (2004). Parasite ligand-host receptor interactions during invasion of erythrocytes by *Plasmodium* merozoites. *Int J Parasitol* **34**, 1413–1429.

Georgiou, G. and Valax, P. (1996). Expression of correctly folded proteins in *Escherichia coli*. *Curr Opin Biotechnol* **7**, 190–197.

Gilberger, T.-W., Thompson, J. K., Reed, M. B., Good, R. T. and Cowman, A. F. (2003). The cytoplasmic domain of the *Plasmodium falciparum* ligand EBA-175 is essential for invasion but not protein trafficking. *J Cell Biol* **162**, 317–327.

Ginsburg, H. and Golenser, J. (2003). Glutathione is involved in the antimalarial action of chloroquine and its modulation affects drug sensitivity of human and murine species of *Plasmodium*. *Redox Rep* **8**, 276–279.

Glaser, P., Frangeul, L., Buchrieser, C., Rusniok, C., Amend, A., Baquero, F., Berche, P., Bloecker, H., Brandt, P., Chakraborty, T., Charbit, A., Chetouani, F., Couvé, E., de Daruvar, A., Dehoux, P., Domann, E., Domínguez-Bernal, G., Duchaud, E., Durant, L., Dussurget, O., Entian, K. D., Fsihi, H., del Portillo, F. G., Garrido, P., Gautier, L., Goebel, W., Gómez-López, N., Hain, T., Hauf, J., Jackson, D., Jones, L. M., Kaerst, U., Kreft, J., Kuhn, M., Kunst, F., Kurapkat, G., Madueno, E., Maitournam, A., Vicente, J. M., Ng, E., Nedjari, H., Nordsiek, G., Novella, S., de Pablos, B., Pérez-Diaz, J. C., Purcell, R., Remmel, B., Rose, M., Schlueter, T., Simoes, N., Tierrez, A., Vázquez-Boland, J. A., Voss, H., Wehland, J. and Cossart, P. (2001). Comparative genomics of *Listeria* species. *Science* **294**, 849–852.

Günther, S., McMillan, P. J., Wallace, L. J. M. and Müller, S. (2005). *Plasmodium falciparum* possesses organelle-specific alpha-keto acid dehydrogenase complexes and lipoylation pathways. *Biochem Soc Trans* **33**, 977–980.

Günther, S., Wallace, L., Patzewitz, E.-M., McMillan, P. J., Storm, J., Wrenger, C., Bissett, R., Smith, T. K. and Müller, S. (2007). Apicoplast lipoic acid protein ligase B is not essential for *Plasmodium falciparum*. *PLoS Pathog* **3**, e189.

Goloubinoff, P., Gatenby, A. A. and Lorimer, G. H. (1989). GroE heat-shock proteins promote assembly of foreign prokaryotic ribulose bisphosphate carboxylase oligomers in *Escherichia coli*. *Nature* **337**, 44–47.

Goodman, C. D., Su, V. and McFadden, G. I. (2007). The effects of anti-bacterials on the malaria parasite *Plasmodium falciparum*. *Mol Biochem Parasitol* **152**, 181–191.

Green, D. E., Morris, T. W., Green, J., Cronan, J. E. and Guest, J. R. (1995). Purification and properties of the lipoate protein ligase of *Escherichia coli*. *Biochem J* **309 (Pt 3)**, 853–862.

Greenwood, B. and Mutabingwa, T. (2002). Malaria in 2002. *Nature* **415**, 670–672.

Greenwood, B. M., Bojang, K., Whitty, C. J. M. and Targett, G. A. T. (2005). Malaria. *Lancet* **365**, 1487–1498.

Gregson, A. and Plowe, C. V. (2005). Mechanisms of resistance of malaria parasites to antifolates. *Pharmacol Rev* **57**, 117–145.

Gueguen, V., Macherel, D., Jaquinod, M., Douce, R. and Bourguignon, J. (2000). Fatty acid and lipoic acid biosynthesis in higher plant mitochondria. *J Biol Chem* **275**, 5016–5025.

Gueguen, V., Macherel, D., Neuburger, M., Pierre, C. S., Jaquinod, M., Gans, P., Douce, R. and Bourguignon, J. (1999). Structural and functional characterization of H protein mutants of the glycine decarboxylase complex. *J Biol Chem* **274**, 26344–26352.

Hall, N., Karras, M., Raine, J. D., Carlton, J. M., Kooij, T. W. A., Berriman, M., Florens, L., Janssen, C. S., Pain, A., Christophides, G. K., James, K., Rutherford, K., Harris, B., Harris, D., Churcher, C., Quail, M. A., Ormond, D., Doggett, J., Trueman, H. E., Mendoza, J., Bidwell, S. L., Rajandream, M.-A., Carucci, D. J., Yates, J. R., Kafatos, F. C., Janse, C. J., Barrell, B., Turner, C. M. R., Waters, A. P. and Sinden, R. E. (2005). A comprehensive survey of the *Plasmodium* life cycle by genomic, transcriptomic, and proteomic analyses. *Science* **307**, 82–86.

Hasse, D., Mikkat, S., Thrun, H.-A., Hagemann, M. and Bauwe, H. (2007). Properties of recombinant glycine decarboxylase P- and H-protein subunits from the cyanobacterium *Synechocystis* sp. strain PCC 6803. *FEBS Lett* **581**, 1297–1301.

He, C. Y., Shaw, M. K., Pletcher, C. H., Striepen, B., Tilney, L. G. and Roos, D. S. (2001). A plastid segregation defect in the protozoan parasite *Toxoplasma gondii*. *EMBO J* **20**, 330–339.

Hill, J., Lines, J. and Rowland, M. (2006). Insecticide-treated nets. *Adv Parasitol* **61**, 77–128.

Hiller, N. L., Bhattacharjee, S., van Ooij, C., Liolios, K., Harrison, T., Lopez-Estraño, C. and Haldar, K. (2004). A host-targeting signal in virulence proteins reveals a secretome in malarial infection. *Science* **306**, 1934–1937.

Hodges, M., Yikilmaz, E., Patterson, G., Kasvosve, I., Rouault, T. A., Gordeuk, V. R. and Loyevsky, M. (2005). An iron regulatory-like protein expressed in *Plasmodium falciparum* displays aconitase activity. *Mol Biochem Parasitol* **143**, 29–38.

Holmquist, L., Stuchbury, G., Berbaum, K., Muscat, S., Young, S., Hager, K., Engel, J. and Münch, G. (2007). Lipoic acid as a novel treatment for Alzheimer's disease and related dementias. *Pharmacol Ther* **113**, 154–164.

Hoppe, H. C., Ngô, H. M., Yang, M. and Joiner, K. A. (2000). Targeting to rhoptry organelles of *Toxoplasma gondii* involves evolutionarily conserved mechanisms. *Nat Cell Biol* **2**, 449–456.

Howard, R. F. and Schmidt, C. M. (1995). The secretary pathway of *Plasmodium falciparum* regulates transport of p82/RAP1 to the rhoptries. *Mol Biochem Parasitol* **74**, 43–54.

Huang, J., Mullapudi, N., Lancto, C. A., Scott, M., Abrahamsen, M. S. and Kissinger, J. C. (2004). Phylogenomic evidence supports past endosymbiosis, intracellular and horizontal gene transfer in *Cryptosporidium parvum*. *Genome Biol* **5**, R88.

Hyde, J. E. (2005). Exploring the folate pathway in *Plasmodium falciparum*. *Acta Trop* **94**, 191–206.

Hyde, J. E. (2007). Drug-resistant malaria - an insight. *FEBS J* **274**, 4688–4698.

Jackson-Constan, D. and Keegstra, K. (2001). *Arabidopsis* genes encoding components of the chloroplastic protein import apparatus. *Plant Physiol* **125**, 1567–1576.

Janse, C. J., Franke-Fayard, B., Mair, G. R., Ramesar, J., Thiel, C., Engelmann, S., Matuschewski, K., van Gemert, G. J., Sauerwein, R. W. and Waters, A. P. (2006). High efficiency transfection of *Plasmodium berghei* facilitates novel selection procedures. *Mol Biochem Parasitol* **145**, 60–70.

Jocelyn, P. C. (1967). The standard redox potential of cysteine-cystine from the thiol-disulphide exchange reaction with glutathione and lipoic acid. *Eur J Biochem* **2**, 327–331.

Jomaa, H., Wiesner, J., Sanderbrand, S., Altincicek, B., Weidemeyer, C., Hintz, M., Türbachova, I., Eberl, M., Zeidler, J., Lichtenthaler, H. K., Soldati, D. and Beck, E. (1999). Inhibitors of the nonmevalonate pathway of isoprenoid biosynthesis as antimalarial drugs. *Science* **285**, 1573–1576.

Jones, D. and Perham, R. (2007). The role of loop and beta-turn residues as structural and functional determinants for the lipoyl domain from the *Escherichia coli* 2-oxoglutarate dehydrogenase complex. *Biochem J* **[Epub ahead of print]**.

Jones, W., Li, X., chao Qu, Z., Perriott, L., Whitesell, R. R. and May, J. M. (2002). Uptake, recycling, and antioxidant actions of alpha-lipoic acid in endothelial cells. *Free Radic Biol Med* **33**, 83–93.

Jordan, S. W. and Cronan, J. E. (1997). A new metabolic link. The acyl carrier protein of lipid synthesis donates lipoic acid to the pyruvate dehydrogenase complex in *Escherichia coli* and mitochondria. *J Biol Chem* **272**, 17903–17906.

Jordan, S. W. and Cronan, J. E. (2002). Chromosomal amplification of the *Escherichia coli lipB* region confers high-level resistance to selenolipoic acid. *J Bacteriol* **184**, 5495–5501.

Kang, S. G., Jeong, H. K., Lee, E. and Natarajan, S. (2007). Characterization of a lipoate-protein ligase A gene of rice (*Oryza sativa* L.). *Gene* **393**, 53–61.

Kather, B., Stingl, K., van der Rest, M. E., Altendorf, K. and Molenaar, D. (2000). Another unusual type of citric acid cycle enzyme in *Helicobacter pylori*: the malate:quinone oxidoreductase. *J Bacteriol* **182**, 3204–3209.

Keeney, K. M., Stuckey, J. A. and O'Riordan, M. X. D. (2007). LplA1-dependent utilization of host lipoyl peptides enables *Listeria* cytosolic growth and virulence. *Mol Microbiol* **66**, 758–770.

Kelly, S. M., Jess, T. J. and Price, N. C. (2005). How to study proteins by circular dichroism. *Biochim Biophys Acta* **1751**, 119–139.

Keresztessy, Z., Hughes, J., Kiss, L. and Hughes, M. A. (1996). Co-purification from *Escherichia coli* of a plant beta-glucosidase-glutathione S-transferase fusion protein and the bacterial chaperonin GroEL. *Biochem J* **314 (Pt 1)**, 41–47.

Kessl, J. J., Ha, K. H., Merritt, A. K., Lange, B. B., Hill, P., Meunier, B., Meshnick, S. R. and Trumpower, B. L. (2005). Cytochrome b mutations that modify the ubiquinol-binding pocket of the cytochrome bc1 complex and confer anti-malarial drug resistance in *Saccharomyces cerevisiae*. *J Biol Chem* **280**, 17142–17148.

Khan, S. M., Franke-Fayard, B., Mair, G. R., Lasonder, E., Janse, C. J., Mann, M. and Waters, A. P. (2005). Proteome analysis of separated male and female gametocytes reveals novel sex-specific *Plasmodium* biology. *Cell* **121**, 675–687.

Kilejian, A. (1979). Characterization of a protein correlated with the production of knob-like protrusions on membranes of erythrocytes infected with *Plasmodium falciparum*. *Proc Natl Acad Sci U S A* **76**, 4650–4653.

Kim, D. J., Kim, K. H., Lee, H. H., Lee, S. J., Ha, J. Y., Yoon, H. J. and Suh, S. W. (2005). Crystal structure of lipoate-protein ligase A bound with the activated intermediate: insights into interaction with lipoyl domains. *J Biol Chem* **280**, 38081–38089.

Kirkman, L. A., Su, X. Z. and Wellems, T. E. (1996). *Plasmodium falciparum*: isolation of large numbers of parasite clones from infected blood samples. *Exp Parasitol* **83**, 147–149.

Klemba, M., Beatty, W., Gluzman, I. and Goldberg, D. E. (2004a). Trafficking of plasmepsin II to the food vacuole of the malaria parasite *Plasmodium falciparum*. *J Cell Biol* **164**, 47–56.

Klemba, M., Gluzman, I. and Goldberg, D. E. (2004b). A *Plasmodium falciparum* dipeptidyl aminopeptidase I participates in vacuolar hemoglobin degradation. *J Biol Chem* **279**, 43000–43007.

Knuepfer, E., Rug, M., Klonis, N., Tilley, L. and Cowman, A. F. (2005). Trafficking of the major virulence factor to the surface of transfected *P. falciparum*-infected erythrocytes. *Blood* **105**, 4078–4087.

Konrad, D. (2005). Utilization of the insulin-signaling network in the metabolic actions of alpha-lipoic acid-reduction or oxidation? *Antioxid Redox Signal* **7**, 1032–1039.

Krnajski, Z., Gilberger, T.-W., Walter, R. D., Cowman, A. F. and Müller, S. (2002). Thioredoxin reductase is essential for the survival of *Plasmodium falciparum* erythrocytic stages. *J Biol Chem* **277**, 25970–25975.

Kyes, S., Horrocks, P. and Newbold, C. (2001). Antigenic variation at the infected red cell surface in malaria. *Annu Rev Microbiol* **55**, 673–707.

Laemmli, U. K. (1970). Cleavage of structural proteins during the assembly of the head of bacteriophage T4. *Nature* **227**, 680–685.

Lambros, C. and Vanderberg, J. P. (1979). Synchronization of *Plasmodium falciparum* erythrocytic stages in culture. *J Parasitol* **65**, 418–420.

Lang-Unnasch, N. (1995). *Plasmodium falciparum*: antiserum to malate dehydrogenase. *Exp Parasitol* **80**, 357–359.

Learngaramkul, P., Petmitr, S., Krungkrai, S. R., Prapunwattana, P. and Krungkrai, J. (1999). Molecular characterization of mitochondria in asexual and sexual blood stages of *Plasmodium falciparum*. *Mol Cell Biol Res Commun* **2**, 15–20.

Leed, A., DuBay, K., Ursos, L. M. B., Sears, D., Dios, A. C. D. and Roepe, P. D. (2002). Solution structures of antimalarial drug-heme complexes. *Biochemistry* **41**, 10245–10255.

Lobley, A., Whitmore, L. and Wallace, B. A. (2002). DICHROWEB: an interactive website for the analysis of protein secondary structure from circular dichroism spectra. *Bioinformatics* **18**, 211–212.

Lobo, C. A., Fujioka, H., Aikawa, M. and Kumar, N. (1999). Disruption of the *Pfg27* locus by homologous recombination leads to loss of the sexual phenotype in *P. falciparum*. *Mol Cell* **3**, 793–798.

Lopez-Estraño, C., Bhattacharjee, S., Harrison, T. and Haldar, K. (2003). Cooperative domains define a unique host cell-targeting signal in *Plasmodium falciparum*-infected erythrocytes. *Proc Natl Acad Sci U S A* **100**, 12402–12407.

Loria, P., Miller, S., Foley, M. and Tilley, L. (1999). Inhibition of the peroxidative degradation of haem as the basis of action of chloroquine and other quinoline antimalarials. *Biochem J* **339 (Pt 2)**, 363–370.

Lotierzo, M., Bui, B. T. S., Florentin, D., Escalettes, F. and Marquet, A. (2005). Biotin synthase mechanism: an overview. *Biochem Soc Trans* **33**, 820–823.

Lutziger, I. and Oliver, D. J. (2000). Molecular evidence of a unique lipoamide dehydrogenase in plastids: analysis of plastidic lipoamide dehydrogenase from *Arabidopsis thaliana*. *FEBS Lett* **484**, 12–16.

Ma, Q., Zhao, X., Eddine, A. N., Geerlof, A., Li, X., Cronan, J. E., Kaufmann, S. H. E. and Wilmanns, M. (2006). The *Mycobacterium tuberculosis* LipB enzyme functions as a cysteine/lysine dyad acyltransferase. *Proc Natl Acad Sci U S A* **103**, 8662–8667.

Mackenzie, S. A. (2005). Plant organellar protein targeting: a traffic plan still under construction. *Trends Cell Biol* **15**, 548–554.

Maier, A. G., Braks, J. A. M., Waters, A. P. and Cowman, A. F. (2006). Negative selection using yeast cytosine deaminase/uracil phosphoribosyl transferase in *Plasmodium falciparum* for targeted gene deletion by double crossover recombination. *Mol Biochem Parasitol* **150**, 118–121.

Maier, A. G., Rug, M., O'Neill, M. T., Beeson, J. G., Marti, M., Reeder, J. and Cowman, A. F. (2007). Skeleton-binding protein 1 functions at the parasitophorous vacuole membrane to traffic PfEMP1 to the *Plasmodium falciparum*-infected erythrocyte surface. *Blood* **109**, 1289–1297.

Marti, M., Good, R. T., Rug, M., Knuepfer, E. and Cowman, A. F. (2004). Targeting malaria virulence and remodeling proteins to the host erythrocyte. *Science* **306**, 1930–1933.

Matuschewski, K. (2006). Getting infectious: formation and maturation of *Plasmodium* sporozoites in the *Anopheles* vector. *Cell Microbiol* **8**, 1547–1556.

Matuschewski, K. and Mueller, A.-K. (2007). Vaccines against malaria - an update. *FEBS J* **274**, 4680–4687.

Mazumdar, J., Wilson, E. H., Masek, K., Hunter, C. A. and Striepen, B. (2006). Apicoplast fatty acid synthesis is essential for organelle biogenesis and parasite survival in *Toxoplasma gondii*. *Proc Natl Acad Sci U S A* **103**, 13192–13197.

McFadden, G. I. and Roos, D. S. (1999). Apicomplexan plastids as drug targets. *Trends Microbiol* **7**, 328–333.

McManus, E., Luisi, B. F. and Perham, R. N. (2006). Structure of a putative lipoate protein ligase from *Thermoplasma acidophilum* and the mechanism of target selection for post-translational modification. *J Mol Biol* **356**, 625–637.

McMillan, P. J., Stimmler, L. M., Foth, B. J., McFadden, G. I. and Müller, S. (2005). The human malaria parasite *Plasmodium falciparum* possesses two distinct dihydrolipoamide dehydrogenases. *Mol Microbiol* **55**, 27–38.

Meshnick, S. R. (1998). Artemisinin antimalarials: mechanisms of action and resistance. *Med Trop (Mars)* **58**, 13–17.

Militello, K. T., Dodge, M., Bethke, L. and Wirth, D. F. (2004). Identification of regulatory elements in the *Plasmodium falciparum* genome. *Mol Biochem Parasitol* **134**, 75–88.

Millar, A. H., Whelan, J. and Small, I. (2006). Recent surprises in protein targeting to mitochondria and plastids. *Curr Opin Plant Biol* **9**, 610–615.

Miller, J. R., Busby, R. W., Jordan, S. W., Cheek, J., Henshaw, T. F., Ashley, G. W., Broderick, J. B., Cronan, J. E. and Marletta, M. A. (2000). *Escherichia coli* LipA is a lipoyl synthase: *in vitro* biosynthesis of lipoylated pyruvate dehydrogenase complex from octanoyl-acyl carrier protein. *Biochemistry* **39**, 15166–15178.

Miller, L. H., Baruch, D. I., Marsh, K. and Doumbo, O. K. (2002). The pathogenic basis of malaria. *Nature* **415**, 673–679.

Müller, R., Marchetti, M., Kratzmeier, M., Elgass, H., Kuschel, M., Zenker, A. and Allmaier, G. (2007). Comparison of planar SDS-PAGE, CGE-on-a-chip, and MALDI-TOF mass spectrometry for analysis of the enzymatic de-N-glycosylation of antithrombin III and coagulation factor IX with PNGase F. *Anal Bioanal Chem* **[Epub ahead of print]**.

Müller, S. (2004). Redox and antioxidant systems of the malaria parasite *Plasmodium falciparum*. *Mol Microbiol* **53**, 1291–1305.

Ménard, R. (2005). Medicine: knockout malaria vaccine? *Nature* **433**, 113–114.

Mooney, B. P., Miernyk, J. A. and Randall, D. D. (2002). The complex fate of alpha-ketoacids. *Annu Rev Plant Biol* **53**, 357–375.

Morgan, R. R., Errington, R. and Elder, G. H. (2004). Identification of sequences required for the import of human protoporphyrinogen oxidase to mitochondria. *Biochem J* **377**, 281–287.

Morris, T. W., Reed, K. E. and Cronan, J. E. (1994). Identification of the gene encoding lipoate-protein ligase A of *Escherichia coli*. Molecular cloning and characterization of the *lplA* gene and gene product. *J Biol Chem* **269**, 16091–16100.

Morris, T. W., Reed, K. E. and Cronan, J. E. (1995). Lipoic acid metabolism in *Escherichia coli*: the *lplA* and *lipB* genes define redundant pathways for ligation of lipoyl groups to apoprotein. *J Bacteriol* **177**, 1–10.

Mu, J., Ferdig, M. T., Feng, X., Joy, D. A., Duan, J., Furuya, T., Subramanian, G., Aravind, L., Cooper, R. A., Wootton, J. C., Xiong, M. and zhuan Su, X. (2003). Multiple transporters associated with malaria parasite responses to chloroquine and quinine. *Mol Microbiol* **49**, 977–989.

Mullin, K. A., Lim, L., Ralph, S. A., Spurck, T. P., Handman, E. and McFadden, G. I. (2006). Membrane transporters in the relict plastid of malaria parasites. *Proc Natl Acad Sci U S A* **103**, 9572–9577.

Na-Bangchang, K., Ruengweerayut, R., Karbwang, J., Chauemung, A. and Hutchinson, D. (2007). Pharmacokinetics and pharmacodynamics of fosmidomycin monotherapy and combination therapy with clindamycin in the treatment of multidrug resistant *falciparum* malaria. *Malar J* **6**, 70.

Nielsen, H., Engelbrecht, J., Brunak, S. and von Heijne, G. (1997). Identification of prokaryotic and eukaryotic signal peptides and prediction of their cleavage sites. *Protein Eng* **10**, 1–6.

Nikolau, B. J., Ohlrogge, J. B. and Wurtele, E. S. (2003). Plant biotin-containing carboxylases. *Arch Biochem Biophys* **414**, 211–222.

Notredame, C., Higgins, D. G. and Heringa, J. (2000). T-Coffee: A novel method for fast and accurate multiple sequence alignment. *J Mol Biol* **302**, 205–217.

O'Donnell, R. A., Freitas-Junior, L. H., Preiser, P. R., Williamson, D. H., Duraisingh, M., McElwain, T. F., Scherf, A., Cowman, A. F. and Crabb, B. S. (2002). A genetic screen for improved plasmid segregation reveals a role for Rep20 in the interaction of *Plasmodium falciparum* chromosomes. *EMBO J* **21**, 1231–1239.

Oliver, D. J., Neuburger, M., Bourguignon, J. and Douce, R. (1990). Interaction between the component enzymes of the glycine decarboxylase multienzyme complex. *Plant Physiol* **94**, 833–839.

O'Riordan, M., Moors, M. A. and Portnoy, D. A. (2003). *Listeria* intracellular growth and virulence require host-derived lipoic acid. *Science* **302**, 462–464.

Pacheco-Alvarez, D., Solórzano-Vargas, R. S. and Río, A. L. D. (2002). Biotin in metabolism and its relationship to human disease. *Arch Med Res* **33**, 439–447.

Packer, L., Kraemer, K. and Rimbach, G. (2001). Molecular aspects of lipoic acid in the prevention of diabetes complications. *Nutrition* **17**, 888–895.

Packer, L., Witt, E. H. and Tritschler, H. J. (1995). alpha-Lipoic acid as a biological antioxidant. *Free Radic Biol Med* **19**, 227–250.

Painter, H. J., Morrisey, J. M., Mather, M. W. and Vaidya, A. B. (2007). Specific role of mitochondrial electron transport in blood-stage *Plasmodium falciparum*. *Nature* **446**, 88–91.

Patrick, L. (2000). Nutrients and HIV: part three - N-acetylcysteine, alpha-lipoic acid, L-glutamine, and L-carnitine. *Altern Med Rev* **5**, 290–305.

Perham, R. N. (1991). Domains, motifs, and linkers in 2-oxo acid dehydrogenase multienzyme complexes: a paradigm in the design of a multifunctional protein. *Biochemistry* **30**, 8501–8512.

Perham, R. N. (2000). Swinging arms and swinging domains in multifunctional enzymes: catalytic machines for multistep reactions. *Annu Rev Biochem* **69**, 961–1004.

Pfanner, N. and Geissler, A. (2001). Versatility of the mitochondrial protein import machinery. *Nat Rev Mol Cell Biol* **2**, 339–349.

Pino, P., Foth, B. J., Kwok, L.-Y., Sheiner, L., Schepers, R., Soldati, T. and Soldati-Favre, D. (2007). Dual targeting of antioxidant and metabolic enzymes to the mitochondrion and the apicoplast of *Toxoplasma gondii*. *PLoS Pathog* **3**, e115.

Poirot, O., O'Toole, E. and Notredame, C. (2003). Tcoffee@igs: A web server for computing, evaluating and combining multiple sequence alignments. *Nucleic Acids Res* **31**, 3503–3506.

Ponpuak, M., Klemba, M., Park, M., Gluzman, I. Y., Lamppa, G. K. and Goldberg, D. E. (2007). A role for falcilysin in transit peptide degradation in the *Plasmodium falciparum* apicoplast. *Mol Microbiol* **63**, 314–334.

Prapunwattana, P., O'Sullivan, W. J. and Yuthavong, Y. (1988). Depression of *Plasmodium falciparum* dihydroorotate dehydrogenase activity in *in vitro* culture by tetracycline. *Mol Biochem Parasitol* **27**, 119–124.

Prasad, P. D. and Ganapathy, V. (2000). Structure and function of mammalian sodium-dependent multivitamin transporter. *Curr Opin Clin Nutr Metab Care* **3**, 263–266.

Prudêncio, M., Rodriguez, A. and Mota, M. M. (2006). The silent path to thousands of merozoites: the *Plasmodium* liver stage. *Nat Rev Microbiol* **4**, 849–856.

Quinn, J., Diamond, A. G., Masters, A. K., Brookfield, D. E., Wallis, N. G. and Yeaman, S. J. (1993). Expression and lipoylation in *Escherichia coli* of the inner lipoyl domain of the E2 component of the human pyruvate dehydrogenase complex. *Biochem J* **289 (Pt 1)**, 81–85.

Ralph, S. A. (2007). Subcellular multitasking - multiple destinations and roles for the *Plasmodium* falcilysin protease. *Mol Microbiol* **63**, 309–313.

Ralph, S. A., van Dooren, G. G., Waller, R. F., Crawford, M. J., Fraunholz, M. J., Foth, B. J., Tonkin, C. J., Roos, D. S. and McFadden, G. I. (2004). Tropical infectious diseases: metabolic maps and functions of the *Plasmodium falciparum* apicoplast. *Nat Rev Microbiol* **2**, 203–216.

Rangarajan, R., Bei, A. K., Jethwaney, D., Maldonado, P., Dorin, D., Sultan, A. A. and Doerig, C. (2005). A mitogen-activated protein kinase regulates male gametogenesis and transmission of the malaria parasite *Plasmodium berghei*. *EMBO Rep* **6**, 464–469.

Reche, P., Li, Y. L., Fuller, C., Eichhorn, K. and Perham, R. N. (1998). Selectivity of post-translational modification in biotinylated proteins: the carboxy carrier protein of the acetyl-CoA carboxylase of *Escherichia coli*. *Biochem J* **329 (Pt 3)**, 589–596.

Reche, P. and Perham, R. N. (1999). Structure and selectivity in post-translational modification: attaching the biotinyl-lysine and lipoyl-lysine swinging arms in multifunctional enzymes. *EMBO J* **18**, 2673–2682.

Reche, P. A. (2000). Lipoylating and biotinylating enzymes contain a homologous catalytic module. *Protein Sci* **9**, 1922–1929.

Reddy, D. V., Rothemund, S., Shenoy, B. C., Carey, P. R. and Sönnichsen, F. D. (1998). Structural characterization of the entire 1.3S subunit of transcarboxylase from *Propionibacterium shermanii*. *Protein Sci* **7**, 2156–2163.

Reed, K. E. and Cronan, J. E. (1993). Lipoic acid metabolism in *Escherichia coli*: sequencing and functional characterization of the *lipA* and *lipB* genes. *J Bacteriol* **175**, 1325–1336.

Reed, K. E., Morris, T. W. and Cronan, J. E. (1994). Mutants of *Escherichia coli* K-12 that are resistant to a selenium analog of lipoic acid identify unknown genes in lipoate metabolism. *Proc Natl Acad Sci U S A* **91**, 3720–3724.

Reed, L. J., DeBusk, B. G., Gunsalus, I. C. and Hornberger, C. S. (1951). Crystalline alpha-lipoic acid; a catalytic agent associated with pyruvate dehydrogenase. *Science* **114**, 93–94.

Reed, L. J. and Hackert, M. L. (1990). Structure-function relationships in dihydrolipoamide acyltransferases. *J Biol Chem* **265**, 8971–8974.

Reed, M. B., Saliba, K. J., Caruana, S. R., Kirk, K. and Cowman, A. F. (2000). Pgh1 modulates sensitivity and resistance to multiple antimalarials in *Plasmodium falciparum*. *Nature* **403**, 906–909.

Richter, S. and Lamppa, G. K. (1998). A chloroplast processing enzyme functions as the general stromal processing peptidase. *Proc Natl Acad Sci U S A* **95**, 7463–7468.

Robin, M.-A., Anandatheerthavarada, H. K., Biswas, G., Sepuri, N. B. V., Gordon, D. M., Pain, D. and Avadhani, N. G. (2002). Bimodal targeting of microsomal CYP2E1 to mitochondria through activation of an N-terminal chimeric signal by cAMP-mediated phosphorylation. *J Biol Chem* **277**, 40583–40593.

Rowe, J. A., Moulds, J. M., Newbold, C. I. and Miller, L. H. (1997). *P. falciparum* rosetting mediated by a parasite-variant erythrocyte membrane protein and complement-receptor 1. *Nature* **388**, 292–295.

Rudzinska, M. A. (1969). The fine structure of malaria parasites. *Int Rev Cytol* **25**, 161–199.

Rug, M., Wickham, M. E., Foley, M., Cowman, A. F. and Tilley, L. (2004). Correct promoter control is needed for trafficking of the ring-infected erythrocyte surface antigen to the host cytosol in transfected malaria parasites. *Infect Immun* **72**, 6095–6105.

Salcedo, E., Sims, P. F. G. and Hyde, J. E. (2005). A glycine-cleavage complex as part of the folate one-carbon metabolism of *Plasmodium falciparum*. *Trends Parasitol* **21**, 406–411.

Sati, S. P., Singh, S. K., Kumar, N. and Sharma, A. (2002). Extra terminal residues have a profound effect on the folding and solubility of a *Plasmodium falciparum* sexual stage-specific protein over-expressed in *Escherichia coli*. *Eur J Biochem* **269**, 5259–5263.

Sato, S., Clough, B., Coates, L. and Wilson, R. J. M. (2004). Enzymes for heme biosynthesis are found in both the mitochondrion and plastid of the malaria parasite *Plasmodium falciparum*. *Protist* **155**, 117–125.

Sato, S., Rangachari, K. and Wilson, R. J. M. (2003). Targeting GFP to the malarial mitochondrion. *Mol Biochem Parasitol* **130**, 155–158.

Sayers, J. R., Price, H. P., Fallon, P. G. and Doenhoff, M. J. (1995). AGA/AGG codon usage in parasites: implications for gene expression in *Escherichia coli*. *Parasitol Today* **11**, 345–346.

Schlitzer, M. (2007). Malaria chemotherapeutics part I: History of antimalarial drug development, currently used therapeutics, and drugs in clinical development. *ChemMedChem* **2**, 944–986.

Seeber, F. (2002). Biogenesis of iron-sulphur clusters in amitochondriate and apicomplexan protists. *Int J Parasitol* **32**, 1207–1217.

Shaw, N. M., Birch, O. M., Tinschert, A., Venetz, V., Dietrich, R. and Savoy, L. A. (1998). Biotin synthase from *Escherichia coli*: isolation of an enzyme-generated intermediate and stoichiometry of S-adenosylmethionine use. *Biochem J* **330 (Pt 3)**, 1079–1085.

Sherman, I. W., ed. (2005). *Molecular Approaches to Malaria*. American Society for Microbiology.

Shevchenko, A., Wilm, M., Vorm, O. and Mann, M. (1996). Mass spectrometric sequencing of proteins silver-stained polyacrylamide gels. *Anal Chem* **68**, 850–858.

Silva-Filho, M. C. (2003). One ticket for multiple destinations: dual targeting of proteins to distinct subcellular locations. *Curr Opin Plant Biol* **6**, 589–595.

Sinden, R. E., Canning, E. U., Bray, R. S. and Smalley, M. E. (1978). Gametocyte and gamete development in *Plasmodium falciparum*. *Proc R Soc Lond B Biol Sci* **201**, 375–399.

Sinden, R. E. and Croll, N. A. (1975). Cytology and kinetics of microgametogenesis and fertilization in *Plasmodium yoelii nigeriensis*. *Parasitology* **70**, 53–65.

Small, I., Peeters, N., Legeai, F. and Lurin, C. (2004). Predotar: A tool for rapidly screening proteomes for N-terminal targeting sequences. *Proteomics* **4**, 1581–1590.

Smith, S., Witkowski, A. and Joshi, A. K. (2003). Structural and functional organization of the animal fatty acid synthase. *Prog Lipid Res* **42**, 289–317.

Soll, J. and Schleiff, E. (2004). Protein import into chloroplasts. *Nat Rev Mol Cell Biol* **5**, 198–208.

Spielmann, T., Hawthorne, P. L., Dixon, M. W. A., Hannemann, M., Klotz, K., Kemp, D. J., Klonis, N., Tilley, L., Trenholme, K. R. and Gardiner, D. L. (2006). A cluster of ring stage-specific genes linked to a locus implicated in cytoadherence in *Plasmodium falciparum* codes for PEXEL-negative and PEXEL-positive proteins exported into the host cell. *Mol Biol Cell* **17**, 3613–3624.

Spycher, C., Klonis, N., Spielmann, T., Kump, E., Steiger, S., Tilley, L. and Beck, H.-P. (2003). MAHRP-1, a novel *Plasmodium falciparum* histidine-rich protein, binds ferriprotoporphyrin IX and localizes to the Maurer's clefts. *J Biol Chem* **278**, 35373–35383.

Spycher, C., Rug, M., Klonis, N., Ferguson, D. J. P., Cowman, A. F., Beck, H.-P. and Tilley, L. (2006). Genesis of and trafficking to the Maurer's clefts of *Plasmodium falciparum*-infected erythrocytes. *Mol Cell Biol* **26**, 4074–4085.

Srivastava, I. K., Rottenberg, H. and Vaidya, A. B. (1997). Atovaquone, a broad spectrum antiparasitic drug, collapses mitochondrial membrane potential in a malarial parasite. *J Biol Chem* **272**, 3961–3966.

Streaker, E. D. and Beckett, D. (1999). Ligand-linked structural changes in the *Escherichia coli* biotin repressor: the significance of surface loops for binding and allostery. *J Mol Biol* **292**, 619–632.

Suh, J. H., Shenvi, S. V., Dixon, B. M., Liu, H., Jaiswal, A. K., Liu, R.-M. and Hagen, T. M. (2004a). Decline in transcriptional activity of Nrf2 causes age-related loss of glutathione synthesis, which is reversible with lipoic acid. *Proc Natl Acad Sci U S A* **101**, 3381–3386.

Suh, J. H., Zhu, B.-Z., deSzoeke, E., Frei, B. and Hagen, T. M. (2004b). Dihydrolipoic acid lowers the redox activity of transition metal ions but does not remove them from the active site of enzymes. *Redox Rep* **9**, 57–61.

Suraveratum, N., Krungkrai, S. R., Leangaramgul, P., Prapunwattana, P. and Krungkrai, J. (2000). Purification and characterization of *Plasmodium falciparum* succinate dehydrogenase. *Mol Biochem Parasitol* **105**, 215–222.

Surolia, N. and Padmanaban, G. (1992). *De novo* biosynthesis of heme offers a new chemotherapeutic target in the human malarial parasite. *Biochem Biophys Res Commun* **187**, 744–750.

Surolia, N. and Surolia, A. (2001). Triclosan offers protection against blood stages of malaria by inhibiting enoyl-ACP reductase of *Plasmodium falciparum*. *Nat Med* **7**, 167–173.

Takeo, S., Kokaze, A., Ng, C. S., Mizuchi, D., Watanabe, J. I., Tanabe, K., Kojima, S. and Kita, K. (2000). Succinate dehydrogenase in *Plasmodium falciparum* mitochondria: molecular characterization of the SDHA and SDHB genes for the catalytic subunits, the flavoprotein (Fp) and iron-sulfur (Ip) subunits. *Mol Biochem Parasitol* **107**, 191–205.

Talman, A. M., Domarle, O., McKenzie, F. E., Ariey, F. and Robert, V. (2004). Gametocytogenesis: the puberty of *Plasmodium falciparum*. *Malar J* **3**, 24.

Targett, G. A. (2005). Malaria vaccines 1985-2005: a full circle? *Trends Parasitol* **21**, 499–503.

Tewari, R., Dorin, D., Moon, R., Doerig, C. and Billker, O. (2005). An atypical mitogen-activated protein kinase controls cytokinesis and flagellar motility during male gamete formation in a malaria parasite. *Mol Microbiol* **58**, 1253–1263.

Thompson, J. D., Higgins, D. G. and Gibson, T. J. (1994). CLUSTAL W: improving the sensitivity of progressive multiple sequence alignment through sequence weighting, position-specific gap penalties and weight matrix choice. *Nucleic Acids Res* **22**, 4673–4680.

Thomsen-Zieger, N., Schachtner, J. and Seeber, F. (2003). Apicomplexan parasites contain a single lipoic acid synthase located in the plastid. *FEBS Lett* **547**, 80–86.

Tonkin, C. J., Roos, D. S. and McFadden, G. I. (2006a). N-terminal positively charged amino acids, but not their exact position, are important for apicoplast transit peptide fidelity in *Toxoplasma gondii*. *Mol Biochem Parasitol* **150**, 192–200.

Tonkin, C. J., Struck, N. S., Mullin, K. A., Stimmler, L. M. and McFadden, G. I. (2006b). Evidence for Golgi-independent transport from the early secretory pathway to the plastid in malaria parasites. *Mol Microbiol* **61**, 614–630.

Tonkin, C. J., van Dooren, G. G., Spurck, T. P., Struck, N. S., Good, R. T., Handman, E., Cowman, A. F. and McFadden, G. I. (2004). Localization of organellar proteins in *Plasmodium falciparum* using a novel set of transfection vectors and a new immunofluorescence fixation method. *Mol Biochem Parasitol* **137**, 13–21.

Trager, W. and Jensen, J. B. (1976). Human malaria parasites in continuous culture. *Science* **193**, 673–675.

Treeck, M., Struck, N. S., Haase, S., Langer, C., Herrmann, S., Healer, J., Cowman, A. F. and Gilberger, T. W. (2006). A conserved region in the EBL proteins is implicated in microneme targeting of the malaria parasite *Plasmodium falciparum*. *J Biol Chem* **281**, 31995–32003.

Triglia, T., Wang, P., Sims, P. F., Hyde, J. E. and Cowman, A. F. (1998). Allelic exchange at the endogenous genomic locus in *Plasmodium falciparum* proves the role of dihydropteroate synthase in sulfadoxine-resistant malaria. *EMBO J* **17**, 3807–3815.

Turner, G. D., Morrison, H., Jones, M., Davis, T. M., Looareesuwan, S., Buley, I. D., Gatter, K. C., Newbold, C. I., Pukritayakamee, S. and Nagachinta, B. (1994). An immunohistochemical study of the pathology of fatal malaria. Evidence for widespread endothelial activation and a potential role for intercellular adhesion molecule-1 in cerebral sequestration. *Am J Pathol* **145**, 1057–1069.

Ugulava, N. B., Sacanell, C. J. and Jarrett, J. T. (2001). Spectroscopic changes during a single turnover of biotin synthase: destruction of a [2Fe-2S] cluster accompanies sulfur insertion. *Biochemistry* **40**, 8352–8358.

Umlas, J. and Fallon, J. N. (1971). New thick-film technique for malaria diagnosis. Use of saponin stromatolytic solution for lysis. *Am J Trop Med Hyg* **20**, 527–529.

Uyemura, S. A., Luo, S., Vieira, M., Moreno, S. N. J. and Docampo, R. (2004). Oxidative phosphorylation and rotenone-insensitive malate- and NADH-quinone oxidoreductases in *Plasmodium yoelii yoelii* mitochondria *in situ*. *J Biol Chem* **279**, 385–393.

van Dooren, G. G., Marti, M., Tonkin, C. J., Stimmler, L. M., Cowman, A. F. and McFadden, G. I. (2005). Development of the endoplasmic reticulum, mitochondrion and apicoplast during the asexual life cycle of *Plasmodium falciparum*. *Mol Microbiol* **57**, 405–419.

van Dooren, G. G., Schwartzbach, S. D., Osafune, T. and McFadden, G. I. (2001). Translocation of proteins across the multiple membranes of complex plastids. *Biochim Biophys Acta* **1541**, 34–53.

van Dooren, G. G., Stimmler, L. M. and McFadden, G. I. (2006). Metabolic maps and functions of the *Plasmodium* mitochondrion. *FEMS Microbiol Rev* **30**, 596–630.

Varadharajan, S., Dhanasekaran, S., Bonday, Z. Q., Rangarajan, P. N. and Padmanaban, G. (2002). Involvement of delta-aminolaevulinate synthase encoded by the parasite gene in *de novo* haem synthesis by *Plasmodium falciparum*. *Biochem J* **367**, 321–327.

Villarejo, A., Burén, S., Larsson, S., Déjardin, A., Monné, M., Rudhe, C., Karlsson, J., Jansson, S., Lerouge, P., Rolland, N., von Heijne, G., Grebe, M., Bako, L. and Samuelsson, G. (2005). Evidence for a protein transported through the secretory pathway *en route* to the higher plant chloroplast. *Nat Cell Biol* **7**, 1224–1231.

Vothknecht, U. C. and Soll, J. (2000). Protein import: the hitchhikers guide into chloroplasts. *Biol Chem* **381**, 887–897.

Walker, J. L. and Oliver, D. J. (1986). Glycine decarboxylase multienzyme complex. Purification and partial characterization from pea leaf mitochondria. *J Biol Chem* **261**, 2214–2221.

Waller, R. F., Keeling, P. J., Donald, R. G., Striepen, B., Handman, E., Lang-Unnasch, N., Cowman, A. F., Besra, G. S., Roos, D. S. and McFadden, G. I. (1998). Nuclear-encoded proteins target to the plastid in *Toxoplasma gondii* and *Plasmodium falciparum*. *Proc Natl Acad Sci U S A* **95**, 12352–12357.

Waller, R. F., Reed, M. B., Cowman, A. F. and McFadden, G. I. (2000). Protein trafficking to the plastid of *Plasmodium falciparum* is via the secretory pathway. *EMBO J* **19**, 1794–1802.

Wallis, N. G. and Perham, R. N. (1994). Structural dependence of post-translational modification and reductive acetylation of the lipoyl domain of the pyruvate dehydrogenase multienzyme complex. *J Mol Biol* **236**, 209–216.

Wang, S. C. and Frey, P. A. (2007). S-adenosylmethionine as an oxidant: the radical SAM superfamily. *Trends Biochem Sci* **32**, 101–110.

Waterkeyn, J. G., Crabb, B. S. and Cowman, A. F. (1999). Transfection of the human malaria parasite *Plasmodium falciparum*. *Int J Parasitol* **29**, 945–955.

Waters, A. P. and Janse, C. J., eds. (2004). *Malaria Parasites: Genomes and Molecular Biology*. Caister Academic Press.

White, S. W., Zheng, J., Zhang, Y.-M. and Rock (2005). The structural biology of type II fatty acid biosynthesis. *Annu Rev Biochem* **74**, 791–831.

Whitmore, L. and Wallace, B. A. (2004). DICHROWEB, an online server for protein secondary structure analyses from circular dichroism spectroscopic data. *Nucleic Acids Res* **32**, W668–W673.

WHO (2007). Malaria - Fact sheet N94. www.who.int/topics/malaria/en/.

Wickham, M. E., Rug, M., Ralph, S. A., Klonis, N., McFadden, G. I., Tilley, L. and Cowman, A. F. (2001). Trafficking and assembly of the cytoadherence complex in *Plasmodium falciparum*-infected human erythrocytes. *EMBO J* **20**, 5636–5649.

Wiesner, J., Henschker, D., Hutchinson, D. B., Beck, E. and Jomaa, H. (2002). *In vitro* and *in vivo* synergy of fosmidomycin, a novel antimalarial drug, with clindamycin. *Antimicrob Agents Chemother* **46**, 2889–2894.

Wilson, R. J., Gardner, M. J., Feagin, J. E. and Williamson, D. H. (1991). Have malaria parasites three genomes? *Parasitol Today* **7**, 134–136.

Winstanley, P. and Ward, S. (2006). Malaria chemotherapy. *Adv Parasitol* **61**, 47–76.

Witkowski, A., Joshi, A. K. and Smith, S. (2007). Coupling of the *de novo* fatty acid biosynthesis and lipoylation pathways in mammalian mitochondria. *J Biol Chem* **282**, 14178–14185.

Wrenger, C. and Müller, S. (2003). Isocitrate dehydrogenase of *Plasmodium falciparum*. *Eur J Biochem* **270**, 1775–1783.

Wrenger, C. and Müller, S. (2004). The human malaria parasite *Plasmodium falciparum* has distinct organelle-specific lipoylation pathways. *Mol Microbiol* **53**, 103–113.

Wu, Y., Kirkman, L. A. and Wellems, T. E. (1996). Transformation of *Plasmodium falciparum* malaria parasites by homologous integration of plasmids that confer resistance to pyrimethamine. *Proc Natl Acad Sci U S A* **93**, 1130–1134.

Wu, Y., Sifri, C. D., Lei, H. H., Su, X. Z. and Wellems, T. E. (1995). Transfection of *Plasmodium falciparum* within human red blood cells. *Proc Natl Acad Sci U S A* **92**, 973–977.

Yasuno, R. and Wada, H. (2002). The biosynthetic pathway for lipoic acid is present in plastids and mitochondria in *Arabidopsis thaliana*. *FEBS Lett* **517**, 110–114.

Yi, X. and Maeda, N. (2005). Endogenous production of lipoic acid is essential for mouse development. *Mol Cell Biol* **25**, 8387–8392.

Young, J. A., Fivelman, Q. L., Blair, P. L., de la Vega, P., Roch, K. G. L., Zhou, Y., Carucci, D. J., Baker, D. A. and Winzeler, E. A. (2005). The *Plasmodium falciparum* sexual development transcriptome: a microarray analysis using ontology-based pattern identification. *Mol Biochem Parasitol* **143**, 67–79.

Zhang, W. J. and Frei, B. (2001). Alpha-lipoic acid inhibits TNF-alpha-induced NF-kappaB activation and adhesion molecule expression in human aortic endothelial cells. *FASEB J* **15**, 2423–2432.

Zhao, X., Miller, J. R. and Cronan, J. E. (2005). The reaction of LipB, the octanoyl-[acyl carrier protein]:protein N-octanoyltransferase of lipoic acid synthesis, proceeds through an acyl-enzyme intermediate. *Biochemistry* **44**, 16737–16746.

Zhao, X., Miller, J. R., Jiang, Y., Marletta, M. A. and Cronan, J. E. (2003). Assembly of the covalent linkage between lipoic acid and its cognate enzymes. *Chem Biol* **10**, 1293–1302.

Zhu, G. (2004). Current progress in the fatty acid metabolism in *Cryptosporidium parvum*. *J Eukaryot Microbiol* **51**, 381–388.

Zhu, G., Marchewka, M. J., Woods, K. M., Upton, S. J. and Keithly, J. S. (2000). Molecular analysis of a type I fatty acid synthase in *Cryptosporidium parvum*. *Mol Biochem Parasitol* **105**, 253–260.

Zuegge, J., Ralph, S., Schmuker, M., McFadden, G. I. and Schneider, G. (2001). Deciphering apicoplast targeting signals–feature extraction from nuclear-encoded precursors of *Plasmodium falciparum* apicoplast proteins. *Gene* **280**, 19–26.

A. Appendix

A.1. Amino acids

Table A.1.: Amino acid abbreviations

Amino acid	Abbreviation	Single letter code
Alanine	Ala	A
Arginine	Arg	R
Asparagine	Asn	N
Aspartate	Asp	D
Cysteine	Cys	C
Glutamate	Glu	E
Glutamine	Gln	Q
Glycine	Gly	G
Histidine	His	H
Isoleucine	Ile	I
Leucine	Leu	L
Lysine	Lys	K
Methionine	Met	M
Phenylalanine	Phe	F
Proline	Pro	P
Serine	Ser	S
Threonine	Thr	T
Tryptophan	Trp	W
Tyrosine	Tyr	Y
Valine	Val	V

A.2. Vector map of pBluescript II SK

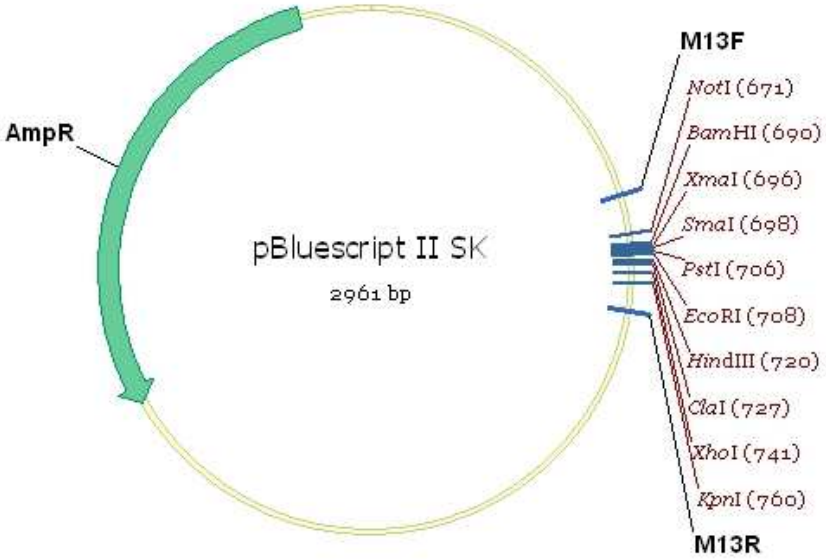

Figure A.1.: Vector map of pBluescript II SK
This figure displays the important features of the pBluescript II SK plasmid (Stratagene). The plasmid contains the ampicillin resistance cassette (AmpR; 861 bp) for selection in *E. coli*, and a multiple cloning site (NotI-KpnI). The primers M13F and M13R were used to verify the sequence of the cloned inserts.

A.3. Vector map of pQE-2

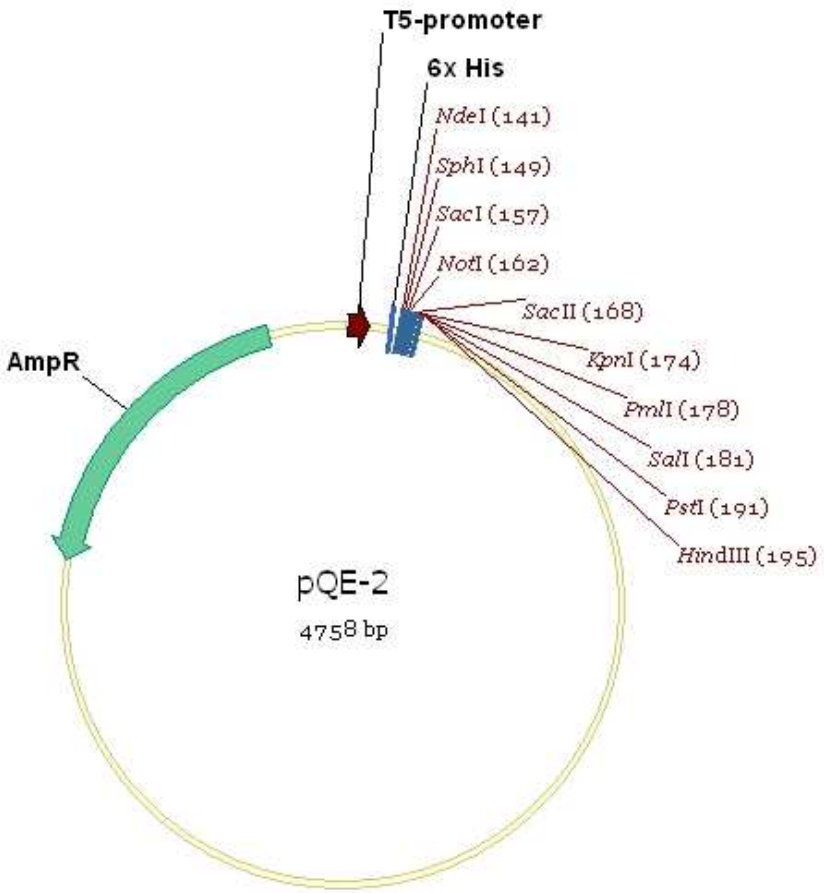

Figure A.2.: Vector map of pQE-2
This figure displays the important features of the pQE-2 (Quiagen) recombinant expression plasmid. These include the ampicillin resistance cassette (AmpR; 861 bp) and the multiple cloning site (NdeI-HindIII). Recombinant expression using this plasmid is under control of the T5 promoter and attaches a $(His)_6$-tag at the N-terminus of the recombinant protein.

A.4. Gene and/or protein IDs

The ID numbers of the genes and proteins described in this study are as follows:

P. falciparum **(obtained from PlasmoDB)**

ACP	PFB0385w
BCDH-E2	PFC0170c
H-protein	PF11_0339
KGDH-E2	PF13_0121
LipA	MAL13P1.220
LipB	MAL8P1.37
LipDH (apicoplast)	PF08_0066
LplA1	PF13_0083
LplA2	PFI1160w
PDH-E2	PF10_0407

P. berghei **(obtained from PlasmoDB)**

BCDH-E2	PB001239.02.0
H-protein	PB000228.00.0
KGDH-E2	PB000860.02.0
LipA	PB300672.00.0
LipB	PB001047.01.0
LipDH (apicoplast)	PB001049.01.0
LplA1	PB000283.02.0
LplA2	PB001158.00.0
PDH-E2	PB000163.02.0

Other apicopmlexan LplA2s

P. chabaudi LplA2	PC000179.03.0 (obtained from PlasmoDB)
P. knowlesi LplA2	PKH_072080 (obtained from PlasmoDB)
P. vivax LplA2	Pv099590 (obtained from PlasmoDB)
P. yoelii LplA2	PY02395 (obtained from PlasmoDB)
T. gondii LplA2	83.m01296 (obtained from ToxoDB)
T. parva LplA2	XP_954802 (obtained from NCBI-DB)

Bacterial genes/proteins (obtained from NCBI-DB)

E. coli H-protein	CAA52145
E. coli KGDH-E2	NP_415255
E. coli LipA	AAB40828
E. coli LipB	NP_415163
E. coli LplA	NP_418803
E. coli PDH-E2	NP_414657
L. monocytogenes LplA1	NP_464456
L. monocytogenes LplA2	NP_464291
T. acidophilum LplA	CAC11654

Plant and mammalian genes/proteins (obtained from NCBI-DB)

Arabidopsis thaliana LplA	BAA95754
Bos taurus lipoate-activating enzyme	BAB40420
Bos taurus lipoyltransferase	BAA24354